STUDIES OF REINFORCED CONCRETE REGIONS NEAR DISCONTINUITIES

by

WILLIAM DIGBY COOK

Department of Civil Engineering and Applied Mechanics

McGill University

Montreal, Canada

July 1987

A thesis submitted to the Faculty of Graduate Studies and Research in partial fulfillment of the requirements for the degree of Doctor of Philosophy

ABSTRACT

A non-linear finite element computer program capable of predicting the complete response of two-dimensional reinforced concrete members was developed. This tool which accounts for the stress strain characteristics of cracked concrete was used to predict the responses of a number of members containing discontinuities. These members included corbels, dapped end beams, beams with web holes, and deep beams. The results of tests performed by the author as well as tests performed by other researchers were compared with the non-linear predictions. In addition, simple strut and tie models suitable for designing regions near discontinuities were developed. The predictions obtained by these models were compared with the non-linear finite element predictions and with the test results.

RESUME

Un programme d'ordinateur effectuant une analyse non-linéaire à élément fini afin de prédire le comportement d'éléments bi-dimensionnels en béton armé fut conçu. Cet outil analytique qui tient compte des caractéristiques de déformation du béton fissuré fut utilizé afin de prédir le comportement d'un certain nombre d'éléments possédant des régions discontinues, tels supports à encorbellement, poutres aux extrémités entailleés, poutres possédant une ouverture dans l'âme, et poutres profondes. Les résultats de tests exécutés par l'auteur ainsi que ceux exécutés par divers chercheurs furent comparés avec les prédictions non-linéaires. De plus, des modèles simples constitués de réseaux d'éléments agissant en compression ou en tension furent conçus en tant que méthode de design des régions discontinues. Les resùltats obtenus par ces modèles furent comparés avec les prédictions d'analyse non-linéaire à élément fini ainsi qu'avec les résultats de tests.

ACKNOWLEDGEMENTS

The author would like to take this opportunity to express his sincere thanks to Professor Denis Mitchell for his knowledgeable and skillful guidance, his continual encouragement and his patience throughout this research programme.

In addition the writer wishes to express his gratitude to Lionel Lemay for his assistance in the construction and testing of the specimens with web holes.

The experimental research was carried out in the Jamieson Structures Laboratory in the Department of Civil Engineering and Applied Mechanics at McGill University. The author is particularly grateful for the assistance given by B. Cockayne and R. Sheppard.

Thanks are extended to Alain Dandurand for his expert assistance in preparing the figures and to Patrick Paultre for taking some of the photographs.

The financial assistance provided by the Natural Sciences and Engineering Research Council of Canada and by the Fonds pour la Formation de Chercheurs et l'Aide à la Recherche of the Government of Quebec is gratefully acknowledged.

This manuscript was prepared using the PCTEX typesetting program and was printed on a Hewlett Packard LaserJet$^+$ Printer.

TABLE OF CONTENTS

ABSTRACT i
RESUME ii
ACKNOWLEDGEMENTS iii
LIST OF FIGURES vi
LIST OF TABLES ix
LIST OF SYMBOLS x

1 INTRODUCTION 1
1.1 Introduction 1
1.2 Previous Research 3
1.3 Objectives 7

2 ANALYSIS AND DESIGN METHODS 8
2.1 Introduction 8
2.2 Strut and Tie Models 8
2.2.1 Design Procedure of the Canadian Concrete Code 9
2.2.2 Example Strut and Tie Models and Truss Idealizations 12
2.2.2.1 Brackets and Corbels 12
2.2.2.2 Dapped End Beams and Beams with Holes in the Web . 12
2.2.2.3 Deep Beams 14
2.3 Program FIELDS 17
2.3.1 General Description of Program 17
2.3.2 Program Logic 18
2.3.3 Element Formulations 19

3. EXPERIMENTAL PROGRAMME 28
3.1 Introduction 28
3.2 Material Properties 29
3.2.1 Concrete 29
3.2.2 Reinforcing Steel 29
3.3 Corbel Specimen C-1 30
3.4 Dapped End Specimens D-1 and D-2 35
3.5 Dapped End Specimens D-3 and D-4 38
3.6 Web Hole Specimens H-1 and H-2 42

TABLE OF CONTENTS *(Continued)*

4 EXPERIMENTAL RESULTS 47
4.1 Introduction 47
4.2 Corbel Specimen C-1 47
4.3 Dapped End Specimen D-1 48
4.4 Dapped End Specimen D-2 56
4.5 Comparison of Behaviour of Dapped End Specimens D-1 and D-2 . . 58
4.6 Dapped End Specimen D-3 61
4.7 Dapped End Specimen D-4 66
4.8 Web Hole Specimen H-1 68
4.9 Web Hole Specimen H-2 73

5 PREDICTIONS OF EXPERIMENTAL RESULTS 78
5.1 Introduction 78
5.2 Reinforced Concrete Shear Panels Tested by Vecchio and Collins . . . 79
5.3 Uniformly Loaded Beams Tested by Mailhot 82
5.4 Continuous Deep Beams Tested by Rogowski, MacGregor and Ong . . 85
5.5 Corbel Specimen C-1 89
5.6 Dapped End Beam Tests D-1 and D-2 91
5.7 Dapped End Beam Test D-4 95
5.8 Dapped End Beam Test D-3 97
5.9 Web Hole Specimen H-1 100
5.10 Web Hole Specimen H-2 102

6 SUMMARY AND CONCLUSIONS 105

STATEMENT OF ORIGINALITY 108
REFERENCES 109

APPENDIX A – EXPERIMENTAL DATA 111
A.1 Introduction 111
A.2 Corbel Specimen C-1 112
A.3 Dapped End Specimens D-1 and D-2 119
A.4 Dapped End Specimens D-3 and D-4 131
A.5 Web Hole Specimens H-1 and H-2 140

LIST OF FIGURES

1.1 Examples of Typical Disturbed Regions 2
1.2 Shear Panel Test Set-Up used by Vecchio and Collins 4
1.3 Discretization of Concrete Beam for Analysis Using Program SMAL . . 6
2.1 Strut and Tie Modelling of a Dapped End Beam 10
2.2 Strut and Tie Models and Truss Idealizations for Brackets and Corbels . 13
2.3 Strut and Tie Models and Truss Idealizations for Dapped End Beams and Beams with Holes in the Web 15
2.4 Strut and Tie Models and Truss Idealizations for Deep Beams 16
2.5 Evaluating Stresses at a Gauss Point in Element CFTQ 20
2.6 Average Concrete Stress-Strain Relationships 22
2.7 Investigating Stresses at Crack Interface 24
3.1 Typical Reinforcement Stress-Strain Relationships 31
3.2 Dimensions and Reinforcement Details of Corbel Specimen C-1 32
3.3 Photograph of Reinforcing Cage for Corbel Specimen C-1 33
3.4 Test Set-Up and Instrumentation for Corbel Specimen C-1 34
3.5 Dimensions and Reinforcement Details of Dapped End Specimens D-1 and D-2 36
3.6 Photographs of Reinforcing Cages for Dapped End Specimens D-1 and D-2 37
3.7 Test Set-Up and Instrumentation for Dapped End Specimens D-1 and D-2 39
3.8 Dimensions and Reinforcement Details of Dapped End Specimens D-3 and D-4 40
3.9 Photographs of Reinforcing Cages for Dapped End Specimens D-3 and D-4 41
3.10 Test Set-Up and Instrumentation for Dapped End Specimens D-3 and D-4 43
3.11 Dimensions and Reinforcement Details of Web Hole Specimens H-1 and H-2 44
3.12 Photographs of Reinforcing Cages for Web Hole Specimens H-1 and H-2 45
3.13 Test Set-Up and Instrumentation for Web Hole Specimens H-1 and H-2 46

LIST OF FIGURES *(Continued)*

4.1 Photograph of Corbel Specimen C-1 at V = 336 kN 48
4.2 Measured Reinforcement Strains in Corbel Specimen C-1 49
4.3 Principal Strains Determined from Rosette Readings for Corbel Specimen C-1 50
4.4 Photograph of Corbel Specimen C-1 after Failure, V = 502 kN 51
4.5 Photographs of Dapped End Specimen D-1 52
4.6 Measured Strains in Vertical and Horizontal Reinforcement in Dapped End Specimen D-1 53
4.7 Principal Strains Determined from Rosette Readings for Dapped End Specimen D-1 54
4.8 Photographs of Dapped End Specimen D-1 55
4.9 Photographs of Dapped End Specimen D-2 57
4.10 Measured Strains in Vertical and Horizontal Reinforcement in Dapped End Specimen D-2 58
4.11 Principal Strains Determined from Rosette Readings for Dapped End Specimen D-2 59
4.12 Photographs of Dapped End Specimen D-2 after Failure 60
4.13 Photographs of Dapped End Specimens D-1 and D-2 after Failure . . . 62
4.14 Photographs of Dapped End Specimen D-3 63
4.15 Measured Strains in Vertical, Diagonal, and Horizontal Reinforcement in Dapped End Specimen D-3 64
4.16 Principal Strains Determined from Rosette Readings for Dapped End Specimen D-3 65
4.17 Photographs of Dapped End Specimen D-3 66
4.18 Photographs of Dapped End Specimen D-4 67
4.19 Measured Strains in Vertical, Inclined, and Horizontal Reinforcement in Dapped End Specimen D-4 69
4.20 Principal Strains Determined from Rosette Readings for Dapped End Specimen D-4 70
4.21 Photographs of Dapped End Specimen D-4 after Failure 71
4.22 Photographs of Web Hole Specimen H-1 72
4.23 Measured Stirrup Strains in Web Hole Specimen H-1 73
4.24 Photographs of Web Hole Specimen H-1 at Failure, w = 177 kN/m . . . 74

LIST OF FIGURES *(Continued)*

4.25 Photographs of Web Hole Specimen H-2 75
4.26 Measured Stirrup Strains in Web Hole Specimen H-2 76
4.27 Photographs of Web Hole Specimen H-2 after Failure 77
5.1 Comparison of Predicted Responses and Measured Responses of Shear Panels Tested by Vecchio and Collins 81
5.2 Details of Uniformly Loaded Beam B Tested by Mailhot 83
5.3 Principal Strains Determined from Strain Rosettes for Specimen B 84
5.4 Predicted Principal Concrete Stresses and Principal Strains for Specimen B 85
5.5 Comparison of Measured and Predicted Strains in Transverse Reinforcement for Specimen B 86
5.6 Continuous Deep Beams Tested by Rogowsky, MacGregor, and Ong . . . 88
5.7 Corbel Specimen C-1 90
5.8 Dapped End Specimen D-1 93
5.9 Dapped End Specimen D-4 96
5.10 Dapped End Specimen D-3 98
5.11 Web Hole Specimen H-1 101
5.12 Web Hole Specimen H-2 104
A.1 Test Set-Up and Instrumentation for Corbel Specimen C-1 112
A.2 Initial Test Set-Up and Instrumentation for Dapped End Specimens D-1 and D-2 119
A.3 Initial Test Set-Up and Instrumentation for Dapped End Specimens D-3 and D-4 131
A.4 Initial Test Set-Up and Instrumentation for Web Hole Specimens H-1 and H-2 140

LIST OF TABLES

3.1 Summary of Concrete Strengths 29
3.2 Reinforcement Properties 30
5.1 Parameters of Shear Panels Tested By Vecchio and Collins 79
A.1 Corbel Specimen C-1 – Measured Loads 113
A.2 Corbel Specimen C-1 – Strain Measurements 113
A.3 Dapped End Specimens D-1 and D-2 – Measured Loads – Loading 1 . . . 120
A.4 Dapped End Specimens D-1 and D-2 – Strain Measurements – Loading 1 120
A.5 Dapped End Specimen D-1 – Measured Loads – Loading 2 126
A.6 Dapped End Specimen D-1 – Strain Measurements – Loading 2 127
A.7 Dapped End Specimens D-3 and D-4 – Measured Loads – Loading 1 . . . 132
A.8 Dapped End Specimens D-3 and D-4 – Strain Measurements – Loading 1 132
A.9 Dapped End Specimen D-3 – Measured Loads – Loading 2 137
A.10 Dapped End Specimens D-3 and D-4 – Strain Measurements – Loading 2 137
A.11 Web Hole Specimens H-1 and H-2 – Measured Loads – Loading 1 . . . 141
A.12 Web Hole Specimens H-1 and H-2 – Strain Measurements – Loading 1 142
A.13 Web Hole Specimen H-1 – Measured Loads – Loading 2 150
A.14 Web Hole Specimen H-1 – Strain Measurements – Loading 2 150

LIST OF SYMBOLS

a	maximum aggregate size
A	element surface area
A_s	area of tension tie reinforcement
B	strain-displacement matrix
D	incremental stress-strain constitutive matrix
E_c	initial tangent modulus of elasticity of concrete
E_s	modulus of elasticity of reinforcement
E_{st}	tangent modulus after yielding of reinforcement
E_{sx}	modulus of elasticity of reinforcement in x direction
E_{sy}	modulus of elasticity of reinforcement in y direction
f'_c	compressive strength of concrete (from a standard cylinder test)
f_{cr}	stress in concrete at cracking
f_{c1}	average principal tensile stress in concrete
f_{c2}	principal compressive stress in concrete
f_{c2max}	compressive strength of cracked concrete
f_{sx}	average stress in x reinforcement
$f_{sx,cr}$	stress in x reinforcement at a crack
f_{sy}	average stress in y reinforcement
$f_{sy,cr}$	stress in y reinforcement at a crack
f_y	yield stress of reinforcement
H	horizontal force
$\mathbf{k_T}$	element tangent stiffness matrix
ℓ_d	development length of reinforcement
s_{mx}	crack spacing expected for axial tension in the local x direction
s_{my}	crack spacing expected for axial tension in the local y direction
$s_{m\theta}$	average crack spacing expected at angle θ from the global X axis
t	element thickness
v_{ci}	shear stress on crack interface
v_{cimax}	maximum shear stress permitted on a crack interface
v_{xy}	shear stress in reinforced concrete element
V	shear force
w	uniform load per unit length
w	crack width

LIST OF SYMBOLS *(Continued)*

α_s	angle between tension tie and compressive strut
β	factor accounting for the reduction in compressive strength of cracked concrete
Δf_{sx}	additional incremental stress in x reinforcement at a crack location
Δf_{sy}	additional incremental stress in y reinforcement at a crack location
ϵ'_c	strain in concrete at peak stress, f'_c (from a standard cylinder test)
ϵ_{cr}	strain in concrete at cracking
ϵ_s	tensile strain in tension tie
ϵ_x	strain in x reinforcement
ϵ_y	strain in y reinforcement
ϵ_1	principal tensile strain
ϵ_2	principal compressive strain
θ	angle of inclination of principal compressive strain measured from global X axis
θ_{sx}	angle between the local x reinforcement and the global X axis
θ_{sy}	angle between the local y reinforcement and the global X axis
λ	factor to account for low density concrete ($\lambda = 1.00$ for normal density, 0.85 for structural semi-low density, and 0.75 for structural low density concretes
ρ_{sx}	reinforcement ratio for the local x reinforcement
ρ_{sy}	reinforcement ratio for the local y reinforcement
ϕ_c	resistance factor for concrete ($\phi_c = 0.60$)
ϕ_s	resistance factor for reinforcement ($\phi_s = 0.85$)

CHAPTER 1

INTRODUCTION

1.1 Introduction

There are many situations in the design of reinforced concrete members where discontinuities, such as abrupt changes in geometry or the presence of concentrated loads or reactions, cause disturbances in the flow of the internal forces in the member. These disturbances in the flow of internal forces around discontinuities result in "disturbed regions" as shown in Fig. 1.1. For example, the concentrated reaction acting on the beam shown in Fig. 1.1a interrupts the uniform field of compressive stresses in the concrete and causes a disturbed region due to the fanning of the compressive stresses into the support. The nib of the dapped end beam shown in Fig. 1.1b causes a disturbance in the flow of the forces resulting in fanning of the compressive stresses in the full depth portion of the beam and concentrated compressive stresses or struts in the nib. The disturbed region in the corbel is characterized by high local compressive stresses at the beam bearing area, with these stresses fanning into the column. The concentrated load acting on the deep beam shown in Fig. 1.1c is transmitted directly to the supports by concentrated uni-directional compressive stresses in the concrete. Since the flow of the forces is transmitted by compressive struts the entire deep beam is considered a disturbed region. The concentrated loads acting on the wall shown in Fig. 1.1d cause a disturbed region due to the fanning of the high compressive stresses

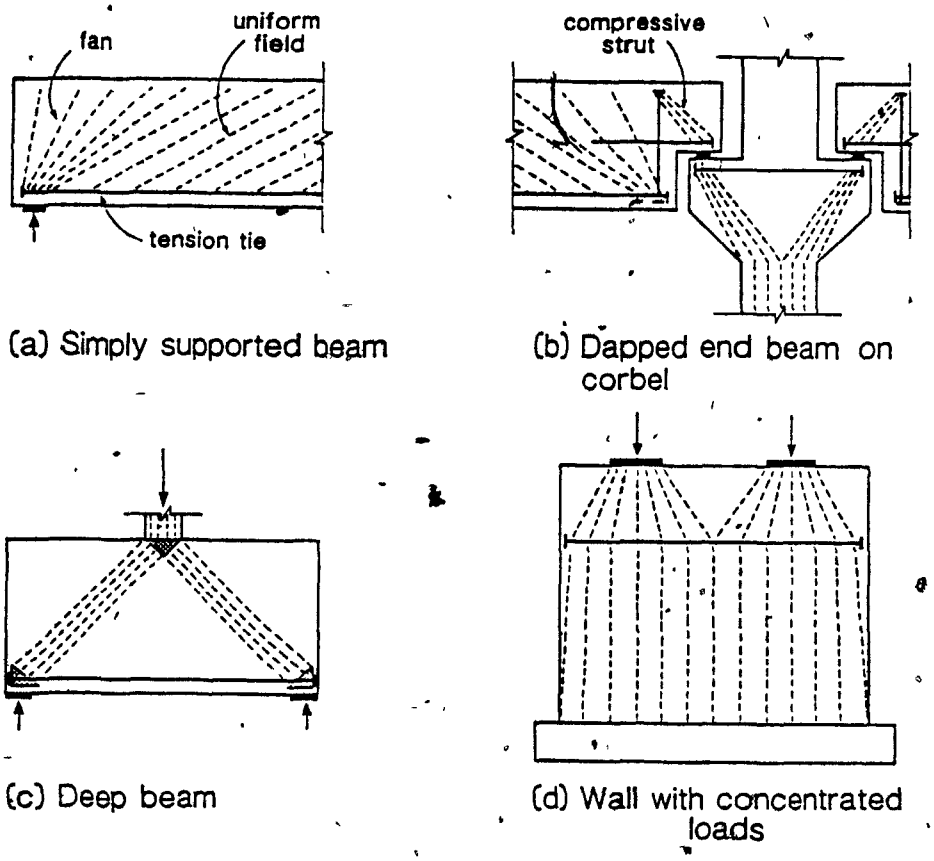

Figure 1.1 Examples of Typical Disturbed Regions.

into the uniform field of compressive stresses. It is not appropriate to design these types of disturbed regions using the usual beam theory which assumes that plane sections remain plane. While elastic finite element analysis may be used to determine the stresses in the concrete prior to cracking, this analysis method may not be appropriate for design since considerable redistribution of stresses occurs after cracking.

The purpose of this research programme is to study the behaviour of disturbed regions (zones near discontinuities) in reinforced concrete members. To meet this goal a two-dimensional non-linear finite element program, FIELDS, capable of predicting the complete response of reinforced concrete members was developed. An additional design and analysis tool referred to as "the strut and tie model" was also investigated. In this model the flow of the forces in a disturbed region is idealized by a truss in which

the zones of concentrated compressive stresses are represented by compressive struts and the principal reinforcement is represented by tension ties. In addition, a number of full scale experiments were carried out on reinforced concrete members which contained disturbed regions. The non-linear finite element analyses are compared with test results and with analyses using simple strut and tie models.

1.2 Previous Research

Truss equilibrium models were developed by Ritter as early as 1899[1] to model the behaviour of reinforced concrete members subjected to shear and moment. These models were further generalized by Mörsch in 1926.[2]

These early truss models led to design procedures[3,4] for shear in Europe and North America which assumed a constant angle of inclination, θ, of the diagonal compressive struts (i.e., $\theta = 45$ degrees) and which also included an empirical concrete contribution to resist a portion of the shear.

More refined truss models were developed by Thürlimann *et al.*[5], Marti[6], and Schlaich and Shäfer[7] in order to predict not only regions containing uniform fields of compressive stresses, but also regions near discontinuities in which these uniform fields are disturbed. The internal flow of forces in these disturbed regions can be idealized by a truss model in which the zones of concentrated compressive stresses are represented by concrete compressive struts and the principal reinforcement is represented by tension ties as shown in Fig. 1.1. The truss design approach suggested by Thürlimann *et al.*[5] and Marti[6] assumes a limiting concrete compressive stress in the struts of $0.6f'_c$. Schlaich and Shäfer[7] have suggested a strut and tie design procedure for these disturbed regions which involves choosing compressive struts oriented to approximate the flow of stresses obtained from an elastic analysis.

Recent developments[8,9,10] leading to a rational model called the compression field theory, have enabled a better understanding of the behaviour of non-prestressed and

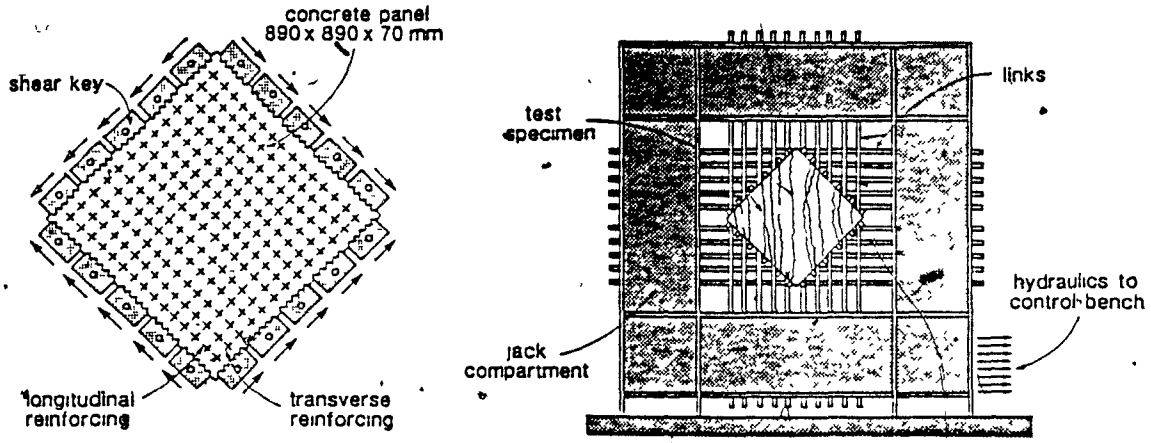

Figure 1.2 Shear Panel Test Set-Up used by Vecchio and Collins.

prestressed concrete members subjected to shear and torsion. Unlike the equilibrium truss models the compression field theory satisfies equilibrium, compatibility of strains and also utilizes the appropriate stress-strain relationships for the reinforcing steel and the cracked concrete.

A detailed study by Vecchio and Collins[11,12] of the shear response of reinforced concrete panels (see Fig. 1.2) has enabled a better understanding of the inelastic response of cracked concrete. The compressive and tensile stress-strain relationships for the cracked concrete were determined by applying shear stresses to the test panels, in stages, up to failure. At each stage, detailed strain measurements enabled the strains in both sets of reinforcement and the principal compressive strain direction, θ, to be determined. Knowing the strains in the reinforcement enabled the stresses in the reinforcement to be determined. From equilibrium the principal tensile stress,* f_{c1}, and the principal compressive stress, f_{c2}, in the concrete were obtained. Repeating these calculations for each load stage resulted in the determination of the tensile and compressive stress-strain relationships for cracked concrete. Vecchio and Collins found that the maximum compressive stress that the concrete can carry was a function of both

*Note: Tensile stresses and strains are taken as positive quantities, while compressive stresses and strains are taken as negative quantities.

the principal compressive strain, ϵ_2, and the principal tensile strain, ϵ_1. The compressive stress-strain relationship for the cracked concrete accounting for the softening and weakening effects due to ϵ_1 is:

$$f_{c2} = f_{c2max}\left[2\left(\frac{\epsilon_2}{\epsilon'_c}\right) - \left(\frac{\epsilon_2}{\epsilon'_c}\right)^2\right] \tag{1-1}$$

where

$$f_{c2max} = \frac{f'_c}{0.8 - 0.34(\epsilon_1/\epsilon'_c)} \qquad \leq f'_c$$

and ϵ'_c = compressive strain in concrete corresponding to the peak stress obtained from a cylinder test.

The principal tensile stress-strain relationship for the concrete can be assumed to be linear up to the cracking stress, f_{cr}, of the concrete, then after cracking the following average principal tensile stress-strain relationship suggested by Vecchio and Collins is used:

$$\begin{aligned} &\text{if} \quad \epsilon_1 \leq \epsilon_{cr} \quad \text{then} \quad f_{c1} = E_c\epsilon_1 \\ &\text{if} \quad \epsilon_1 > \epsilon_{cr} \quad \text{then} \quad f_{c1} = \frac{f_{cr}}{\sqrt{1 + 200\epsilon_1}} \end{aligned} \tag{1-2}$$

where E_c = initial tangent modulus of elasticity of concrete
ϵ_{cr} = concrete strain at cracking.

The stress-strain relationships for cracked concrete are described in more detail in Chapter 2. In addition, the ability of the reinforced concrete to transmit forces across cracks is discussed in Chapter 2.

Vecchio and Collins developed a computer program[11] (SMAL) which can be used to predict the response of a segment of a beam subjected to shear, moment and axial load. In order to analyze a beam using this approach the cross-section is first divided into a series of horizontal strips (see Fig. 1.3) and the position and areas of the steel reinforcement are given along with the material properties. In the analysis, an initial

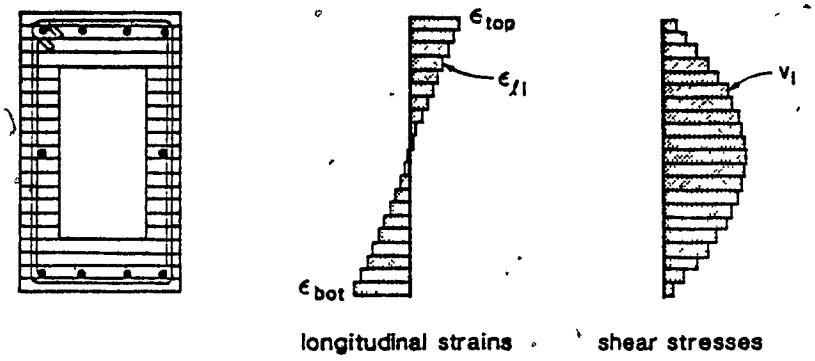

Figure 1.3 Discretization of Concrete Beam for Analysis Using Program SMAL.

shear stress distribution is first estimated and then using a linear longitudinal strain distribution over the member depth, the program SMAL iterates the shear stress distribution until equilibrium and compatibility are achieved. This incremental analysis enables the response of a short segment of the beam to be determined.

The 1984 Canadian Concrete Code[13] introduced a general method for shear and torsion design. This general method[14] uses the compression field theory for regions of members having a uniform field of diagonal compression in the concrete. For regions near discontinuities a method incorporating concrete compressive struts and reinforcing steel tension ties is given. This strut and tie design procedure is described in Chapter 2.

1.3 Objectives

The objectives of this research programme are:

- to develop a non-linear plane stress finite element program, FIELDS, using the stress-strain characteristics of cracked concrete including the effects of strain softening in compression and the effects of tensile stresses in the concrete between the cracks. The micro-computer program must be capable of predicting the complete response of reinforced concrete members.
- to design and test full scale, well-instrumented reinforced concrete members with disturbed regions in order to study the complete responses.
- to predict the responses of the members with disturbed regions tested at McGill University and by other investigators using program FIELDS.
- to compare the response predictions with the experimental results.
- to provide design guidance on the use of simple strut and tie models for disturbed regions.

CHAPTER 2

ANALYSIS AND DESIGN METHODS

2.1 Introduction

During the early phases of this research programme the strut and tie model design procedure for disturbed regions given in the 1984 Canadian Concrete Code[13] was under development. The results from some of the tests performed in this research programme (described in Chapters 3 and 4) provided guidance for sample design examples[14,15] of corbels and beams with dapped ends. A description of the strut and tie model design procedure is given in Section 2.2. Strut and tie models and truss idealizations developed during the course of this research for a number of different disturbed regions are also given in Section 2.2.

Section 2.3 provides a brief description of program FIELDS.

2.2 Strut and Tie Models

It is appropriate to design regions of reinforced concrete members which contain uniform fields of compressive stresses in the concrete by a sectional design approach which assumes that the shear stress is uniformly distributed over the depth of the member and that the uniform field can be represented by a series of parallel compressive struts. However, in the design of disturbed regions (see Fig. 1.1) the flow of the forces in the member is more appropriately modelled by a series of concrete compressive struts

and reinforcement tension ties. These struts and ties are interconnected at nodal regions of multi-directionally compressed concrete. The struts and ties can be represented by truss members where the truss nodes represent the nodal regions.

The geometry of the strut and tie model is determined by following the flow of the forces from the loading points to the support reactions. The intersection of compressive struts with the tension ties or the support reactions delineate the nodal zones. Once the geometry of the truss is known the forces in the struts and ties are determined by statics.

2.2.1 Design Procedure of the Canadian Concrete Code

This section summarizes the design procedure for disturbed regions with reference to the provisions of the Canadian Concrete Code.[13] The design steps are summarized below with reference to the dapped end beam shown in Fig. 2.1.

(1) Sketch the flow of the forces in the member under consideration. Identify regions of uniform fields, fans, and concentrated compressive stresses in the concrete as shown in Fig. 2.1a. Sectional shear design provides an estimate of the angle of principal compressive stresses in the uniform field regions. Represent the fans and concentrated compressive stresses by compressive struts acting along their centrelines (see Fig. 2.1b). Sketch the tension ties required for equilibrium. The tension ties and compressive struts form a truss representation of the flow of the forces.

(2) Choose bearing areas at the loading points and the support reactions such that the nodal zone stress limits are not exceeded under the action of factored loads. The nodal zone stress limits, unless special confinement is present, are:

a) $0.85\phi_c f'_c$ in nodal zones bounded by compressive struts and bearing areas;

b) $0.75\phi_c f'_c$ in nodal zones anchoring only one tension tie; and

c) $0.60\phi_c f'_c$ in nodal zones anchoring tension ties in more than one direction.

where ϕ_c = material resistance factor for concrete.

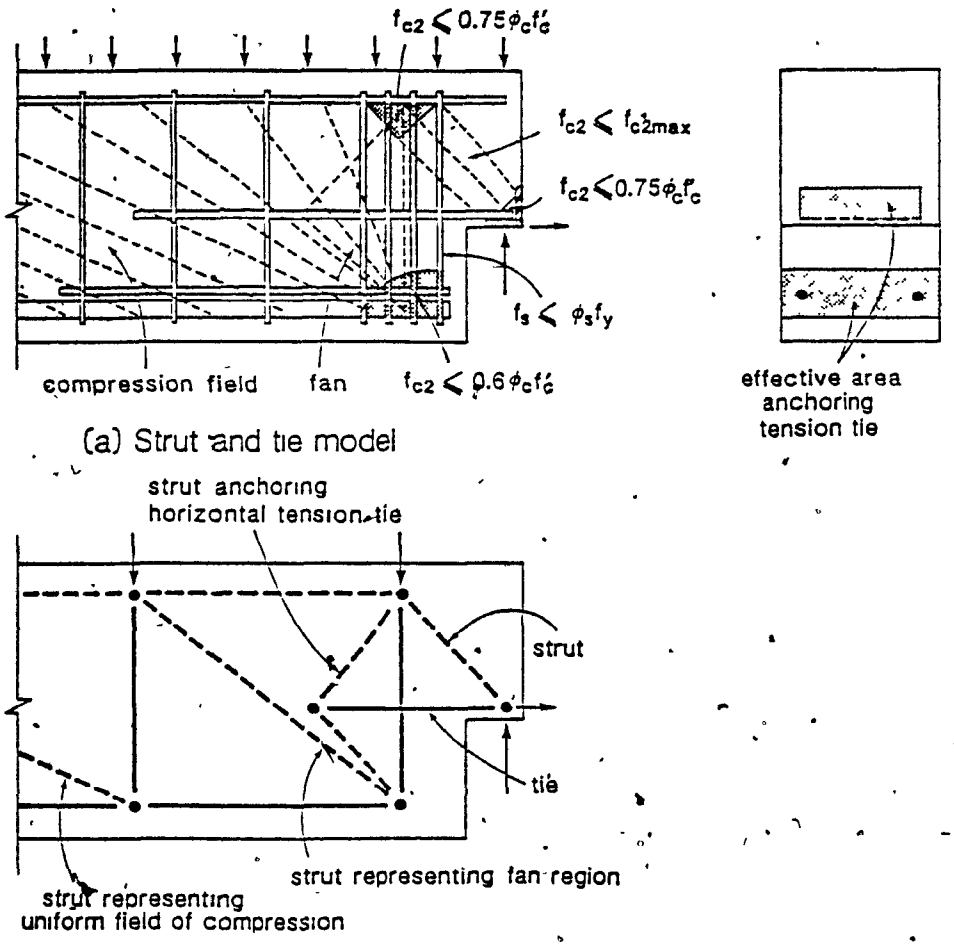

Figure 2.1 Strut and Tie Modelling of a Dapped End Beam.

(3) Determine the geometry of the truss by first locating the nodes of the truss at the points of intersection of the forces in the truss members meeting at the nodal zones.

(4) Solve for the forces in the members of the truss when the truss is subjected to factored loads.

(5) Choose the tension tie reinforcement assuming a factored resistance of $\phi_s A_s f_y$, where ϕ_s = material resistance factor for reinforcement, A_s = area of tension tie reinforcement, and f_y = yield stress of reinforcement.

(6) Distribute the tension tie reinforcement such that the stress limits in the nodal

zones anchoring the tension tie are not exceeded.

(7) Detail the anchorage of the tension tie so that it can develop the required tensile force at the innermost edge of the nodal zone. If the embedment length is not sufficient then hooked or mechanical anchorages must be provided.

(8) Check that the compressive stress, f_{c2}, in the strut is less than the crushing limit, f_{c2max}. The strut compressive stress, f_{c2}, is determined by dividing the force in the strut by the area of the strut. The cross-sectional area of a compressive strut is determined by the dimensions of the nodal zones at the ends of the strut. The maximum allowable stress, f_{c2max}, must be reduced to account for the presence of the principal tensile strain, ϵ_1. This principal tensile strain is determined from strain compatibility in the regions where a tension ties crosses a compressive strut. The principal strain may be determined by conservatively assuming that the strain, ϵ_s, in the tension tie, is f_y/E_s, where E_s is modulus of elasticity of steel, and then finding ϵ_1 as follows:

$$\epsilon_1 = \epsilon_s + \frac{\epsilon_s + 0.002}{\tan^2 \alpha_s} \qquad (2\text{-}1)$$

where α_s = the angle between the tie and the strut.

The crushing strength, f_{c2max}, accounting for the reduction of strength due to the presence of the principal tensile strain, ϵ_1, is found from:

$$f_{c2max} = \frac{\lambda \phi_c f'_c}{0.8 + 170\epsilon_1} \qquad \leq \lambda \phi_c f'_c \qquad (2\text{-}2)$$

where λ is a factor to account for low density concrete ($\lambda = 1.00$ for normal density, 0.85 for structural semi-low density, and 0.75 for structural low density concrete).

2.2.2 Example Strut and Tie Models and Truss Idealizations

2.2.2.1 Brackets and Corbels

The strut and tie models, together with truss idealizations for a variety of brackets and corbels are given in Fig. 2.2. The double-sided corbel resists the loads by compressive struts feeding directly into the column as shown in Fig. 2.2a. As can be seen, a tension tie is required from equilibrium to resist the out-of-balance forces at the loading points. Figure 2.2b illustrates the flow of the forces in a single-sided corbel. It is assumed that the anchorage of the main horizontal tension tie takes place at the 90° bend in this tie reinforcement. Therefore, two compressive struts are required to anchor the tension tie. The capacity of a corbel depends greatly on the anchorage details of the tension tie reinforcement. Recommended details for anchorage of the tension ties are given in References 4 and 16. For example, a structural steel angle welded to the main tension tie reinforcement to enable the development of the yield strength of the tie will also serve as a bearing surface and serve to armour the outer corner of the bracket or corbel.

In the ledger beam shown in Fig. 2.2c the hanger steel transmits the vertical component from the inclined compressive struts towards the top of the beam. As can be seen this hanger steel can be spread over a short length of the ledger beam and should be provided in addition to the shear and torsion reinforcement required in the ledger beam. The beam with the single ledge support shown in Fig. 2.2d requires two compression struts in the region of the ledge to anchor the horizontal tension tie. It is interesting to note that the force in the vertical tension hanger is larger than the vertical force acting on the ledge.

2.2.2.2 Dapped End Beams and Beams with Holes in the Web

Figure 2.3 illustrates the application of strut and tie models to members with dapped ends and members with holes in the web. The change in flow of forces from

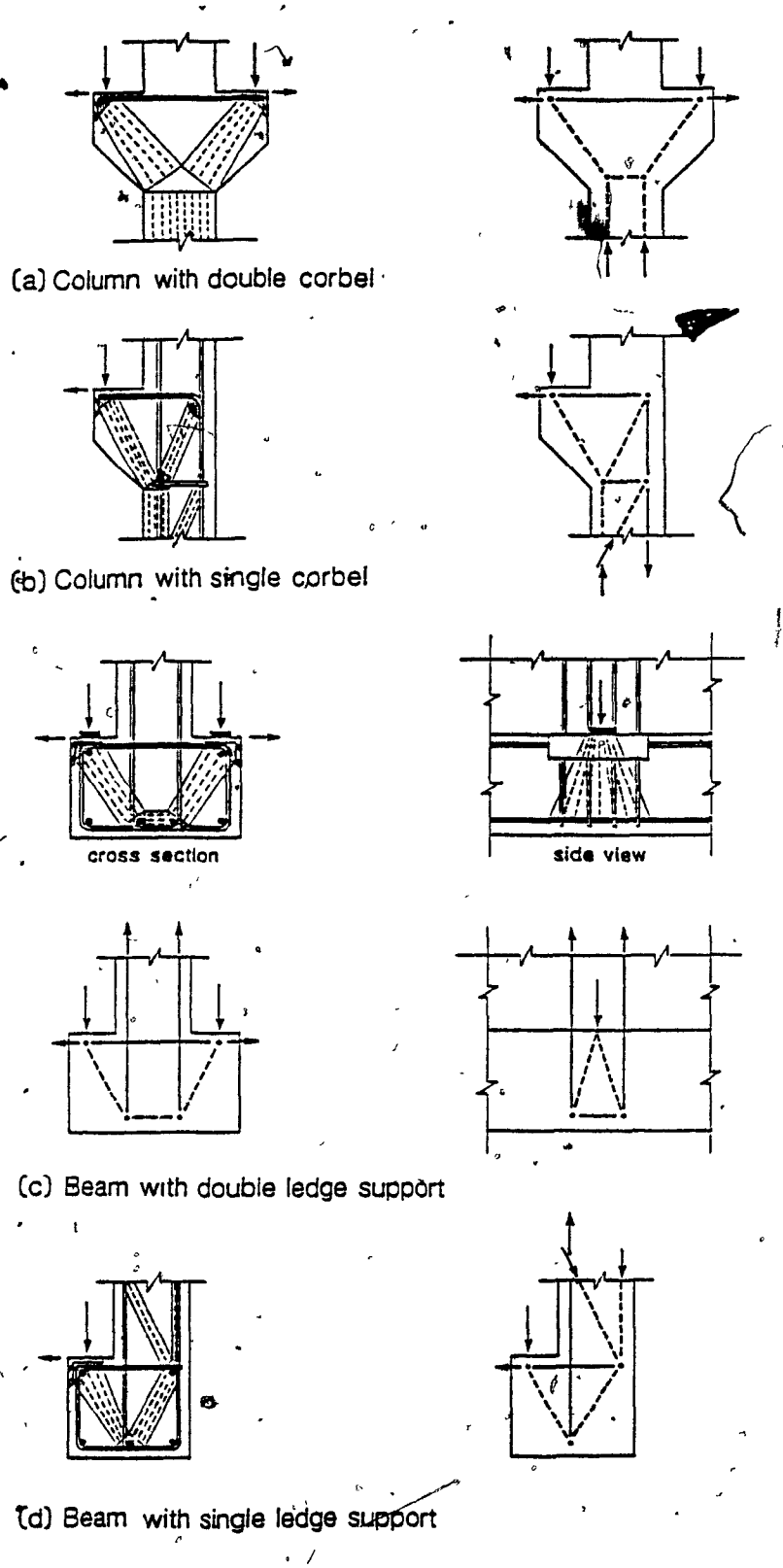

Figure 2.2 Strut and Tie Models and Truss Idealizations for Brackets and Corbels.

a uniform compression field to a fan which delivers compression to the bottom of the main vertical tension tie in a dapped end beam is illustrated in Fig. 2.3a. The role of this vertical tension tie is to lift the force to the top of the beam, thus permitting the forces to flow into the support by means of a direct compressive strut. Horizontal tension ties are required to balance the outward thrusts of compression at the support reaction and at the bottom of the main vertical tension tie. In order to anchor the horizontal tension tie at the level of the support reaction the tie is welded to an angle at one end and the other end must continue well into the region of fanning compressive stresses to achieve proper development. The anchorage of this tie is simulated by the two struts radiating from an anchor point assumed to be located $0.5\ell_d$ beyond the centre of the vertical tension tie, where ℓ_d is the tension development length. It is noted that this reinforcement must continue well beyond this assumed anchor point into the full depth portion of the beam.

Figure 2.3b shows the strut and tie model for an inclined dapped end beam. The bent-up tension tie creates large local stresses at the bar bend and must be anchored above the support reaction (e.g., a welded plate) in order to create a nodal zone.

The manner in which an opening in the web affects the flow of the forces in a uniformly loaded T-beam is illustrated in Fig. 2.3c. The uniform field of diagonal compression is interrupted by the opening causing higher shear stresses in the section beneath the opening, requiring an increase in the amount of stirrup reinforcement in this region. In order to make use of the full depth of the section beyond the opening, a vertical tension tie is provided to lift the shear force to the top of the beam. This vertical tension tie enables the force to flow into the support reaction area by means of a direct compressive strut.

2.2.2.3 Deep Beams

Figure 2.4 illustrates the strut and tie models and truss idealizations for some deep beams. The simply supported deep beam is easily modelled with a statically

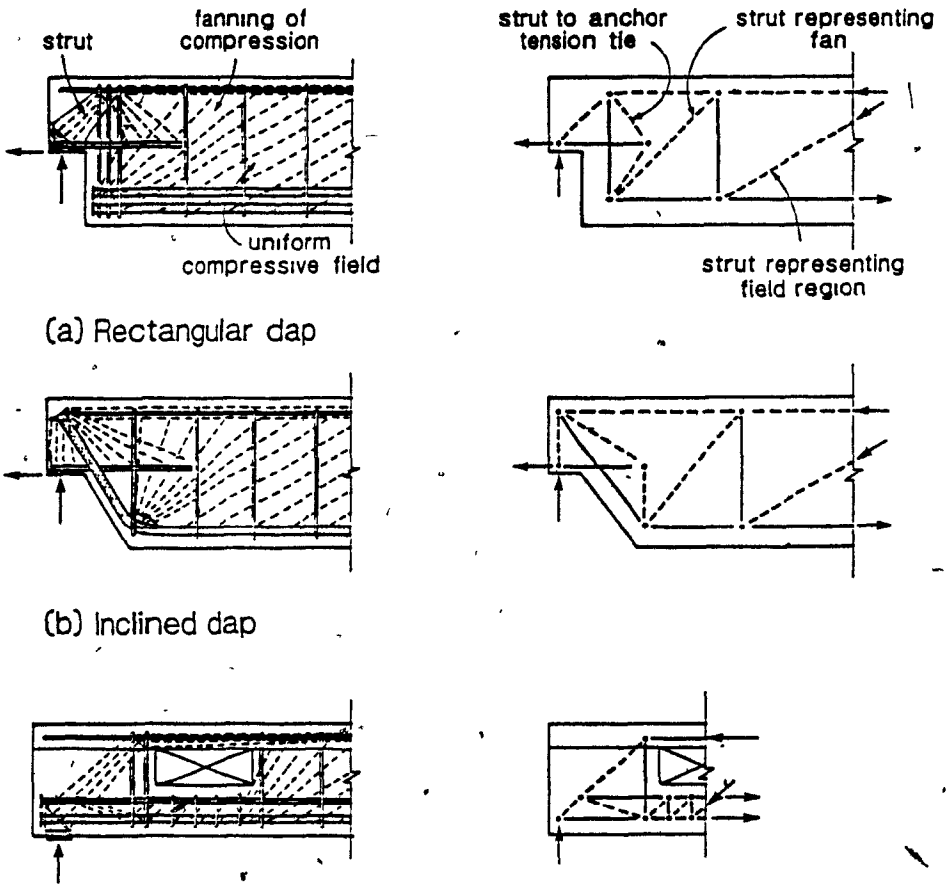

Figure 2.3 Strut and Tie Models and Truss Idealizations for Dapped End Beams and Beams with Holes in the Web.

determinate truss as shown in Fig. 2.4a. The design must ensure that premature failures due to inadequate amount of tension tie reinforcement, insufficient anchorage of tension ties, crushing of bearing areas, and crushing of compressive struts do not occur. In addition to the main tension tie reinforcement, the Canadian Concrete Code requires a minimum reinforcement ratio in the transverse and longitudinal directions of 0.002 in order to control cracking and to increase the ductility of the member. This small amount of uniformly distributed reinforcement is usually neglected in designing deep beams using a simple strut and tie model. Examples of the design of simply supported deep beams are given in References 14 and 15.

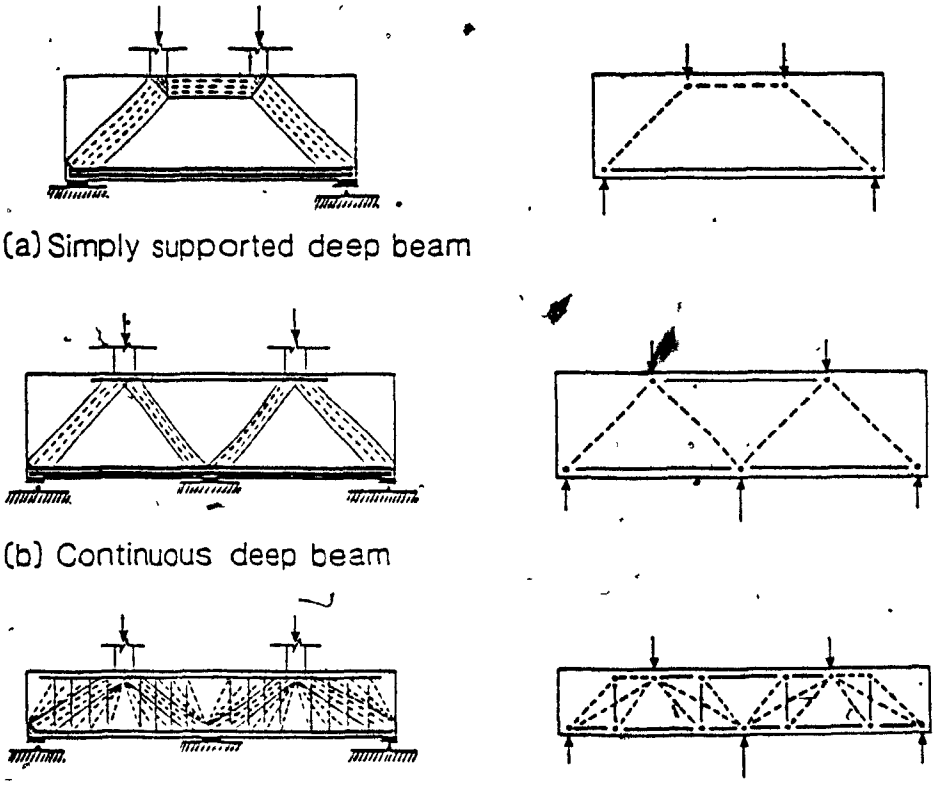

Figure 2.4 Strut and Tie Models and Truss Idealizations for Deep Beams.

Strut and tie models and the resulting statically indeterminate truss idealizations for continuous deep beams are shown in Figs. 2.4b and c. In order to solve for the truss member forces, it is necessary to account for the relative stiffness of the members. If a significant amount of transverse reinforcement is provided in a deep beam then the load will be carried by both compressive struts and fans. The truss idealization for such a case is given in Fig. 2.4c where it has been assumed that the transverse reinforcement between the loading points and the reactions is modelled as a single tension tie. Beams containing transverse reinforcement that are in the transition region between deep beam action and shallow beam action can also be modelled in this manner. As the beam becomes more shallow a uniform compression field could develop between the fanning regions near the supports and loading points.

The design of these more complex transfer girders can be carried out by assuming a simplified truss idealization in which the relative stiffness of the members is assumed. Guidance on the use of more sophisticated truss models is given by Rogowsky and MacGregor.[17]

2.3 Program FIELDS

2.3.1 General Description of Program

A non-linear finite element program was developed for predicting the response of reinforced concrete members. This program, which uses two-dimensional plane stress elements, utilizes the compression field theory in the evaluation of the element tangent stiffnesses. The reinforcement and the cracking are assumed to be smeared uniformly within the element.

In analyzing the complete response of a member, the program starts with the self weight of the member and increments the applied loading in steps chosen by the user. For a given load step the program uses an iterative solution technique (Newton-Raphson) where the out-of-balance loads and the tangent stiffness from the last displaced configuration are used to compute incremental displacements. Iteration continues until convergence requirements are met, that is, until the norms of out-of-balance loads and incremental displacements are within tolerance limits.

This program includes the following features:

- choice of truss, triangular, and quadrilateral elements,
- effects of compressive strain softening and tension stiffening of concrete,
- personal computer based (IBM PC/XT/AT series),
- results saved to files for graphical post-processing and display,
- ability to restart an analysis,
- dynamic allocation of memory,

- selective output of results, and
- screen log showing the progress of the analysis.

Most of the program is written in Microsoft FORTRAN 77, with some subroutines written in 8086 assembly language for speed (e.g., matrix multiplication, vector addition, norms of vectors, etc.). Program FIELDS contains about 10 000 lines of code.

The analysis is limited to two-dimensional problems in which the load is assumed to increase monotonically. Although effects such as spalling of the concrete cover and local bond stresses are not treated directly by the program, ways of including these effects have been investigated.

2.3.2 Program Logic

The main steps in the program are listed below:

(1) Read and verify the input data. The input data includes: a) nodal coordinates, b) nodal restraints, c) element properties (including concrete and reinforcing steel parameters), d) element connectivity, and e) unit loading cases for variable loads and constant load cases (self-weight).

(2) Read unit load case multiplier, solution type (e.g., choice between iteration with constant stiffness or with updated stiffnesses), maximum number of equilibrium iterations, relaxation factor (a factor used to increase or decrease the incremental displacements), convergence tolerances on out-of-balance loads and incremental displacements.

(3) Determine the total applied load for this load increment.

(4) Based on the displaced configuration from the last iteration, evaluate the element tangent stiffnesses and assemble the global stiffness matrix (only if updated stiffness solution technique is used).

(5) Based on the displaced configuration evaluate the internal forces in the elements and assemble the global internal force vector.

(6) Calculate the out-of-balance force vector which is the difference between the total applied load vector and the global internal force vector.

(7) Solve for incremental displacements based on the updated tangent stiffness matrix and the out-of-balance loads.

(8) Update the total displacements.

(9) Check for convergence by evaluating the norm of the incremental displacement over the total displacements and the norm of the out-of-balance loads over the total applied load.

(10) If the convergence tolerances are not both satisfied and if the maximum number of equilibrium iterations has not been exceeded then go to Step 4.

(11) Output the current forces, displacements, strains and stresses and save all results on files for graphical post-processing.

(12) If more unit loading case multipliers exist, go to Step 2.

A Gaussian matrix solver with the stiffness matrix stored in "skyline format" has been used. An in-core matrix solver is used in order to speed up the solution time.

2.3.3 Element Formulations

An isoparametric quadrilateral element, CFTQ (with up to 9 nodes), and an isoparametric triangular element, CFTT (with up to 6 nodes), are used to model the reinforced concrete behaviour. Within each element the reinforcement and any cracking that occurs are assumed to be smeared uniformly. Two different sets of reinforcement may be specified for each element. The orientation of the sets of reinforcement within the element are specified by angles, θ_{sx} and θ_{sy}, measured from the global X axis. The reinforcement ratio in the x direction, ρ_{sx}, is taken as the total area of steel in the x direction divided by the gross concrete area in the x direction. The reinforcement ratio in the y direction, ρ_{sy}, is similarly defined.

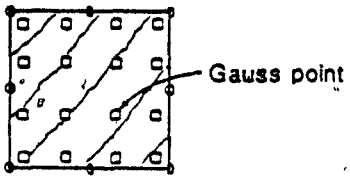

(a) Element with 4 x 4 quadrature

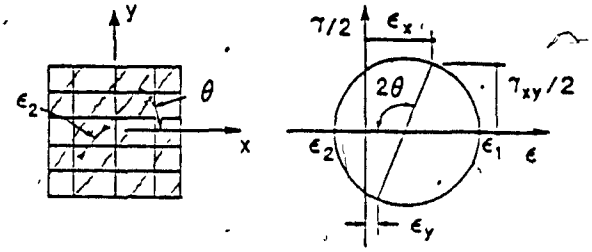

(b) State of strain at a single Gauss point

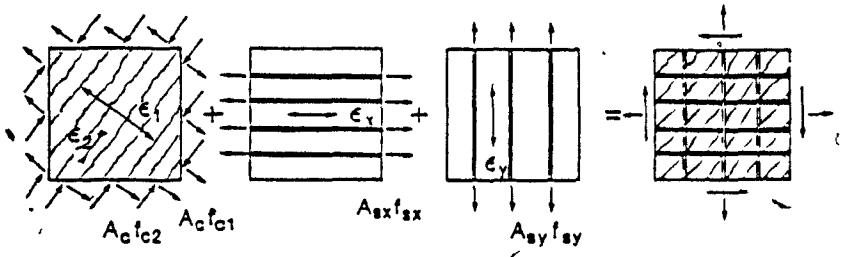

(c) Determining stresses at a Gauss point corresponding to strain state

Figure 2.5 Evaluating Stresses at a Gauss Point in Element CFTQ.

In order to account for the significant non-linearities within an element, which could result in wide variations of stiffness, a number of integration or Gauss points are used to determine the tangent stiffness matrix. Figure 2.5 illustrates the manner in which the stresses are evaluated at each Gauss point. The principal tensile strain, ϵ_1, the principal compressive strain, ϵ_2, the strain in the x direction, ϵ_x, the strain in the y direction, ϵ_y, and the angle of the principal compressive strain, θ, are interrelated by the requirements of strain compatibility (see Fig. 2.5b). It is assumed that the principal compressive stress direction coincides with the principal compressive strain direction, θ.

For a given state of strain in an element it is straight forward to determine the

steel stresses, f_{sx} and f_{sy}, corresponding to the strains, ϵ_x and ϵ_y, from the stress-strain relationships of the reinforcement (see Fig. 2.5c). A bi-linear stress-strain relationship is assumed for the reinforcement with the ability to model strain hardening. It is not as easy to determine the principal stresses, f_{c1} and f_{c2}, in the cracked concrete. For a given state of strain the principal compressive stress, f_{c2}, in the concrete, can be determined as shown in Fig. 2.6a. The principal compressive stress, f_{c2}, is not only a function of the principal compressive strain, ϵ_2, but also depends on the principal tensile strain, ϵ_1, if cracks are present. As ϵ_1 increases f_{c2} decreases, an effect which has been termed as strain softening. From the work carried out by Vecchio and Collins[11,12] the compressive stress-strain relationship of the cracked concrete can be written as:

$$f_{c2} = \beta f'_c \left[2\left(\frac{\epsilon_2}{\epsilon'_c}\right) - \left(\frac{\epsilon_2}{\epsilon'_c}\right)^2 \right] \tag{2-3}$$

where

$$\beta = \frac{1}{0.8 - 0.34(\epsilon_1/\epsilon'_c)} \qquad \leq 1.00$$

and ϵ'_c = compressive strain in concrete at peak stress.

After cracking, the principal tensile stress in the concrete varies from zero at a crack location to a maximum value between cracks. Figure 2.6b illustrates the average principal tensile stress-strain relationship for the concrete as suggested by Vecchio and Collins.[11,12] The average principal tensile stress is given by:

$$\begin{aligned} &\text{if} \quad \epsilon_1 \leq \epsilon_{cr} \quad \text{then} \quad f_{c1} = E_c \epsilon_1 \\ &\text{if} \quad \epsilon_1 > \epsilon_{cr} \quad \text{then} \quad f_{c1} = \frac{f_{cr}}{\sqrt{1 + 200\epsilon_1}} \end{aligned} \tag{2-4}$$

where E_c = initial tangent modulus of elasticity of concrete
f_{cr} = concrete cracking stress
ϵ_{cr} = strain in concrete at cracking.

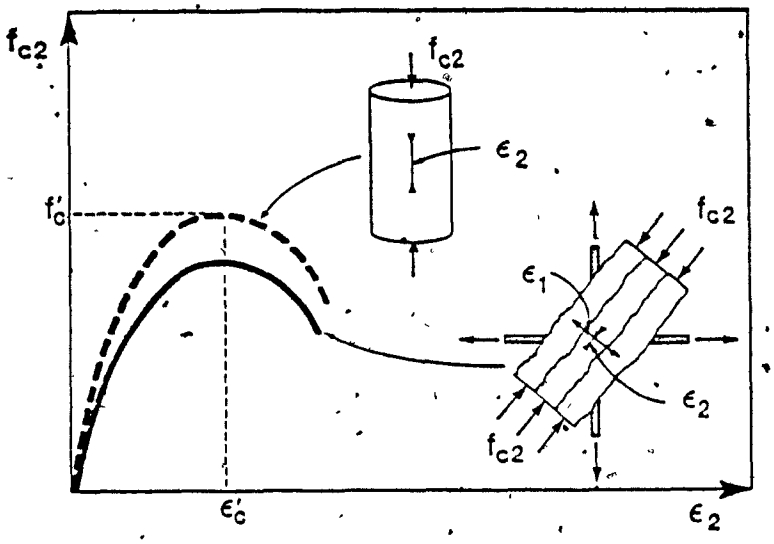

(a) Determining average concrete compressive stress, f_{c2}, from strains ϵ_1 and ϵ_2

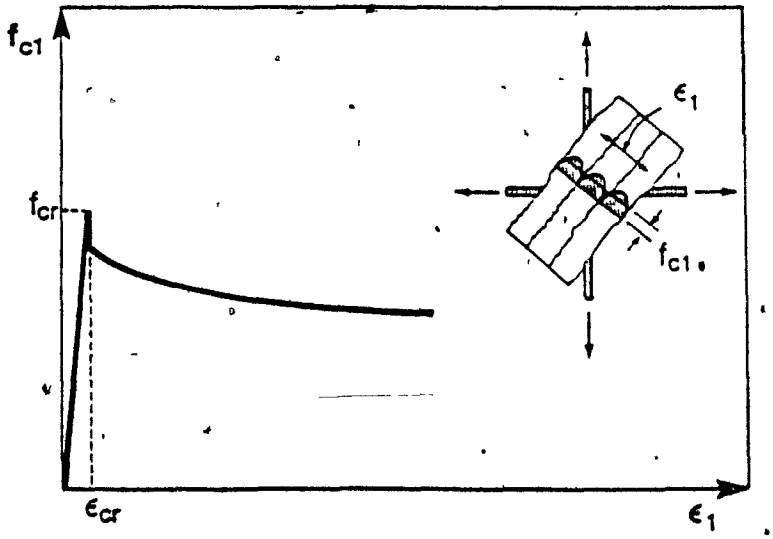

(b) Determining average concrete tensile stress, f_{c1}, from strain ϵ_1

Figure 2.6 Average Concrete Stress-Strain Relationships.

As shown in Fig. 2.7 this average principal tensile stress, f_{c1}, may be limited by yielding of the steel reinforcement across the cracks or by sliding along the crack interface. Between the cracks the concrete and the steel are assumed to have average values of stress, (see Fig. 2.7c) while at a crack the tensile stress in the concrete is zero, the stresses in the reinforcement, $f_{sx,cr}$ and $f_{sy,cr}$, are at a maximum and a shear stress, v_{ci}, may exist at the crack interface (see Fig. 2.7d). Based on the interface shear transfer tests carried out by Walraven[18] an approximate expression to limit the shear stress along the crack was developed.[12] This expression was further simplified as follows:

$$v_{cimax} = \frac{0.18\sqrt{-f'_c}}{0.31 + 24w/(a+16)} \qquad (2\text{-}5)$$

where v_{cimax} = maximum shear stress permitted on a crack interface
w = average crack width assumed to be equal to the average crack spacing, $s_{m\theta}$, times ϵ_1
a = maximum aggregate size
and f'_c is in MPa units and w and a are in mm (for Imperial units of psi and inches replace the 0.18 by 2.16 and the 16 by 0.63)

The average inclined crack spacing $s_{m\theta}$ is taken as:

$$s_{m\theta} = \left[\left|\frac{\sin(\theta_{sx}-\theta)}{s_{mx}}\right| + \left|\frac{\sin(\theta_{sy}-\theta)}{s_{my}}\right|\right]^{-1} \qquad (2\text{-}6)$$

where s_{mx} = the crack spacing expected for axial tension in the x direction
s_{my} = the crack spacing expected for axial tension in the y direction.

Since the states of stress in Figs. 2.7c and d are statically equivalent it is possible to investigate whether yielding of the reinforcement across the crack (i.e., $f_{sx,cr}$ or $f_{sy,cr}$ equals f_y) or sliding of the crack interface (i.e., v_{ci} equals v_{cimax}) will result in a value of f_{c1} lower than that given by Eq. (2-4) after cracking. The manner in which the average principal tensile stress, f_{c1}, after cracking can be calculated is described below for different situations:

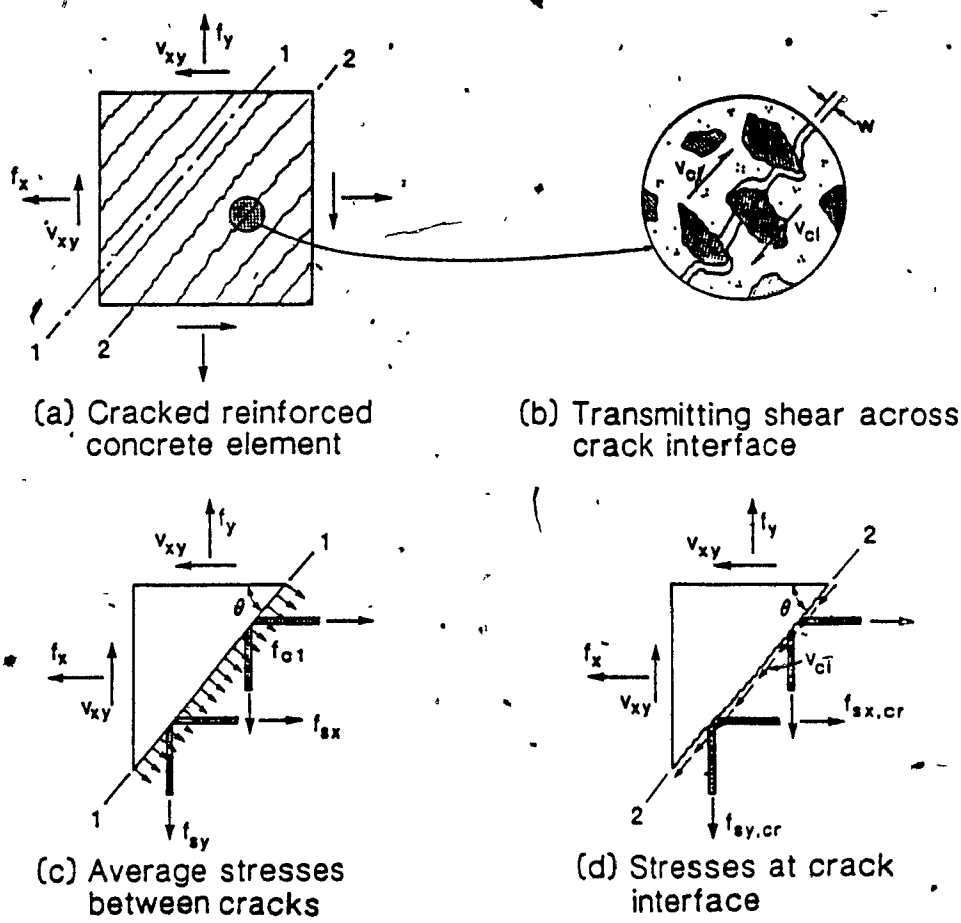

Figure 2.7 Investigating Stresses at Crack Interface.

(a) Plain concrete element – since no reinforcement is present it is evident from equilibrium that f_{c1} must be zero,

(b) Reinforced concrete element with reinforcement in one arbitrary direction – the equations given below are for reinforcement assumed to be at an angle of θ_{sx} from the global X direction. From Figs. 2.7c and d, assuming $A_{sy} = 0$, the average principal tensile stress, f_{c1}, is limited by the maximum shear stress that can develop on the crack interface and hence from equilibrium:

$$f_{c1} = |v_{ci\,max} \tan(\theta_{sx} - \theta)| \qquad (2\text{-}7)$$

but it is also limited by the yielding of the reinforcement across the crack, that is:

$$f_{c1} = \rho_{sx} \Delta f_{sx} \sin^2(\theta_{sx} - \theta) \tag{2-8}$$

where $\Delta f_{sx} = f_{sx,cr} - f_{sx}$ = the stress increase in the x reinforcement at the crack.

(c) Reinforced concrete element with reinforcement in two arbitrary directions – the equations derived below are for x and y reinforcement assumed to be at angles of θ_{sx} and θ_{sy} from the global X direction. Equating the stress conditions in Figs. 2.7c and d gives the following relationships:

$$f_{c1} = \rho_{sx} \Delta f_{sx} \sin^2(\theta_{sx} - \theta) + \rho_{sy} \Delta f_{sy} \sin^2(\theta_{sx} - \theta) \tag{2-9}$$

and

$$\begin{aligned} v_{cimax} = &-\rho_{sx} \Delta f_{sx} \sin(\theta_{sx} - \theta) \cos(\theta_{sx} - \theta) \\ &- \rho_{sy} \Delta f_{sy} \sin(\theta_{sx} - \theta) \cos(\theta_{sy} - \theta) \end{aligned} \tag{2-10}$$

where $\Delta f_{sx} = f_{sx,cr} - f_{sx}$ = the stress increase in the x reinforcement at the crack

$\Delta f_{sy} = f_{sy,cr} - f_{sy}$ = the stress increase in the y reinforcement at the crack.

If both sets of reinforcement in an element have average stresses, f_{sx} and f_{sy}, equal to the yield strength, f_y of the reinforcement then both Δf_{sx} and Δf_{sy} will be zero if the reinforcing steel has no strain hardening and hence, f_{c1} will be zero.

If neither set of reinforcement is yielding at a crack then an additional compatibility relationship is required in order to determine the strains and stresses in each set of reinforcement. In order to examine the compatibility of strains in the reinforcement across the crack it was assumed that the crack opens in the direction of ϵ_1 and does

not slip. The resulting relationships are summarized below:

$$\Delta f_{sx} = \frac{f_{c1} E_{sx} \sin^2(\theta_{sx} - \theta)}{\rho_{sx} E_{sx} \sin^4(\theta_{sx} - \theta) + \rho_{sy} E_{sy} \sin^4(\theta_{sy} - \theta)} \tag{2-11}$$

and

$$\Delta f_{sy} = \frac{f_{c1} E_{sy} \sin^2(\theta_{sy} - \theta)}{\rho_{sx} E_{sx} \sin^4(\theta_{sx} - \theta) + \rho_{sy} E_{sy} \sin^4(\theta_{sy} - \theta)} \tag{2-12}$$

where E_{sx} = modulus of elasticity of reinforcement in x direction
E_{sy} = modulus of elasticity of reinforcement in y direction

It can be seen from Eqs.(2-11) and (2-12) that Δf_{sx} and Δf_{sy} are related by the following equation:

$$\Delta f_{sy} = \Delta f_{sx} \frac{E_{sy} \sin^2(\theta_{sy} - \theta)}{E_{sx} \sin^2(\theta_{sx} - \theta)} \tag{2-13}$$

If one of the sets of reinforcement is yielding at the crack then Δf_{sx} or Δf_{sy} will be zero and the system can be treated as case (b) above.

It is noted that in the above relationships f_{c1} can never exceed the value obtained from the average tensile stress–average tensile strain relationship given in Eq. (2-4). In order to solve for the stresses and the strains in the cracked concrete and steel a value of f_{c1} is first assumed from Eq. (2-4) and then the conditions in the sets of reinforcement at the crack and the ability of the crack to transmit the necessary shear are investigated. For small values of principal tensile strain where significant reinforcement is present then f_{c1} will be governed by Eq. (2-4). For large values of principal tensile strain, f_{c1} will be lower than the values given by Eq. (2-4) and hence will be governed by the condition at the crack.

It is important to recognize that the above constitutive relationships for the cracked concrete are not only highly non-linear but also interdependent. Thus, in order to determine the incremental (tangent) stress-strain relationships for a given strained state, incremental strains were applied, one at a time, to the existing strains in order

to find the corresponding changes in stress. From the incremental strains and the resulting changes in stress the incremental stress-strain constitutive matrix, $\mathbf{D}$, at the current load stage is determined and hence the incremental tangent stiffness, $\mathbf{k_T}$, of each element can be found from:

$$\mathbf{k_T} = \int_A \mathbf{B}^T \mathbf{D} \mathbf{B} t dA \qquad (2\text{-}14)$$

where $\mathbf{B}$ = the strain-displacement matrix
t = element thickness
A = element surface area.

Numerical integration is used to evaluate the above expression. In order to avoid numerical instabilities in the solution process it is assumed that the concrete has a small positive stiffness (E_c / 10000) beyond strains of ϵ'_c for determining the incremental element stiffness. It is noted however that Eq. (2-3) is used to determine the concrete stress.

In addition to the CFTQ and CFTT elements, a non-linear truss element, TRUS, for modelling external steel reinforcement and support conditions is also provided.

CHAPTER 3

EXPERIMENTAL PROGRAMME

3.1 Introduction

A series of experiments of reinforced concrete members with disturbed regions was carried out in order to investigate the complete response of these members to provide comparisons with predicted responses. Although many tests have been carried out on a number of different types of members with either load or geometric discontinuities, they typically lack detailed strain measurements on both the concrete and the reinforcement.

The test specimens were instrumented with pairs of targets (DEMEC points) glued to the surface of the concrete. A mechanical gauge was used to determine the change in length between target points, thus enabling the strain to be determined. Sets of readings in the horizontal, vertical, and diagonal directions created a series of strain rosettes. The horizontal and vertical readings had a gauge length of 100 mm while the diagonal readings were taken over a gauge length of 141 mm. In addition to the strain readings on the concrete surface, targets were epoxied directly to the reinforcing bars before casting. Small access holes in the concrete permitted strain readings directly on the steel reinforcing bars.

All the specimens were designed using the strut and tie approach of the Canadian Concrete Code assuming material resistance factors $\phi_c = \phi_s = 1.0$ and assuming a concrete compressive strength, $f'_c = 35$ MPa and a steel yield strength, $f_y = 400$ MPa.

During the design stage the strut and tie model design approach of the Canadian Concrete Code was evolving and hence, during the course of this research programme the models used in design have been modified as more has been learned about appropriate modelling techniques. Chapter 5 presents the strut and tie models and truss idealizations used to analyze all of the specimens tested. These analyses are based on measured material properties and actual specimen dimensions.

3.2 Material Properties

3.2.1 Concrete

The concrete used in all specimens was obtained from a local concrete ready mix company and had the following specifications: 30 MPa design strength, Type 30 (High early strength) cement, 20 mm maximum aggregate size, 100 mm slump, and 4–6% entrained air. The concrete was obtained in two batches, batch 1 was used to cast dapped end specimens D-1 and D-2, and web hole specimens H-1 and H-2, while dapped end specimens D-3 and D-4 and the corbel specimen C-1 were cast from batch 2. The compressive strengths as determined from a minimum of three cylinder tests on the date of each test are shown in Table 3.1.

Table 3.1 Summary of Concrete Strengths.

Test Specimen	f'_c (MPa)	Age (days)	Batch
C-1	40.4	96	2
D-1 and D-2	29.8	78	1
D-3 and D-4	36.3	18	2
H-1 and H-2	26.3	7	1

3.2.2 Reinforcing Steel

The steel reinforcement used in all specimens consisted of deformed bars with a specified yield strength of 400 MPa. The actual properties of the reinforcement as

determined from at least three tension tests are shown in Table 3.2. The #3 (9.5 mm diameter) and No. 10 stirrups and vertical tension ties in web hole specimens H-1 and H-2 were heat treated to reduce the yield strength and improve the ductility. The heat treatment consisted of heating the formed stirrups and ties at 800° C for 75 minutes, followed by air cooling. Typical stress-strain curves for the reinforcement are shown in Fig. 3.1. The modulus of elasticity for the steel for all design and analysis has been taken as 200 000 MPa.

Table 3.2 Reinforcement Properties.

Test Specimen	Size	Area (mm^2)	f_y (MPa)	f_u (MPa)
C-1	#3	71	489*	626
	No. 10	100	436	643
	No. 15	200	444	702
D-1 and D-2	No. 10	100	445	676
	No. 15	200	445	693
	No. 30	700	430	688
D-3 and D-4	No. 10	100	436	643
	No. 15	200	444	702
	No. 20	300	478	755
	No. 25	500	445	677
	No. 30	700	443	743
H-1 and H-2	#3**	71	388	561
	No. 10**	100	365	583
	No. 10	100	445	676
	No. 30	700	430	688

* 0.2% offset stress, rounded stress-strain curve

** annealed reinforcement, 800° C for 75 mins., air cool

3.3 Corbel Specimen C-1

The details of corbel specimen C-1 are shown in Figs. 3.2 and 3.3. This specimen contains both a geometric and a load discontinuity. A horizontal tensile load equal to 20 percent of the vertical was applied to the corbel during the test. The corbel was originally designed for a vertical load of 350 kN and a horizontal load of 70 kN using

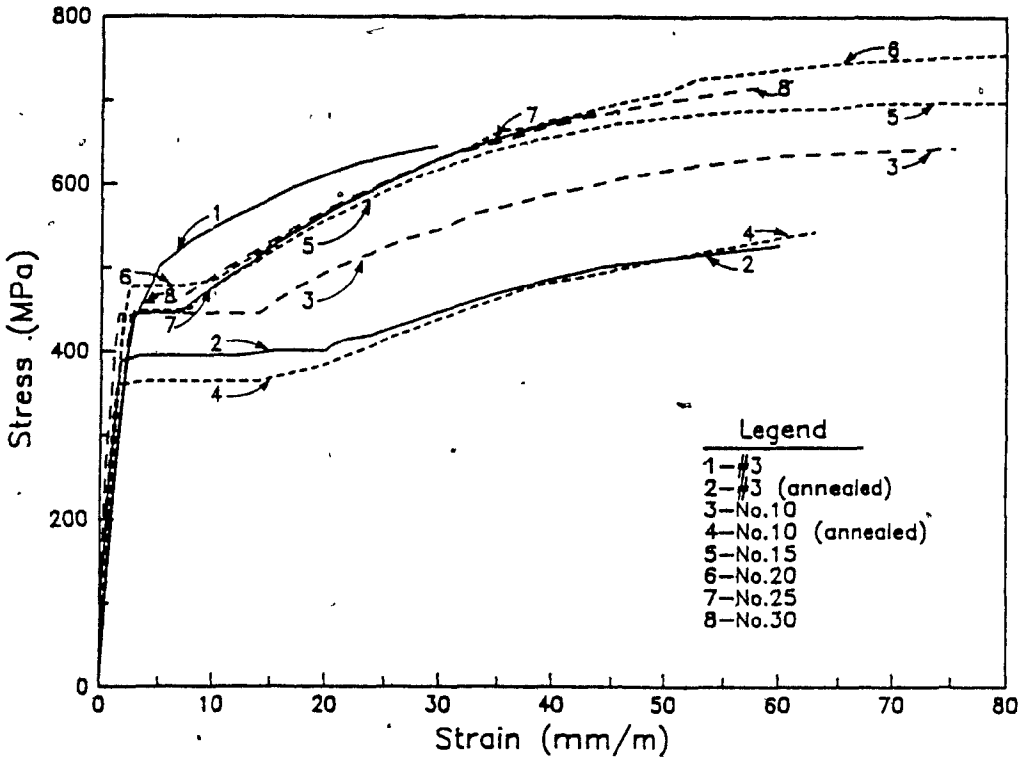

Figure 3.1 Typical Reinforcement Stress-Strain Relationships.

the strut and tie model shown in Fig. 2.2. A strut and tie model analysis of the corbel using measured material properties is described in Chapter 5.

The 350 mm wide corbels frame into a 250 x 350 mm column. The depth of the corbel at the column face is 350 mm and the depth of the corbel is 200 mm at its outer face. The main tension tie reinforcement consisted of four No. 15 reinforcing bars welded to a steel plate which was embedded in the top of the corbel (see Fig. 3.2). The steel plate was 50 mm wide, 25 mm thick and 300 mm long. The welding of the reinforcement to the plate provides positive anchorage of the main tension tie reinforcement. As required by the Canadian Concrete Code[13] additional horizontal reinforcement (two No. 10 closed stirrups) was provided over the depth of the corbel to control cracking. Two No. 10 trim bars were used to support these No. 10 closed horizontal stirrups. The column reinforcement consisted of six No. 15 bars together with #3 ties at 225 mm spacing. Table 3.2 summarizes the material properties for the

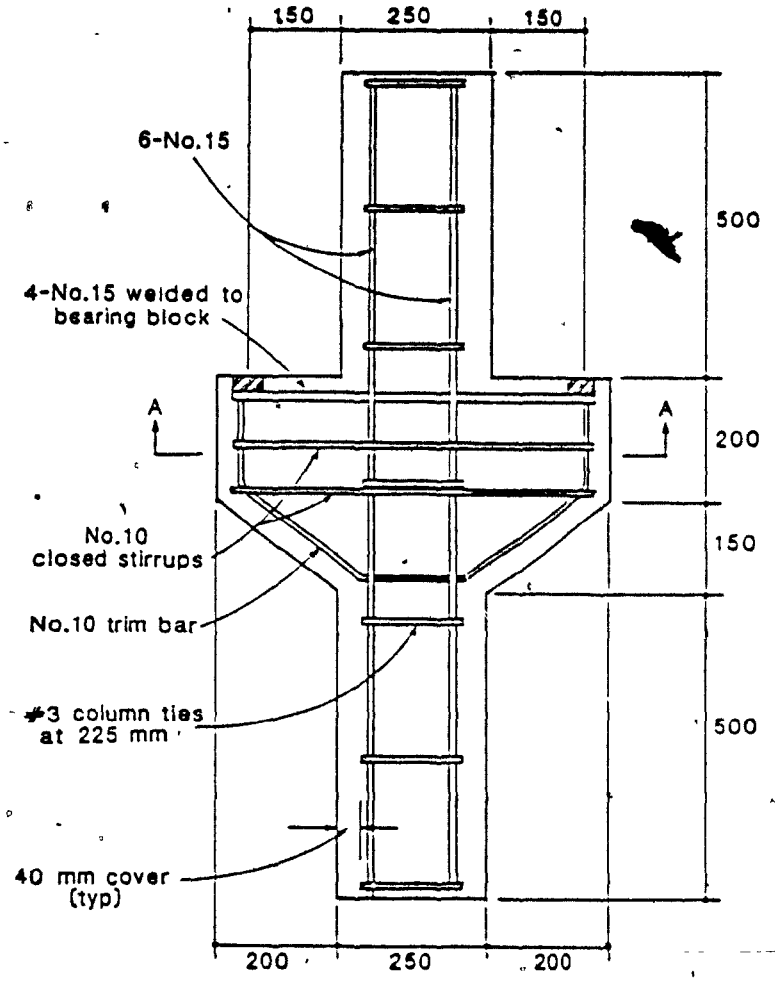

elevation view

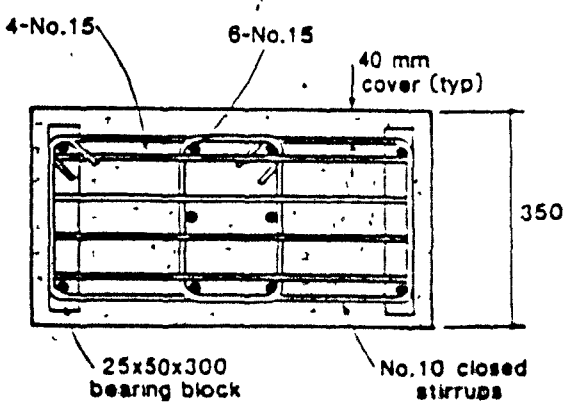

Section A-A

Figure 3.2 Dimensions and Reinforcement Details of Corbel Specimen C-1.

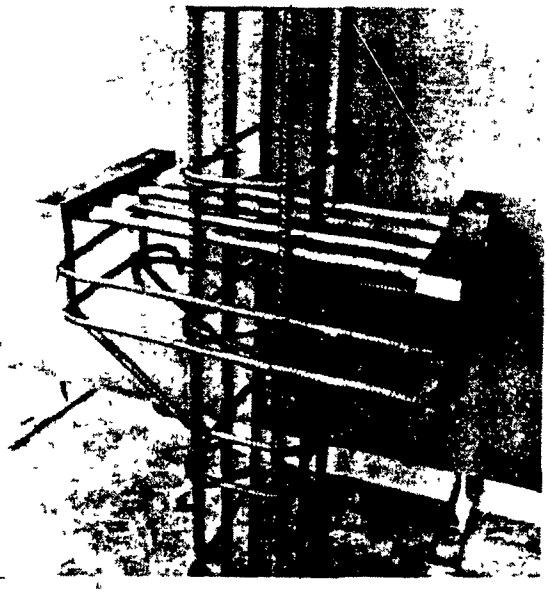

Figure 3.3 Photograph of Reinforcing Cage for Corbel Specimen C-1.

reinforcing bars used in this specimen. The average concrete compressive strength was 40.4 MPa (see Table 3.1). The column-corbel unit was cast in a horizontal position.

The vertical loads were located 150 mm from the face of the column and the horizontal load (which is 20% of the vertical load) was applied through a loading block as shown in Fig. 3.4. To facilitate testing the column-corbel unit was tested in an inverted position as shown in Fig. 3.4.

Figure 3.4 also illustrates the instrumentation for strain measurements on the specimen. Targets were placed on the concrete surface along grid lines spaced 50 mm apart to form strain rosettes.

The loading procedure consisted of applying a vertical load to the column by a universal testing machine which produced equal vertical reactions on the corbels (see Fig. 3.4). This loading was applied in small increments and the horizontal load was made equal to 20% of the vertical reaction in each corbel in each increment by means of independent hydraulic jacks. The vertical loading was monitored by the calibrated loading machine, while load cells were used to determine the horizontal loads applied to

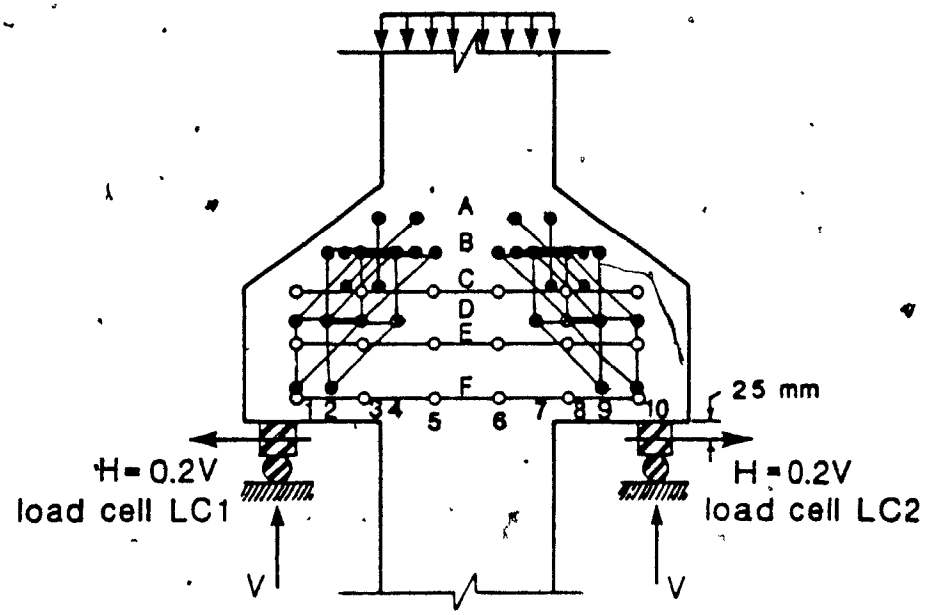

(a) North face instrumentation

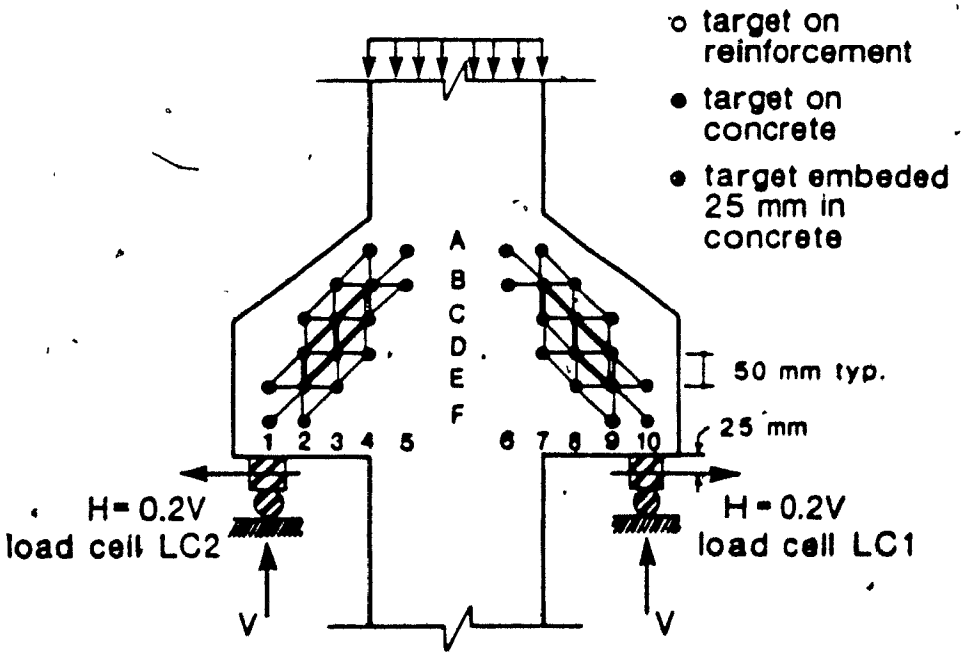

(b) South face instrumentation

Figure 3.4 Test Set-Up and Instrumentation for Corbel Specimen C-1.

the corbels. Full sets of strain readings were taken at regular load intervals throughout the test.

3.4 Dapped End Specimens D-1 and D-2

The details of dapped end specimens D-1 and D-2 are shown in Figs. 3.5 and 3.6. The 3.275 m long by 300 mm wide dapped end beam was 600 mm deep, with 137.5 mm long by 250 mm deep rectangular nibs at each end. The loading span was 3.2 m. Both D-1 and D-2 were originally designed using the strut and tie model shown in Fig. 2.3 for support reactions of 225 kN. The central region of the beam was over-designed by 20% to force failure to occur in the dapped end regions.

Five No. 30 main longitudinal bars in two layers were used as flexural reinforcement in the middle region along with No. 10 U-stirrups at 225 mm spacing (see Fig. 3.5). Three No. 10 horizontal U-bars were included at the ends of the main flexural reinforcement to provide anchorage for the nodal zone region which would develop there. Two No. 10 longitudinal bars were used to anchor the stirrups along the top of the beam.

The main vertical tension tie consisted of four No. 10 stirrups at 33 mm spacing. This main tension tie in specimen D-1 consisted of closed stirrups which were anchored with 135° bends. The vertical tension tie in specimen D-2 consisted of open U-stirrups anchored around the No. 10 longitudinal bars with 135° hooks.

The horizontal tension tie in the nib consisted of four No. 15 bars welded to a 75 x 75 x 6 mm thick by 300 mm long angle which was embedded in the concrete at the bottom of the nib. The welding provided positive anchorage of this reinforcement while the back leg of the angle provided a reaction area for the compressive strut. Two additional No. 10 horizontal U-bars were provided in the nib to control cracking as required by the code.

The only difference between specimens D-1 and D-2 was the detailing of the main

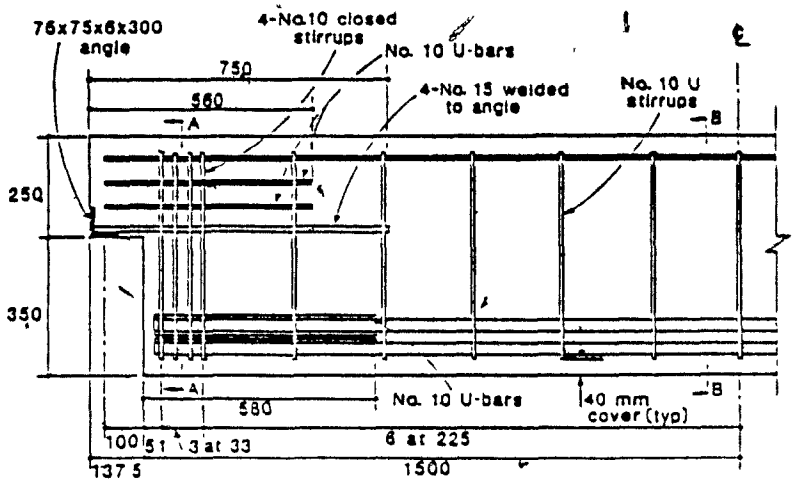

(a) Dapped end D-1

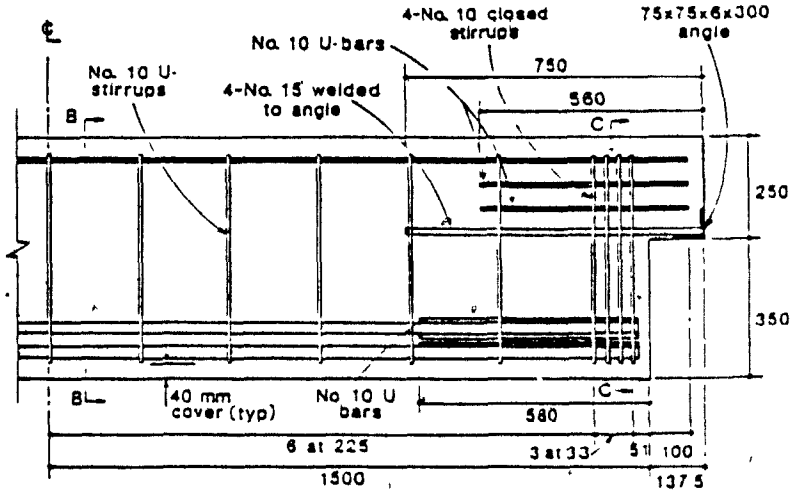

(b) Dapped end D-2

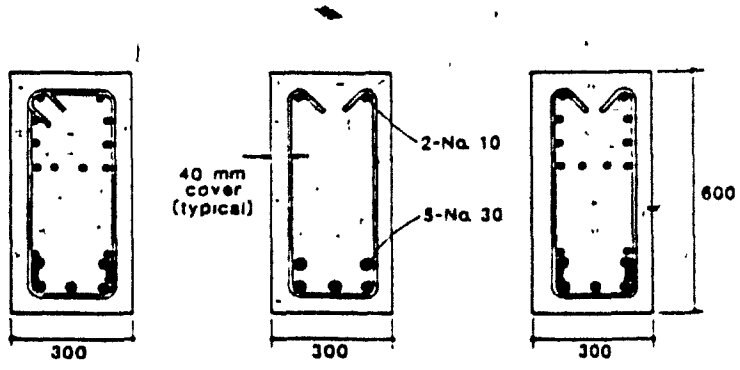

Figure 3.5 Dimensions and Reinforcement Details of Dapped End Specimens D-1 and D-2.

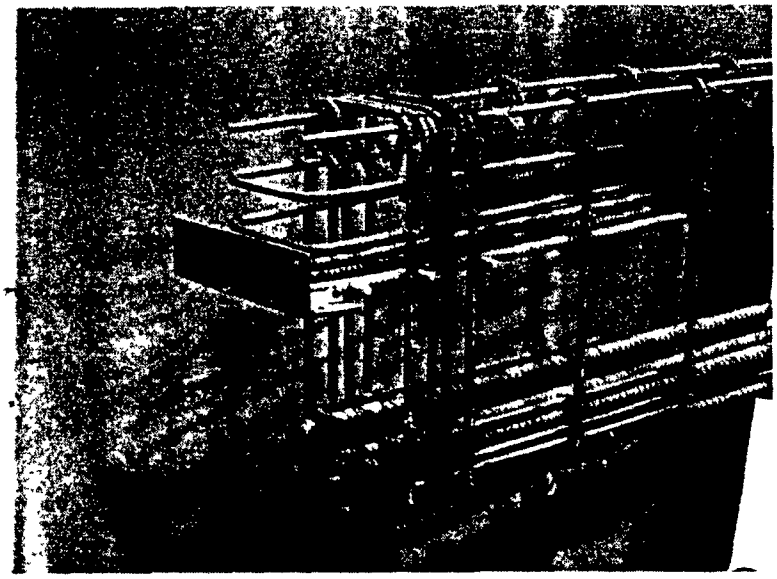

(a) Dapped End D-1

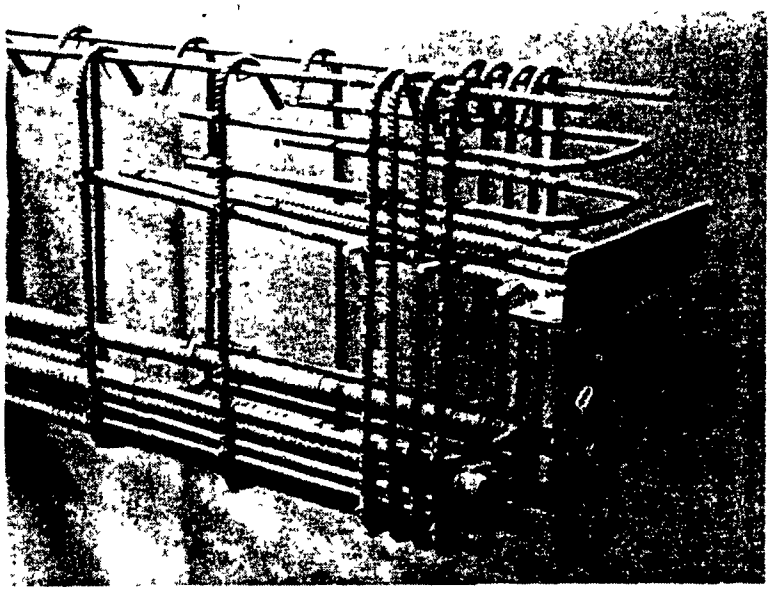

(b) Dapped End D-2

Figure 3.6 Photographs of Reinforcing Cages for Dapped End Specimens D-1 and D-2.

vertical tension tie reinforcement in the upper nodal zone region. The purpose of performing tests on these two different details was to demonstrate the need for careful detailing of the reinforcement.

The material properties of the reinforcement used can be found in Table 3.2. The

average compressive strength of concrete was 29.8 MPa (see Table 3.1).

Figure 3.7 illustrates the instrumentation used for taking strain measurements for specimens D-1 and D-2. In addition, five dial gauges were used to measure deflections. The beam was initially loaded with a single point load at midspan as shown in Fig. 3.7. The load was applied in small increments by a universal testing machine. Full readings of all strains and deflections were taken at regular intervals throughout the tests. After dapped end specimen D-2 failed a support was inserted under the full depth portion of dapped end D-2, 100 mm from the end of the dap, to permit further loading of dapped end D-1.

3.5 Dapped End Specimens D-3 and D-4

The details of dapped end specimens D-3 and D-4 are shown in Figs. 3.8 and 3.9. The 3.275 m long by 300 mm wide dapped end beam was 600 mm deep at midspan and spanned 3.2 m. Specimen D-3 had a 137.5 mm long by 250 mm deep rectangular nib as shown in Fig. 3.8a and contained vertical hanger reinforcement and inclined tension tie reinforcement. Specimen D-4 contained inclined tension tie reinforcement parallel to the sloping end face of the beam as shown in Fig. 3.8b.

Specimens D-3 and D-4 were originally designed for end support reactions of 250 kN using the strut and tie models shown in Fig. 2.3. The detailed analysis of both of these specimens is given in Chapter 5. The main flexural reinforcement consisted of five No. 30 bars placed in two layers and the transverse reinforcement in the full depth beam consisted of No. 10 U-stirrups at 225 mm spacing (see Fig. 3.8). Two No. 10 longitudinal bars were used to anchor the top of the transverse reinforcement. The hanger reinforcement in specimen D-3 consisted of two No. 10 vertical closed U-stirrups together with two No. 20 bars inclined at an angle of 52.5 degrees from the horizontal. The main horizontal tension tie reinforcement in the nib consisted of two No. 15 bars welded to an angle. Horizontal No. 10 U-bars were placed in the nib and at the level

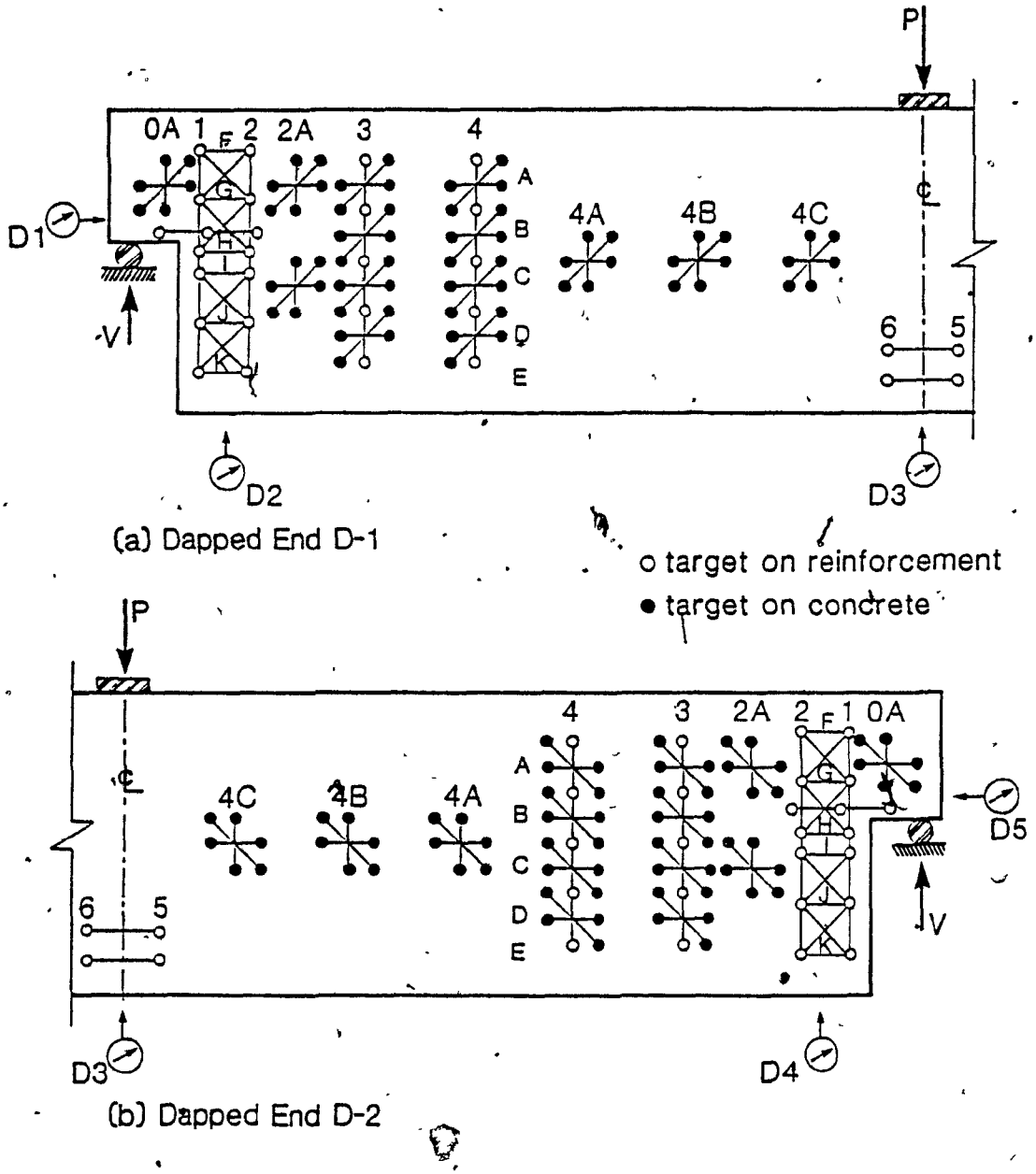

Figure 3.7 Test Set-Up and Instrumentation for Dapped End Specimens D-1 and D-2.

of the main flexural reinforcement as shown in Fig. 3.8.

Instead of a combination of vertical and inclined hanger reinforcement specimen D-4 contained two No. 25 inclined bars as shown in Fig. 3.8. The main horizontal tension tie reinforcement in the nib consisted of three No. 10 bars welded to a steel plate.

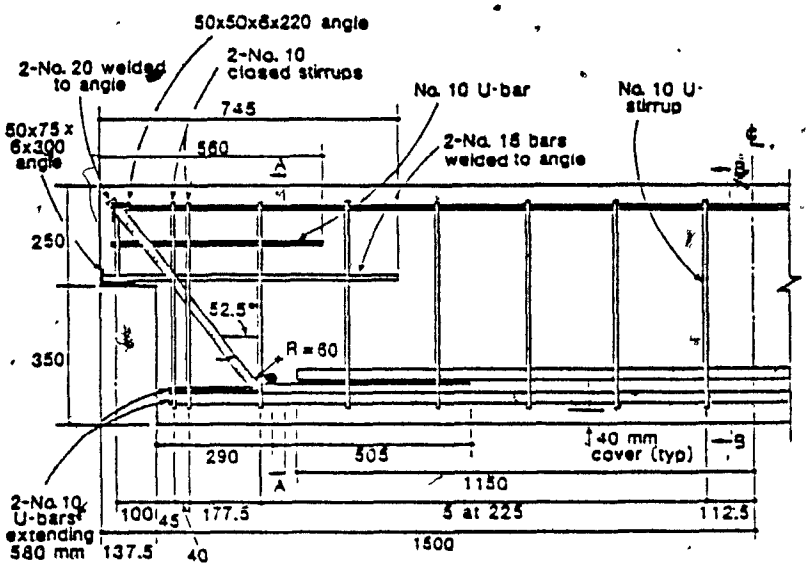

(a) Dapped end D-3

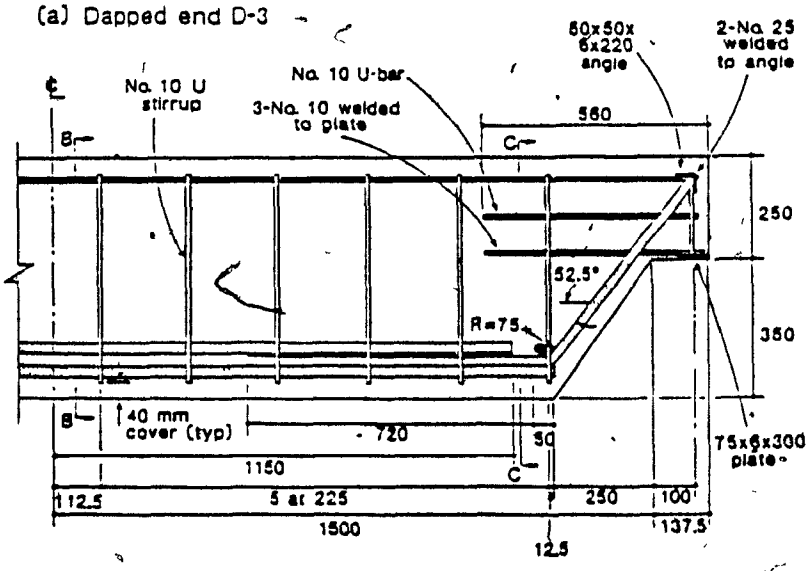

(b) Dapped end D-4

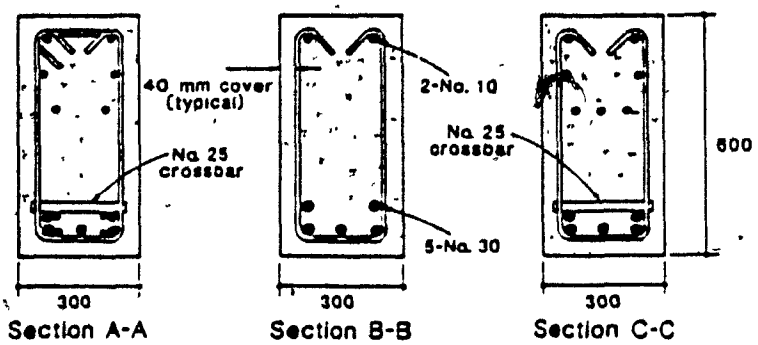

Figure 3.8 Dimensions and Reinforcement Details of Dapped End Specimens D-3 and D-4.

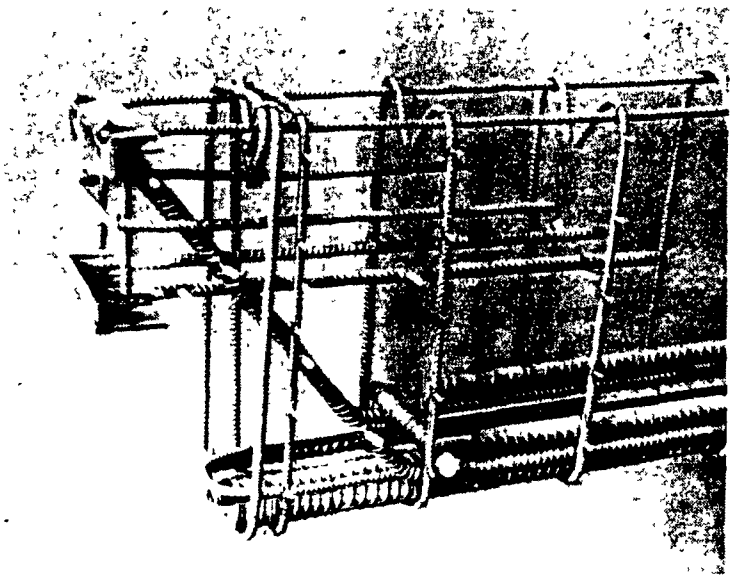

(a) Dapped End D-3

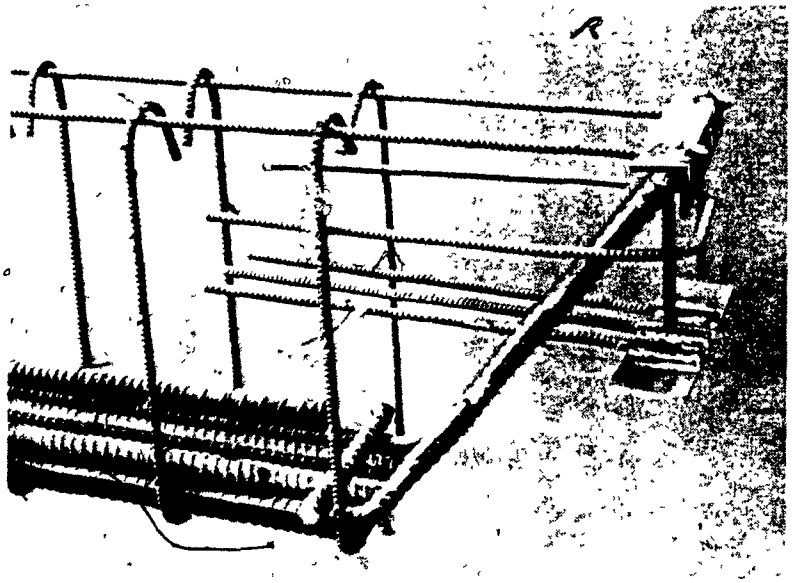

(b) Dapped End D-4

Figure 3.9 Photographs of Reinforcing Cages for Dapped End Specimens D-3 and D-4.

The material properties of the reinforcement are given in Table 3.2. The average compressive strength of the concrete was 36.6 MPa.

Figure 3.10 shows the instrumentation for strain measurements for both specimens. In addition five dial gauges were used to measure the deflections of the specimens. The

beam was initially loaded with a single concentrated load at midspan as shown in Fig. 3.10. The load was applied in small increments by a universal testing machine. Full readings of all strains and deflections were taken at regular intervals throughout the tests. After dapped end D-4 failed the loading set-up was changed to permit further loading of dapped end D-3. A support was added under the full depth portion of dapped end D-4 located 160 mm from the bottom of the inclined dap and the loading was shifted so that it was centred in the remaining 2.79 m span.

3.6 Web Hole Specimens H-1 and H-2

The details of the web hole specimens H-1 and H-2 are shown in Figs. 3.11 and 3.12. The 5.6 m long T-beam had a 800 mm wide, 100 mm thick flange and a 200 mm thick web. The beam was 400 mm deep, had a clear span of 4.8 m and had two 130 mm x 500 mm rectangular web openings. The centre of the web hole was 1.0 m from the support centreline for specimen H-1, while for specimen H-2 it was 0.75 m from the support centreline.

Specimens H-1 and H-2 were originally designed using the simple strut and tie model illustrated in Fig. 2.3 for a uniform load of 130 kN/m. Detailed analyses of these specimens are given in Chapter 5.

The main longitudinal reinforcement consisted of four No. 30 bars in two layers. The slab contained four No. 10 full length longitudinal bars together with an additional four No. 10 longitudinal bars in the region over the opening. The slab also contained pairs of No. 10 transverse reinforcing bars at a spacing of 250 mm. The stirrups between the centreline and the holes consisted of #3 heat-treated U-stirrups at a spacing of 190 mm. Beneath the holes #3 closed stirrups were used as shown in Fig. 3.11. On the support sides of the openings two full-depth U-stirrups were provided to act as vertical tension hangers. Some additional stirrups were provided between the holes and the supports as shown in Fig. 3.11. The details of the reinforcement properties are given

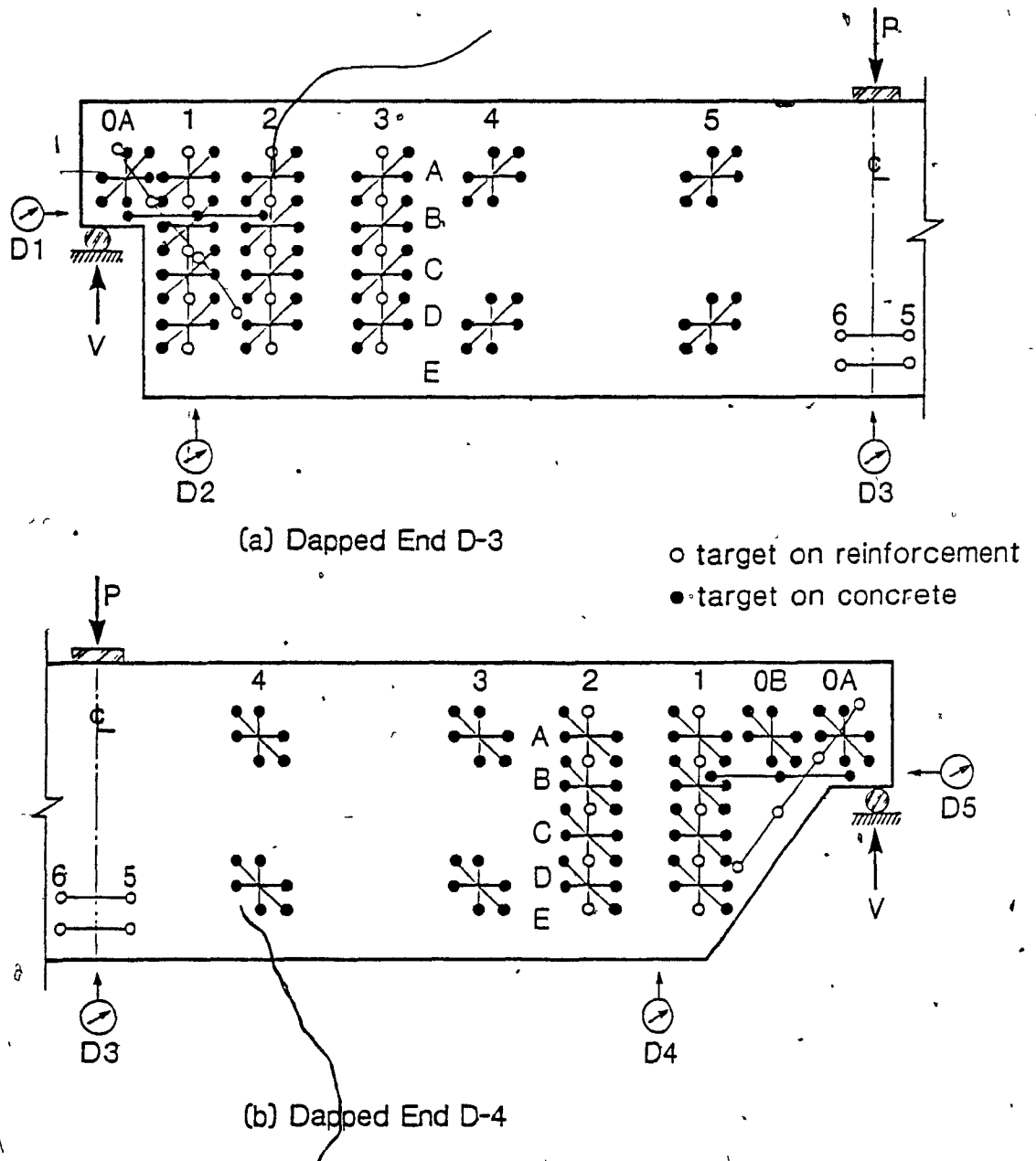

Figure 3.10 Test Set-Up and Instrumentation for Dapped End Specimens D-3 and D-4.

in Table 3.2. The average concrete strength at the time of testing was 26.3 MPa (see Table 3.1).

Figure 3.13 shows the instrumentation for strain measurements for both specimens. In addition five dial gauges were used to measure the deflections of the specimens. The beam was loaded with a series of point loads at 250 mm spacing simulating a

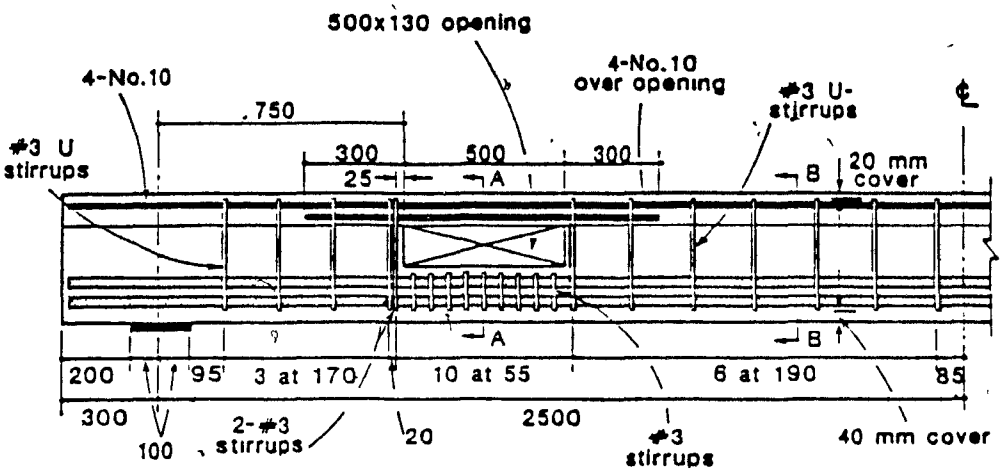

(a) Web hole H-1

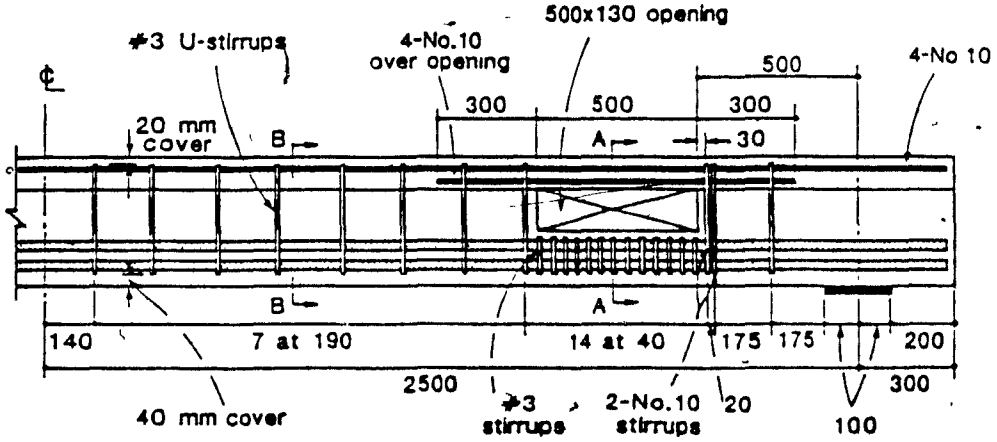

(b) Web hole H-2

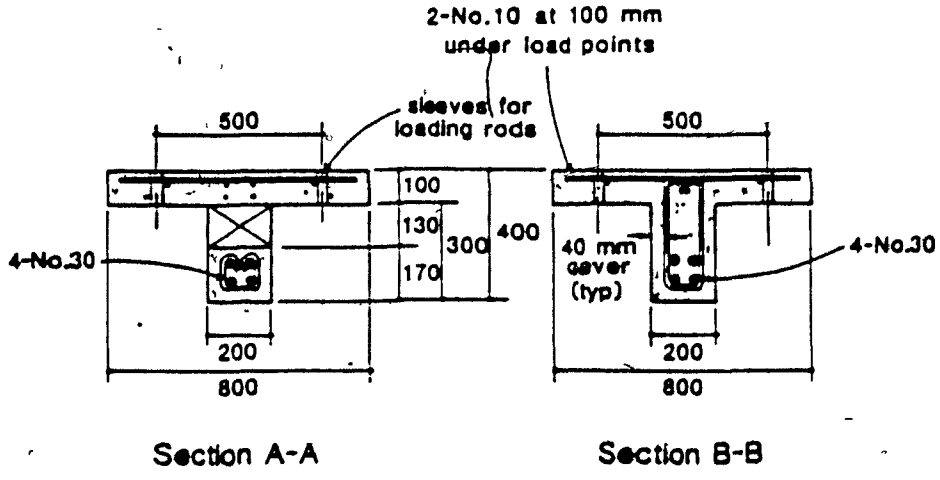

Figure 3.11 Dimensions and Reinforcement Details of Web Hole Specimens H-1 and H-2.

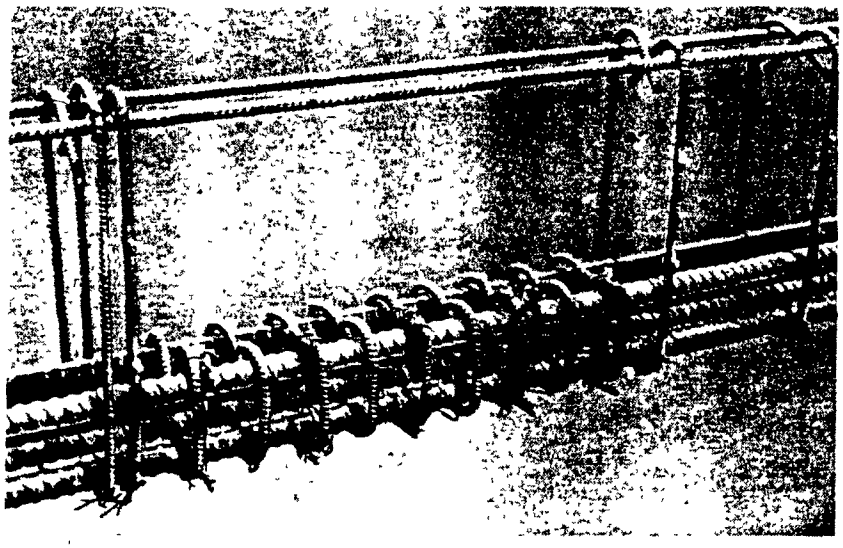

(a) Web Hole H-1

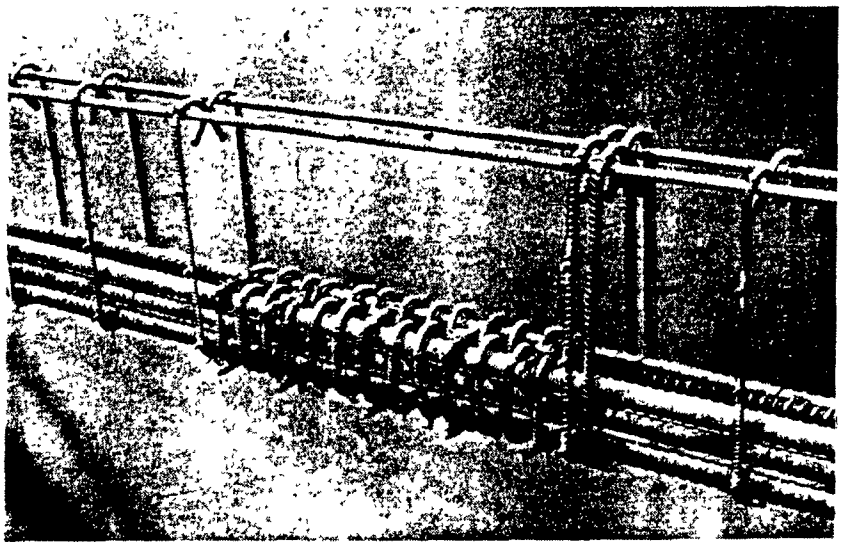

(b) Web Hole H-2

Figure 3.12 Photographs of Reinforcing Cages for Web Hole Specimens H-1 and H-2.

uniform loading as shown in Fig. 3.13. The simulated uniform load was applied in small increments and full readings of all strains and deflections were taken at regular intervals throughout the tests. After the failure of the end containing opening H-2 the support at this end of the beam was moved inwards by 1.16 m to permit further loading of end H-1.

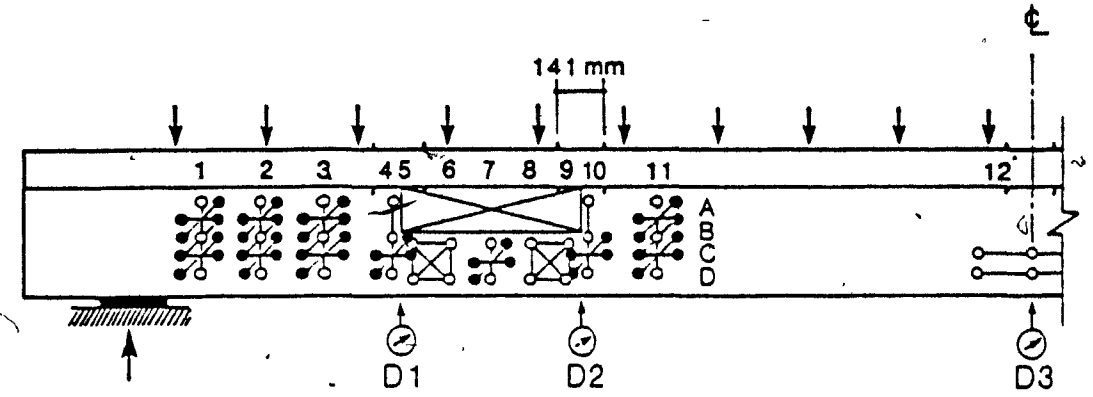

(a) Hole H-1

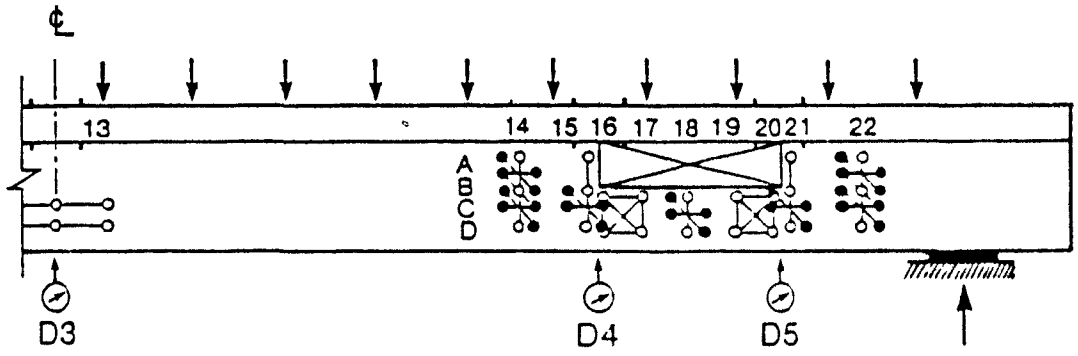

(b) Hole H-2

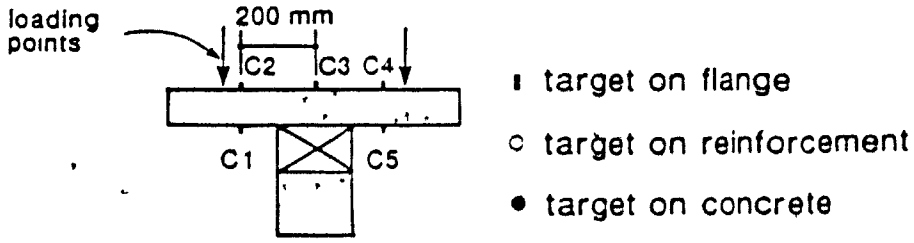

(c) Section showing location of concrete targets on flange

Figure 3.13 Test Set-Up and Instrumentation for Web Hole Specimens H-1 and H-2.

CHAPTER 4

EXPERIMENTAL RESULTS

4.1 Introduction

The responses of the specimens tested in this research programme are described in this chapter. Complete response data for each specimen are given in Appendix A.

4.2 Corbel Specimen C-1

First cracking in the corbel specimen occurred at a vertical load, V, of 102 kN near the column faces. A hairline crack had formed at the inner face of the bearing plate at a load of 169 kN. First yielding occurred in the tension tie between targets 8 and 10 at a load, V, of 336 kN. A photograph of the cracking pattern in the corbel at first yielding is shown in Fig. 4.1. At this load stage the maximum crack width observed was 0.15 mm. Figure 4.2a shows the variation of strains in the reinforcement at first yielding. The measured strains at the face of the column were larger than those measured near the loading plates. This is due to the larger moment in the corbel closer to the face of the column.

Figure 4.3a shows the magnitude of the principal strains and their directions as determined from the strain rosette readings at first yield.

The corbel reached a maximum shear load, V, of 502 kN with a corresponding horizontal load of 99.5 kN. Failure occurred by yielding of the main tension tie together

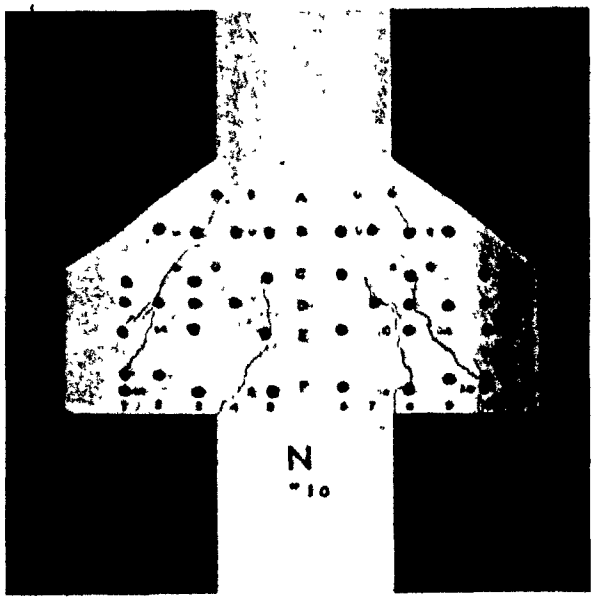

Figure 4.1 Photograph of Corbel Specimen C-1 at V = 336 kN.

with yielding of the lower tension ties (see Fig. 4.2b) followed by crushing of the concrete under the bearing plate. As can be seen the tension tie is yielding along its length between the face of the column and the loading plate. Figure 4.4 shows the specimen after failure. The rotation of the bearing plate is evident, as well as spalling of the concrete in the region of the bearing plate. The presence of large principal tensile strains together with concentrations of principal compressive strains is evident from Fig. 4.3b.

4.3 Dapped End Specimen D-1

First flexural cracking occurred at midspan at a load causing an end reaction, V, of 40.0 kN. Cracking at the re-entrant corner was observed at a load, V, of 73.3 kN. The first shear crack in the web occurred when the end reaction was 107 kN. At this loading stage the maximum flexural crack width measured at midspan was 0.13 mm and the maximum width of the cracks at the re-entrant corner was 0.25 mm. The corresponding cracking pattern for D-1 is illustrated in Fig. 4.5a. As can be seen,

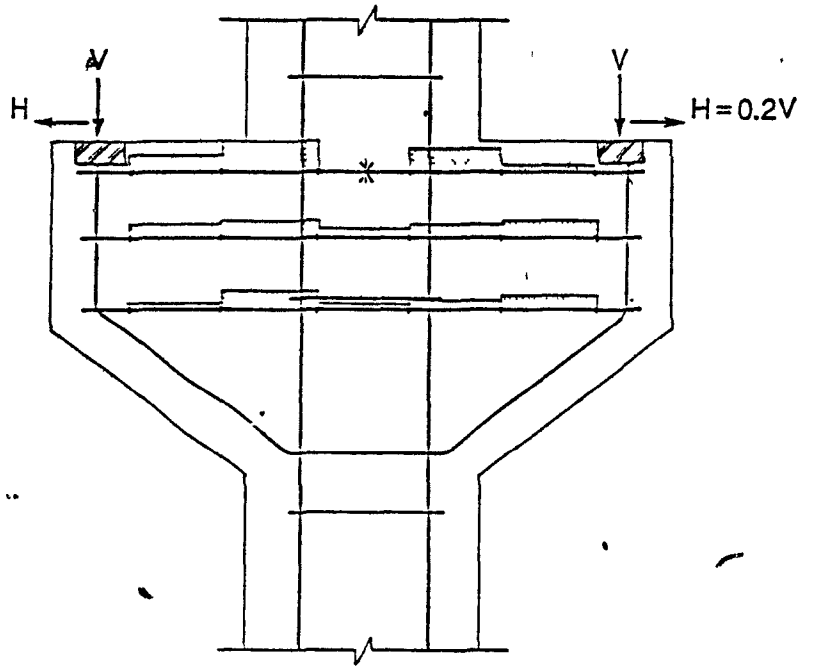

(a) Load, V = 336 kN

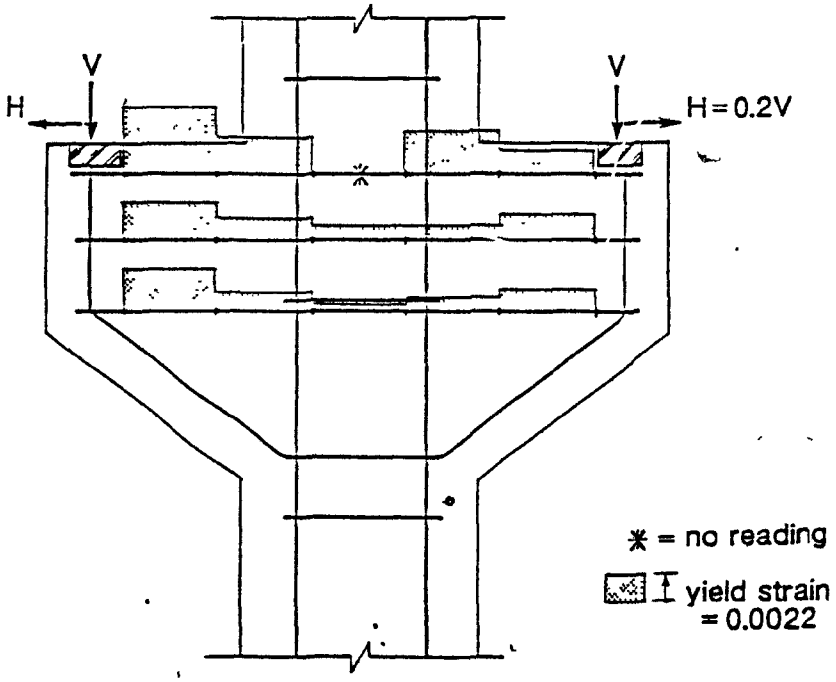

(b) Load, V = 502 kN

Figure 4.2 Measured Reinforcement Strains in Corbel Specimen C-1.

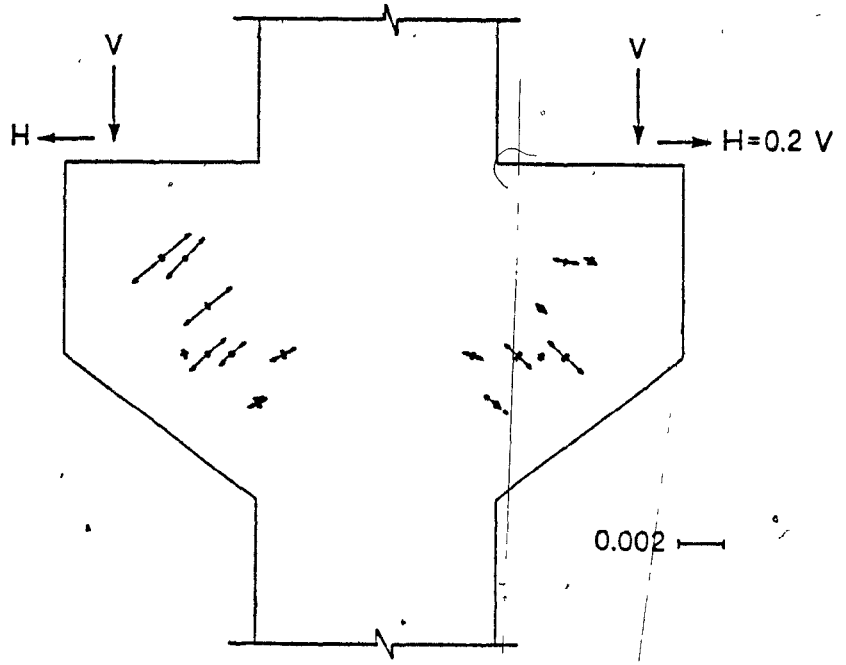

(a) Support reaction, V = 336 kN

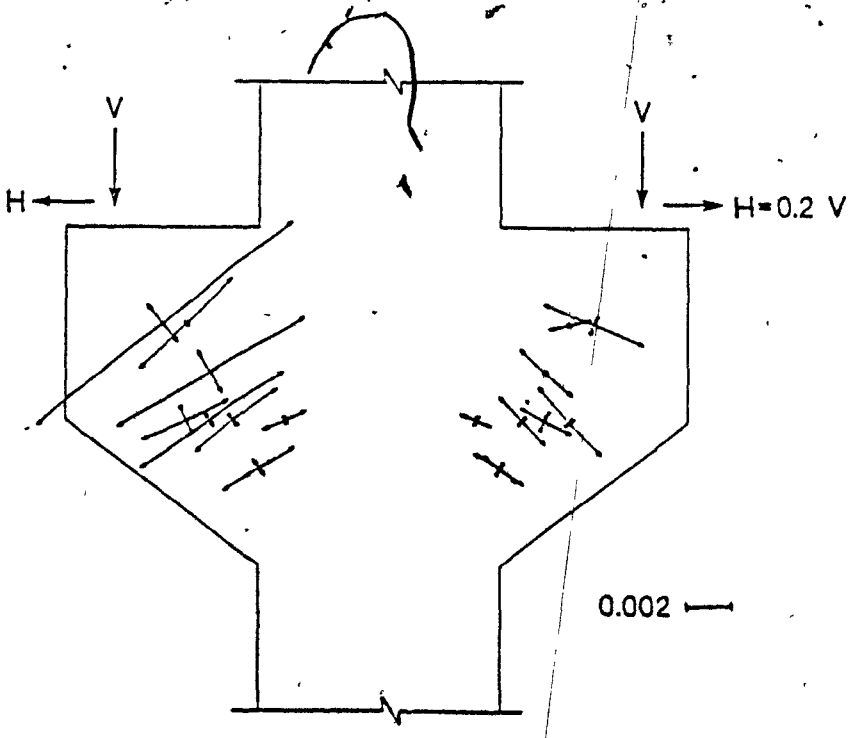

(b) Support reaction, V = 502 kN

Figure 4 3 Principal Strains Determined from Rosette Readings for Corbel Specimen C-1.

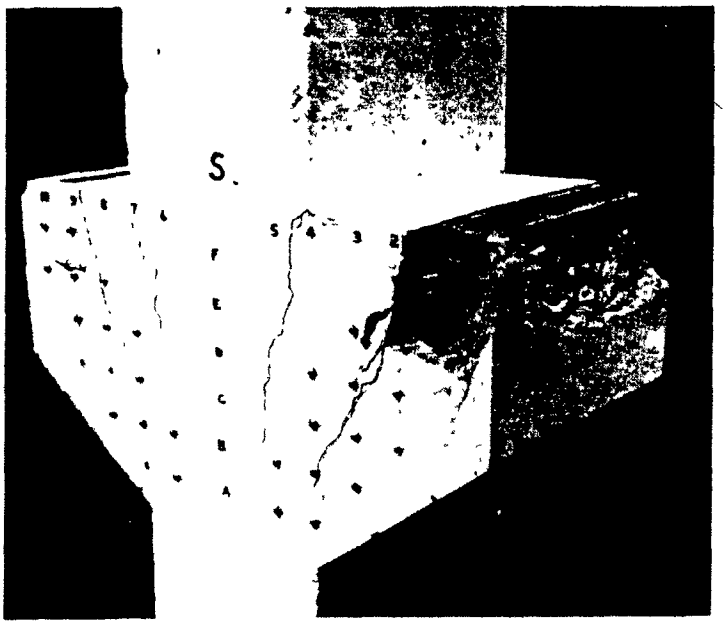

Figure 4.4 Photograph of Corbel Specimen C-1 after Failure, V = 502 kN.

inclined cracks had crossed the main vertical tension tie reinforcement.

Both the vertical and horizontal reinforcement yielded at a load of 173 kN in the region of the re-entrant corner. At this stage additional inclined cracks occurred in the nib running from the centreline of the support up to the top of the vertical tension tie reinforcement. Figure 4.6a shows the variations of measured strains in the vertical and horizontal reinforcement for specimen D-1 at this load stage while Fig. 4.7a shows the principal strains calculated from the rosette readings. The fanning of the compressive stresses into the bottom of the main vertical tension tie is evident.

Figure 4.5b shows the cracking pattern at an end reaction of 207 kN. By this stage, inclined shear cracking in the main beam was well developed and a number of inclined cracks crossed the vertical tension tie reinforcement. The inclined cracking in the nib outlines the compressive strut going from the top of vertical tension tie down to the support reaction area.

Loading progressed using the test set-up shown in Fig. 3.7. However, after end D-2 failed, an addition support was placed at the failed end, 100 mm from the end face

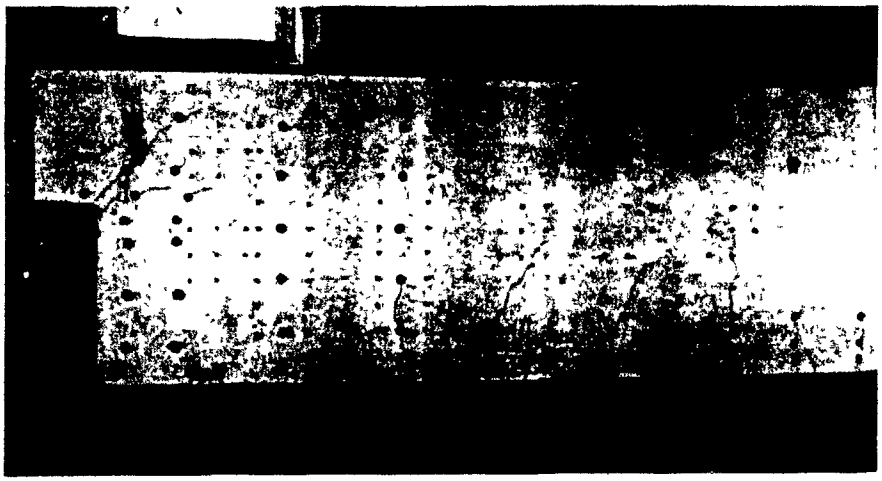

(a) Support reaction, V = 107 kN

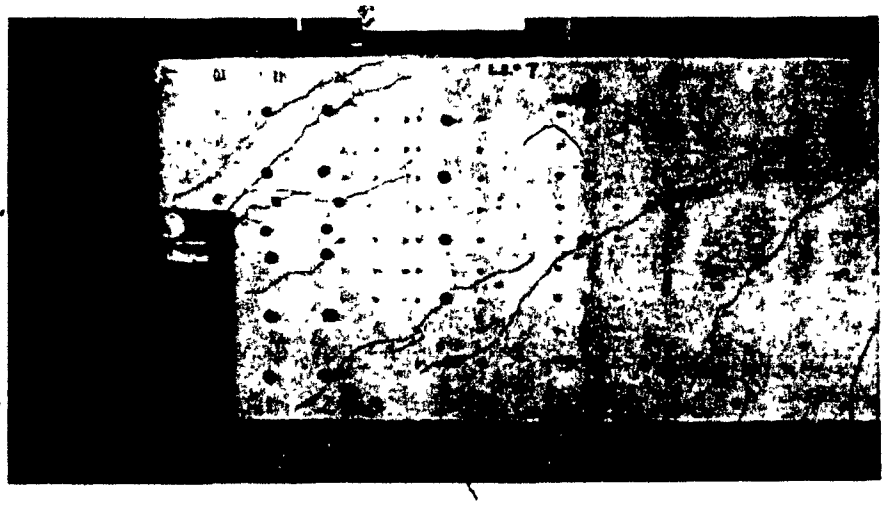

(b) Support reaction, V = 207 kN

Figure 4.5 Photographs of Dapped End Specimen D-1.

of the full depth beam. Specimen D-1 failed when the vertical reaction reached 307 kN. Significant splitting and spalling of the concrete cover occurred. Figure 4.8 shows the appearance of specimen D-1 after failure.

The closed stirrups used in specimen D-1 provided excellent anchorage for the inclined compressive strut. It is clear from Fig. 4.8b that in highly stressed nodal regions it is necessary to account for the spalling of the concrete cover. The 135° bend anchorages in specimen D-1 performed very well. It is noted that spalling occurred

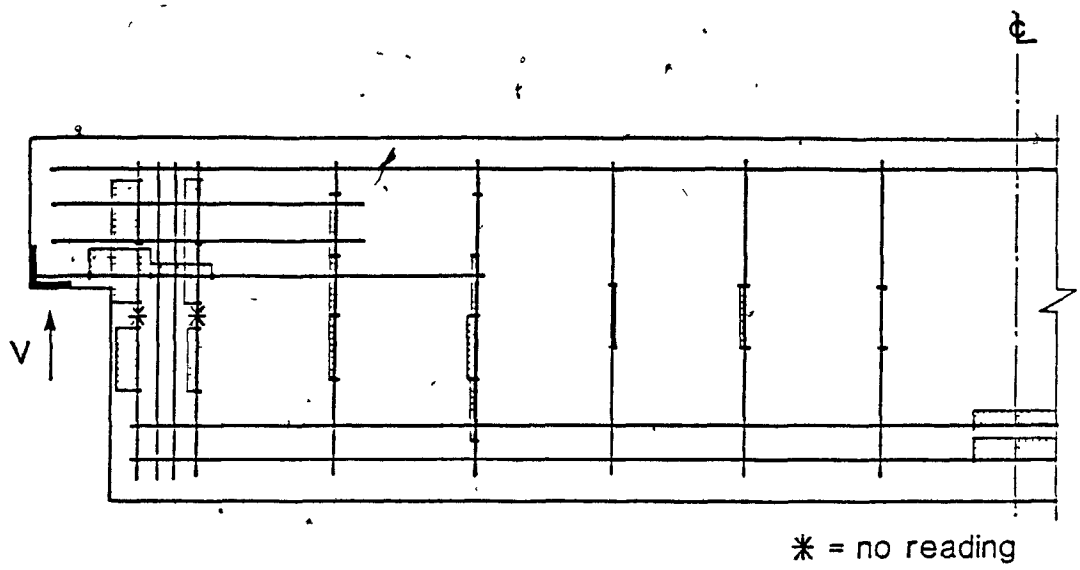

(a) Support reaction, V = 173 kN

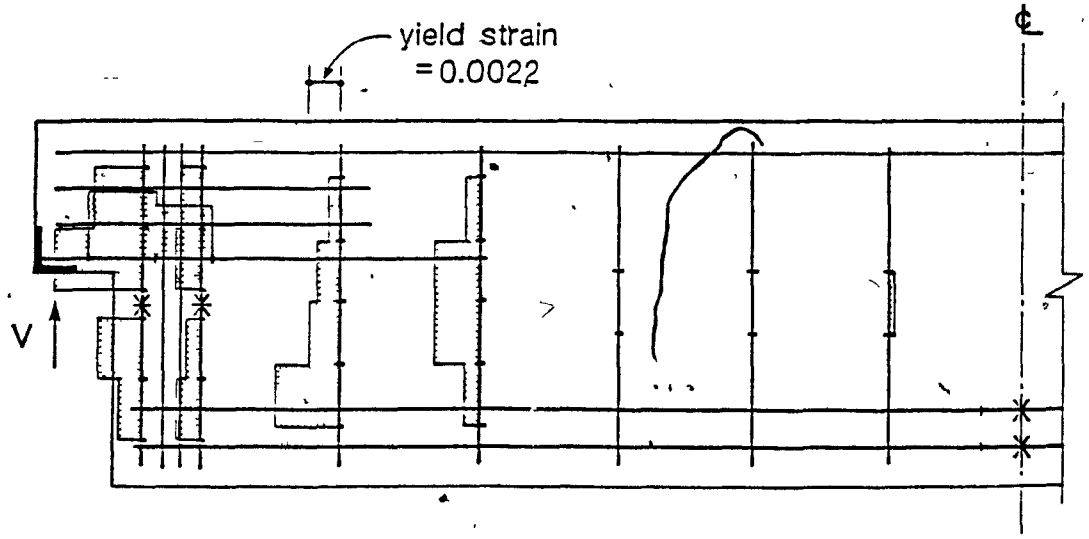

(b) Support reaction, V = 307 kN

Figure 4.6 Measured Strains in Vertical and Horizontal Reinforcement in Dapped End Specimen D-1.

down to about the centreline of the vertical tension tie reinforcement.

At the maximum load level of 307 kN yielding took place over most of the height of the outermost vertical stirrup, with the innermost stirrup of the main vertical tension

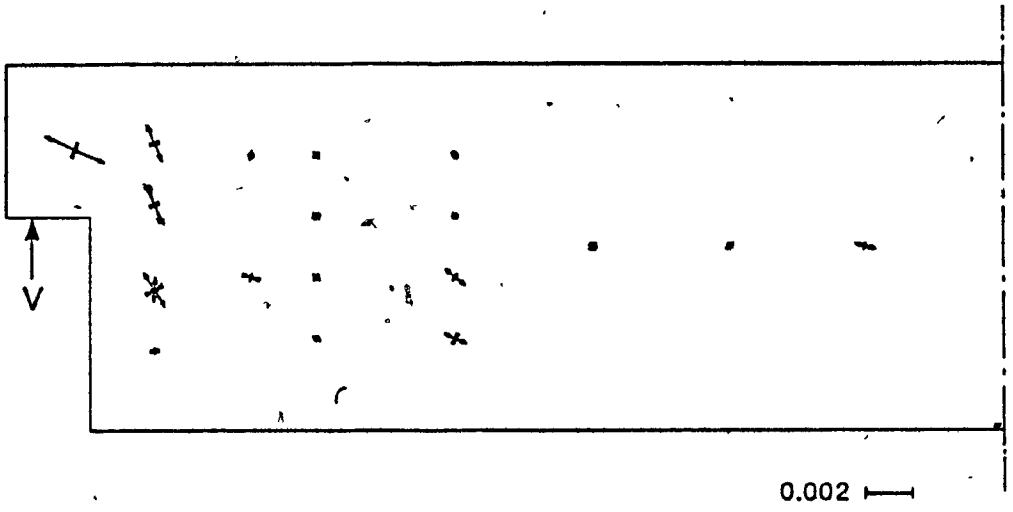

(a) Support reaction, V=173 kN

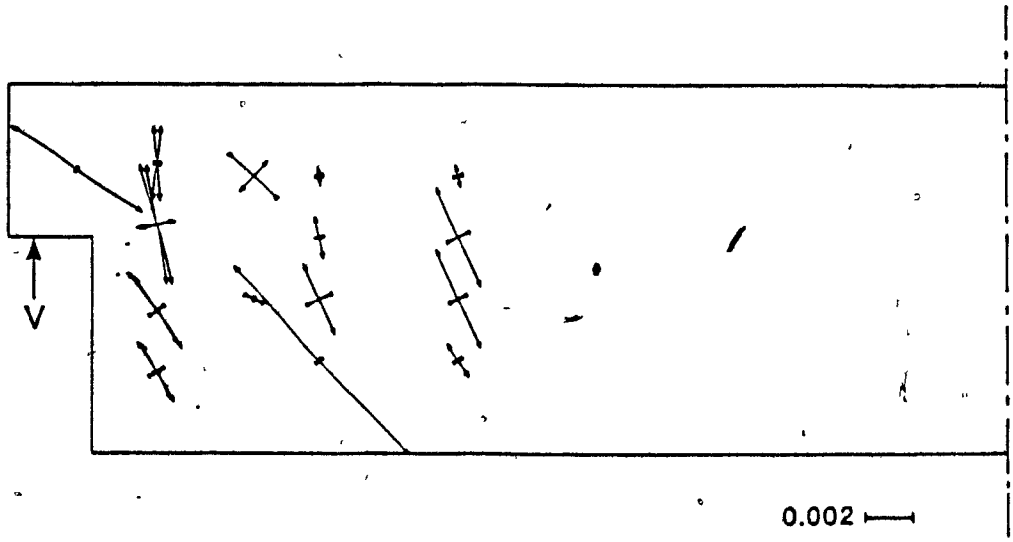

(b) Support reaction, V = 307 kN

Figure 4.7 Principal Strains Determined from Rosette Readings for Dapped End Specimen D-1.

tie yielding in the region of the re-entrant corner. Yielding was also recorded in the two U-stirrups closest to the dapped end as shown in Fig. 4.6b. The zones of yielding in these stirrups delineate a region of fanning of the compressive stresses near the dapped end. The horizontal tension tie anchored in the nib had fully yielded at this stage.

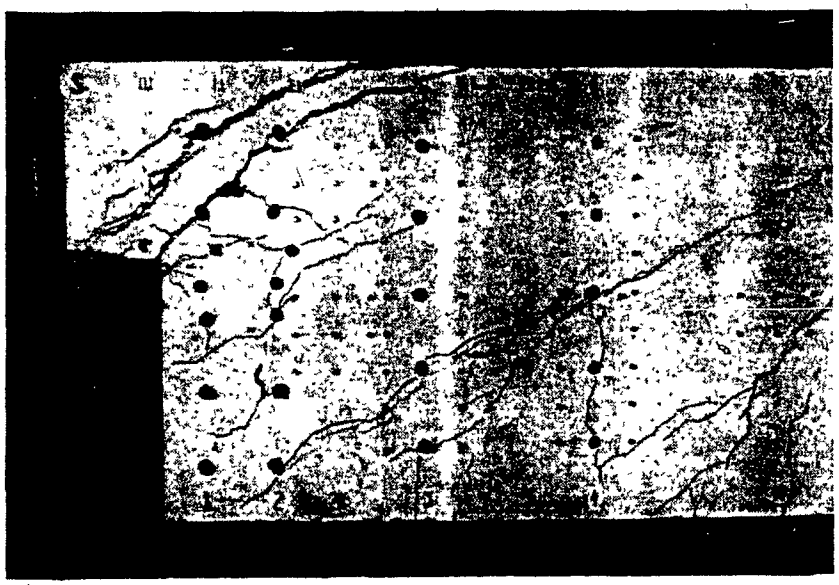

(a) Support reaction, V = 307 kN

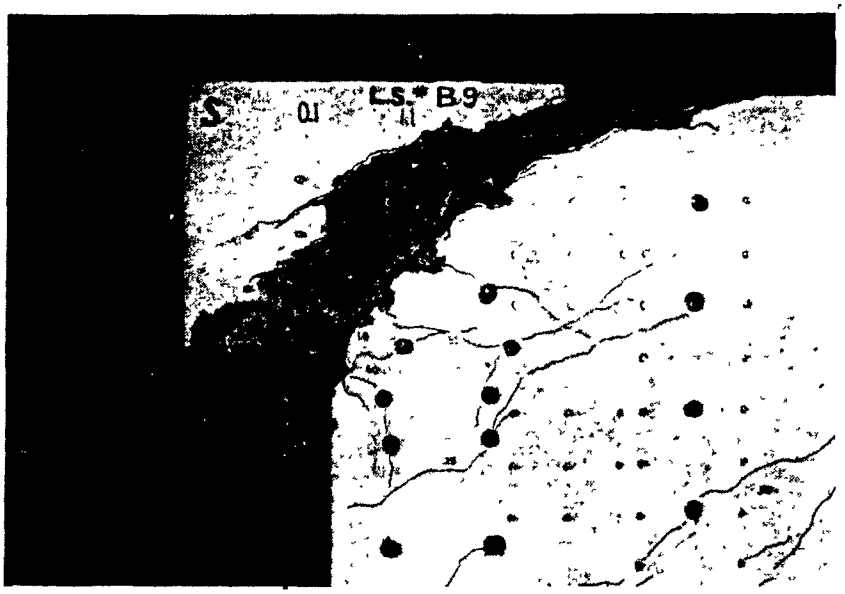

(b) Close-up of nib after failure

Figure 4.8 Photographs of Dapped End Specimen D-1.

The yielding of the main horizontal and vertical tension ties precipitated failure of the specimen. As can be seen from Fig. 4.7b large principal tensile strains occur in the direction of the main tension tie and perpendicular to the highly stressed compressive struts. At higher load levels the compressive strain in the strut located in the nib

dropped. This drop in the surface strains was due to spalling of the concrete cover in this region.

4.4 Dapped End Specimen D-2

First flexural cracking occurred at midspan at a load causing an end reaction, V, of 40.0 kN. Cracking at the re-entrant corner was observed at a load, V, of 73.3 kN. A hairline shear crack in the web occurred when the end reaction was 106 kN. At this loading stage the maximum flexural crack width measured at midspan was 0.13 mm and the maximum width of the cracks at the re-entrant corner was 0.25 mm. The cracking pattern for specimen D-2 at an end reaction of 140 kN is illustrated in Fig. 4.9a. As can be seen, inclined cracks had crossed the main vertical tension tie reinforcement. When the vertical reaction reached 173 kN additional inclined cracks occurred in the nib running from the centreline of the support up to the top of the vertical tension tie reinforcement.

The main vertical tension tie reinforcement yielded at a load of 207 kN in the region of the re-entrant corner where significant cracking had developed. Figure 4.10a shows the variations of measured strains in the vertical and horizontal reinforcement for specimen D-2 at this load level. Figure 4.11a shows the principal strains calculated from the rosette readings. The fanning of the compressive stresses into the bottom of the main vertical tension tie is evident in this figure. Figure 4.9b illustrates the cracking pattern for D-2 at this loading stage. As can be seen, inclined shear cracking in the main beam was well developed and a number of inclined cracks crossed the vertical tension tie reinforcement. The inclined cracking in the nib outlines the compressive strut going from the top of vertical tension tie down to the support reaction area.

Specimen D-2 failed when the end reaction reached 258 kN. Figure 4.12a illustrates the cracking pattern at failure. The concrete cover on the top surface of the beam and on the sides of the nib was loose due to the significant splitting and spalling that had

(a) Support reaction, V = 140 kN

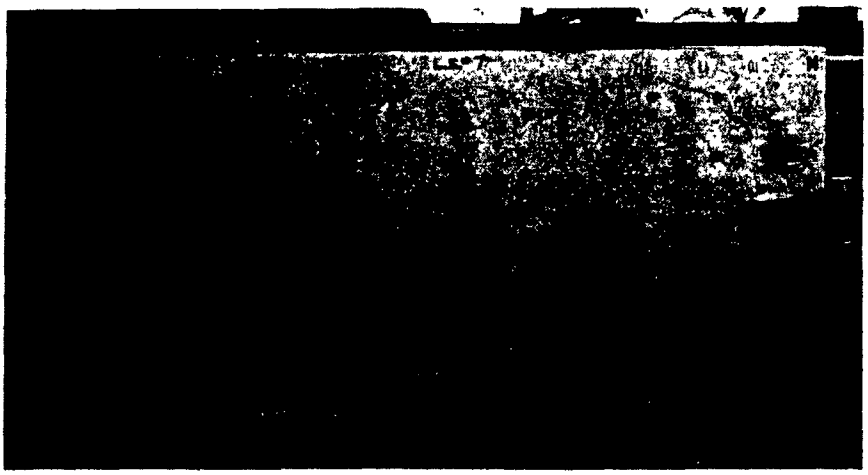

(b) Support reaction, V = 207 kN

Figure 4.9 Photographs of Dapped End Specimen D-2.

occurred.

Specimen D-2 failed by crushing of the concrete compressive strut between the top of the tension tie and the support. Only the concrete confined by the stirrup hook anchorages was effective. The resulting reduction in the effective width of the nodal zone caused a premature failure of the compressive strut near the top of the vertical tension tie (see Fig. 4.12b).

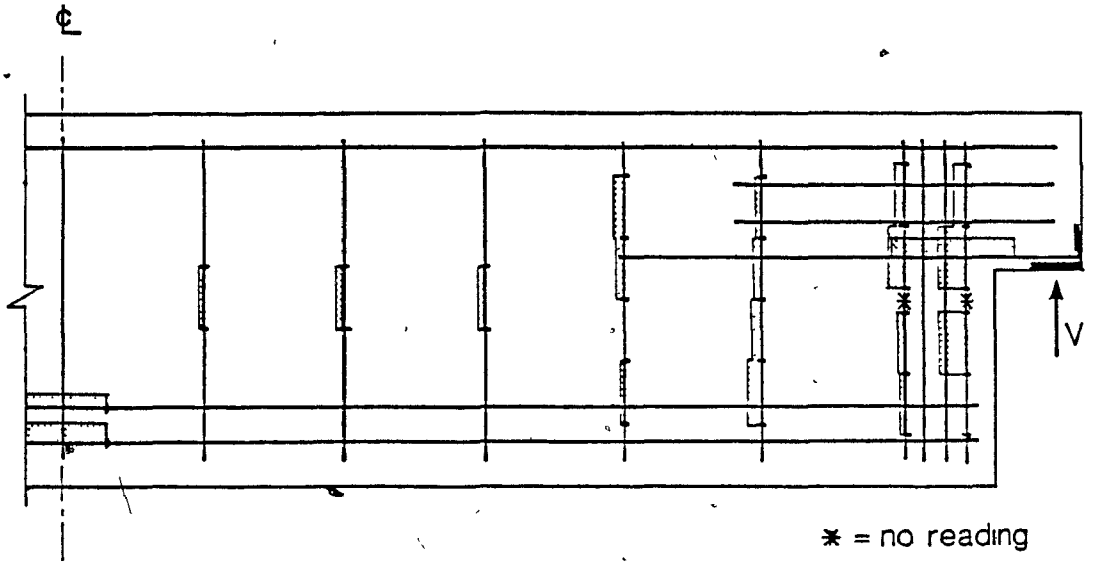

(a) Support reaction, V = 207 kN

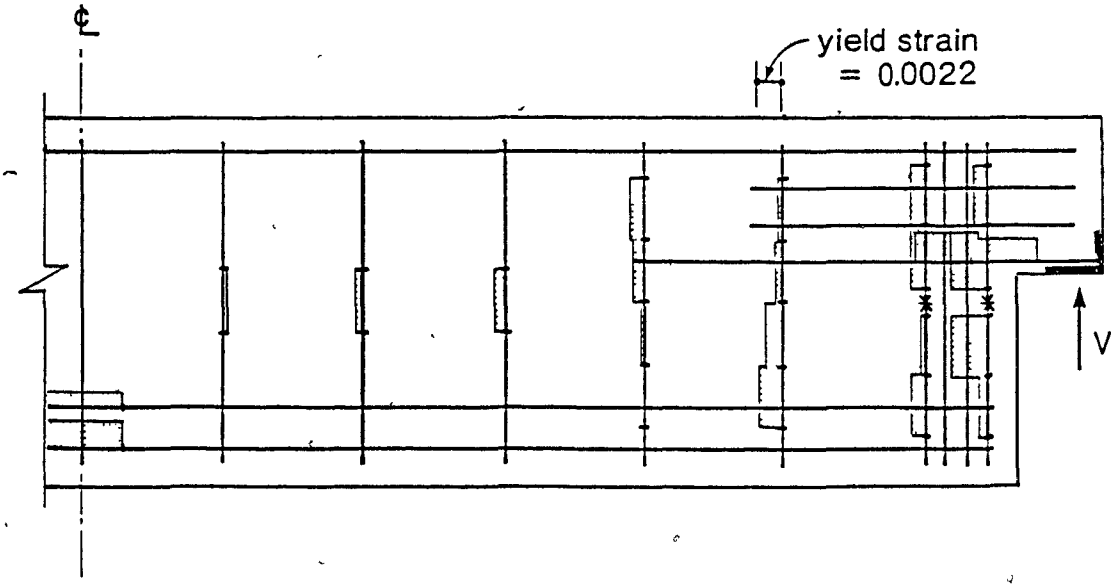

(b) Support reaction, V = 240 kN

Figure 4.10 Measured Strains in Vertical and Horizontal Reinforcement in Dapped End Specimen D-2.

4.5 Comparison of Behaviour of Dapped End Specimens D-1 and D-2

Dapped end specimens D-1 and D-2 had identical reinforcement details except for the detailing of the main vertical tension tie reinforcement at the top of the beams. This

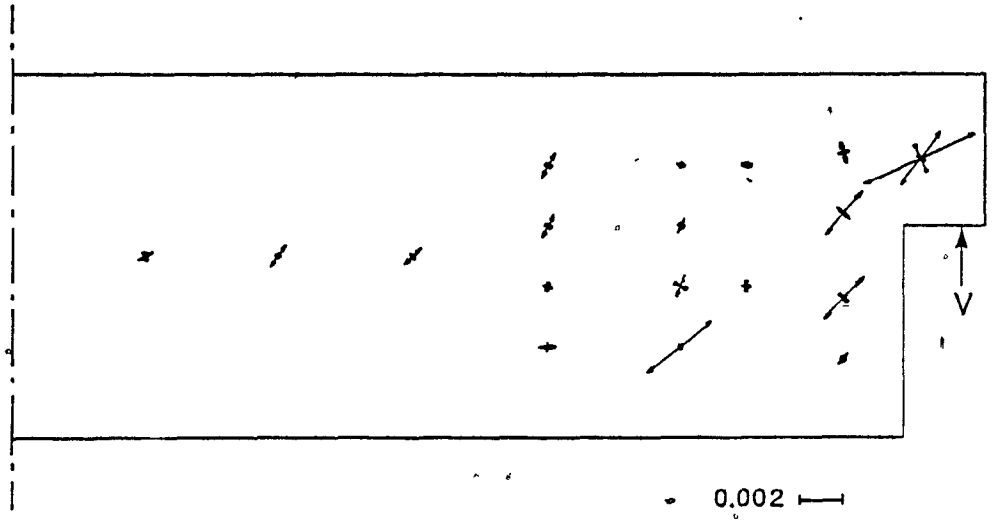

(a) Support reaction, V=207 kN

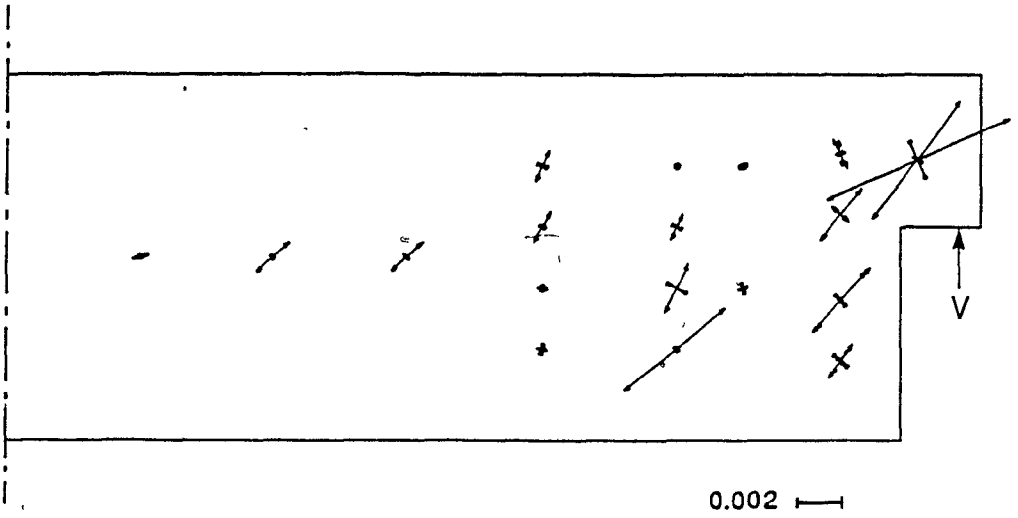

(b) Support reaction, V=240 kN

Figure 4.11 Principal Strains Determined from Rosette Readings for Dapped End Specimen D-2.

tension tie in specimen D-1 consisted of closed stirrups, while specimen D-2 contained open U-stirrups (see Fig. 3.5 for details).

It is evident from the comparisons of the cracking patterns, reinforcement strain

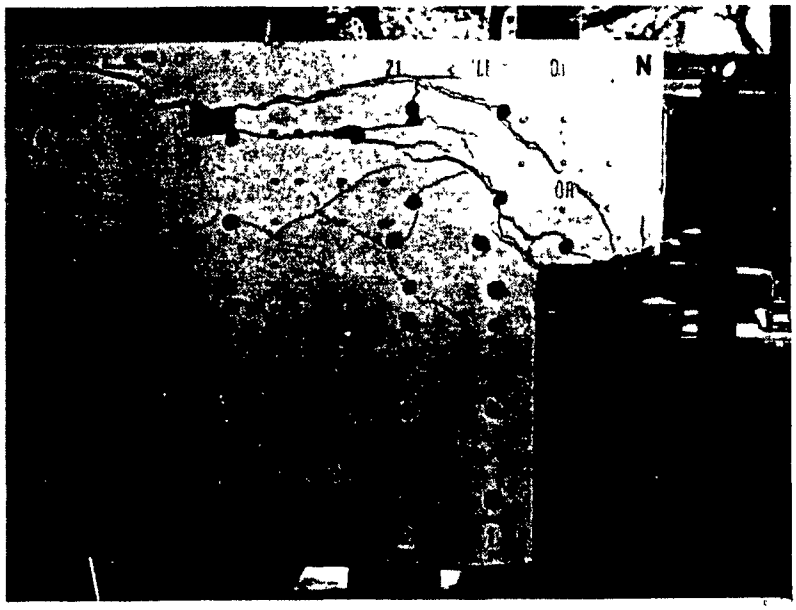

(a) Side view

(b) Close-up of nib after removing spalled concrete

Figure 4.12 Photographs of Dapped End Specimen D-2 after Failure.

distributions and the principal strains given in Sections 4.3 and 4.4 that both of these specimens behaved in a similar manner until specimen D-2 failed prematurely.

Figure 4.13 shows the condition of specimens D-1 and D-2 after failure. The

premature failure of specimen D-2 was caused by crushing of the compressive strut at the top of the main vertical tension tie. This failure was initiated by the strut losing its support anchorage due to the inappropriate detailing of the vertical tension tie (see Fig. 4.13b). The 15.9% reduction in capacity is attributed to the use of open versus closed stirrups.

It is also evident from Fig. 4.13 that it is necessary to account for spalling of the concrete cover when detailing the end anchorages of tension ties. Hence, it is necessary to detail such tension ties with closed stirrups having 135° bend anchorages, in order to anchor the compressive struts and to develop yielding in the tension ties.

4.6 Dapped End Specimen D-3

First flexural cracking occurred at midspan at a load causing a vertical end reaction, V, of 39.9 kN. A hairline crack was observed at the re-entrant corner at a load, V, of 73.3 kN. This crack had a width of 0.15 mm at an end reaction of 140 kN. The first shear crack in the full depth web occurred when the end reaction was 207 kN. The cracking pattern in the beam at this load stage is shown in Fig. 4.14a. At this loading stage the maximum crack width at the re-entrant corner was 0.20 mm. As can be seen, inclined cracks had crossed the vertical and inclined tension tie reinforcement.

First yielding occurred in the stirrups near the bottom of the full depth beam at a load of 274 kN. Figure 4.15a shows the variations of measured strains in the vertical, diagonal, and horizontal reinforcement for specimen D-3 at this load level. Figure 4.16a shows the principal strains calculated from the rosette readings. The fanning of the compressive stresses into the bottom of the main tension ties is evident.

When the vertical reaction reached 307 kN additional inclined cracks occurred in the nib running from the centreline of the support up to the top of the vertical tension tie reinforcement. Figure 4.14b illustrates the cracking pattern for D-3 at this loading stage. As can be seen, inclined shear cracking in the main beam was well developed and

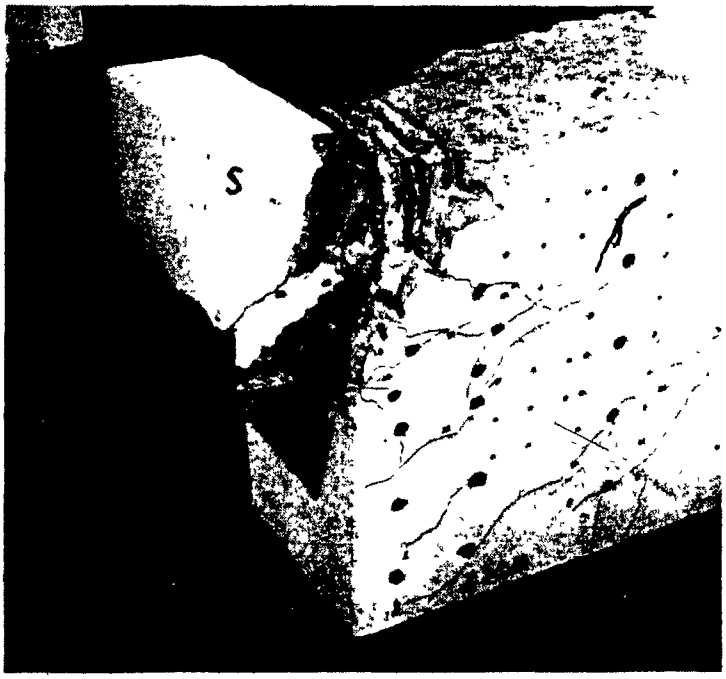

(a) Dapped End D-1

(b) Dapped End D-2

Figure 4.13 Photographs of Dapped End Specimens D-1 and D-2 after Failure.

(a) Support reaction, V = 207 kN

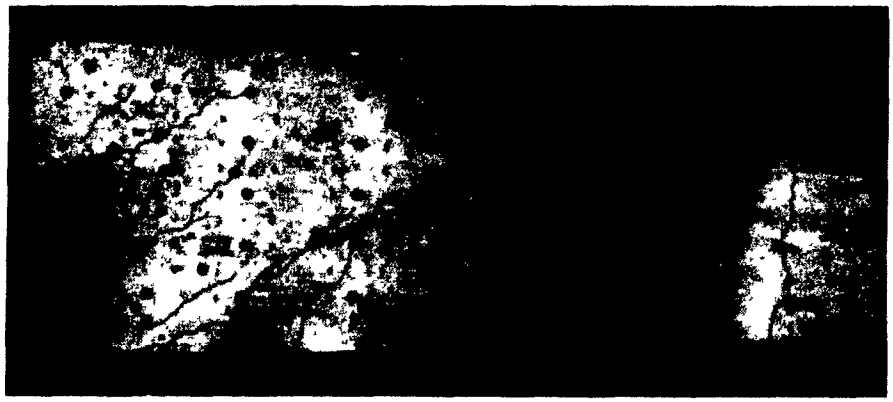

(b) Support reaction, V = 307 kN

Figure 4.14 Photographs of Dapped End Specimen D-3.

a number of inclined cracks crossed the vertical and inclined tension tie reinforcement.

Loading progressed using the test set-up shown in Fig. 3.10, however, in order to permit further loading of end D-3 after end D-4 failed, an additional support was placed at the failed end, 160 mm from the end of the full depth portion of the beam. The concentrated load was positioned at the centre of this new span of 2.69 m.

Specimen D-3 failed when the vertical reaction reached 372 kN. Figure 4.17 shows the appearance of specimen D-3 after failure. Significant splitting and spalling of the concrete occurred in the region near the nodal zone at the bottom of the full depth beam. A large inclined crack occurred after significant yielding of three stirrups near the

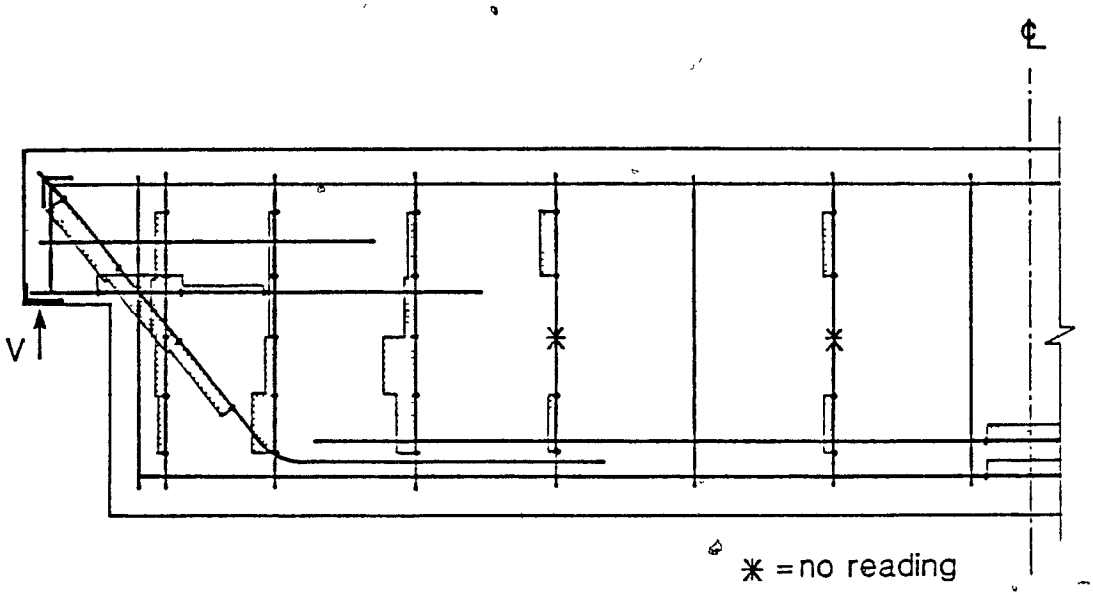

(a) Support reaction , V = 274 kN

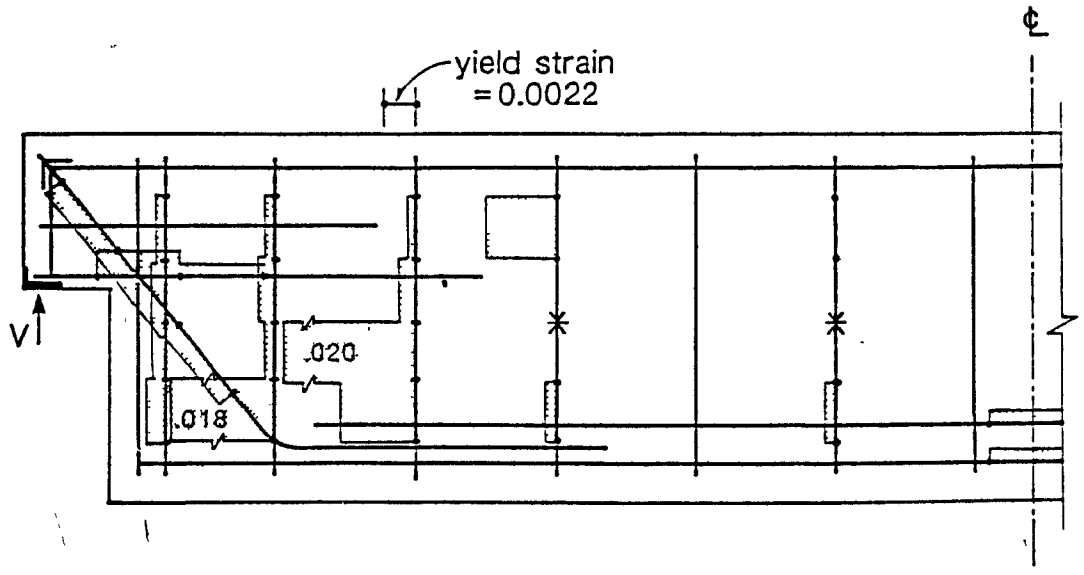

(b) Support reaction , V = 372 kN

Figure 4.15 Measured Strains in Vertical, Diagonal, and Horizontal Reinforcement in Dapped End Specimen D-3.

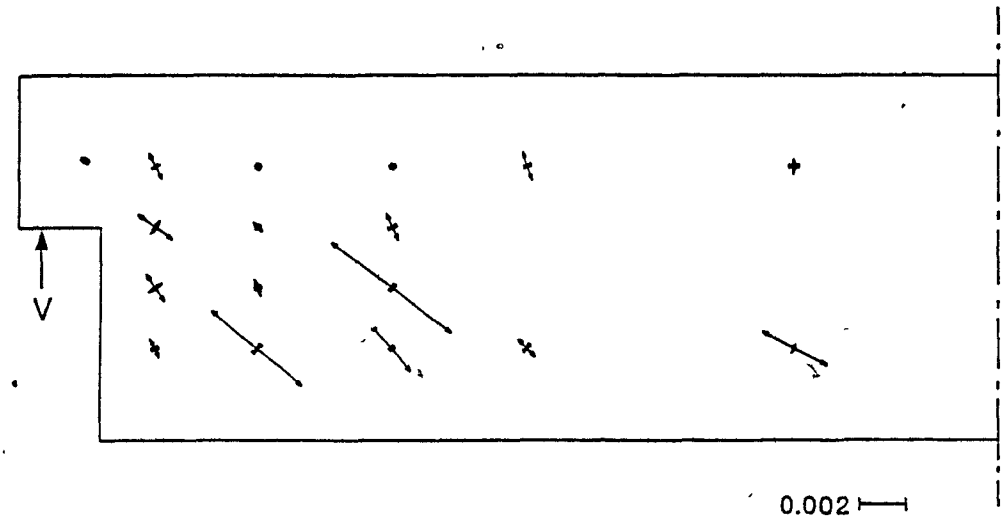

(a) Support reaction, V = 274 kN

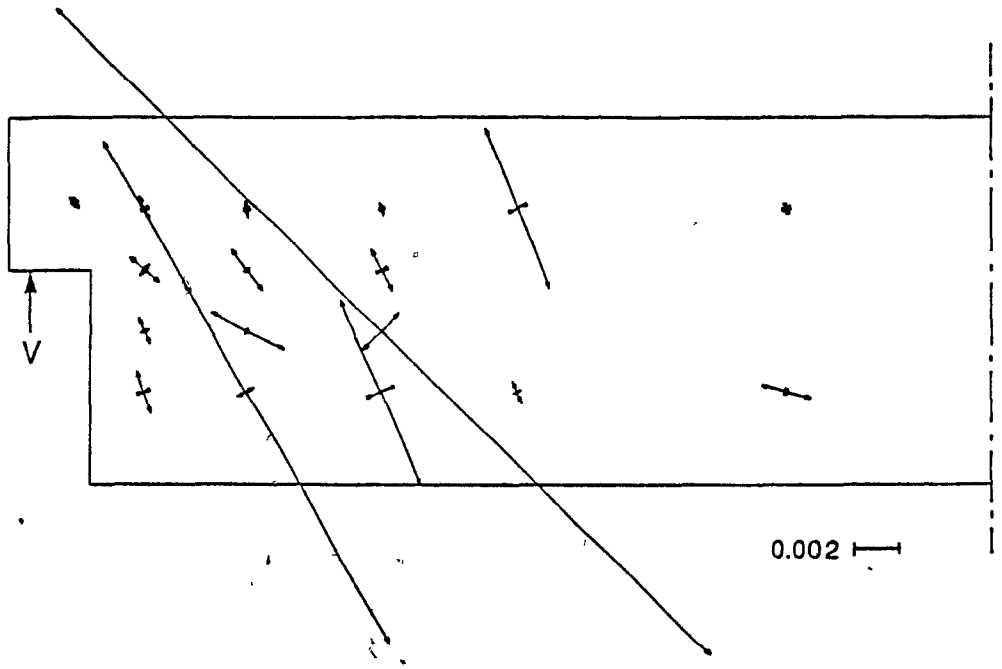

(b) Support reaction, V=372 kN

Figure 4.16 Principal Strains Determined from Rosette Readings for Dapped End Specimen D-3.

end of the beam as shown in Fig. 4.15b. It is noted that the inclined and vertical tension tie reinforcement did not reach yield, however, the horizontal tension tie reinforcement in the nib yielded in the region of the re-entrant corner.

Figure 4.16b shows the large principal tensile strains in the region of stirrup yielding and the significant tensile strains in the directions of the vertical and inclined tension ties.

4.7 Dapped End Specimen D-4

First flexural cracking occurred at midspan at a load causing an end reaction of 39.7 kN. Cracking at the re-entrant corner was observed when the end reaction reached 73.0 kN. When the reaction was 140 kN an inclined shear crack having a maximum width of 0.10 mm intersected the inclined end face. This crack opened to 0.30 mm when the reaction was 207 kN. The corresponding cracking pattern for D-4 is illustrated in Fig. 4.18a. As can be seen there are a number of inclined cracks which had formed perpendicular to the inclined face.

First yielding occurred in the stirrups near the bottom of the full depth beam at a load of 273 kN. Figure 4.19a shows the variations of measured strains in the vertical, inclined, and horizontal reinforcement for specimen D-4 at this stage. Figure 4.20a shows the principal strains calculated from the rosette readings. The fanning of the compressive stresses into the bottom of the main tension ties is evident. Figure 4.18b illustrates the cracking pattern for D-4 at this loading stage. As can be seen, inclined shear cracking in the main beam was well developed and a number of inclined cracks crossed the inclined tension tie reinforcement.

The inclined dapped end failed when the reaction reached 340 kN. Figure 4.21 shows the appearance of specimen D-4 after failure. Significant splitting and spalling of the concrete occurred in the region near the nodal zone at the bottom of the full depth beam. This large inclined crack occurred after significant yielding of three stirrups

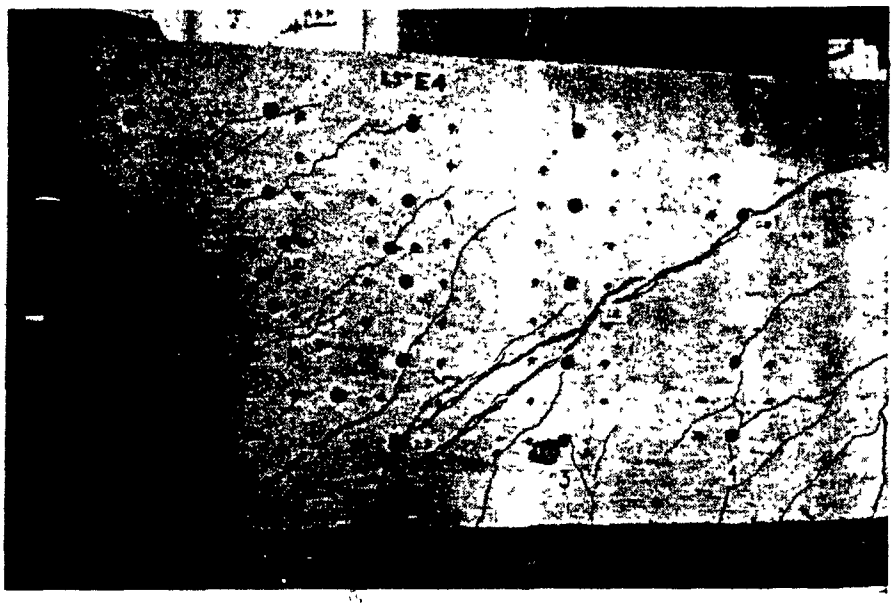

(a) Support reaction, V = 372 kN

(b) Close-up of lower nodal region after failure

Figure 4.17 Photographs of Dapped End Specimen D-3.

(a) Support reaction, V = 207 kN

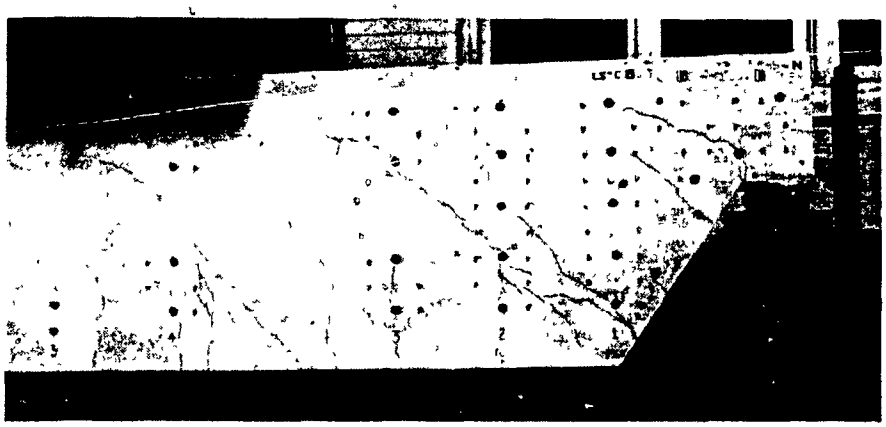

(b) Support reaction, V = 273 kN

Figure 4.18 Photographs of Dapped End Specimen D-4.

near the end of the beam as shown in Fig. 4.19b. It is noted that the inclined tension tie reinforcement and the horizontal tension tie reinforcement in the nib did not reach yield.

Figure 4.20b shows the large principal tensile strains in the region of stirrup yielding and the significant tensile strains in the direction of the inclined tension tie.

4.8 Web Hole Specimen H-1

Hairline flexural cracks first appeared at midspan at a load of 15.4 kN/m. At a load of 32.4 kN/m the maximum flexural crack width was 0.1 mm with a negative

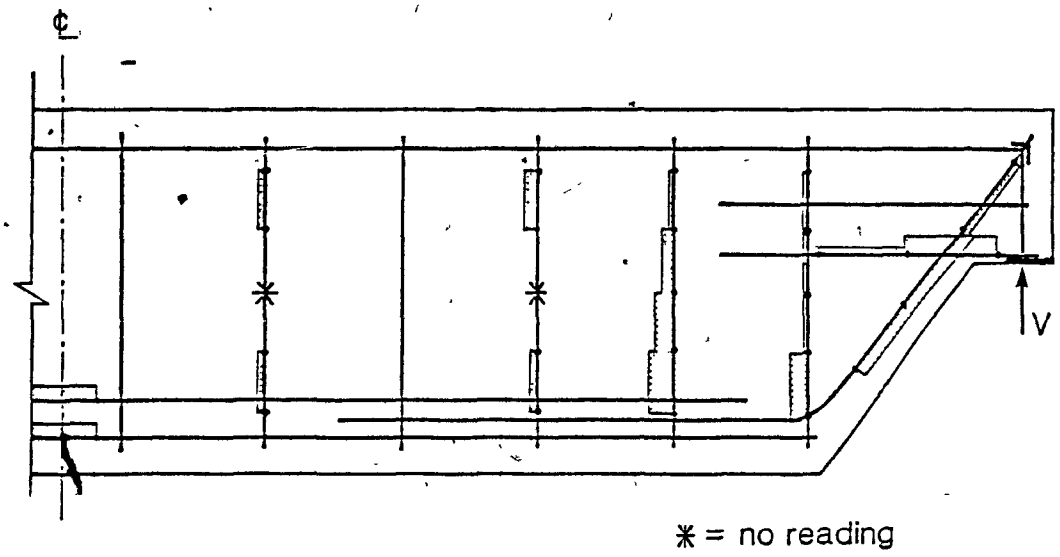

(a) Support reaction , V=273 kN

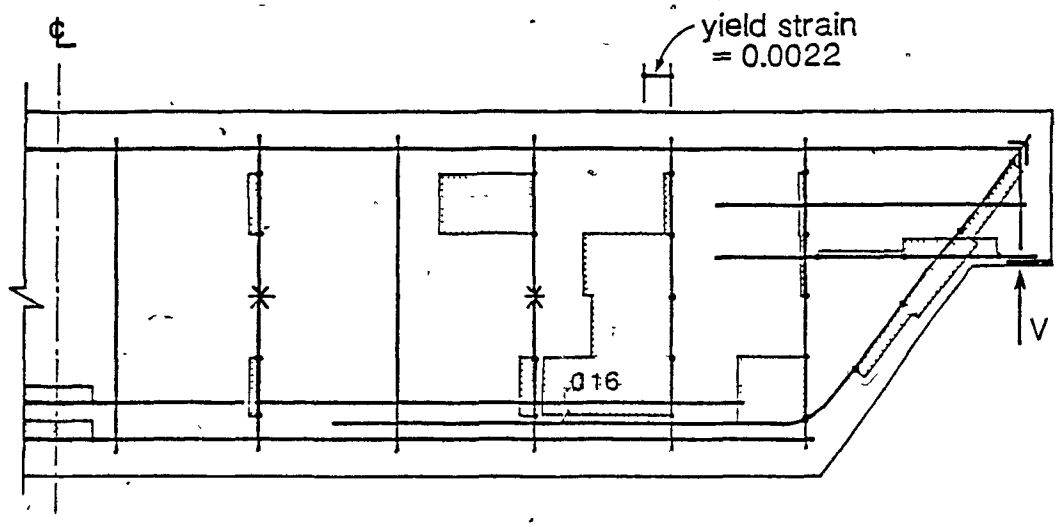

(b) Support reaction , V=329 kN

Figure 4.19 Measured Strains in Vertical, Inclined, and Horizontal Reinforcement in Dapped End Specimen D-4.

moment flexural crack appearing in the portion of the web beneath the opening together with positive moment cracks appearing in the flange above the opening. First shear cracking was observed between the opening and the support reaction area at a load of 43.6 kN/m. Figure 4.22a shows the appearance of the specimen at this stage. Positive

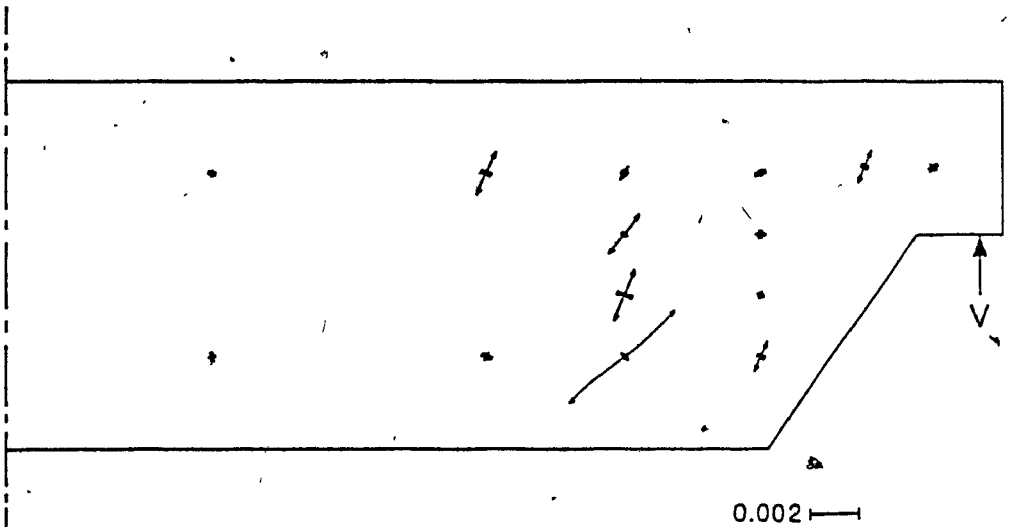

(a) Support reaction, V = 273 kN

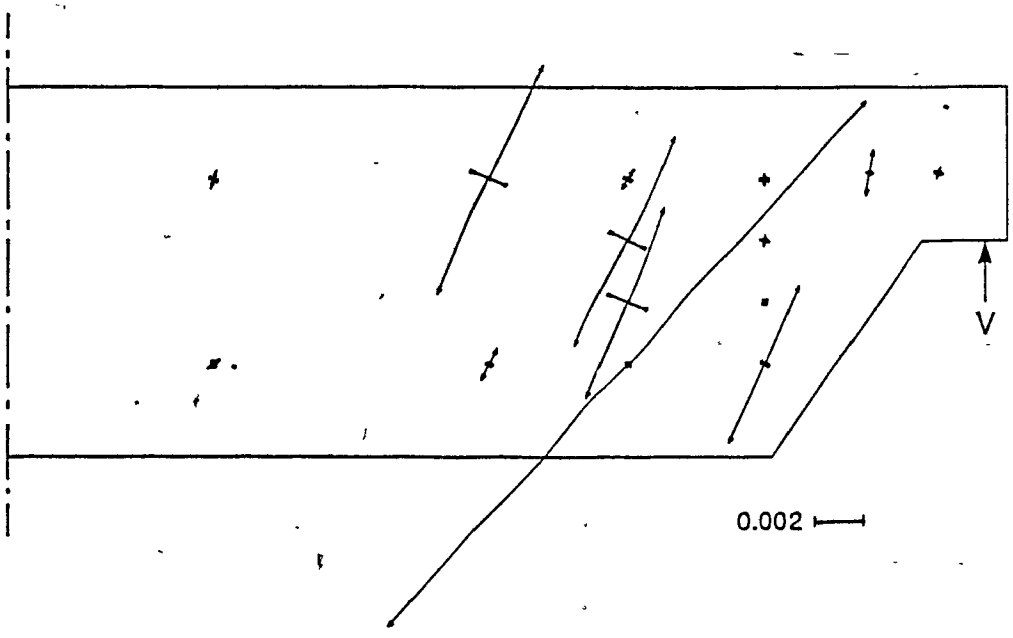

(b) Support reaction, V = 329 kN

Figure 4.20 Principal Strains Determined from Rosette Readings for Dapped End Specimen D-4.

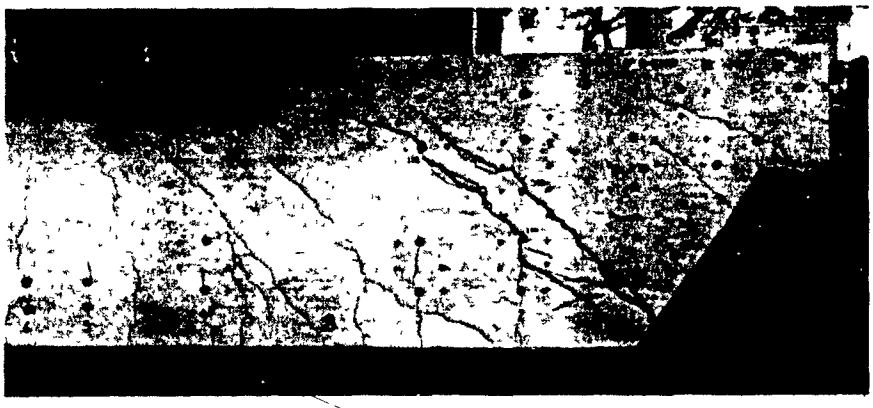

(a) Side view

(b) Close-up of lower nodal zone region

Figure 4.21 Photographs of Dapped End Specimen D-4 after Failure.

and negative moment flexural cracks having a width of 0.15 mm were observed in the flange at the ends of the opening.

At a load of 52.7 kN/m midspan flexural cracks were 0.2 mm and the shear cracking below the opening had a maximum crack width of 0.15 mm. First yielding of the

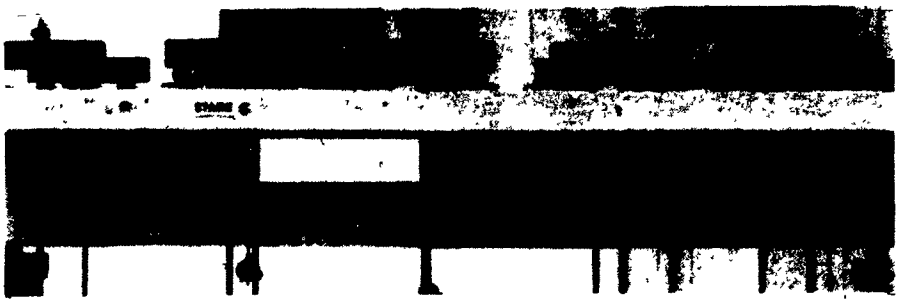

(a) Uniform load, w = 43.6 kN/m

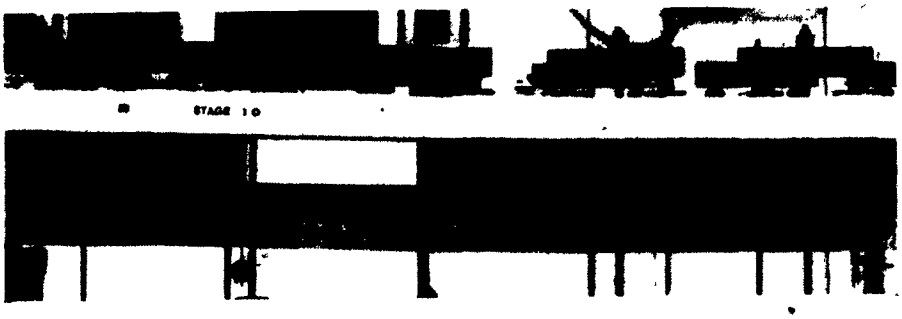

(b) Uniform load, w = 88.1 kN/m

Figure 4.22 Photographs of Web Hole Specimen H-1.

stirrups beneath the opening occurred when the load was 88.1 kN/m. Figure 4.22b shows the appearance of specimen H-1 at first yielding, while Fig. 4.23a shows the variations in the measured stirrup strains. At this load stage concrete crushing was evident in the web at the lower corner of the opening furthest from the support. The maximum width of shear cracking between the opening and the support was 0.5 mm. The maximum crack width in the web below the opening was 0.35 mm.

At a load of 97.3 kN/m significant crushing of the concrete occurred in the web near the upper corner of the opening closest to the support. At a load of 99.7 kN/m the end of the beam with opening H-2 failed. Testing was continued on specimen H-1 after a support was placed at the other end reducing the clear span to 3.64 m (see Section 3.6).

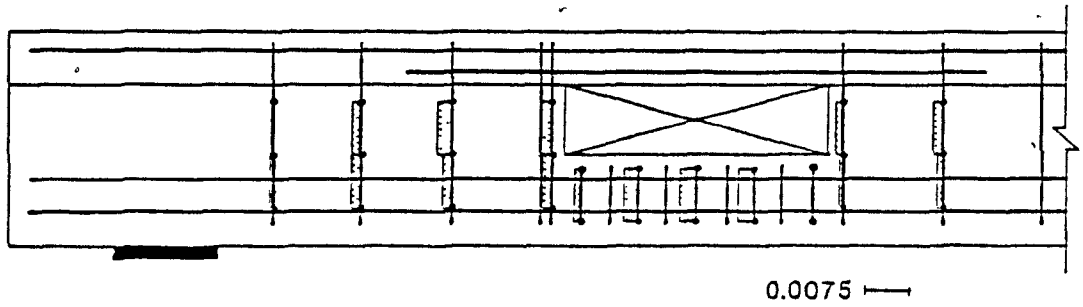

(a) Uniform load, w_u = 88.1 kN/m

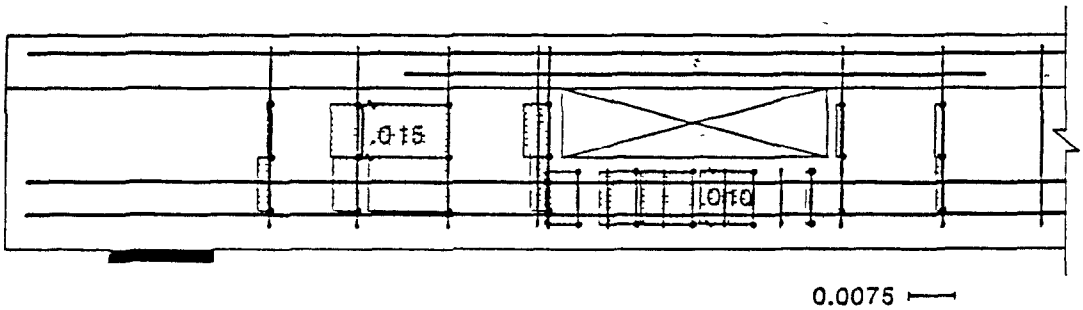

(b) Uniform load, w_u = 177 kN/m

Figure 4.23 Measured Stirrup Strains in Web Hole Specimen H-1.

Failure occurred at a uniform load of 177 kN/m by shear failure of the region beneath the opening accompanied by spalling of the concrete cover in this region. Figure 4.24 shows the appearance of specimen H-1 at failure. The variation in the stirrup strains in the region around the opening in the T-beam at failure is given in Fig. 4.23b. The significantly higher strains in the stirrups beneath the opening and the large strains in the main vertical tension tie are apparent.

4.9 Web Hole Specimen H-2

Flexural hairline cracks first appeared at midspan at a load of 15.4 kN/m. At a load of 32.4 kN/m the maximum flexural crack width was 0.1 mm with a negative moment

(a) Side view

(b) Detail of opening

Figure 4.24 Photographs of Web Hole Specimen H-1 at Failure, w = 177 kN/m.

flexural crack appearing in the portion of the web beneath the opening together with positive moment cracks appearing in the flange above the opening. First shear cracking was observed between the opening and the support reaction area at a load of 43.6 kN/m. Positive and negative moment flexural cracks having a width of 0.15 mm were observed in the flange at the ends of the opening. Figure 4.25a shows the appearance of specimen H-2 at this load level.

At a load of 52.7 kN/m, midspan flexural cracks were 0.2 mm and the shear crack-

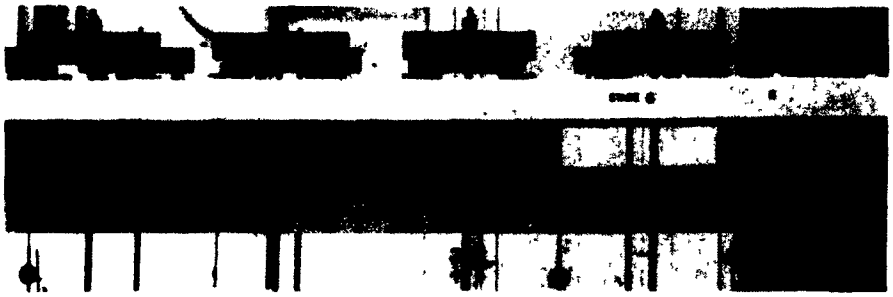

(a) Uniform load, w = 43.6 kN/m

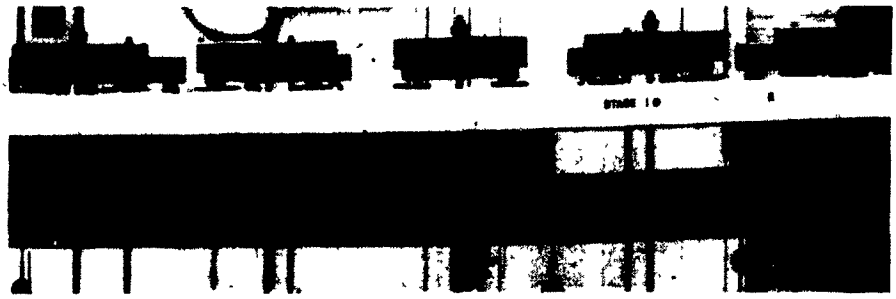

(b) Uniform load, w = 88.1 kN/m

Figure 4.25 Photographs of Web Hole Specimen H-2.

ing below the opening had a maximum crack width of 0.15 mm. First yielding of the stirrups beneath the opening occurred between loads of 79.3 kN/m and 88.1 kN/m with significant strains developing at a load of 88.1 kN/m. Figure 4.25b shows appearance of specimen H-2 at first yielding. At this load stage concrete crushing was evident in the web at the lower corner of the opening furthest from the support. The maximum width of shear cracking between the opening and the support was 0.8 mm. The maximum crack width in the web below the opening was 0.5 mm. The measured stirrup strains at first yielding are shown in Fig. 4.26a.

At a load of 97.3 kN/m significant crushing of the concrete occurred in the web near the upper corner of the opening closest to the support. The maximum load reached was 99.7 kN/m when shear failure took place beneath the opening accompanied by spalling

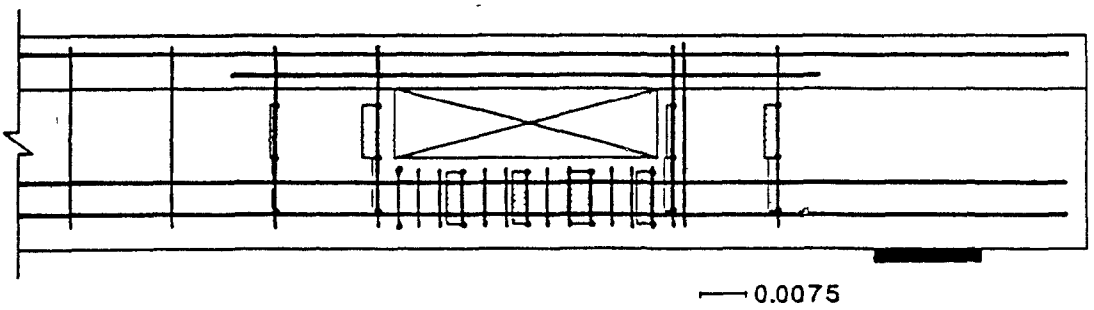

(a) Uniform load, w_u = 88.1 kN/m

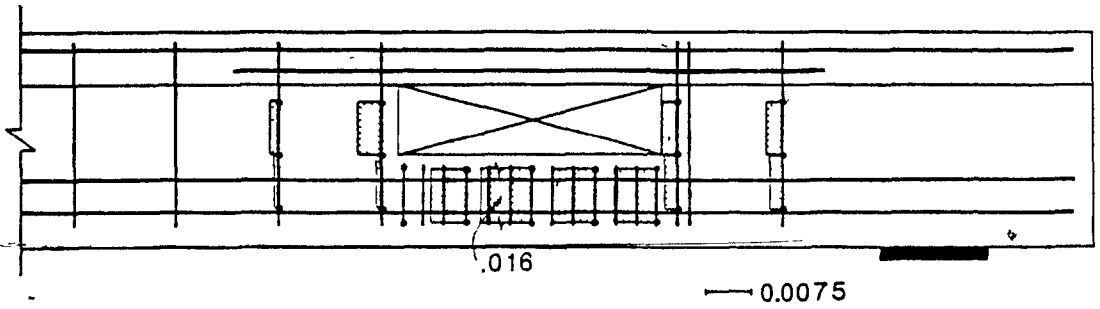

(b) Uniform load, w_u = 99.7 kN/m

Figure 4.26 Measured Stirrup Strains in Web Hole Specimen H-2.

of the concrete cover in this region. Signs of shear failure in the flange above the opening were evident at this stage. Figure 4.27 shows the appearance of the specimen at the failure load. Figure 4.26b gives the variation in the stirrup strains in the region of the opening of the T-beam at the ultimate load stage. The significantly higher strains in the stirrups beneath the opening and the large strains in the main vertical tension tie are apparent.

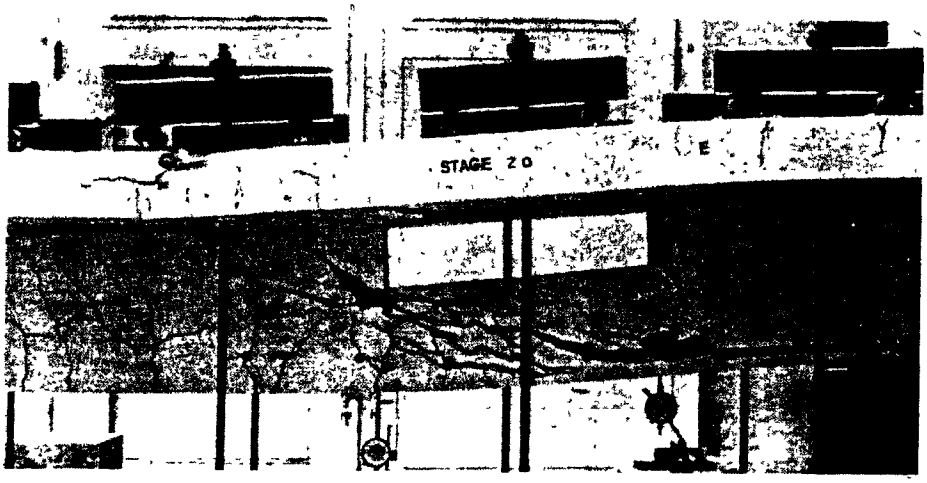

(a) Side view

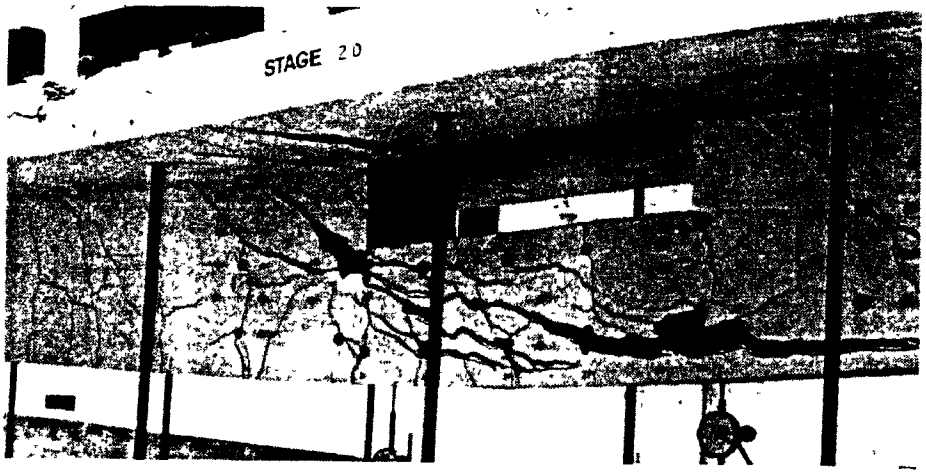

(b) Detail of opening

Figure 4.27 Photographs of Web Hole Specimen H-2 after Failure.

CHAPTER 5

PREDICTIONS OF EXPERIMENTAL RESULTS

5.1 Introduction

In this chapter the responses of a number of test specimens containing disturbed regions are compared with the predictions using the non-linear finite element analysis program, FIELDS, and with the predictions using simple strut and tie models. In order to validate the non-linear finite element program the predictions using this program are first compared with reinforced concrete members having uniform fields of diagonal compression. Recent experimental results that were well-instrumented are used in the comparisons.

In the finite element analyses the compressive strength of concrete, f'_c, was taken from the standard cylinder results given in Table 3.1. The tensile strength of concrete, f_{cr}, was taken as $0.33\sqrt{-f'_c}$ and the strain at peak compressive stress, ϵ'_0, was taken as $2f'_c/(5\,500\sqrt{-f'_c})$ unless otherwise noted. Poisson's ratio was taken as 0.10. The steel reinforcement was modelled with a bi-linear stress-strain relationship. The yield stress, f_y, assumed in the analyses are given in Table 3.2. The initial steel elastic modulus, E_s, was taken as 200 000 MPa, while the tangent modulus after yielding, E_{st}, was taken as 2 000 MPa, unless otherwise noted.

The finite elements were nine-noded quadrilaterals (CFTQ) and six-noded triangles (CFTT) with four by four quadrature used for numerical integration. In all cases

the applied loads were simulated with consistent nodal loads. The analyses typically used load increments equal to one tenth of the expected failure load.

5.2 Reinforced Concrete Shear Panels Tested by Vecchio and Collins

The program FIELDS was used to predict the responses of a number of reinforced concrete panels tested in pure shear by Vecchio and Collins[11,12] (see Fig. 1.2), in order to verify the capabilities of elements CFTQ and CFTT used in FIELDS.

These well instrumented tests were used to develop[11,12] the stress-strain characteristics of cracked concrete that are described in Chapter 2. Since these specimens failed in different ways they provide a means of checking the computer program in a variety of circumstances for simple elements displaying uniform fields of diagonal compressive stresses in the concrete.

Each of the shear panels tested was 890 x 890 mm by 70 mm thick (see Fig. 1.2). Some of the important parameters for six of the shear panels are summarized in Table 5.1.

Table 5.1 Parameters of Shear Panels Tested By Vecchio and Collins.

Specimen	Longitudinal Steel		Transverse Steel		Concrete	
	ρ_{sx}	f_y (MPa)	ρ_{sy}	f_y (MPa)	ϵ'_c	f'_c (MPa)
PV4	0.01056	242	0.01056	242	0.00250	26.6
PV11	0.01785	235	0.01306	235	0.00260	15.6
PV12	0.01785	469	0.00446	269	0.00250	16.0
PV20	0.01785	460	0.00885	297	0.00180	19.6
PV22	0.01785	458	0.01524	420	0.00200	19.6
PV27	0.01785	442	0.01785	442	0.00190	20.5

Each of the shear panels was idealized with either a single nine-noded CFTQ element or with two six-noded CFTT elements. Consistent nodal loads were applied to simulate the applied pure shear loads. The reinforcement tangent modulus after yielding, E_{st}, was taken as 500 MPa for this series of analyses.

Figure 5.1 compares the predicted shear stress – shear strain responses with the test results for the six reinforced concrete panels described in Table 5.1.

Specimen PV4 contained equal amounts of reinforcement in the x and y directions with failure occurring by yielding of both sets of reinforcement. As can be seen from Fig 5.1a the predictions using program FIELDS agrees reasonably well with the test response.

Specimen PV11 contained different amounts of reinforcement in the x and y directions with failure taking place by yielding of the y reinforcement followed by yielding of the x reinforcement. This mode of failure was predicted by program FIELDS.

Specimen PV12 contained about four times as much steel in the x direction as in the y direction. Observations during the testing indicated that considerable redistribution of stresses takes place after the yielding of the reinforcement in the y direction. As can be seen the response is predicted well by program FIELDS.

Specimen PV20 contained twice as much reinforcement in the x direction as in the y direction. In addition, the reinforcement in the x direction had a yield stress of 460 MPa, while the reinforcement in the y direction had a yield stress of only 297 MPa. Yielding was observed in the test at a shear stress level of 4.14 MPa with failure occurring at a shear stress level of 4.26 MPa by sliding along a crack interface. The predicted yield load is 4.00 MPa with failure predicted to occur at a shear stress of 4.49 MPa. At the maximum predicted load the principal compressive stress in the concrete is about 90% of the crushing strength and there is a significant shear stress on the crack interface.

Specimen PV22 contained a slightly larger amount of reinforcement in the x direction than in the y direction. In addition, the reinforcement in the x direction had a slightly higher yield stress. Specimen PV27 had identical reinforcement in the x and y directions. Specimens PV22 and PV27 failed by crushing of the concrete without yielding of the reinforcement at shear stress levels of 6.07 and 6.35 MPa, respectively.

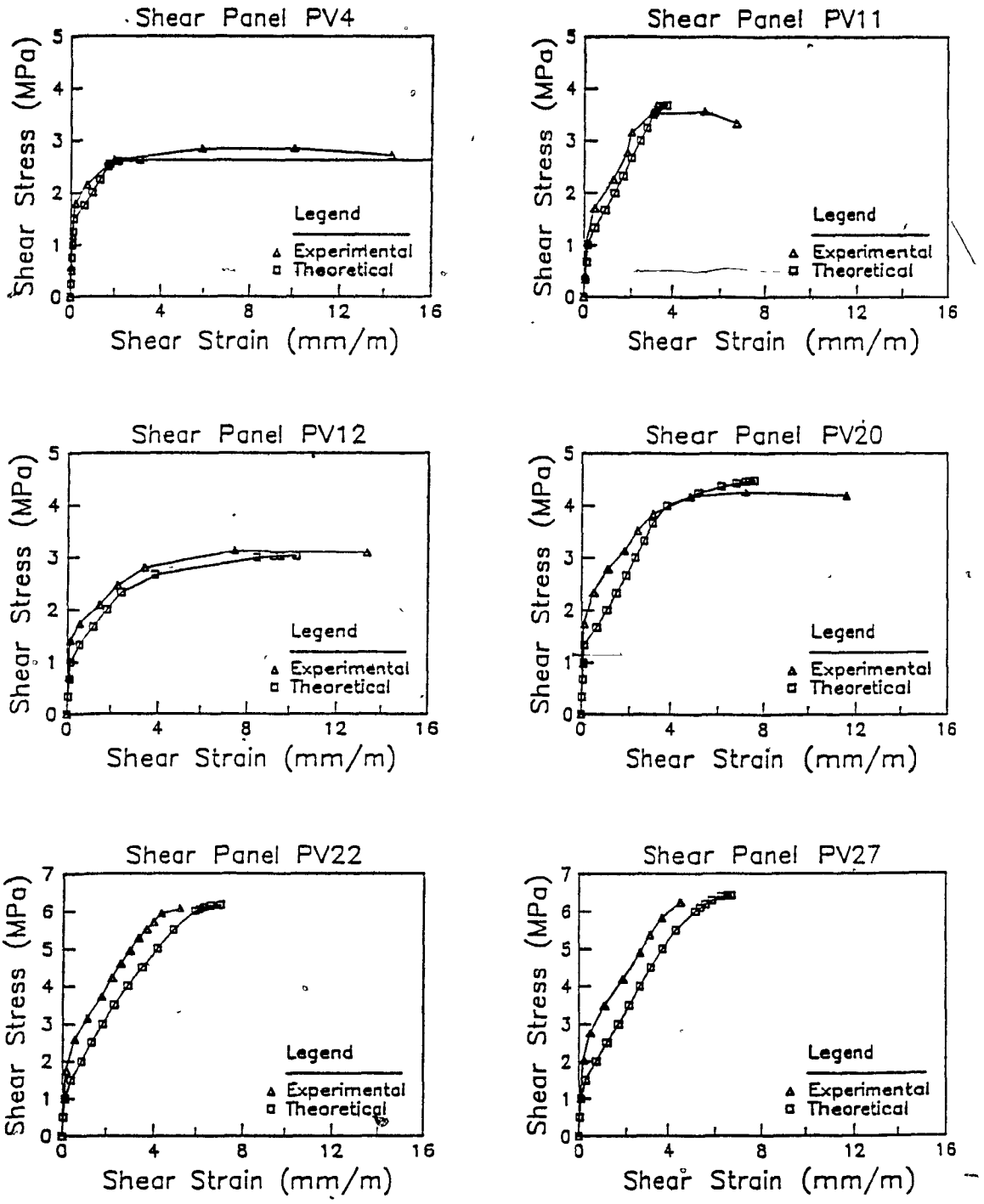

Figure 5.1 Comparison of Predicted Responses and Measured Responses of Shear Panels Tested by Vecchio and Collins[11,12]

This crushing was followed by sliding shear failures in both cases. For specimens PV22 and PV27 failure is predicted to occur by crushing of the concrete with f_{c2max} equal to about 60% of f'_c at shear stress levels of 6.18 and 6.43 MPa, respectively.

In predicting the responses of these six shear panel tests it was assumed that the concrete cracking stress was $0.33\sqrt{-f'_c}$. In reporting the test results of the panels Vecchio and Collins[11,12] found cracking stresses somewhat higher than $0.33\sqrt{-f'_c}$. For example, the cracking stress assumed in predicting the response of specimen PV22 was 1.46 MPa while the measured cracking stress was 2.42 MPa. It is noted that if higher cracking stresses are assumed then greater values of f_{c1} would be possible and the response predictions would be stiffer after cracking.

5.3 Uniformly Loaded Beams Tested by Mailhot

In order to verify the ability of program FIELDS to predict the response of a flexural member containing large regions of uniform fields of diagonal compressive stresses and few disturbances, the program was used to analyze a uniformly loaded T-beam. The details of specimen B tested by Mailhot[19] are given in Fig. 5.2. This beam was part of a research programme to investigate the "staggering concept" used for the design of stirrups and to demonstrate the design procedures of the 1984 Canadian Concrete Code.[13]

The T-beam specimen was designed for a uniform load of 106 kN/m and the stirrups were provided in bands of $d_v / \tan\theta$ equal to 586 mm. The principal compressive angle, θ, used in design was 27°.

Figure 5.3a shows the positions of the strain targets located on the concrete surface and on the steel reinforcement for one end of the beam. These targets on the web formed strain rosettes which enabled the principal strains and their directions to be determined as shown in Fig. 5.3b. As can be seen the large principal tensile strains and low principal compressive strains near midspan reflect the high moment and low

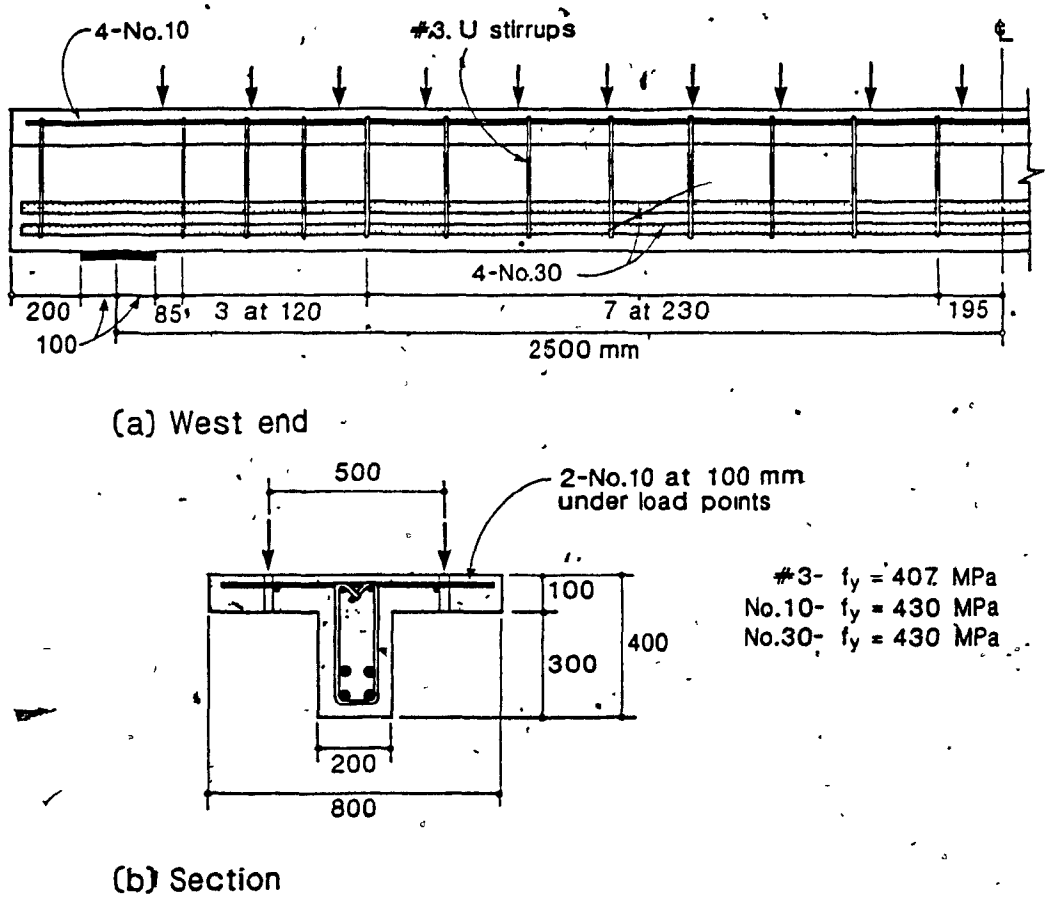

Figure 5.2 Details of Uniformly Loaded Beam B Tested by Mailhot[19]

shear in this region. It is apparent that at midspan the longitudinal reinforcement was well beyond yield at ultimate. It is possible to identify a region between the support and midspan in which relatively uniform fields of diagonal compression exist.

As can be seen from Fig. 5.4 the finite element model consisted of four elements over the depth of the member. Due to the symmetrical nature of the loading and of the supports only half the beam was modelled. The finite element mesh was chosen such that the elements coincided with the actual stirrup spacing. The support condition of the steel plate bearing surface was simulated with the truss elements shown in Fig. 5.4, to account for the relatively small actual bearing surface after the beam rotates on its supports. Consistent nodal loads were used to simulate the uniform load applied

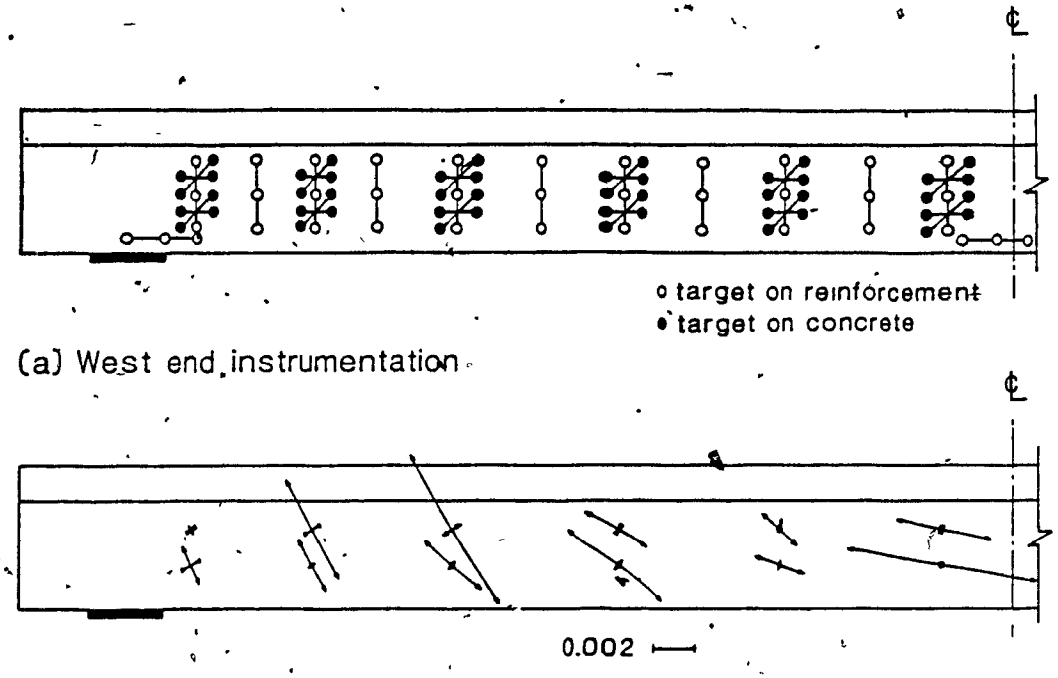

Figure 5.3 Principal Strains Determined from Strain Rosettes for Specimen B.[19]

to the top face of the top row of elements. The flow of the compressive stresses from the top flange of the T-beam at midspan to the support reaction area is evident from Fig. 5.4a. The finite element analysis predicts a failure load of 122 kN/m by flexural yielding of the longitudinal reinforcement after significant yielding occurred in some of the stirrups. The test specimen failed at a load of 130 kN/m after experiencing large strains in the longitudinal steel at midspan and after some stirrup strains reached about three times the yield strain. It is noted that the predicted response did not account for the horizontal restraint at the ends of the beam due to the friction between the beam and the steel bearing supports, thus giving a conservative strength prediction.

The predicted principal strains and their directions are given in Fig. 5.4b. As can be seen these predicted strains agree reasonably well with the experimentally determined values (see Fig. 5.3b).

A comparison of the predicted and measured strains in the transverse reinforcement

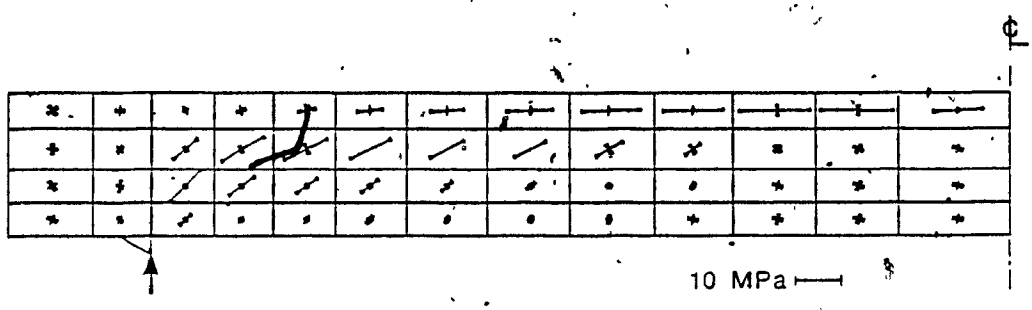

(a) Principal stresses, $w_u = 124$ kN/m

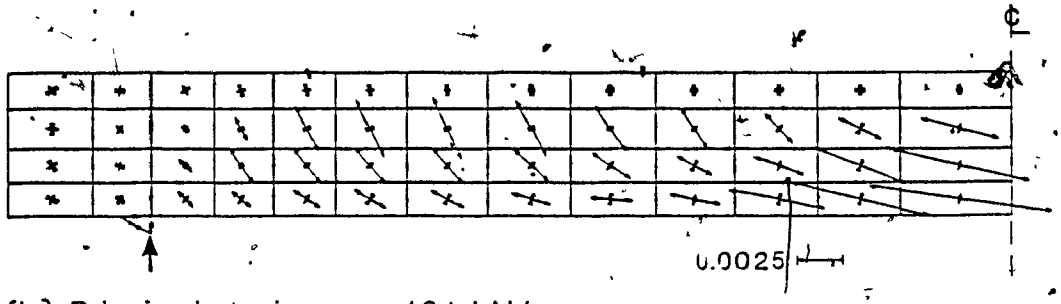

(b) Principal strains, $w_u = 124$ kN/m

Figure 5.4 Predicted Principal Concrete Stresses and Principal Strains for Specimen B.

is given in Fig. 5.5. The strain measurements permit this comparison to be made for the top and bottom of each stirrup. As can be seen the general trend of the predicted values agrees reasonably well with the measured values taken at the load stage closest to the predicted failure load.

It is noted that in comparing the predicted and measured strain values the discrete nature of the cracks result in significant fluctuations in the measured values, whereas the predicted values are averages based on a smeared cracking pattern.

5.4 Continuous Deep Beams Tested by Rogowski, MacGregor and Ong

In order to demonstrate the versatility of program FIELDS it was used to predict the responses of statically indeterminate members containing disturbed regions. Two of the continuous deep beams tested by Rogowsky, MacGregor and Ong[20] demonstrate the

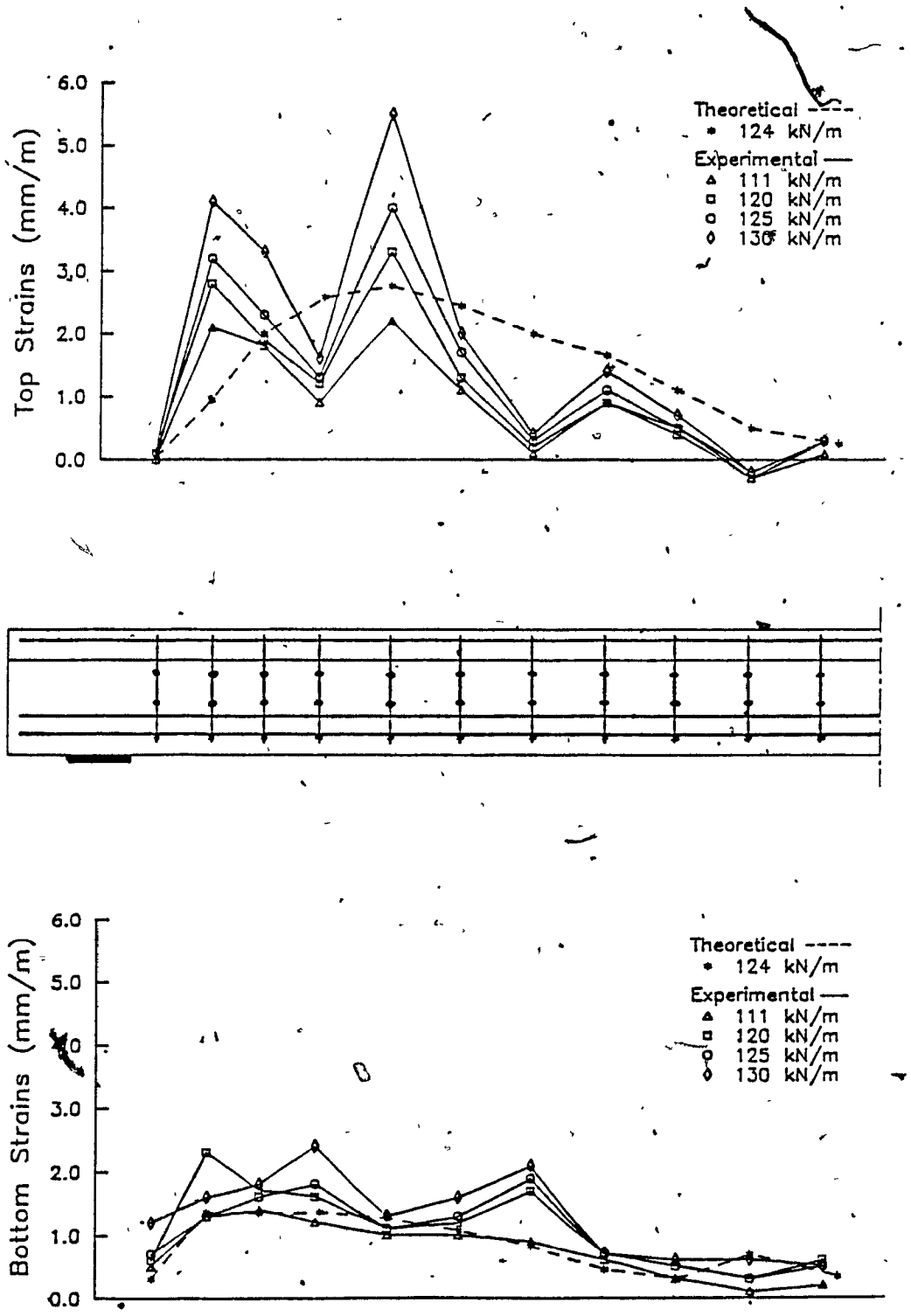

Figure 5.5 Comparison of Measured and Predicted Strains in Transverse Reinforcement for Specimen B.[19]

influence of shear span to depth ratio on the response. Specimens 5/1.5 and 5/2.0 have shear span to depth ratios of 1.5 and 2.0 respectively. The main reinforcement details are shown in Fig. 5.6a. In addition to the reinforcement shown the columns contained significant amounts of longitudinal and transverse reinforcement. Both specimens have similar concrete strengths (f'_c = 39.6 MPa and 41.1 MPa) and are 200 mm thick.

Figure 5.6b shows the finite element mesh used to model these two beams. Due to symmetry about the central supports only half the beams were modelled with a 5 by 14 grid of CFTQ elements. Four additional elements were used to model the loading columns. All of the reinforcement in the deep beam and the columns was modelled. The elements were chosen such that they were centred on the main horizontal reinforcement. Figure 5.6b also shows the predicted deflected shapes for these two deep beams.

Figures 5.6c and d show the principal stresses and the principal strains at the centres of the elements predicted by program FIELDS at ultimate load. Specimen 5/1.5 failed in the north shear span when the applied load in this span reached 858 kN. After strengthening the north side the south shear span failed at a load of 879 kN. The predicted capacity is 890 kN. Specimen 5/2.0 failed at corresponding loads of 677 kN and 693 kN which compare well with the predicted capacity of 695 kN. Since both specimens had the same total amount of transverse reinforcement in each shear span, the 21% drop in load carrying capacity between these two specimens is due to the difference in their geometries. This geometric difference resulted in a larger direct compressive strut action in the "deeper" specimen (5/1.5). As can be seen from Fig. 5.6c, the compressive struts in both specimens become wider between the loading point and the reaction areas. In both cases failure is predicted to occur in the interior shear span by yielding of the transverse reinforcement, followed by crushing of the concrete. Specimen 5/1.5 exhibited an inclined crack which opened by 6 mm which indicates that yielding of the transverse reinforcement occurred. Specimen 5/2.0 also exhibited yielding of the transverse reinforcement. The negative moment near the

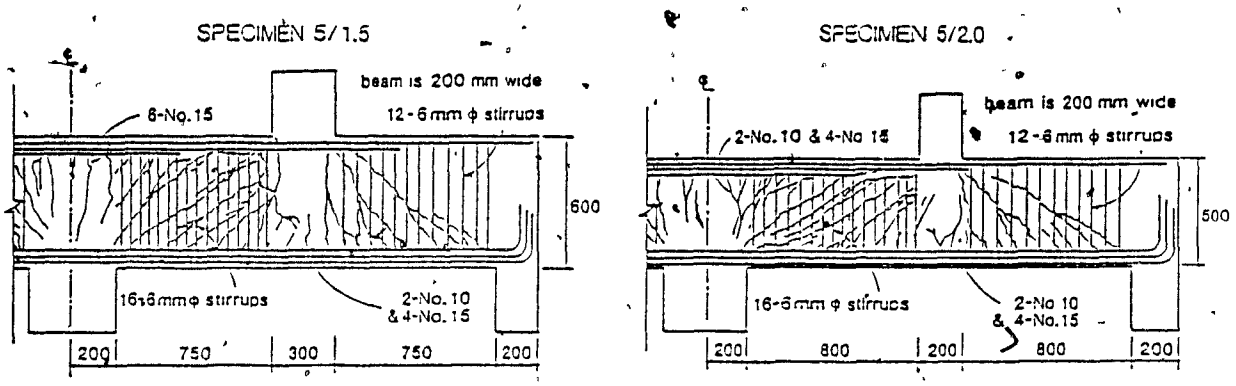

(a) Reinforcement details and failure concitions

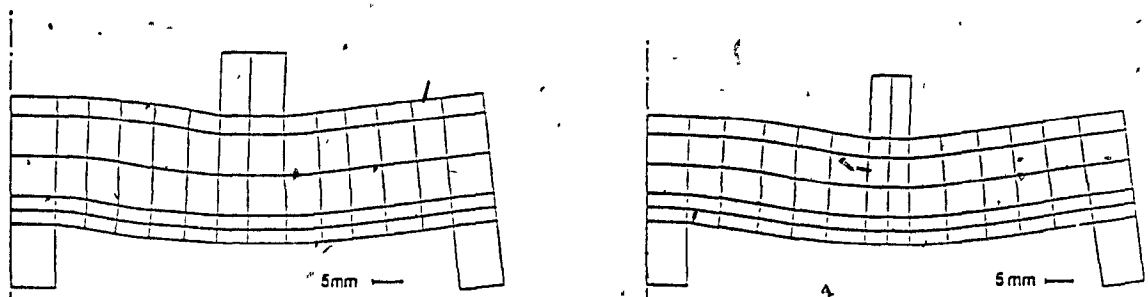

(b) Finite element mesh and deflected shapes at ultimate

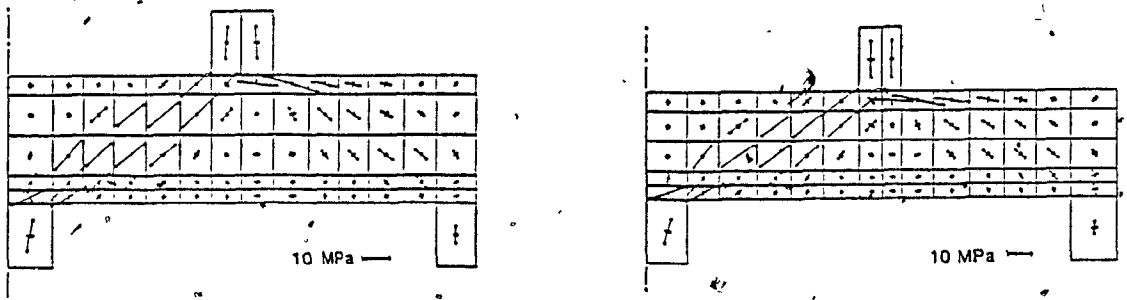

(c) Predicted principal stresses

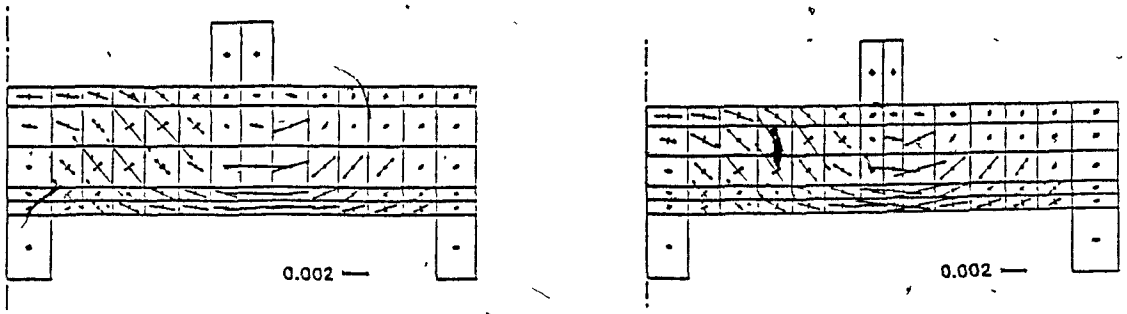

(d) Predicted principal strains

Figure 5.6 Continuous Deep Beams Tested by Rogowsky, MacGregor and Ong.[20]

central support results in larger principal tensile strains (see Fig. 5.6d), thus softening the concrete and reducing its compressive strength. Due to the large tensile strains the principal tensile stresses are reduced to zero in some elements (see Fig. 5.6c). The regions of crushing of the concrete are illustrated in Fig. 5.6a for the west face of the beam. Although the concrete cover remained intact near the top and bottom of the beams considerable spalling and splitting along the plane of the stirrup centrelines were observed in the middle regions.

5.5 Corbel Specimen C-1

Figure 5.7 summarizes the reinforcement details of the double-sided corbel specimen C-1. Further details about this specimen are given in Section 3.3 and the experimental results are given in Section 4.2.

Figure 5.7 also illustrates the analysis of specimen C-1 using a simple strut and tie model. Using the measured material properties (all material resistance factors are taken as 1.0) the main tension tie can supply a force of $A_s f_y$ = 800 mm^2 x 444 MPa = 355 kN. If we assume that the yield force of the tension tie will govern the corbel failure then from the statics of the truss (see Fig. 5.7b) the predicted failure loads are 408 kN vertically and 81.6 kN horizontally. The fanning compressive strut has its maximum stress in the nodal zone at the top of the corbel. The nodal zone stress under the 50 mm wide by 300 mm long by 25 mm thick bearing plate is 408 kN / (50 mm x 300 mm) = 27.2 MPa. The nodal zone stress limit is $0.75 f'_c$ = 0.75 x 40.4 MPa = 30.3 MPa. Hence, it is predicted that yielding of the main tension tie will initiate the failure of the corbel followed closely by crushing of the concrete in the top nodal zone. The actual reinforcement details for this corbel are shown in Fig. 5.7c. As can be seen additional closed horizontal ties, having an area of at least 50% of A_s and distributed within the top two-thirds of the corbel, have been provided in accordance with code detailing requirements[4,13] for brackets and corbels. In the analysis using

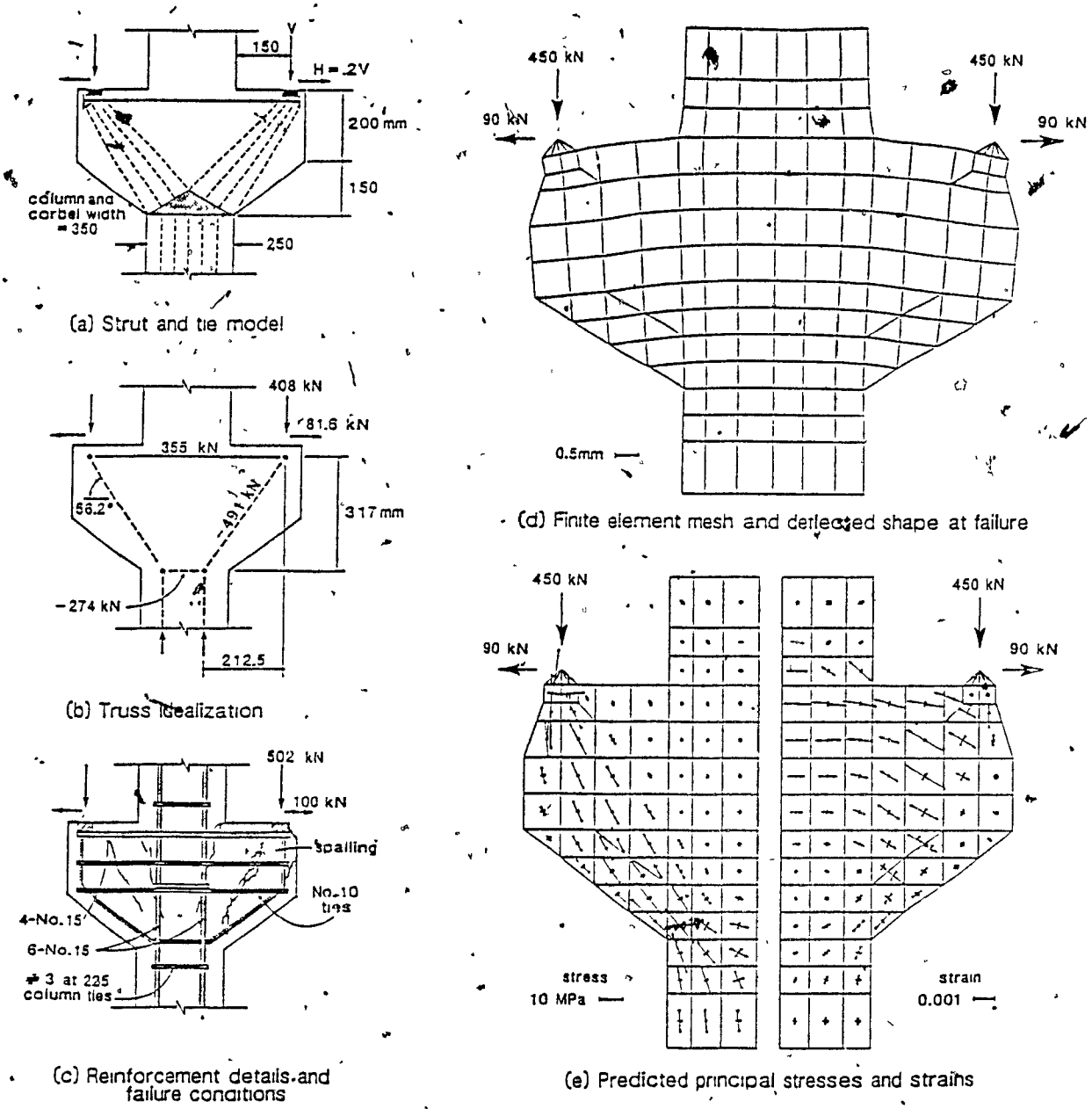

Figure 5.7 Corbel Specimen C-1.

the simplified strut and tie model this additional reinforcement was neglected. Failure occurred in specimen C-1 at a vertical load of 502 kN by concrete crushing under the bearing plate after large strains were recorded in the main tension tie and after the occurrence of severe spalling of the concrete cover surrounding the bearing plate (see Figs. 4.4 and 5.7c).

Figure 5.7d shows the finite element mesh and the deformed shape predicted by program FIELDS close to failure. Only half of the specimen was modelled due to the symmetry of the specimen and the loading. A total of 65 CFTQ and 8 CFTT elements were used. Figure 5.7e illustrates the principal stresses and principal strains in the concrete predicted by the finite element analysis. In the modelling of this corbel, stiff truss elements were used to simulate the presence of a steel loading block which was attached to the top of the steel bearing plate. The two elements in the top row surrounding the bearing area were given thicknesses of 300 mm to simulate the spalling of the 25 mm of concrete outside the bearing plate. As can be seen from Fig. 5.7d the mesh also simulated the likely concrete spalling zones in the unarmoured region outside of the bearing plate. All of the reinforcement in the corbel and column was modelled in the finite element analysis. As can be seen from Fig. 5.7e the predicted flow of concrete compressive stresses is somewhat different than that assumed in the simple strut and tie model. Due to the presence of the additional horizontal reinforcement and due to the vertical cracking in the corbel, these compressive stresses are more curved towards the outer surface of the corbel and become more concentrated as they funnel into the column. Program FIELDS predicts failure to occur at a vertical load of 450 kN, that is, at 90% of the actual failure load, by yielding of the main tension tie reinforcement. The large predicted tensile strains are evident in Fig. 5.7e.

An additional finite element analysis was carried out with the horizontal loading located directly at the top of the steel bearing plate. This resulted in a predicted failure load of 525 kN which demonstrates the sensitivity of these types of connections to small changes in load eccentricities.

5.6 Dapped End Beam Tests D-1 and D-2

Figures 5.8a and b show the strut and tie model and truss idealization used to analyze the rectangular dapped end test specimen D-1. The reinforcement details are

summarized in Fig. 5.8c. More details about this specimen are given in Section 3.4 and the experimental results are given in Section 4.3. The additional horizontal bars, provided in the nib to satisfy the code detailing requirements,[4,13] were not included in the simple truss idealization. In predicting the failure load it is assumed that the material resistance factors were equal to 1.0. If it is assumed that failure will be governed by yielding of the vertical tension tie then the force in this tie will be $A_s f_y$ = 800 mm^2 x 445 MPa = 356 kN. The forces in the other truss members can be determined from statics (see Fig. 5.8b).

In order to investigate the capacity of the nodal zone region at the top of the vertical tension tie we first assume that the concrete cover spalls off down to the centreline of the stirrups in this highly stressed region. Hence, the stress on the top face of the nodal zone anchoring this tension tie is 356 kN / 110 mm x 210 mm = 15.4 MPa. This is less than the nodal zone stress limit of $0.75 f'_c$ = 0.75 x 29.8 = 22.4 MPa.

The most critical section of the compressive strut going from the support to the top of the vertical tension tie is located at the interface with the top nodal zone. Since it is assumed that the faces of of the nodal zone are equally stressed then the compressive stress, f_{c2}, in the strut at the face of the nodal zone is also equal to 15.4 MPa. The maximum compressive stress, f_{c2max}, that this strut can carry can be determined from Eq. (2-2) if we assume that the strain ϵ_s in the vertical tension tie crossing the strut is at the yield strain (2.23 x 10^{-3}). Hence, from Eq. (2-1):

$$\epsilon_1 = \epsilon_s + \frac{\epsilon_s + 0.002}{\tan^2 \alpha_s} = 0.00223 + \frac{0.00223 + 0.002}{\tan^2 47.3^\circ} = 0.00583$$

and from Eq. (2-2):

$$f_{c2max} = \frac{f'_c}{0.8 + 170\epsilon_1} = \frac{29.8}{0.8 + 170 \times 0.00583} = 16.6 \text{ MPa}$$

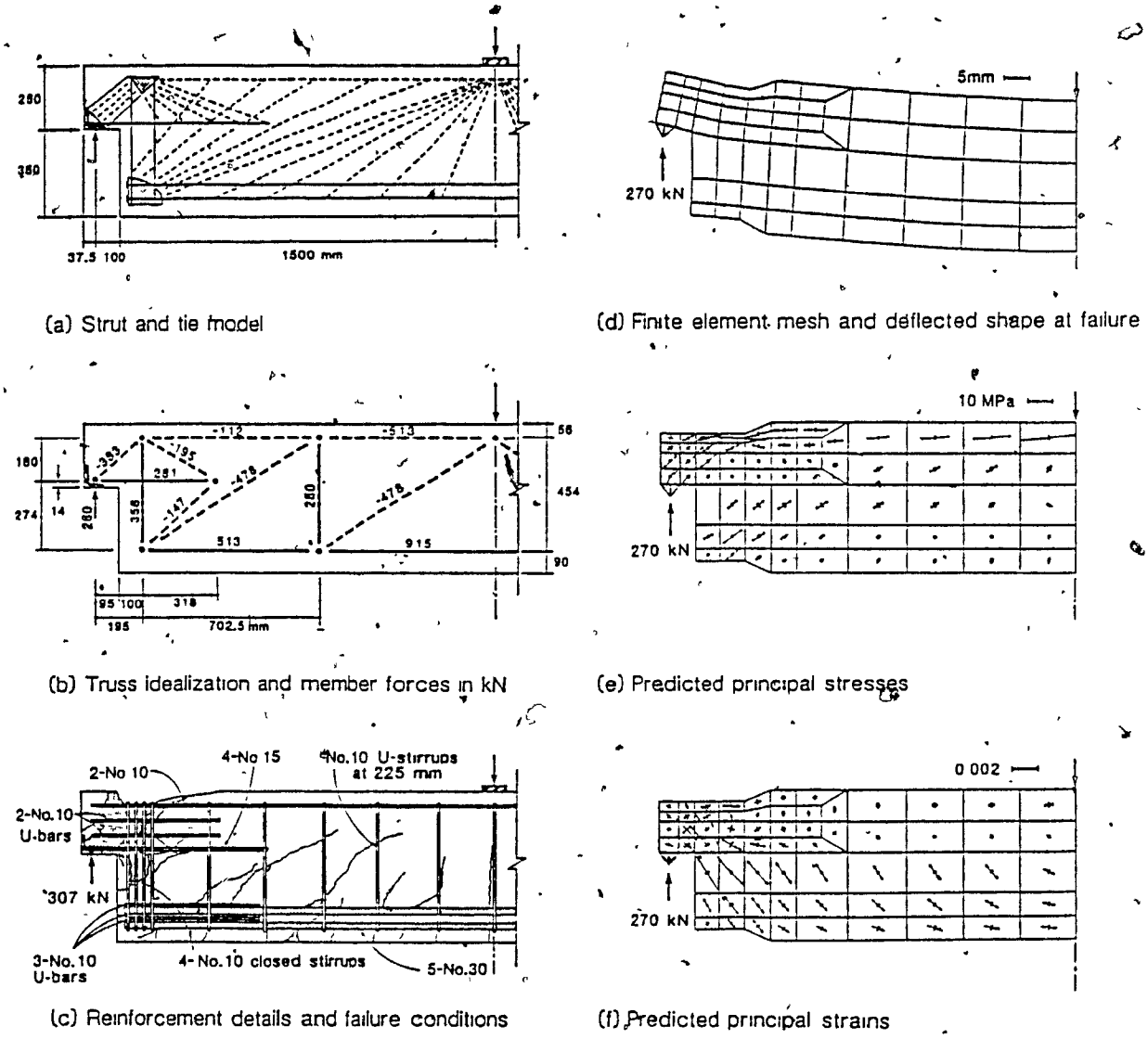

Figure 5.8 Dapped End Specimen D-1.

As can be seen the presence of the tension tie significantly reduces the compressive strength of the strut. Since the compressive stress, f_{c2}, is slightly less than f_{c2max}, the strut and tie model predicts that the tension tie will just yield before the strut crushes.

From an investigation of the bond characteristics of the longitudinal tension tie at the bottom of the main vertical tension tie, it can be shown that the available tension tie force is just sufficient. It can also be shown that all of the other truss members are adequate, thus, it is predicted that failure will occur when the vertical reaction is

260 kN by yielding of the main vertical tension tie. Failure occurred in specimen D-1 when the reaction reached 307 kN. The conditions of the beam at failure are shown in Figs. 4.8 and 5.8c.

The results of the finite element analysis of specimen D-1 are shown in Figs. 5.8d, e and f. Sixty-five CFTQ elements were used to model half the beam with symmetrical boundary conditions applied at the beam centreline. This was done even though the two ends of the beam were not identical since the differences were minor and would not affect the behaviour in the disturbed region of the nib. The support conditions were simulated with a grid of truss elements which idealized the angle embedded in the concrete. All reinforcement was included in the finite element modelling. The spalling of the concrete cover outside of the stirrups shown in Figs. 4.8 and 5.8c was simulated in the finite element model by reducing the thickness of elements near the vertical tension tie and by adjusting the mesh geometry (see Fig. 5.8d). The failure load predicted by FIELDS is 270 kN, that is, 88% of the actual failure load. The finite element analysis predicts a curving of the compressive stresses which are flowing from the top of the vertical tension tie to the support (see Fig. 5.8e). As can be seen from the principal tensile strains shown in Fig. 5.8f the vertical tension tie yields before the concrete compressive strut crushes as was predicted by the simple strut and tie model. Since the finite element analysis correctly accounts for the changing stiffness of elements as well as the presence of all reinforcement it more accurately models the stress flow. It therefore correctly predicts that the shear is transferred by both compressive struts and fields into the nib.

Specimen D-2 failed at a shear of 258 kN, that is, at 84% of the failure shear of specimen D-1. As described in Section 4.4, failure of specimen D-2 took place by crushing of the concrete compressive strut in the region near the top of the vertical tension tie. Since specimen D-1 was close to crushing of the compressive strut at failure we can approximate the effective width of the compressive strut for specimen D-2 as

0.84 x 210 mm = 176 mm. The reduction in effective width of specimen D-2 is evident from Fig. 4.13. This figure also shows the lateral arching action of the compressive strut as it seeks anchorage in the region of the vertical tension tie hooks. A conservative estimate of the effective width is the inside bend diameter of the tension tie hook plus the diameter of the tension tie on each side of the specimen. This conservative estimate would give an effective width of $2 \times (50+11.3) = 123$ mm. It is clear that it is important to account for the detailing in the modelling of the response.

5.7 Dapped End Beam Test D-4

Figures 5.9a and b show the strut and tie model and truss idealization used to analyze the inclined dapped end test specimen D-4. The reinforcement details are summarized in Fig. 5.9c. More details about this specimen are given in Section 3.5 and the experimental results are given in Section 4.7. The additional horizontal bars, provided in the nib were not included in the simple truss idealization. It is noted that these bars are required to control cracking in the nib and would also be required if any horizontal force existed at the support. In predicting the failure load it is assumed that the material resistance factors are equal to 1.0. The truss idealization has two vertical tension ties which represent groups of three stirrups. If it is assumed that failure will be governed by yielding of the stirrups then the force in each tie will be $A_s f_y$ = 3 x 200 mm^2 x 436 MPa = 262 kN. The forces in the other truss members can be determined from statics (see Fig. 5.9b). It can be shown that none of the other tension ties yield. The yield force in the two No. 25 inclined bars is 2 x 500 mm^2 x 445 MPa = 445 kN which is less than required tension of 330 kN. The resulting end reaction is 262 kN.

In the test, first yielding occurred in the stirrup reinforcement at a load of 273 kN with failure taking place at a load of 340 kN by general yielding of the transverse reinforcement in the full depth beam. The strut and tie model conservatively predicts

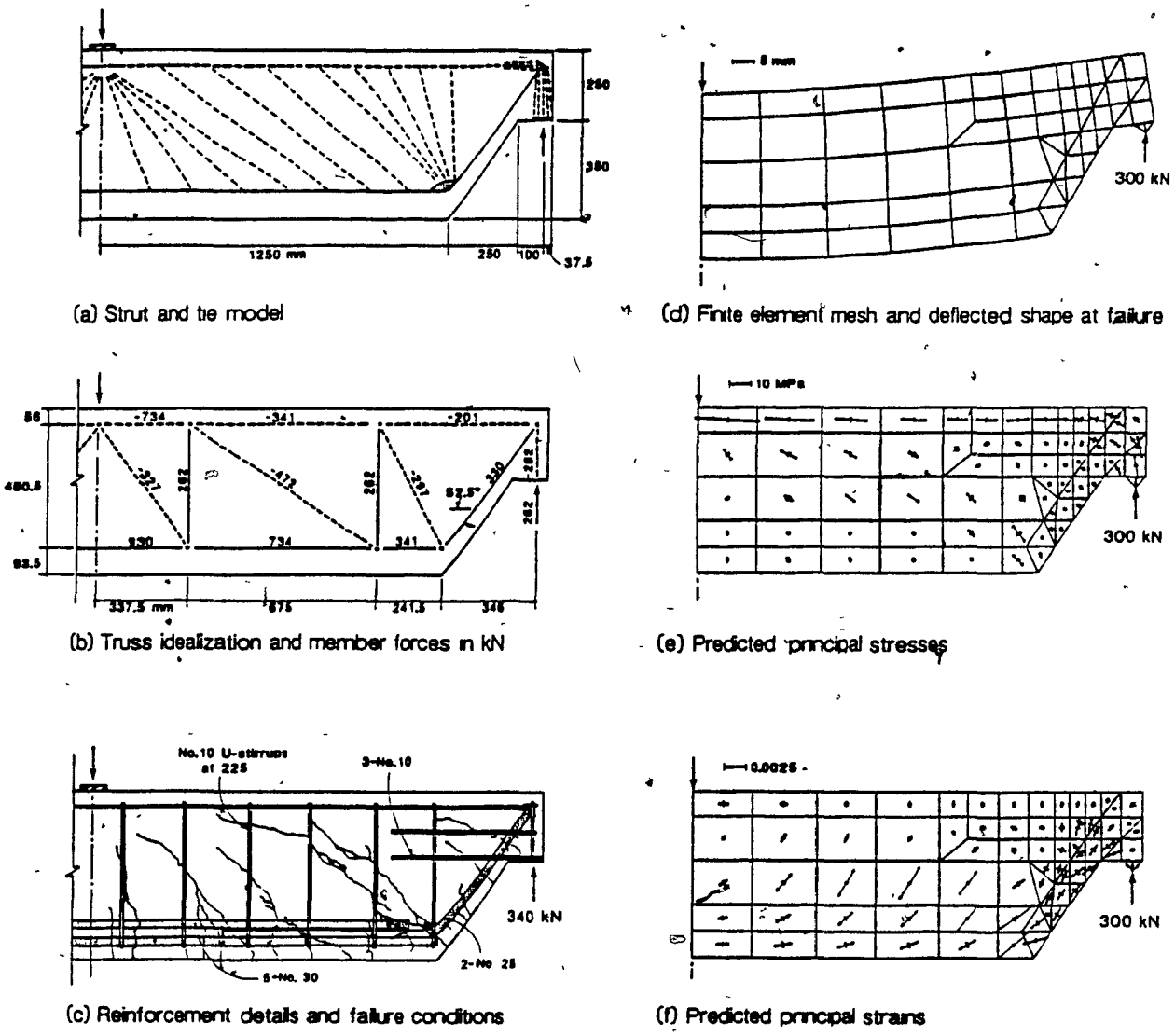

Figure 5.9 Dapped End Specimen D-4.

the failure load.

The results of the finite element analysis of specimen D-4 are shown in Figs. 5.9d, e and f. The specimen was modelled with symmetrical boundary conditions at the beam centreline and a total of 49 CFTQ and 21 CFTT elements were used. The bearing plate embedded in the nib was simulated with a series of truss elements. All reinforcement was included in the finite element modelling. The development of the main longitudinal reinforcement and the inclined tension tie was simulated by reducing the area of the

reinforcement to simulate the available force. The failure load predicted by FIELDS is 300 kN, that is, 88% of the actual failure load. The finite element analysis predicts a curving of the compressive stresses which are flowing from the top of the beam into the nib (see Fig. 5.9e). This figure also indicates a concentration of compression stresses which collect near the bottom of the inclined reinforcement. As can be seen from the principal tensile strains shown in Fig. 5.9f, the stirrups in the full depth beam yield at failure. This corresponds with the observed large inclined cracking near the end of the beam (see Section 4.7).

5.8 Dapped End Beam Test D-3

Dapped end beam D-3 contains both inclined and vertical hanger reinforcement near the dapped end and hence, has two means of hanging up the load. In deciding on the strut and tie model and the truss idealization it is necessary to account for these two sets of hanger reinforcement. Figures 5.10a and b show the strut and tie model and truss idealization used to analyze dapped end test specimen D-3. The reinforcement details are summarized in Fig. 5.10c. More details about this specimen are given in Section 3.4 and the experimental results are given in Section 4.6. The additional horizontal bars, provided in the nib were not included in the simple truss idealization. It is noted that these bars are required to control cracking in the nib and would also be required if any horizontal force existed at the support. Four stirrups in the full depth beam were represented by a single tension tie located at the centre of the group of stirrups. The truss model is statically indeterminate because of the two sets of hanger reinforcement. In the analysis to find the reaction it was assumed that both sets of hanger reinforcement yielded. The yield force in the inclined reinforcement is $A_s f_y$ = 2 x 300 mm^2 x 478 MPa = 287 kN, while the yield force in the vertical hanger is $A_s f_y$ = 4 x 100 mm^2 x 436 MPa = 174 kN. The forces in the other truss members have been determined from statics as shown in Fig. 5.10b. It can be shown that none

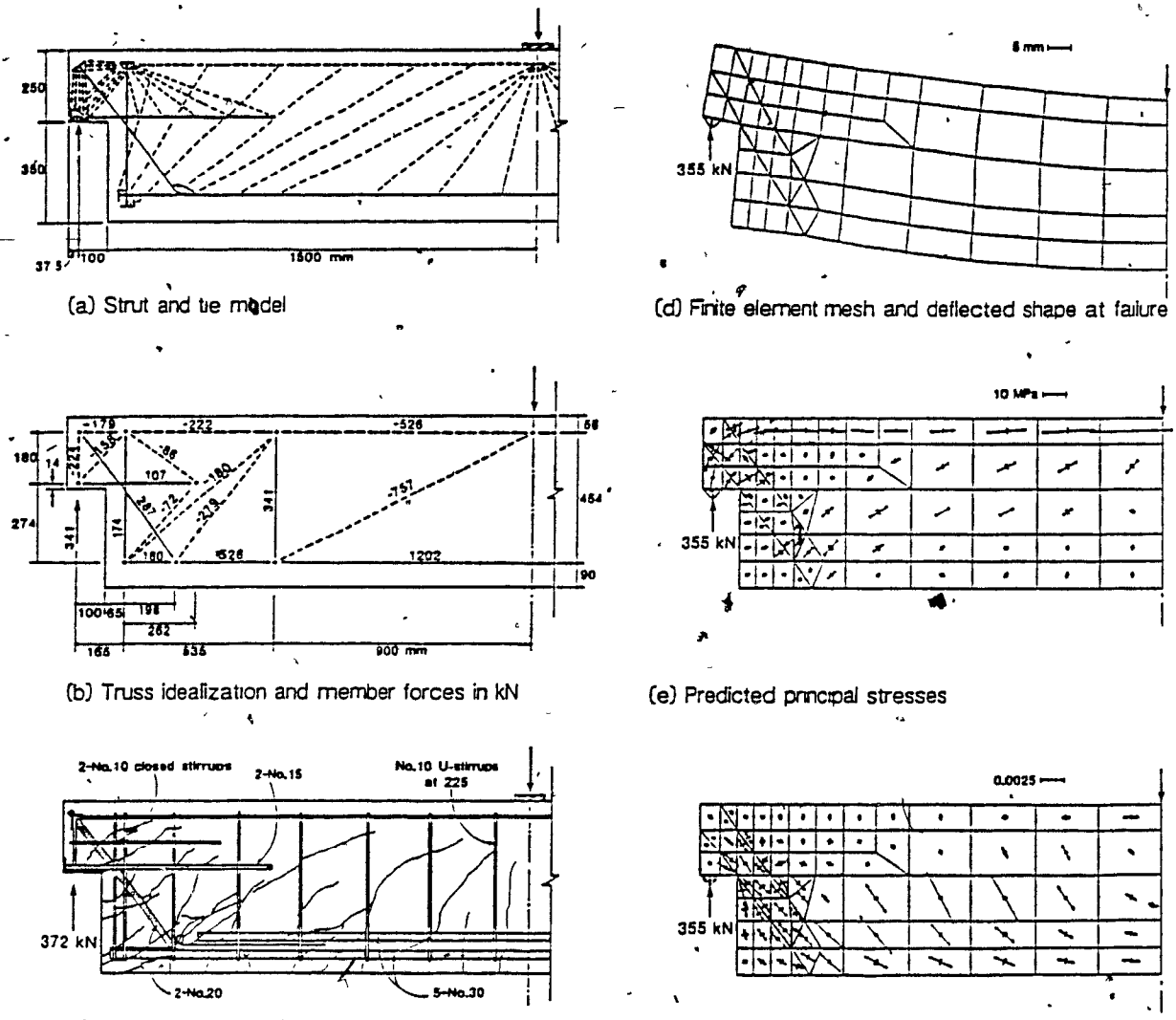

Figure 5.10 Dapped End Specimen D-3.

of the other tension ties yield. It is noted that the vertical tension tie representing four stirrups has a tension of 341 kN, i.e., 98% of the yield force. The force in the U-bars together with the force developed in the three No. 30 longitudinal bars at the bottom of the beam is just sufficient to develop the required force. The resulting end reaction is 341 kN.

In the test, first yielding occurred in the stirrup reinforcement near the end of the beam at a load of 274 kN with failure taking place at a load of 372 kN by yielding of

the transverse reinforcement in the full depth beam. Significant strains were developed in all the main tension ties in the region of the dap as shown in Fig. 4.15. The strut and tie model conservatively predicts the failure load.

The results of the finite element analysis of specimen D-3 are shown in Figs. 5.10d, e and f. The specimen was modelled with symmetrical boundary conditions at the beam centreline and a total of 55 CFTQ and 25 CFTT elements were used to model the beam. The angle embedded in the nib was simulated with a series of truss elements. All reinforcement was included in the finite element modelling. The development of the main longitudinal reinforcement and the inclined tension tie was accounted for by reducing the area of the reinforcement to simulate the available force. In the region of the re-entrant corner and in the lower nodal zone region it was necessary to model three layers of reinforcement, the inclined tension tie, the vertical stirrup reinforcement, and horizontal reinforcement. This was handled by adding a second CFTQ or CFTT element with a minimal concrete thickness (0.1 mm) and reinforcement equal to the stirrup contribution over the top of the full thickness element containing the inclined and horizontal reinforcement. Since the thinner elements will have a negligible tension stiffening contribution, it is important to model principal tension ties in the thicker elements so that their tension stiffening effects will be included. The failure load predicted by FIELDS is 355 kN, that is, 95% of the actual failure load. An examination of the predicted principal concrete stresses and principal strains reveals that there are actually three different major load paths into the nib. These load paths are provided by both the inclined and vertical hanger reinforcement as well as compressive stresses which are flowing directly into the nib (see Fig. 5.10e). This figure also indicates a concentration of compression stresses which collect near the bottom of the inclined reinforcement. As can be seen from the principal tensile strains shown in Fig. 5.10f, the stirrups in the full depth beam yield at failure. This corresponds with the observed large inclined cracking near the end of the beam and with the measured strains in the reinforcement (see Section 4.6).

5.9 Web Hole Specimen H-1

Figure 2.3c illustrates a simple strut and tie model and truss idealization for a beam with a web opening. If it is assumed that the capacity will be governed by yielding of the main vertical tension tie on the support side of the opening then a prediction of the failure load can be made. The yield force of the four #3 legs is 4 x 71 mm^2 x 388 MPa = 110 kN. The simple strut and tie model assumes that the flange is ineffective in carrying shear and therefore, all of the shear past the centreline of the opening is assumed to pass through the portion of the beam beneath the opening. Thus, the corresponding uniform load is equal to the tension tie capacity divided by the distance from the beam centreline to the centre of the opening, that is, 110 kN / (1.92 m - 1.00 m) = 120 kN/m.

Figure 5.11a shows the appearance of specimen H-1 at failure. First yielding of the transverse reinforcement occurred in the main tension tie at a uniform loading of 97.3 kN/m. Failure occurred at a uniform load of 177 kN/m and as can be seen failure took place after severe spalling of the concrete cover in the region under the opening. In addition extremely large strains developed in the stirrups beneath the opening and in the main vertical tension tie (see photograph in Fig. 4.24 and strain distributions in Fig. 4.23). At failure there was also evidence of shear cracking in the slab over the opening indicating that there was some shear being transferred through the slab.

The full span of specimen H-1 in the testing configuration used to load the beam to failure was modelled in the finite element idealization. Figure 5.11b illustrates the portion of the mesh up to the geometric centreline of the T-beam. A total of 20 columns of CFTQ elements were used with 4 elements through the depth of the beam. In the vicinity of the opening the mesh was refined to include two elements in the top flange. The support conditions were modelled with truss elements located such that their edge coincides with the inner edge of the steel bearing support. In this analysis the tensile strength of concrete was taken as $0.37\sqrt{-f'_c}$ which was the value obtained from split cylinder tests. The deformations shown in Fig. 5.11c illustrate the significant

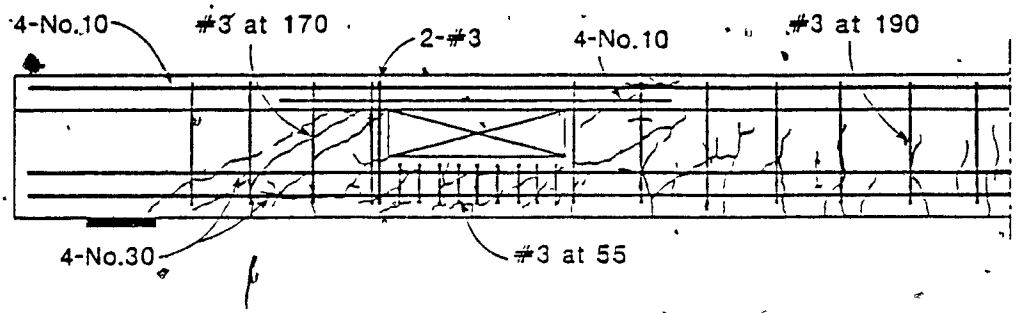

(a) Reinforcement details and failure conditions, w_u=177 kN/m

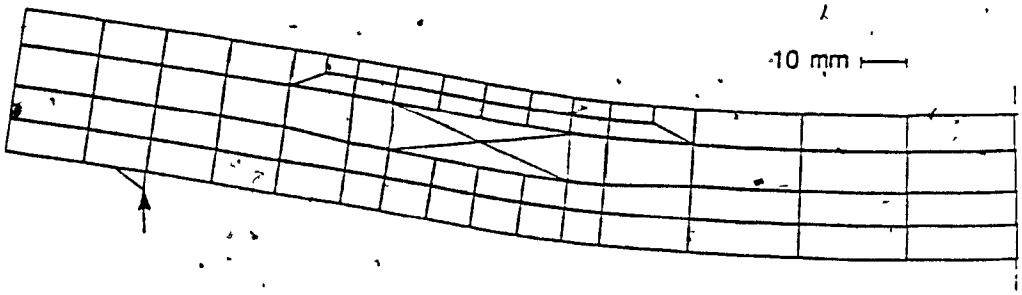

(b) Finite element mesh and deflected shape at failure

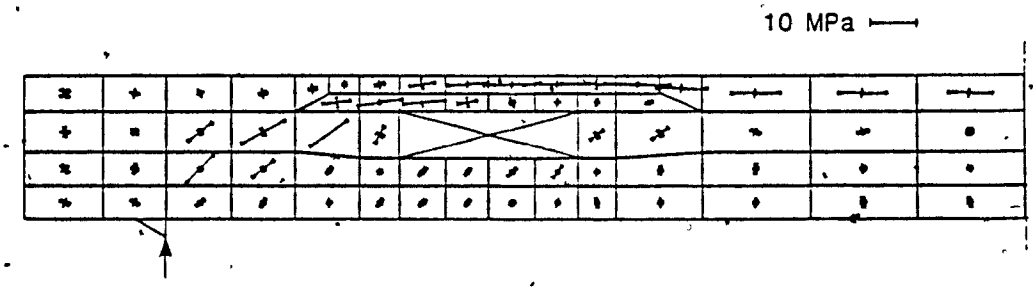

(c) Predicted principal stresses, w_u=141 kN/m

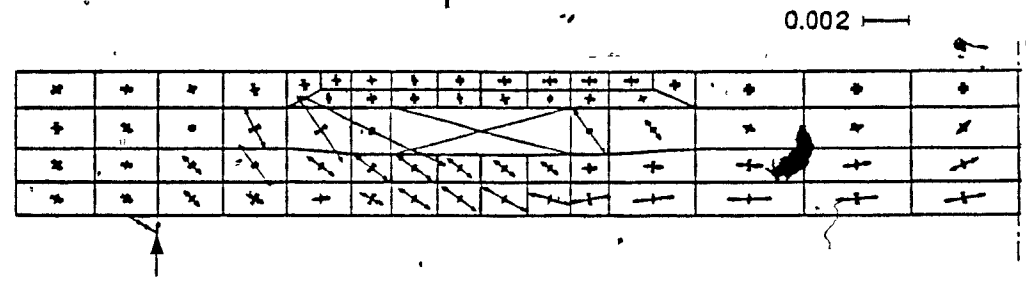

(d) Predicted principal strains, w_u=141 kN/m

Figure 5.11 Web Hole Specimen H-1.

distortions in the regions immediately around the opening. Failure is predicted to occur at uniform loading of 141 kN/m. The steeply inclined compressive field in the region beneath the opening is apparent from Fig. 5.11d due to the very high shear stress in this heavily reinforced region. The slight inclination of the compressive stresses in the slab above the opening indicates that the finite element model is predicting that some shear is transmitted directly by the 800 mm wide slab. The flow of compressive stresses from the top of the main tension tie is also evident in this figure. The principal strains shown in Fig. 5.11e indicate that failure has taken place by yielding of the main tension tie reinforcement and by yielding of the stirrups in the region between the support and the opening.

The failure load predicted by the simple strut and tie model is 69% of the actual failure load, while program FIELDS predicts the failure to be 80% of the actual failure load. It is noted that the predicted responses did not account for the horizontal restraint at the ends of the beam due to the friction between the beam and the steel bearing supports, thus giving conservative strength predictions.

5.10 Web Hole Specimen H-2

Using the simple strut and tie model and truss idealization shown in Fig. 2.3c and assuming that the capacity will be governed by yielding of the main vertical tension tie on the support side of the opening, the predicted failure shear can be obtained. The yield force of the four No. 10 legs is 4 x 100 mm^2 x 365 MPa = 146 kN. The simple strut and tie model assumes that the flange is ineffective in carrying shear and therefore, all of the shear past the centreline of the opening is assumed to pass through the portion of the beam beneath the opening. Thus, the corresponding uniform load is equal to the tension tie capacity divided by the distance from the beam centreline to the centre of the opening, that is, 146 kN / (2.5 m - .75 m) = 83 kN/m.

Figure 5.12a shows the appearance of specimen H-2 at failure. First yielding of the transverse reinforcement occurred in the main tension tie at a uniform loading of

97.3 kN/m. Failure occurred at a uniform load of 99.7 kN/m. As with specimen H-1, failure took place after severe spalling of the concrete cover in the region under the opening. A very large diagonal crack starting at the side of the opening furthest from the support and extending beneath the opening caused the final failure (see photograph in Fig. 4.27 and strain distributions in Fig. 4.26). The shear cracking in the slab over the opening indicated that there was some shear being transferred through the slab.

Figure 5.12b illustrates the finite element idealization of specimen H-2. The truss elements shown are located such that their centre coincides with the inner edge of the steel bearing support. Half of the span is modelled in the testing configuration used to load the beam to failure. In the analysis it was assumed that the beam was symmetrical about midspan. The tensile strength of concrete for this analysis was taken as $0.37\sqrt{-f'_c}$ which was the value obtained from split cylinder tests. The deformations shown in Fig. 5.12c illustrate the significant distortions in the regions immediately around the opening. Failure is predicted to occur at uniform loading of 78 kN/m. The steeply inclined compressive field in the region beneath the opening is apparent from Fig. 5.12d due to the very high shear stress in this heavily reinforced region. The slight inclination of the compressive stresses in the slab above the opening indicates that the finite element model is predicting that some shear is transmitted directly by the 800 mm wide slab. The flow of compressive stresses from the top of the main tension tie is also evident in this figure. The principal strains shown in Fig. 5.12e indicate that failure has taken place by yielding of the transverse reinforcement on the side of the opening furthest from the support.

The failure load predicted by the simple strut and tie model is 83% of the actual failure load, while program FIELDS predicts the failure to be 78% of the actual failure load. It is noted that the predicted responses did not account for the horizontal restraint at the ends of the beam due to the friction between the beam and the steel bearing supports, thus giving conservative strength predictions.

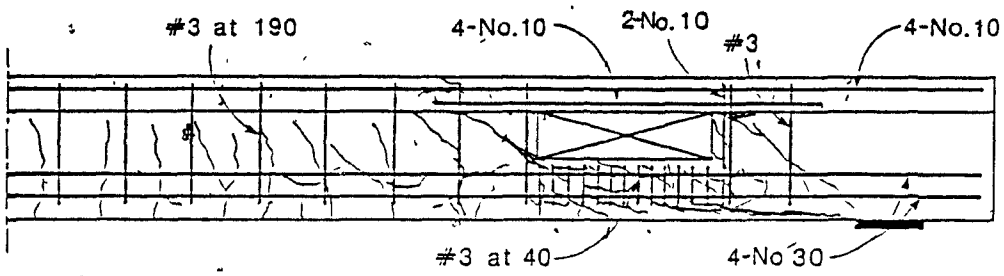

(a) Reinforcement details and failure conditions, $w_u = 99.7$ kN/m

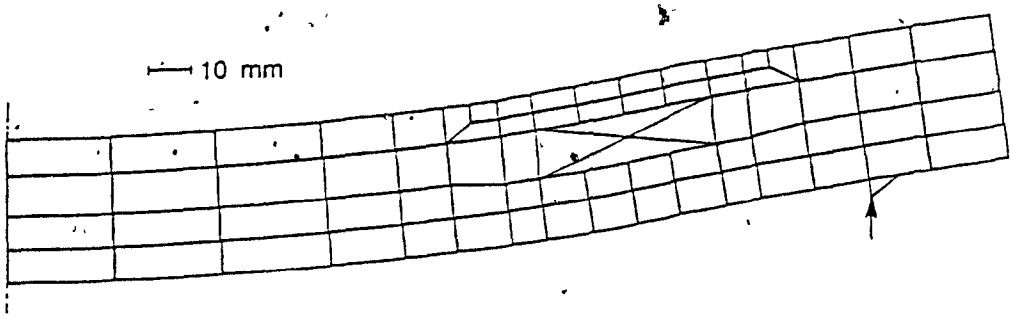

(b) Finite element mesh and deflected shape at failure, $w_u = 78$ kN/m

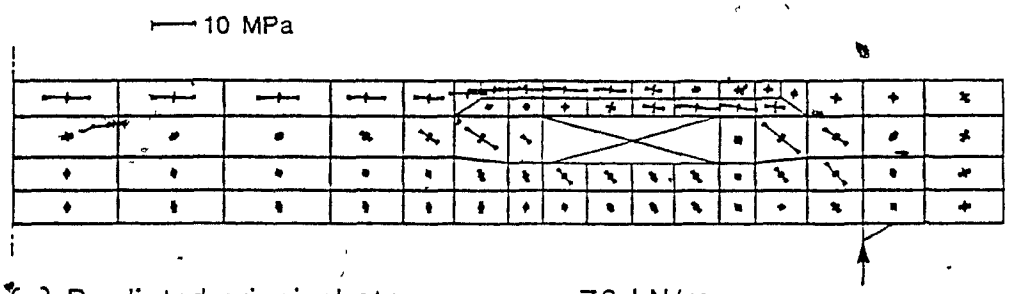

(c) Predicted principal stresses, $w_u = 78$ kN/m

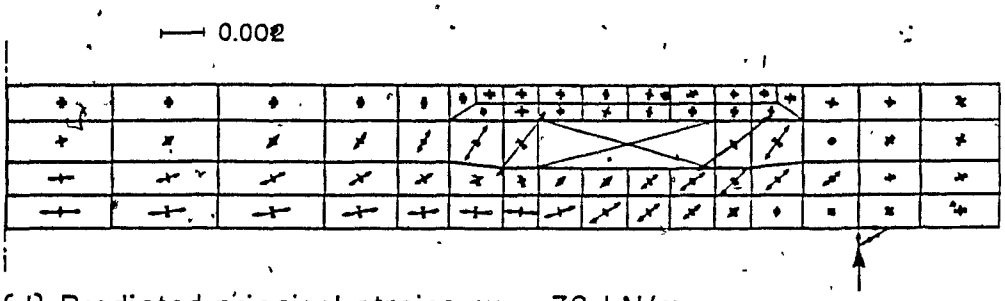

(d) Predicted principal strains, $w_u = 78$ kN/m

Figure 5.12 Web Hole Specimen H-2.

CHAPTER 6

SUMMARY AND CONCLUSIONS

A two dimensional, non-linear finite element computer program, FIELDS, was developed in order to provide a means of predicting the complete response of reinforced concrete members subjected to in-plane loading. It accounts for the non-linear behaviour of the reinforcement as well as the strain softening of the concrete in compression and the tension stiffening of the concrete between the cracks. The program enables the use of truss, triangular, and quadrilateral elements. The triangular and quadrilateral elements permit the use of mid-side nodes. In order to enable the use of larger elements without significant loss of accuracy FIELDS permits the use of up to four by four quadrature in the numerical integration of element stiffnesses. Reinforcement in two arbitrary directions is assigned to each triangular and quadrilateral element. This reinforcement is assumed to be smeared uniformly within the element. Concentrations of reinforcement can be modelled by carefully choosing the mesh with higher percentages of reinforcement in appropriate elements. Additional reinforcement can be modelled using truss elements. Although a smeared cracking model is assumed, the program checks the ability of cracks to transmit shear stresses and the ability of the reinforcement to transfer tension across cracks. Both slippage at the crack and yielding of the reinforcement across cracks reduce the tension stiffening of the concrete between the cracks and lead to significant reductions in stiffness and strength.

Program FIELDS is particularly useful in predicting the response of reinforced concrete members containing major discontinuities or disturbed regions. The ability of this non-linear finite element program to model the flow of the stresses around regions of discontinuities throughout all stages of loading provides a useful tool in studying the response of complex members. The predictions of the responses of a number of test specimens containing regions of major discontinuities were compared with the test results. The program predicted correctly the modes of failure of a number of shear panels tested by Vecchio and Collins, a uniformly loaded beam tested by Mailhot, and continuous deep beams tested by Rogowski, MacGregor and Ong.

As part of this research programme a number of members with major disturbances were tested. These tests included a corbel specimen, four dapped end specimens, and two tests on uniformly loaded beams with web holes. These test specimens were heavily instrumented in order to permit a detailed study of the strains. These test specimens provided useful data for non-linear analyses using program FIELDS and were used to develop simple strut and tie models suitable for design.

The test results and the predictions using non-linear finite element analyses demonstrate the need to account for the following important features of disturbed regions:

a) since the ultimate capacities of corbels and dapped ended beams are sensitive to small changes in load eccentricities it is necessary to carefully model the details of the bearing and loading areas,

b) unrestrained concrete outside of bearing areas and plain concrete cover has the potential to spall and therefore, should be neglected in the analysis of the ultimate failure conditions,

c) the termination of reinforcing bars results in significant bond stresses and variation of forces along the length of the bar. In this study this was accounted for by reducing the area of steel along the development length. In the design using strut and tie models it is necessary to ensure that the reinforcement is detailed such that the

required forces in the tension ties can be achieved.

d) the ultimate capacity is sensitive to the manner in which nodal zones are modelled. Elements modelling the region around main tension ties should be chosen such that the elements are approximately the same width as the effective zone around the tie. Elements modelling nodal zone regions should have a thickness consistent with the available anchorage details (e.g., the difference between open and closed stirrups can be substantial).

Program FIELDS enables an assessment of different strut and tie models for the design of disturbed regions. Simple strut and tie models, along with truss idealizations for a variety of disturbed regions are presented. It was found that these simple strut and tie models conservatively predicted the test failure loads. Program FIELDS enabled better predictions of both the failure loads and the flow of the forces in the test specimens and hence provides a useful tool for the analysis of disturbed regions.

STATEMENT OF ORIGINALITY

A non-linear finite element computer program was developed in order to analyze the full response of reinforced concrete members including regions near discontinuities. This program accounts for the strain softening and tensile stiffening effects on the cracked concrete. The program also accounts for the non-linear response of the steel and investigates the ability of the steel reinforcement to transfer forces across the cracks.

A number of full scale experiments were carried out on members with a variety of major discontinuities. These test results and the non-linear finite element computer analyses enabled simple strut and tie models to be developed for use in design.

REFERENCES

1. Ritter, W., *Die Bauweise Hennebique*, Schweizerische Bauzeitung, Zürich, February 1899.
2. Mörsch, E., *Concrete-Steel Construction*, English Translation by E.P: Goodrich, McGraw-Hill Book Company, New York, 1909, 368 pp. (Translation from third edition of *Der Eisenbetonbau*, first edition, 1902).
3. CEB–FIP, *Model Code for Concrete Structures*, CEB–FIP International Recommendations, Third Edition, Comité Euro-International du Béton, Paris, 1978, 384 pp.
4. ACI Committee 318, "Building Code Requirements for Reinforced Concrete (ACI 318-83)", American Concrete Institute, Detroit, 1983, 111 pp.
5. Thürlimann, B., Marti, P., Pralong, J., Ritz, P. and Zimmerli, B., *Anwendung der Plastizitaetstheorie auf Stahlbeton (Application of the Theory of Plasticity to Reinforced Concrete)*, Institute for Structural Engineering, ETH Zürich, 1983, 252 pp.
6. Marti, P., "Basic Tools of Reinforced Concrete Beam Design", *ACI Journal*, V. 82, No. 1, January-February 1985, pp. 46–56.
7. Schlaich, J. and Schäfer, K., "Konstruieren im Stahlbetonbau", *Sonderdruck aus dem Beton-Kalender 1984*, Wilhelm Ernst und Sohn, Berlin, 1984, pp. 787–1004.
8. Mitchell, D. and Collins, M.P., "Diagonal Compression Field Theory – A Rational Model for Structural Concrete in Pure Torsion", *ACI Journal*, V. 71, August, 1974 pp. 396–408.
9. Collins, M.P., "Towards a Rational Theory for RC Members in Shear", *Journal for the Structural Division*, ASCE, V. 104, April 1978, pp. 649–666.
10. Collins, M.P. and Mitchell, D., "Shear and Torsion Design of Prestressed and Non-Prestressed Concrete Beams", *PCI Journal*, V. 25, No. 5, September-October 1980, pp. 32–100.
11. Vecchio, F.J. and Collins, M.P., "*The Response of Reinforced Concrete to In-Plane Shear and Normal Stresses*", University of Toronto, Dept. of Civil Engineering, *Publication No. 82-03*, March 1982, 332 pp.
12. Vecchio, F.J. and Collins, M.P., "The Modified Compression-Field Theory for Reinforced Concrete Elements Subjected to Shear", *ACI Journal*, V. 83, No. 2, March-April 1986, pp. 219–231.
13. "Design of Concrete Structures for Buildings (CAN3-A23.3-M84)", Canadian Standards Association, Rexdale, 1984, 281 pp.
14. Collins, M.P. and Mitchell, D., "A Rational Approach to Shear Design - The 1984 Canadian Code Provisions", *ACI Journal*, V. 83, No. 6, November-December 1986, pp. 925–933.

15. Collins, M.P. and Mitchell, D., "Chapter 4 - Shear and Torsion", *CPCA Concrete Design Handbook*, Canadian Portland Cement Association, Ottawa, 1985, pp. 4-1–4-51.

16. Mattock, A.H., Chen, K.C. and Soongswang, K., "The Behavior of Reinforced Concrete Corbels", *PCI Journal*, V. 21, No. 2, March-April 1976, pp. 52–77.

17. Rogowsky, D.M. and MacGregor, J.G., "The Design of Reinforced Concrete Deep Beams", *Concrete International: Design & Construction*, V. 8, No. 8, August 1986, pp. 49–58.

18 Walraven, J.C., "Fundamental Analysis of Aggregate Interlock", *Journal for the Structural Division*, ASCE, V. 107, ST11, November 1981, pp. 2245-2270.

19. Mailhot, G., "Experiments on the Staggering Concept for Shear Design", M.Eng. Project Report, McGill University, March 1984.

20. Rogowsky, D.M., MacGregor, J.G. and Ong, S.Y., "Tests of Reinforced Concrete Deep Beams", *ACI Journal*, V. 83, No. 4, July-August 1986, pp. 614–623.

APPENDIX A

EXPERIMENTAL DATA

A.1 Introduction

This appendix includes the experimental data for the corbel specimen C-1, the dapped end specimens D-1 through D-4, and the beam specimens H-1 and H-2 with web openings. A complete description of the specimen, loading, and instrumentation details are given in Chapter 3.

The location and orientation of the strain measurements is described by a number such as D2 H12F, which indicates that the reading is on specimen D-2 in the horizontal direction between lines 1 and 2 at level F (see Fig. A.2).

It is noted that some specimens required a change in test set-up due to the failure of one of the ends of the specimen during testing. The reloading after this change in test set-up is referred to as "Loading 2" in the following tables. Details of these reloading test set-ups are given in Chapter 3. The deflection readings were reset to zero for reloading.

A.2 Corbel Specimen C-1

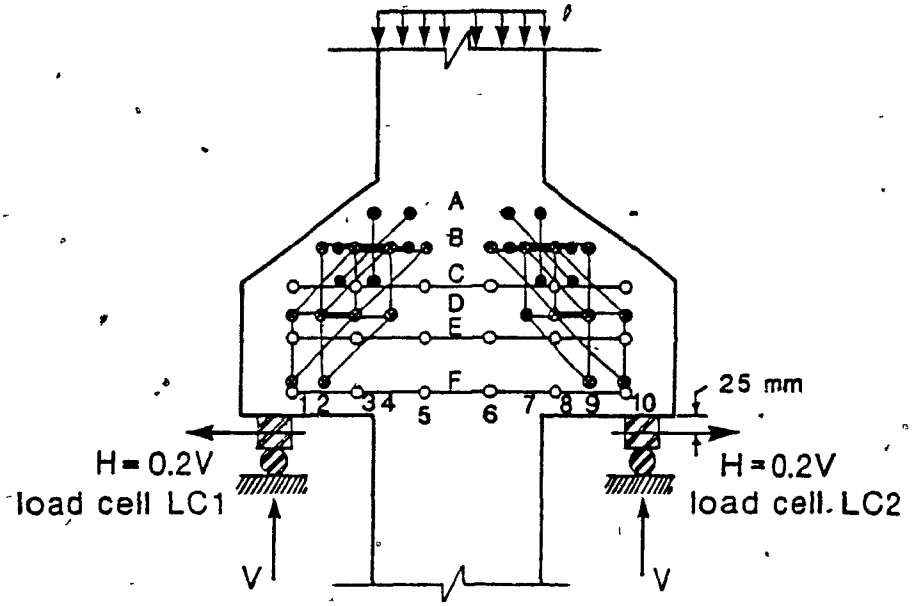

(a) North face instrumentation

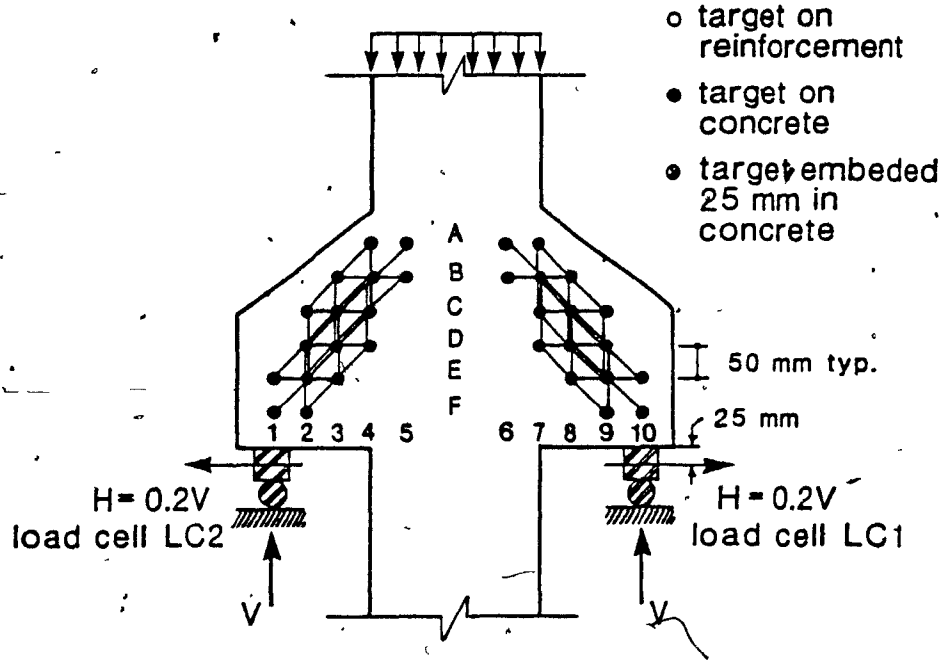

(b) South face instrumentation

Figure A.1 Test Set-Up and Instrumentation for Corbel Specimen C-1.

Table A.1 Corbel Specimen C-1 – Measured Loads.

Load Stage	Measured Loads Shear* (kN)	LC1 (kN)	LC2 (kN)
0A-B	0.0	0.0	0.0
1	33.4	6.9	7.7
2	66.7	12.2	13.4
3	100.1	18.9	20.4
4	133.5	24.8	26.7
5	166.8	31.9	34.1
6	200.2	38.7	41.3
7	233.5	44.7	47.5
8	266.9	50.6	53.8
9	300.3	57.8	61.2
10	333.6	64 4	68.1
11	367.0	71 1	75.1
12	400.3	78 0	82.2
13	433 7	84.4	88.6
14	467.0	91 2	95 5
15	500.4	97.3	101 8

* Does not include self-weight shear of 1 8 kN.

Table A.2 Corbel Specimen C-1 – Strain Measurements.

Load Stage	DEMEC Gauge Readings - Strain (mm/m) 1 N H13C	2 N H13E	3 N H13F	4 N H35C	5 N H35E	6 N H35F	7 N H56C	8 N H56E
0A	0.000	0.050	0.050	0.050	0.000	-0 050	0.000	0 000
0B	0.000	-0.050	-0 050	-0 050	0.000	0 050	0.000	0 000
1	0.000	0.050	0.050	0.050	0.000	-0.450	0 000	-0.100
2	0.100	0.050	0.050	0.150	0.100	-0.450	0 000	0 000
3	0.100	0.050	0.150	0.050	0.100	-0.450	0 100	0 100
4	0.100	0.050	0.050	0.050	0.100	-0 250	0 000	0 100
5	0.100	0.050	0 050	0.250	0 500	0.350	0 200	0 300
6	0.100	0.050	0.050	0 350	0.500	0.750	0 300	0.300
7	0.100	0.250	0 350	0.350	0.700	1 250	0 200	0 400
8	0.500	0.650	0.750	0.650	0 500	1.450	0 300	0.500
9	0.800	0.950	0.950	0.650	0.800	1 550	0.300	0 500
10	0.900	1.050	0.650	0.750	0.900	1.850	0 300	0 600
11	1.100	1.250	0.950	0.850	1 000	2.050	0 300	0 700
12	1.300	1.450	1.250	0.950	1.100	2.450	0 400	0 900
13	1.500	1.550	1.250	1 050	1 200	2.650	0.400	1.000
14	1.700	1.750	1.350	1.150	1.200	2.950	0 500	1.000
15	1.600	1.750	1.650	1.150	1.300	3.250	0.500	1.200

Table A.2 *(Cont'd)* Corbel Specimen C-1 – Strain Measurements.

	DEMEC Gauge Readings - Strain (mm/m)							
Load Stage	9 N H56F	10 N H68C	11 N H68E	12 N H68F	13 N H810C	14 N H810E	15 N H810F	16 N H13D
0A	0.000	0.000	0.050	0.000	0.000	0.000	0.050	0.000
0B	0.000	0.000	-0.050	0.000	0.000	0.000	-0.050	0.000
1	-0.300	0.100	0.150	0.100	0.000	0.000	0.150	0.000
2	-0.400	0.100	0.050	0.000	-0.200	0.000	0.150	0.000
3	—	0.200	0.250	0.100	0.000	-0.100	0.150	0.000
4	—	0.200	0.250	0.600	-0.200	0.100	-0.050	0.000
5	—	0.400	0.550	1.100	0.100	0.300	-0.150	0.100
6	—	0.500	0.750	1.500	-0.100	0.200	-0.050	-0.100
7	—	0.700	0.950	1.900	0.000	0.400	0.250	0.100
8	—	0.800	1.050	2.100	0.200	0.800	0.850	0.900
9	—	1.000	1.150	2.100	0.400	1.000	1.050	1.300
10	—	1.100	1.250	2.500	0.300	1.100	1.250	1.600
11	—	1.200	1.350	2.700	0.600	1.300	1.450	1.900
12	—	1.400	1.450	3.200	0.900	1.600	1.750	2.300
13	—	1.400	1.550	3.000	0.900	2.300	1.750	2.700
14	—	1.300	1.650	3.200	1.700	1.800	2.250	3.000
15	—	1.800	1.550	2.800	3.400	3.000	5.150	3.200

Table A.2 *(Cont'd)* Corbel Specimen C-1 – Strain Measurements.

	DEMEC Gauge Readings - Strain (mm/m)							
Load Stage	17 N H24B+	18 N H24B	19 N H24D	20 N H35B	21 N H68B	22 N H79B+	23 N H79B	24 N H79D
0A	-0.050	0.000	0.000	0.000	0.000	0.050	0.000	0.000
0B	0.050	0.000	0.000	0.000	0.000	-0.050	0.000	0.000
1	-0.050	0.000	0.100	0.000	0.000	-0.050	0.000	0.000
2	-0.050	0.000	0.200	0.100	0.000	0.050	0.000	0.000
3	0.050	0.000	0.100	0.100	0.000	0.050	0.000	0.000
4	-0.050	0.000	0.100	0.000	0.000	-0.050	0.000	0.200
5	0.050	0.000	0.200	0.100	0.100	0.050	0.000	0.400
6	-0.050	-0.100	0.100	0.100	0.000	0.050	0.000	0.600
7	-0.050	-0.100	0.100	0.100	0.000	0.050	-0.100	0.800
8	0.250	0.200	0.100	0.300	0.200	0.250	0.200	1.400
9	0.550	0.500	0.000	0.700	0.400	0.450	0.400	1.700
10	0.850	0.700	0.000	0.800	0.600	0.550	0.500	2.000
11	1.050	1.000	0.000	1.100	0.800	0.750	0.700	2.200
12	1.350	1.200	0.000	1.400	1.000	0.950	0.800	2.400
13	1.550	1.500	0.000	1.600	1.100	1.050	1.000	2.500
14	1.750	1.600	0.000	1.800	1.000	1.050	0.900	2.500
15	1.850	1.800	-0.100	1.900	1.000	0.850	0.900	2.200

Table A.2 *(Cont'd)* Corbel Specimen C-1 – Strain Measurements.

	DEMEC Gauge Readings - Strain (mm/m)							
Load Stage	25 N H810D	26 N V1DF	27 N V2BD	28 N V2DF	29 N V3AC	30 N V3BD	31 N V4BD	32 N V7BD
0A	0.000	0.000	0.000	0.000	-0.050	0.000	0.050	0.050
0B	0.000	0.000	0.000	0.000	0.050	0.000	-0.050	-0.050
1	0.000	0.100	0.000	0.100	0.050	0.200	0.050	0.150
2	0.000	0.100	-0.100	0.000	0.050	0.100	-0.050	0.050
3	0.100	0.100	-0.100	0.000	-0.050	0.100	-0.050	0 050
4	0.100	0.100	-0.100	0.100	-0.050	0.100	-0.150	0.150
5	0.100	0.100	-0.100	0.000	-0.050	0.000	-0.150	0.150
6	0.100	0.100	-0.200	-0.100	-0.150	-0.100	-0 150	0.150
7	0.200	0.000	-0.100	0.000	-0 250	-0.100	-0 150	0 250
8	0.700	0.100	0.400	0 000	-0.150	0.100	-0.150	0.350
9	1.000	0.100	0.700	0.000	-0.150	0.300	-0.150	0 350
10	1.300	0 100	0.900	0.000	0.450	0.500	-0 150	0.350
11	1.500	0.200	1.100	0 000	0.050	0.600	-0.150	0 350
12	1.800	0.100	1.500	0.000	0.150	0.700	-0 250	0 350
13	2.000	0.100	1.700	-0.100	0.150	0.900	-0.250	0.350
14	2.000	0.100	2.000	-0.200	0.250	1.000	-0.150	0.450
15	2.500	0.000	2.100	-0.100	0.250	1.200	-0.150	0 450

Table A.2 *(Cont'd)* Corbel Specimen C-1 – Strain Measurements.

	DEMEC Gauge Readings - Strain (mm/m)							
Load Stage	33 N V8AC	34 N V8BD	35 N V9BD	36 N V9DF	37 N V10AC	38 N D13DB	39 N D13FD	40 N D24CA
0A	0.000	0.000	0.050	0.050	0.000	0.000	-0 035	0 000
0B	0.000	0 000	-0.050	-0 050	0.000	0.000	0 035	0 000
1	0.100	0.100	-0.050	0 050	0.000	-0.284	-0 177	0 000
2	0.000	0.000	-0.250	-0.050	-0.100	-0 071	0.106	0.000
3	0.000	0.100	-0.150	0.050	-0.100	-0.142	-0.035	-0 071
4	0.100	0.100	-0.050	0.050	-0.100	-0.071	0 106	-0 071
5	0.000	0.100	-0.250	0.050	-0.100	-0.142	-0 035	-0 071
6	-0.200	0.000	-0.250	-0.050	-0.200	-0.142	-0.035	-0.213
7	-0.300	-0.100	-0.250	0.050	-0.300	-0.142	0.106	-0.071
8	-0.300	0.300	-0.350	0.750	-0.300	-0.284	0 106	-0 213
9	-0.300	0.400	-0.450	0.950	-0.300	-0.426	0.177	-0.213
10	-0.200	0.600	-0.350	1.250	-0.300	-0.355	0.248	-0.142
11	-0.200	0.800	-0.450	1.450	-0.400	-0.496	0.106	-0 284
12	-0.100	0.900	-0.750	1.650	-0.500	-0.709	0.461	-0.142
13	-0.100	1.100	-0 550	1.950	-0.300	-0.709	0.248	-0.496
14	0.100	1.200	-0.750	2.050	-0.400	-0.567	0.319	-0.284
15	0.000	1.400	-0.350	2.850	0.000	-0.496	1.312	-0 496

Table A.2 *(Cont'd)* Corbel Specimen C-1 – Strain Measurements.

Load Stage	DEMEC Gauge Readings - Strain (mm/m) 41 N D24DB	42 N D24FD	43 N D35DB	44 N D68BD	45 N D79AC	46 N D79BD	47 N D79DF	48 N D810BD
0A	0.000	0.000	0.000	0.000	0.035	0.035	-0.035	-0.035
0B	0.000	0.000	0.000	0.000	-0.035	-0.035	0.035	0.035
1	-0.071	-0.142	0 000	0.071	-0.035	-0.035	-0.035	0.035
2	0.071	0.071	-0.071	0.142	-0.035	-0.035	-0.035	-0.035
3	-0.071	0.000	-0.142	0 071	-0.106	-0.106	-0.035	-0.035
4	0.000	0.142	-0.071	0.142	-0.106	-0.106	-0.035	-0.106
5	-0.142	0.000	-0.071	0.142	-0.177	-0.177	-0.035	-0.106
6	-0.213	0.000	-0.142	0.213	-0.177	-0.177	0.035	-0.177
7	-0.142	0.000	-0.071	0.142	-0.248	-0.248	0.106	-0.248
8	-0.213	0.000	-0 142	0.213	-0.248	-0.248	0.035	-0.319
9	-0.284	0.000	-0.142	0.213	-0.248	-0.248	0.106	-0.319
10	-0.426	0.000	-0.142	0.213	-0.390	-0.248	0.177	-0.248
11	-0.213	0.000	-0.071	0.142	-0.319	-0.248	0 248	-0.319
12	-0.071	0 000	-0.142	0.426	-0.319	-0.177	0.319	-0 390
13	-0.071	-0.071	0.142	0.496	-0.390	-0.461	0 390	-0.745
14	-0.284	0.000	-0.213	0.284	-0.390	-0.319	0 319	-0.390
15	-0.567	0.142	-0.213	0.355	-0.461	-0.603	-2.730	-0 674

Table A.2 *(Cont'd)* Corbel Specimen C-1 – Strain Measurements.

Load Stage	DEMEC Gauge Readings - Strain (mm/m) 49 N D810DF	50 S H13E	51 S H24C	52 S H24D	53 S H35B	54 S H68B	55 S H79C	56 S H79D
0A	-0.035	-0.050	0.000	-0 050	0.000	0.000	0.050	0 000
0B	0.035	0.050	0.000	0.050	0.000	0.000	-0.050	0.000
1	0.035	-0.050	0.000	0.050	0.000	0.000	-0.050	0.000
2	0.035	0.050	0.000	0.150	0.000	0.000	-0.050	-0.100
3	0.035	-0.050	0.000	0.050	0.000	-0.100	-0.050	0.000
4	-0.035	0.050	0.100	0.150	0.000	-0.100	-0.050	0 000
5	-0.106	0.050	0.000	0.050	0.000	0.000	-0.050	0 000
6	-0.177	0.050	-0.100	-0 050	-0.100	-0.100	-0.050	-0.100
7	-0.106	0.550	0.100	0.350	-0.100	-0.100	-0.050	-0 200
8	-0.248	1.150	0.500	0.950	0.100	-0.100	-0.150	-0.200
9	-0.390	1.550	0.900	1.250	0.400	-0.200	-0.150	-0.200
10	-0.177	2.050	1.200	1.750	0.600	-0.100	0.150	0.200
11	-0.177	2.550	1.500	2.050	0.800	0.100	0 450	0.600
12	-0.106	3.050	1.800	2.450	1.000	0.500	0.850	1.100
13	-0.177	3.350	2.100	2.750	1.100	0.600	1.150	1.400
14	0.035	4.050	2.500	3.350	1.400	0.900	1.550	1.900
15	-0.106	9.950	5.500	7.850	2.900	1.100	1.950	1.900

Table A.2 *(Cont'd)* Corbel Specimen C-1 – Strain Measurements.

	DEMEC Gauge Readings - Strain (mm/m)							
Load Stage	57 S H810E	58 S V2CE	59 S V2DF	60 S V3BD	61 S V3CE	62 S V4AC	63 S V4BD	64 S V7AC
0A	0.050	-0.050	-0.050	0.000	0.000	-0.050	-0.050	-0.100
0B	-0.050	0.050	0.050	0.000	0.000	0.050	0.050	0.100
1	-0.050	-0.050	-0.050	0.000	0.000	-0.050	0 050	-0.100
2	-0.050	-0.050	-0.050	0.100	0.100	0.050	0.050	-0.100
3	-0.050	-0.050	-0.050	-0.100	0.000	-0.150	-0.050	-0.100
4	-0.050	0.050	0.050	0.000	0.100	0.050	0.050	-0 100
5	-0.050	-0.150	-0.050	-0.100	-0.100	-0.150	-0.050	-0.100
6	-0.050	-0.150	-0.050	-0.200	-0.100	-0 250	-0.150	-0.200
7	-0.150	-0.250	0.350	-0.100	0.000	-0.250	-0 150	-0 300
8	-0.150	-0.350	0.750	0.200	0.400	-0.250	-0.150	-0 300
9	-0.150	-0.350	1.150	0 500	0.600	-0.150	-0 150	-0.300
10	0.450	-0.450	1.550	0.800	1.000	0.050	-0.150	-0 200
11	0.950	-0.550	1.950	1.000	1.200	0 150	-0.250	-0.100
12	1.850	-0.550	2.250	1.200	1 500	0.250	-0 150	0.100
13	2.350	-0.550	2.550	1.500	1.800	0.250	-0.250	0.200
14	3.250	-0.550	3.050	1.900	2.200	0 450	-0 250	0 400
15	4.050	-0.750	7.250	3 100	4.300	1.750	-0 350	0.600

Table A.2 *(Cont'd)* Corbel Specimen C-1 – Strain Measurements.

	DEMEC Gauge Readings - Strain (mm/m)							
Load Stage	65 S V7BD	66 S V8BD	67 S V8CE	68 S V9CE	69 S V9DF	70 S D13EC	71 S D13FD	72 S D24CA
0A	0.000	-0.050	-0.050	-0.050	0.000	0.000	0.035	0.035
0B	0.000	0.050	0.050	0.050	0 000	0.000	-0.035	-0 035
1	0.000	0.050	-0.050	-0.050	0.000	-0 071	0.106	-0 248
2	0.000	0.050	0.050	-0 050	0.000	-0.142	0 035	0 035
3	0.100	0.050	-0.050	-0 050	0.000	-0.142	-0.035	-0 035
4	0.000	0.050	-0.150	-0.050	0.000	-0.213	0.106	-0.106
5	0.000	0.050	-0.050	-0.050	0.000	-0.213	-0.035	-0 106
6	-0.100	-0.050	-0.150	-0.150	0.000	-0.284	-0 035	-0 248
7	-0.200	-0.050	-0.150	-0.150	-0.100	-0.284	0.035	-0 248
8	-0.200	-0.050	-0.150	-0.250	-0.100	-0.284	0.177	-0 248
9	-0.200	-0.150	-0.150	-0.150	-0.100	-0.355	0.177	-0.390
10	-0.200	-0.150	0.150	-0.250	-0.100	-0.496	0.177	-0.461
11	0.100	-0.250	0.450	-0.250	-0.200	-0.638	0.248	-0.603
12	0.200	-0.250	0.750	-0 250	-0.200	-0.426	0 461	-0 674
13	0.400	-0.350	0.950	-0.250	-0.100	0.355	0.603	-0.248
14	0.600	-0.350	1.350	-0.250	-0.100	-0.567	0.532	-0.745
15	0.900	-0.250	1.550	0.050	0.000	0.071	2.376	-0.177

Table A.2 *(Cont'd)* Corbel Specimen C-1 – Strain Measurements.

Load Stage	DEMEC Gauge Readings - Strain (mm/m) 73 S D24DB	74 S D24EC	75 S D24FD	76 S D35CA	77 S D35DB	78 S D68AC	79 S D68BD	80 S D79AC
0A	0.035	0.000	0.035	0.035	0.035	-0.035	-0.035	0.000
0B	-0.035	0.000	-0.035	-0.035	-0.035	0.035	0.035	0.000
1	0.035	0.071	0.106	0.106	0.035	0.106	0.106	0.071
2	-0.035	0.000	0.035	0.035	-0.106	0.035	0.035	0.000
3	-0.035	0.000	0.106	0.035	-0.106	-0.035	-0.035	-0.071
4	-0.035	0.000	0.106	-0.035	-0.035	-0.106	-0.035	-0.213
5	-0.035	-0.071	0.035	-0.106	-0.035	-0.106	-0.035	-0.142
6	-0.106	-0.071	0.035	-0.177	-0.106	-0.177	-0.106	-0.213
7	-0.177	-0.071	0.035	-0.177	-0.177	-0.177	-0.106	-0.284
8	-0.177	0.000	-0.035	-0.106	-0.177	-0.177	-0.106	-0.355
9	-0.177	-0.071	-0.035	-0.177	-0.248	-0.390	-0.177	-0.426
10	-0.248	0.000	-0.177	-0.177	-0.319	-0.319	-0.177	-0.496
11	-0.532	0.213	-0.532	-0.177	-0.319	-0.319	0.177	-0.355
12	-0.177	0.213	-0.177	0.035	-0.177	-0.390	0.177	-0.426
13	0.035	0.142	0.319	-0.106	-0.177	-0.319	0.106	-0.284
14	-0.248	0.567	-0.603	-0.106	-0.390	-0.106	0.177	-0.355
15	1.028	2.766	0.177	1.099	0.461	-0.248	-0.035	-0.426

Table A.2 *(Cont'd)* Corbel Specimen C-1 – Strain Measurements.

Load Stage	DEMEC Gauge Readings - Strain (mm/m) 81 S D79BD	82 S D79CE	83 S D79DF	84 S D810CE	85 S D810DF
0A	-0.035	-0.035	-0.035	0.000	-0.035
0B	0.035	0.035	0.035	0.000	0.035
1	0.106	0.035	-0.035	-0.071	-0.035
2	-0.035	-0.106	-0.035	-0.142	-0.035
3	0.035	-0.035	-0.035	-0.071	-0.106
4	-0.106	-0.035	-0.106	-0.142	-0.106
5	-0.106	-0.035	-0.106	-0.142	-0.177
6	-0.106	-0.177	-0.177	-0.213	-0.248
7	-0.177	-0.106	-0.248	-0.213	-0.248
8	-0.248	-0.248	-0.248	-0.355	-0.319
9	-0.319	-0.248	-0.248	-0.284	-0.248
10	-0.319	-0.319	-0.177	-0.284	-0.319
11	-0.035	0.106	0.106	-0.213	-0.177
12	-0.319	0.390	0.106	-0.213	-0.248
13	-0.177	0.106	0.319	-0.496	-0.177
14	-0.319	0.035	0.532	-0.355	-0.106
15	-0.603	0.248	0.674	-0.426	-0.035

A.3 Dapped End Specimens D-1 and D-2

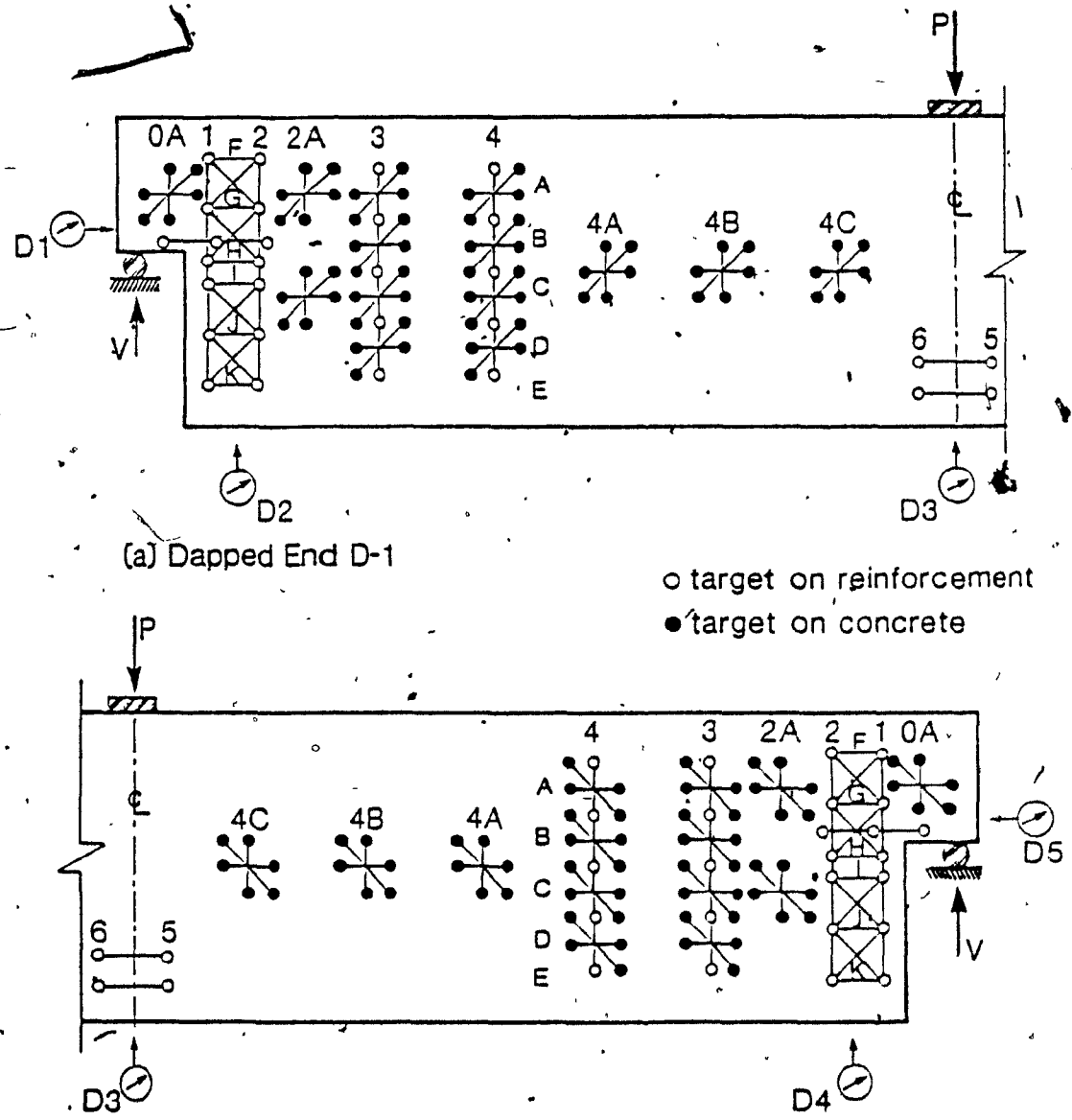

Figure A.2 Initial Test Set-Up and Instrumentation for Dapped End Specimens D-1 and D-2.

Table A.3 Dapped End Specimens D-1 and D-2 – Measured Loads – Loading 1.

Load Stage	Shear* (kN)	Measured Loads and Deflections Dial 1 (mm)	Dial 2 (mm)	Dial 3 (mm)	Dial 4 (mm)	Dial 5 (mm)
1A-C	0.0	0.00	0.00	0.00	0.00	0.00
2	33.4	0.05	0.51	0.99	0.38	0.89
3	66.7	0.05	0.91	2.21	0.61	1.24
4	100.1	0.03	1.40	3.35	1.60	1.37
5	133.5	0.00	1.96	4.72	2.24	1.42
6	166.8	0.03	2.67	6.25	2.95	1.40
7	200.2	0.00	3.51	8.33	3.66	1.35
8	233.5	-0.03	4.29	10.26	5.11	1.27
9	251.3	0.00	3.48	10.52	12.32	-0.79
10	3.3	0.10	2.41	7.04	9.12	-1.55

* Does not include self-weight shear of 6.6 kN.

Table A.4 Dapped End Specimens D-1 and D-2 – Strain Measurements – Loading 1.

Load Stage	1 D2 H0A-A	2 D2 H12F	3 D2 H12G	4 D2 H12H	5 D2 H12I	6 D2 H12J	7 D2 H12K	8 D2 H2A-A
	DEMEC Gauge Readings - Strain (mm/m)							
1A	0.067	0.100	—	0.033	—	0.050	—	0.133
1B	-0.033	0.000	0.150	-0.067	0.100	—	-0.100	-0.167
1C	-0.033	-0.100	-0.150	0.033	-0.100	-0.050	0.100	0.033
2	-0.133	-0.200	0.050	0 033	-0.100	0.050	0.100	0.133
3	-0.033	-0.100	0.150	0.033	-0.200	0.050	0.200	0.033
4	-0.133	-0.100	0.550	0.033	0.000	-0.250	0.100	0.033
5	-0.033	0.000	0.550	0 433	0.200	0.150	0.000	0.233
6	0.567	0.300	0.850	0.833	0.400	-0.050	0.200	0.433
7	1.067	-0.100	1.150	1.533	1.800	0.250	0.100	0.033
8	2.267	0.200	1.150	2.233	2.600	0.150	0.200	-0.367
10	5.067	—	—	1.133	2.000	0.450	0.000	1.533

Table A.4 *(Cont'd)* Dapped End Specimens D-1 and D-2 – Strain Measurements – Loading 1.

Load Stage	9 D2 H2A-D	10 D2 H3A	11 D2 H3B	12 D2 H3D	13 D2 H3E	14 D2 H4A	15 D2 H4B	16 D2 H4D
	DEMEC Gauge Readings - Strain (mm/m)							
1A	0.033	—	0.100	0.067	0.133	0.100	-0.100	0.133
1B	-0.067	0.000	—	-0.033	-0.067	0.000	0.000	-0.067
1C	0.033	0.000	-0.100	-0.033	-0.067	-0.100	0.100	-0.067
2	0.033	-0.100	0.000	-0.233	0.033	0.100	0.200	0.033
3	0.133	-0.500	0.000	0.067	0.033	0.000	0.100	0.033
4	0.033	-0.200	-0.100	-0.133	0.033	-0.100	0.000	-0.067
5	0.033	-0.200	-0 100	-0.033	0.133	-0.200	0.000	0.233
6	0.033	-0.300	-0.100	-0.233	1.033	-0.300	0.000	0.133
7	-0.067	-0.100	-0.100	-0.333	2.033	0.000	0.000	-0.067
8	-0.067	-0.200	-0.200	-0.333	3.133	-0.200	0.100	-0.067
10	-0.067	-1.400	-0.100	-0.333	1.333	0.000	0.100	-0.067

Table A.4 *(Cont'd)* Dapped End Specimens D-1 and D-2 – Strain Measurements – Loading 1.

	DEMEC Gauge Readings - Strain (mm/m)							
Load	17	18	19	20	21	22	23	24
Stage	D2 H4E	D2 H4AC	D2 H4BC	D2 H4CC	D2 H0A1B	D2 H12B	CL H56E	CL H56K
1A	0.067	0.200	0.133	0.067	-0.035	0.000	0.142	-0.189
1B	-0.033	0.000	-0.067	-0.033	—	0.000	0.071	0.024
1C	-0.033	-0.200	-0.067	-0.033	0.035	—	-0.213	0.165
2	0.167	0.100	0.133	0.067	0.248	-0.071	0.000	0.378
3	0.267	-0.200	-0.267	0.067	0.390	0.284	0 284	0.875
4	0.367	0.000	0.033	0.267	0.532	0.638	0.496	—
5	0.467	0.100	0.233	0.367	0.745	0.780	0.780	1.300
6	0.567	0.100	0.133	0.467	1.241	0.993	0.851	1.584
7	0.667	0.400	0.233	0.567	1.525	1.560	1.064	1.797
8	0.367	0.900	0.933	0.667	2.092	2.482	1.348	2.009
10	0.067	0.500	0.833	0.267	5.142	2.199	0.355	0.875

Table A.4 *(Cont'd)* Dapped End Specimens D-1 and D-2 – Strain Measurements – Loading 1.

	DEMEC Gauge Readings - Strain (mm/m)							
Load	25	26	27	28	29	30	31	32
Stage	D2 V0A-A	D2 V1FG	D2 V1GH	D2 V1GI	D2 V1HJ	D2 V1IJ	D2 V1JK	D2 V2FG
1A	0.067	-0.100	0.133	—	0.118	0.133	—	-0.167
1B	0.067	0.100	-0.067	-0.035	0.118	-0.067	0.000	0.133
1C	-0.133	0.000	-0.067	0.035	-0.236	-0.067	0.000	0.033
2	0.067	0.000	-0.167	-0.177	-0.024	0.133	-0.100	0.233
3	-0.033	0.200	0.333	-0.106	0.047	-0.067	-0.400	-0.067
4	-0.033	0.500	0.733	0.319	-0.236	0.133	-0.500	0.033
5	-0.133	0.400	1.133	0.603	-0.236	0.333	-0.500	0.133
6	0.867	0.800	1.533	1.099	0.686	1.233	-0.100	0.433
7	1.767	1.000	2.033	1.454	1.324	2.033	0.100	0.633
8	3.867	1.100	2.733	1.596	1.608	2.833	0.400	1.033
10	16.167	—	—	—	0.898	0.633	0.000	—

Table A.4 *(Cont'd)* Dapped End Specimens D-1 and D-2 – Strain Measurements – Loading 1.

	DEMEC Gauge Readings - Strain (mm/m)							
Load	33	34	35	36	37	38	39	40
Stage	D2 V2GH	D2 V2GI	D2 V2HJ	D2 V2IJ	D2 V2JK	D2 V2A-A	D2 V2A-D	D2 V3A
1A	-0.033	0.000	—	0.033	—	0.050	—	0.033
1B	-0.033	0.000	0.071	0.033	-0.050	—	0.050	-0.067
1C	0.067	0.000	-0.071	-0.067	0.050	-0.050	-0.050	0.033
2	-0.033	-0.071	-0.213	0.033	-0.050	0.050	-0.050	-0.367
3	-0.133	-0.071	-0.426	-0.067	-0.050	-0.050	-0.150	-0.167
4	0.067	-0.071	-0.567	-0.467	-0.050	0.050	-0.250	-0.267
5	0.467	0.000	-0.638	-0.567	-0.250	-0.350	-0.350	-0.167
6	0.767	0.851	-0.142	-0.267	-0.150	-0.350	-0.350	-0.067
7	0.967	0.709	-0.071	-0.067	0.250	-0.250	-0.450	-0.167
8	1.167	1.348	0.213	0.333	1.050	-0.250	-0.450	0.233
10	-0.633	0.355	-0.709	0.033	0.350	—	-0.450	0.733

Table A.4 *(Cont'd)* Dapped End Specimens D-1 and D-2 – Strain Measurements – Loading 1.

Load Stage	DEMEC Gauge Readings - Strain (mm/m) 41 D2 V3B	42 D2 V3D	43 D2 V3E	44 D2 V4A	45 D2 V4B	46 D2 V4D	47 D2 V4E	48 D2 V4A-C
1A	-0.067	-0.033	-0.100	0 000	0.033	0.000	0.033	0.000
1B	-0.167	0.067	0.000	0 000	0.033	0.000	0.033	0.000
1C	0.233	-0.033	-0.100	0.000	-0.067	0.000	-0.067	0 000
2	0.133	-0.833	0.200	0 000	-0.167	0.000	0.033	0.000
3	0.033	-0.133	0.000	-0.100	-0.067	0.000	-0.267	0.100
4	-0.067	-0.433	-0.100	0.000	0.033	-0.100	-0.167	-0.200
5	-0.067	-0.133	0.100	0.000	-0.067	-0.100	-0.067	-0.200
6	0.133	0.167	0.500	0.200	0.133	0.000	-0.067	-0.200
7	0.433	0.667	1.200	0 800	0.733	0.100	-0.067	0.400
8	0.833	1.567	2.000	1 100	1.033	0.200	0.033	0 800
10	0.333	0 567	0.900	0.400	0.433	0.100	0.133	0 500

Table A.4 *(Cont'd)* Dapped End Specimens D-1 and D-2 – Strain Measurements – Loading 1.

Load Stage	DEMEC Gauge Readings - Strain (mm/m) 49 D2 V4B-C	50 D2 V4C-C	51 D2 D0A-A	52 D2 D21FG	53 D2 D21GH	54 D2 D21IJ	55 D2 D21JK	56 D2 D12FG
1A	-0.133	0.000	-0.095	0.095	0.071	0.000	—	0 071
1B	-0.033	-0.100	-0.024	0.024	0.071	0.071	-0.035	0.000
1C	0.167	0.100	0.118	-0.118	-0.142	-0.071	0.035	-0 071
2	0.267	0.100	0.189	-0.189	-0.284	0.071	-0.319	-0.142
3	0.167	0.200	0.118	-0.047	-0.213	-0.071	-0.887	-0.142
4	0.067	-0.100	0.189	0.095	-0.071	-0.142	-0.461	-0.071
5	0.167	-0.200	0.189	0.307	-0.142	-0.355	-0.319	0.142
6	0.567	0.000	0.118	0.378	-0.142	-0.071	-0.390	0.426
7	0.667	0.200	0.118	0.733	0.426	-0.142	-0.248	0.496
8	0.667	-0.200	0.118	0.875	0.851	-0.213	-0.816	0.284
10	1.067	-0.200	-0.165	—	-0.922	-0.426	-0.816	—

Table A.4 *(Cont'd)* Dapped End Specimens D-1 and D-2 – Strain Measurements – Loading 1.

Load Stage	DEMEC Gauge Readings - Strain (mm/m) 57 D2 D12GH	58 D2 D12IJ	59 D2 D12JK	60 D2 D2A-A	61 D2 D2A-D	62 D2 D3A	63 D2 D3B	64 D2 D3D
1A	0.355	0.095	—	0.142	-0.024	0.024	0.047	-0.071
1B	-0.071	0.024	0.000	-0.071	0.047	0.024	-0.024	0.000
1C	-0.284	-0.118	0.000	-0.071	-0.024	-0.047	-0.024	0.071
2	0.071	0.095	-0.213	-0.142	-0.095	-0.118	-0.095	-0.071
3	0.284	0.095	-0.142	-0.071	-0.165	-0.118	-0.165	-0.071
4	0.567	0.236	-0.142	0.000	-0.165	0.024	-0.095	-0.071
5	1.348	0.591	0.071	0.000	-0.236	-0.189	-0.307	-0.213
6	1.844	1.442	0.071	0.000	-0.236	-0.047	-0.165	-0 213
7	2.128	2.506	0.496	-0.071	-0.236	-0.118	-0.236	-0.426
8	2.624	3.641	1.206	-0.284	-0.378	-0.118	-0.307	-0.638
10	—	1.939	0.496	—	-0.236	0.307	0.544	-0.355

Table A.4 *(Cont'd)* Dapped End Specimens D-1 and D-2 – Strain Measurements – Loading 1.

	DEMEC Gauge Readings - Strain (mm/m)							
Load Stage	65 D2 D3E	66 D2 D4A	67 D2 D4B	68 D2 D4D	69 D2 D4E	70 D2 D4A-C	71 D2 D4B-C	72 D2 D4C-C
1A	0.024	0.024	—	-0.024	0.000	0.095	0.047	-0.024
1B	0.024	0.024	0.071	-0.095	-0.071	-0.047	0.047	0.047
1C	-0.047	-0.047	-0.071	0.118	0.071	-0.047	-0.095	-0.024
2	-0.047	-0.118	-0.142	0.047	0.071	0.024	0.047	0.047
3	0.024	-0.189	-0.071	-0.024	0.000	0.024	-0.024	0.047
4	0.024	-0.189	-0.071	-0.024	0.071	-0.047	-0.024	0.118
5	-0.047	-0.047	-0.071	-0.024	0.142	-0.047	-0.095	0.047
6	-0.047	-0.118	-0.142	0.047	0.355	-0.047	-0 024	0.118
7	-0.118	-0.189	-0.213	-0.024	0.284	-0.118	-0.165	0.118
8	-0.189	-0.189	-0.142	0.047	0.284	-0.047	-0.236	-0.024
10	-0.189	-0.118	-0.071	-0.095	0.000	-0.047	-0.095	0.118

Table A.4 *(Cont'd)* Dapped End Specimens D-1 and D-2 – Strain Measurements – Loading 1

	DEMEC Gauge Readings - Strain (mm/m)							
Load Stage	73 D2BK H0A	74 D2BK V0A	75 D2BK D0A	76 D1 H0A-A	77 D1 H12F	78 D1 H12G	79 D1 H12H	80 D1 H12I
1A	0.033	0.033	0.142	0.200	-0.067	0.050	0.200	0.067
1B	0.033	0.033	0.071	0.000	0.133	—	0.200	0.167
1C	-0.067	-0.067	-0.213	-0.200	-0.067	-0 050	-0.400	-0.233
2	-0.067	-0.267	-0.071	-0.300	-0.167	-0.150	-0.300	-0.133
3	0.033	-0.267	-0.284	-0.300	-0.067	0.050	-0.400	-0.533
4	-0.167	-0.267	-0.355	-0.500	-0.067	0.150	0.100	-0 033
5	-0.067	-0.367	-0.426	-0.600	0 233	0 250	0 500	0.367
6	1.933	-0.267	-0.355	2.300	0.333	0.150	0.700	0.467
7	4.033	-0.167	-0.426	2.800	0.333	0,150	1.600	1.167
8	6.733	-0.067	-0.355	3.600	0.433	0 250	2.000	1.567
10	3.033	-0.067	-0.142	1.400	0.533	0.150	1.000	0 967

Table A.4 *(Cont'd)* Dapped End Specimens D-1 and D-2 – Strain Measurements – Loading 1.

	DEMEC Gauge Readings - Strain (mm/m)							
Load Stage	81 D1 H12J	82 D1 H12K	83 D1 H2A-A	84 D1 H2A-D	85 D1 H3A	86 D1 H3B	87 D1 H3D	88 D1 H3E
1A	0.400	0.100	0.000	0.033	-0.067	0.067	0.000	0.033
1B	0.300	0.100	0.000	0.133	0.033	-0.067	0.000	0.133
1C	-0.700	-0.200	0.000	-0.167	0.033	-0.133	0.000	-0.167
2	-0.400	-0.300	0.000	-0.367	-0.067	0.067	0.000	-0.367
3	-0.200	-0.400	0.000	-0.467	0.033	0.167	-0.100	-0.167
4	-0.600	-0.100	0.000	-0.567	0.033	0.067	0.200	-0.067
5	-0.400	0.100	0.000	-0.467	0.133	-0.033	0.200	-0.167
6	-0.700	0.000	-0.200	-0.667	0.133	-0.033	0.200	0.233
7	-0.200	0.500	-0.300	-0.567	0.233	-0.033	-0.100	1.833
8	-0.300	0.500	-0.200	-0.467	0.133	-0.033	-0.100	2.633
10	-0.100	0.600	-0.200	-0.567	0.233	0.067	0.100	0.833

Table A.4 *(Cont'd)* Dapped End Specimens D-1 and D-2 – Strain Measurements – Loading 1.

	DEMEC Gauge Readings - Strain (mm/m)							
Load Stage	89 D1 H4A	90 D1 H4B	91 D1 H4D	92 D1 H4E	93 D1 H4A-C	94 D1 H4B-C	95 D1 H4C-C	96 D1 H0A1B
1A	0.033	0.300	—	-0.167	-0.167	-0.033	0.200	0.024
1B	0.033	-0.100	0.000	-0.067	0.133	-0.033	0.000	0.024
1C	-0.067	-0.200	0.000	0.233	0.033	0.067	-0.200	-0.047
2	-0.067	-0.100	0.100	-0.567	0.033	0.167	0.000	-0.047
3	0.033	-0.200	0 200	0 233	0.133	0.267	0.000	0.449
4	0.033	-0.100	0.200	0.533	0.133	0.167	0.400	0.875
5	-0.067	-0.100	0.500	0 833	0.033	-0.033	0.600	1.442
6	-0.067	-0.100	0.600	0.833	-0.167	0.067	0.800	2.222
7	-0.067	0.100	0.500	0.833	-0.067	0.067	1.000	2.931
8	-0.067	0.000	0.400	0.733	-0.267	0.167	1.100	3.215
10	-0.067	-0.100	0.300	0.333	0.033	0.167	0.400	1.442

Table A.4 *(Cont'd)* Dapped End Specimens D-1 and D-2 – Strain Measurements – Loading 1.

	DEMEC Gauge Readings - Strain (mm/m)							
Load Stage	97 D1 H12B	98 D1 V0A-A	99 D1 V1FG	100 D1 V1GH	101 D1 V1GI	102 D1 V1HJ	103 D1 V1IJ	104 D1 V1JK
1A	0.047	-0.133	-0.167	-0.100	-0.165	-0.024	-0.067	-0.167
1B	-0.024	0.067	0.033	-0.100	0.118	-0.095	0.133	0.133
1C	-0.024	0.067	0.133	0.200	0.047	0.118	-0.067	0.033
2	-0.024	-0.133	0,133	0.300	0.331	0.402	0.133	-0.067
3	-0.024	-0.233	0.433	0.900	0.615	0.260	0.433	0.133
4	0.189	-0.233	0.633	1.400	1.08	0.615	0.433	0.533
5	0.331	-0.333	1.333	1.700	1.537	0.615	0.533	0.433
6	0.686	-0.133	1.833	2.200	2.388	1.08	1.433	0.333
7	1.324	-0.233	2.533	2.900	2 388	1.678	1.733	0.633
8	2.104	0.567	2.733	3.400	2.671	2.246	2.133	0.833
10	1.324	-0.133	1.033	1 300	1.040	0.331	0.433	0.533

Table A.4 *(Cont'd)* Dapped End Specimens D-1 and D-2 – Strain Measurements – Loading 1.

	DEMEC Gauge Readings - Strain (mm/m)							
Load Stage	105 D1 V2FG	106 D1 V2GH	107 D1 V2GI	108 D1 V2HJ	109 D1 V2IJ	110 D1 V2JK	111 D1 V2A-A	112 D1 V2A-D
1A	-0.233	-0.050	—	—	-0.133	-0.033	0.167	0.000
1B	0.167	0.050	-0.177	0.071	0.167	-0.033	-0.233	0.000
1C	0.067	—	-0.177	-0.071	-0.033	0.067	0.067	0.000
2	0.067	0.050	-0.106	-0.567	-0.033	0.067	0.067	-0.100
3	0.267	0.550	-0.177	-0.426	0.267	0.167	0.067	-0.100
4	0.567	0.350	-0.177	-0.355	-0.133	0.167	0.067	-0.100
5	0.667	0.550	0.603	0.213	0.267	0.167	-0.033	-0.100
6	0.867	0.950	0.745	0.000	0.567	0.267	-0.033	-0.100
7	0.967	1.050	0.887	0.638	0.567	0.767	-0.133	-0.100
8	1.167	1.550	0.887	0.567	0 667	0.967	-0.233	-0.200
10	0.467	0.350	0.816	0.213	0.067	0.367	0.167	-0.100

Table A.4 *(Cont'd)* Dapped End Specimens D-1 and D-2 - Strain Measurements - Loading 1.

	DEMEC Gauge Readings - Strain (mm/m)							
Load Stage	113 D1 V3A	114 D1 V3B	115 D1 V3D	116 D1 V3E	117 D1 V4A	118 D1 V4B	119 D1 V4D	120 D1 V4E
1A	-0.167	0.000	0.100	0.033	-0.067	0 033	0.000	0.000
1B	0.133	0.100	0.000	0 033	0 033	-0.067	0 000	0.000
1C	0.033	-0.100	-0.100	-0.067	0 033	0 033	0.000	0 000
2	-0.067	-0.100	-0.100	-0.867	-0.067	0.033	-0.100	-0.100
3	-0.067	-0.100	0.000	-0.167	-0.067	0 033	0.000	0 000
4	-0.067	0.000	0.000	0.133	-0 067	0.033	0.100	0 000
5	0.133	0.100	0.100	-0.067	-0.067	0 133	0.100	0 100
6	0.133	0.100	0.100	-0.067	0 033	0.233	0.400	0.200
7	0.433	0.400	1.100	1.533	0.333	1 633	1 400	0.700
8	0.333	0.900	1.500	1.733	0.633	1.833	1 700	0 800
10	0.133	0.600	0.800	0.433	0.433	0 533	0 400	0 600

Table A.4 *(Cont'd)* Dapped End Specimens D-1 and D-2 - Strain Measurements - Loading 1.

	DEMEC Gauge Readings - Strain (mm/m)							
Load Stage	121 D1 V4A-C	122 D1 V4B-C	123 D1 V4C-C	124 D1 D0A-A	125 D1 D21FG	126 D1 D21GH	127 D1 D21IJ	128 D1 D21JK
1A	-0.067	-0.033	0.000	-0.047	0 213	-0.118	-0 106	-0 165
1B	0.133	0.067	0.100	-0.095	0.000	0.095	—	0 118
1C	-0.067	-0.033	-0.100	0.047	-0.213	0.024	0 106	0 047
2	-0.067	-0.033	-0.100	-0.024	0 000	0.024	0 248	0 118
3	-0.067	-0.033	0.000	-0.095	0.000	0.024	0 319	0 260
4	-0.167	-0.133	-0.100	-0.307	-0.142	0.165	0.390	0.402
5	-0.067	-0.033	-0.100	-0.236	0 000	0 449	0.461	0 544
6	-0.167	0.167	0.000	-0.165	0.355	0.662	0.532	
7	0.133	-0.033	-0.100	-0.095	0.709	1.229	0.390	0 331
8	0.033	-0.133	0.000	-0 095	0.993	1.584	0 106	0 189
10	-0.167	-0.033	0.000	0.047	0.709	1 017	0.248	0 544

Table A.4 *(Cont'd)* Dapped End Specimens D-1 and D-2 - Strain Measurements - Loading 1

	DEMEC Gauge Readings - Strain (mm/m)							
Load Stage	129 D1 D12FG	130 D1 D12GH	131 D1 D12IJ	132 D1 D12JK	133 D1 D2A-A	134 D1 D2A-D	135 D1 D3A	136 D1 D3B
1A	0.142	0.095	-0.047	-0.213	-0 024	0.165	—	0 024
1B	0.000	0.095	-0.260	0 071	0 047	-0.118	-0.035	0.024
1C	-0.142	-0 189	0.307	0.142	-0.024	-0.047	0 035	-0 047
2	0 071	0.307	0.236	0.000	0.118	-0.118	0 035	-0 047
3	0.496	0.591	0.307	-0 355	-0 024	-0.118	-0 106	-0 189
4	0.851	1.087	0.378	-0.284	-0.095	-0 118	-0.106	-0 331
5	1.277	1.513	0.946	0.142	-0.024	-0.118	-0 035	-0 118
6	1.418	1.726	1.513	0.071	-0.095	-0 189	-0 106	-0 331
7	1.418	1.797	2.009	0 426	-0.236	-0 260	-0.106	-0 189
8	1.418	2.009	2.506	0.142	-0.236	-0.331	-0.035	-0 331
10	0.213	0.591	0.875	0 142	-0.165	-0.118	-0 035	-0 189

Table A.4 *(Cont'd)* Dapped End Specimens D-1 and D-2 – Strain Measurements – Loading 1.

Load Stage	DEMEC Gauge Readings - Strain (mm/m) 137 D1 D3D	138 D1 D3E	139 D1 D4A	140 D1 D4B	141 D1 D4D	142 D1 D4E	143 D1 D4A-C	144 D1 D4B-C
1A	-0.095	0.047	0 095	-0.035	-0.071	-0.024	-0.024	-0.095
1B	0.118	0.047	0.095	0.035	0.142	-0.024	0.047	0.047
1C	-0.024	-0.095	-0.189	—	-0.071	0.047	-0.024	0.047
2	0.047	0.118	0.024	-0.035	0.071	0.118	-0.024	-0.024
3	0.047	-0.024	-0.047	-0.177	0.000	0.189	-0.095	-0.024
4	-0.024	-0.024	-0.118	-0 248	0.000	0.189	-0.024	-0.024
5	0.047	-0.095	-0 189	-0 248	0.000	0.189	-0.095	0.047
6	-0.095	-0.165	-0.189	-0.177	-0.071	0.118	-0.024	-0.024
7	-0.236	-0.307	-0 260	-0.390	-0.284	0.047	-0.024	-0.024
8	-0.378	-0.307	-0.260	-0.461	-0.355	0.047	-0.165	-0.165
10	-0.165	-0.165	-0 047	-0.248	-0.071	0.118	-0.024	0.047

Table A.4 *(Cont'd)* Dapped End Specimens D-1 and D-2 – Strain Measurements – Loading 1.

Load Stage	DEMEC Gauge Readings - Strain (mm/m) 145 D1 D4C-C	146 D1BK H0A	147 D1BK V0A	148 D1BK D0A
1A	-0.071	-0.033	0.000	0 024
1B	0.071	-0.033	0.000	0.024
1C	0.000	0.067	0.000	-0.047
2	0.000	-0.133	0.000	-0 047
3	0.071	-0.133	-0.200	-0.047
4	0.071	-0.033	-0.100	-0.118
5	0.071	-0.233	-0.200	-0.331
6	0.142	-0.233	-0.300	-0.331
7	0.142	1.167	1.100	-0.402
8	-0.071	1.767	2.200	-0.118
10	0.000	0.567	0.700	-0.118

Table A.5 Dapped End Specimen D-1 – Measured Loads – Loading 2.

Load Stage	Measured Loads and Deflections Shear* (kN)	Dial 1 (mm)	Dial 2 (mm)	Dial 3 (mm)
B1	10.4	0.00	0.00	0.00
B2	31.1	0.00	0.20	0.61
B3	155.7	-0.05	1.68	4.27
B4	218.0	-0.08	2.41	6.05
B5	238.7	-0.10	2.82	6.91
B6	259.5	-0.10	3.30	7.82
B7	280.2	-0.15	3.86	8.81
B8	301.0	-0.20	4.88	10.29
B8A	138.0	-0.61	12.90	11.13
B9	0.0	-0.53	9.55	5.51

* Does not include self-weight shear of 6.2 kN.

Table A.6 Dapped End Specimen D-1 – Strain Measurements – Loading 2.

Load Stage	DEMEC Gauge Readings - Strain (mm/m) 23 CL H56E	24 CL H56K	76 D1 H0A-A	77 D1 H12F	78 D1 H12G	79 D1 H12H	80 D1 H12I	81 D1 H12J
B1	0.284	1.017	1.200	0.333	0 250	0.800	0.867	-0.300
B2	0.284	1.158	1.100	0.033	0.250	0.600	0.767	-0.400
B3	0.922	1.797	2.300	0.233	0.550	1.400	1.667	0.000
B4	1.489	2.364	2.900	0.183	0.750	2.100	1.767	0.000
B5	1.560	2.577	3.000	0.133	0.250	1.800	1.567	-0.100
B6	1.631	2.577	3.300	0.033	0.650	2.400	2.067	-0.700
B7	1.915	2.861	3.600	0.133	0.550	2.600	2.267	0 500
B8	—	—	4.300	-0.067	0.350	3.100	2.267	-0 600
B9	0.496	1.584	6.800	—	-2 250	1 600	1 267	-0 800

Table A.6 *(Cont'd)* Dapped End Specimen D-1 – Strain Measurements – Loading 2

Load Stage	DEMEC Gauge Readings - Strain (mm/m) 82 D1 H12K	83 D1 H2A-A	84 D1 H2A-D	85 D1 H3A	86 D1 H3B	87 D1 H3D	88 D1 H3E	89 D1 H4A
B1	0.500	0 000	-0.467	0.133	0 067	0.100	0.733	0 033
B2	0.600	-0.500	-0.567	-0.067	-0 033	0.200	1 433	0 233
B3	0.700	-0.100	-0.467	0.233	0 167	-0.300	1 733	-0 067
B4	0.900	-0.300	-0 567	0 233	0 167	0 100	2 733	-0.167
B5	0.800	-0.400	-0.567	0 133	-0.033	-0.400	2 133	-0 167
B6	1.500	-0.400	-0.567	0 033	-0.133	-0 100	3 033	-0 067
B7	0.800	-1.300	-0.867	0 033	0 067	-0 300	3 433	-0 267
B8	1.100	-0 700	-0 767	0 133	0.067	-0 400	4 733	-0 367
B9	0.200	-0.600	-0.567	0.033	-0 033	-0.200	1 133	-0 067

Table A.6 *(Cont'd)* Dapped End Specimen D-1 – Strain Measurements – Loading 2

Load Stage	DEMEC Gauge Readings - Strain (mm/m) 90 D1 H4B	91 D1 H4D	92 D1 H4E	93 D1 H4A-C	94 D1 H4B-C	95 D1 H4C-C	96 D1 H0A1B	97 D1 H12B
B1	0.000	0.200	0.333	0.133	0.167	0 400	1.300	1.111
B2	0.100	0.400	0 533	0 033	0.167	0.400	1 584	1 466
B3	0.100	0.200	0.233	-0.067	0.167	0.900	2.577	2 033
B4	0.100	0.300	0.533	-0.167	0.067	0.900	3.286	2 600
B5	0.000	0.200	0 833	-0.167	0.067	1 200	3 783	2.742
B6	-0.100	0.100	0 433	-0.167	-0.033	1.500	3.995	2.955
B7	0.000	0.200	0 733	-0.167	-0 033	1.800	4.634	3.593
B8	-0.100	0.100	0.533	-0.267	-0.033	2.200	5.485	4.444
B9	-0.100	0.200	0.033	-0 067	0.067	0.500	9.740	1 395

Table A.6 *(Cont'd)* Dapped End Specimen D-1 – Strain Measurements – Loading 2.

Load Stage	DEMEC Gauge Readings - Strain (mm/m) 98 D1 V0A-A	99 D1 V1FG	100 D1 V1GH	101 D1 V1GI	102 D1 V1HJ	103 D1 V1IJ	104 D1 V1JK	105 D1 V2FG
B1	-0.133	0.833	1.300	1.040	0.544	0.833	0.833	0.467
B2	-0.133	0.833	1.500	1.324	0.615	0.533	0.833	0.567
B3	-0.333	1.933	2.600	2.175	1.182	1.333	0.533	1.067
B4	-0.233	2.333	3.300	2.813	1.891	1.633	1.033	1.267
B5	-0.333	2.233	3.500	2.600	2.317	1.633	1.033	1.067
B6	-0.233	2.833	3.900	3.310	1.891	2.133	0.833	1.467
B7	0.267	2.933	5.100	4.161	2.033	2.133	1.333	1.367
B8	1.767	3.933	7.300	—	—	3.333	1.833	2.067
B9	41.767	—	6.000	4.090	0.047	0.633	1.033	0.967

Table A.6 *(Cont'd)* Dapped End Specimen D-1 – Strain Measurements – Loading 2.

Load Stage	DEMEC Gauge Readings - Strain (mm/m) 106 D1 V2GH	107 D1 V2GI	108 D1 V2HJ	109 D1 V2IJ	110 D1 V2JK	111 D1 V2A-A	112 D1 V2A-D	113 D1 V3A
B1	0.250	0.745	-0.142	-0.133	0.467	0.167	-0.100	0.333
B2	0.550	0.532	0.284	-0.333	0.567	-0.233	-0.100	0.333
B3	1.050	1.099	0.426	0.367	0.867	-0.033	-0.200	0.433
B4	1.050	1.525	0.780	0.567	0.967	-0.033	0.000	0.633
B5	1.250	1.241	0.567	0 567	0.967	-0.233	-0.300	0.433
B6	1.550	1.241	0.213	0.467	0.967	0.067	-0.300	0.533
B7	1.750	1.667	0.496	0.667	1.267	-0.233	-0.300	0.633
B8	2.350	—	—	1.067	1.967	-0.333	-0.300	0.733
B9	0.850	7.553	-1.844	-0.033	0.667	-0.333	-0.200	0.333

Table A.6 *(Cont'd)* Dapped End Specimen D-1 – Strain Measurements – Loading 2.

Load Stage	DEMEC Gauge Readings - Strain (mm/m) 114 D1 V3B	115 D1 V3D	116 D1 V3E	117 D1 V4A	118 D1 V4B	119 D1 V4D	120 D1 V4E	121 D1 V4A-C
B1	0.500	0.800	0.633	0.533	0.633	0.300	0.400	0.033
B2	0.200	0.700	0.633	0.333	0.833	0.600	0.500	0.033
B3	0.700	1.400	1.333	0.533	1.433	1.200	0.800	0.033
B4	0.800	1.600	2.333	0.633	1.833	1.600	0.900	0.133
B5	1.000	1.700	2.033	0.533	1.933	1.500	0.800	-0.067
B6	0.800	1.900	2.133	0.633	2.133	1.700	0.900	-0.067
B7	1.400	2.300	2.533	0.633	2.533	2.100	1.300	-0.167
B8	1.700	2.400	5.433	0.833	3.533	3.500	1.200	0.033
B9	0.300	0.800	3.433	0.333	—	—	0.400	-0.067

Table A.6 *(Cont'd)* Dapped End Specimen D-1 – Strain Measurements – Loading 2.

Load Stage	DEMEC Gauge Readings - Strain (mm/m) 122 D1 V4B-C	123 D1 V4C-C	124 D1 D0A-A	125 D1 D21FG	126 D1 D21GH	127 D1 D21IJ	128 D1 D21JK	129 D1 D12FG
B1	0.067	0.000	-0.024	0.709	0.875	0.035	0.260	0.142
B2	-0.033	-0.100	0.189	0.780	1.087	0.461	0.473	0.355
B3	0.067	0.000	0.260	1.277	1.726	0.106	0.686	0.709
B4	0.067	-0.100	0.047	1 418	1.939	1.170	0 473	0.922
B5	-0.133	-0.200	0.118	1.418	2.009	0.887	0.757	0.993
B6	-0.133	-0.400	0.331	1.844	2.364	0 674	0.402	1 277
B7	-0.233	-0.300	-0.095	1.773	2.364	0.248	0.544	1 348
B8	-0.033	-0.300	-0.024	1 915	2.719	-0.035	-0.095	1.844
B9	-0.033	-0.300	—	-0 993	2.080	0.177	0.473	—

Table A.6 *(Cont'd)* Dapped End Specimen D-1 – Strain Measurements – Loading 2.

Load Stage	DEMEC Gauge Readings - Strain (mm/m) 130 D1 D12GH	131 D1 D12IJ	132 D1 D12JK	133 D1 D2A-A	134 D1 D2A-D	135 D1 D3A	136 D1 D3B	137 D1 D3D
B1	0.378	0.804	0.496	0.047	-0 047	-0.035	0.024	-0 095
B2	0.662	1.158	0.638	-0.024	-0 189	-0.035	-0 047	-0 024
B3	1.513	2.080	0 993	-0.024	-0.047	0.248	0.095	-0.165
B4	2.080	2.222	1.135	-0.024	-0 331	0.248	0.165	-0.165
B5	2.364	2.364	1.418	-0.024	-0 047	0.106	0.095	-0.095
B6	2.648	3.144	2.128	0.118	-0.189	0.319	0 307	-0 307
B7	3.499	3.499	2.128	0 615	-0.189	0 248	0.165	-0 307
B8	4.208	3.712	2.695	1 678	-0 260	0.319	0.520	-0 662
B9	0.449	1.371	1.064	0 402	-0.331	-0:035	—	-0.095

Table A.6 *(Cont'd)* Dapped End Specimen D-1 – Strain Measurements – Loading 2.

Load Stage	DEMEC Gauge Readings - Strain (mm/m) 138 D1 D3E	139 D1 D4A	140 D1 D4B	141 D1 D4D	142 D1 D4E	143 D1 D4A-C	144 D1 D4B-C	145 D1 D4C-C
B1	0.047	0.024	-0 248	-0.071	0.118	-0.024	0.118	-0 142
B2	-0.095	0.095	0.035	2.128	0.118	0.047	0.118	0 071
B3	0.118	-0.047	-0.390	-0.213	0.118	0 118	0.047	0 071
B4	0.189	-0.047	-0.177	-0.071	0.118	0.047	-0.095	0.213
B5	0.118	-0.047	-0.461	-0.142	0.260	0.047	0.118	0 000
B6	-0.024	-0 118	-0 319	-0.284	0.189	-0 165	0.189	-0 071
B7	-0.378	-0.260	-0.390	-0 284	0.047	-0.024	0.118	0.142
B8	-0.378	-0.118	-0 390	-0.213	0.118	-0.095	—	—
B9	-0.236	0.024	-0.248	0.000	0.118	0.047	0 118	-0.071

Table A.6 *(Cont'd)* Dapped End Specimen D-1 – Strain Measurements – Loading 2.

Load Stage	DEMEC Gauge Readings - Strain (mm/m) 146 D1BK H0A	147 D1BK V0A	148 D1BK D0A
B1	0.767	0.900	0.024
B2	0.967	1.100	0.165
B3	2.467	2.800	0.024
B4	3.267	3.900	0.165
B5	3.467	4.600	0.095
B6	3.367	4.900	0.236
B7	3.467	5.300	0.165
B8	3.467	6.000	—
B9	—	16.700	2.931

A.4 Dapped End Specimens D-3 and D-4

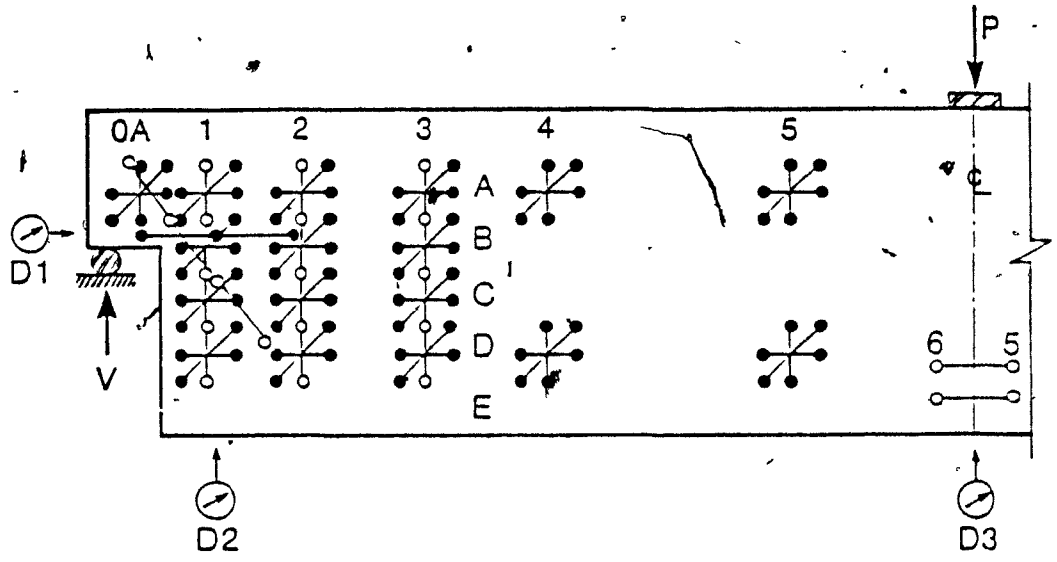

(a) Dapped End D-3

○ target on reinforcement
● target on concrete

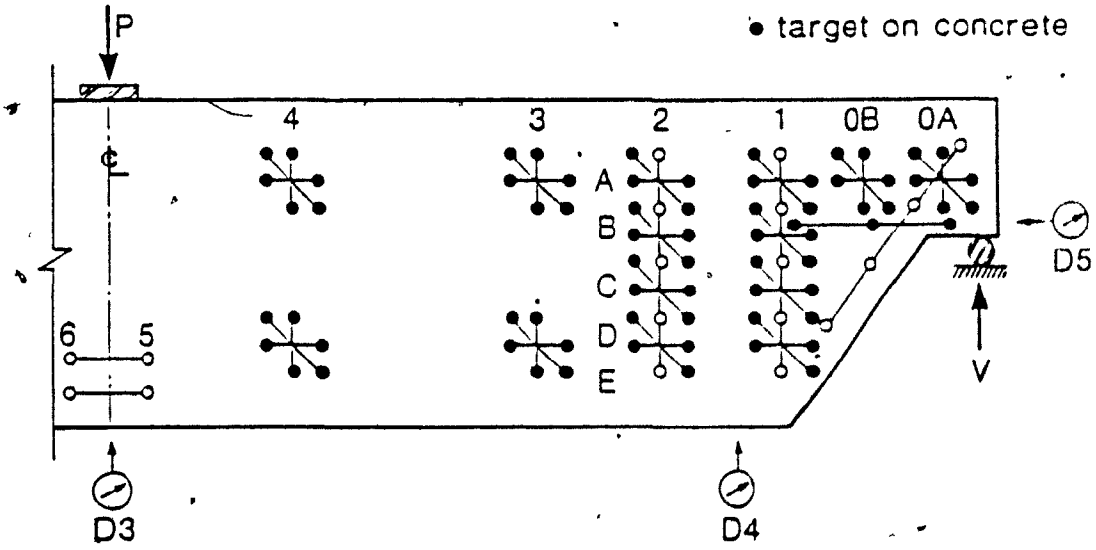

(b) Dapped End D-4

Figure A.3 Initial Test Set-Up and Instrumentation for Dapped End Specimens D-3 and D-4.

Table A.7 Dapped End Specimens D-3 and D-4 – Measured Loads – Loading 1.

Load Stage	Shear* (kN)	Measured Loads and Deflections Dial 1 (mm)	Dial 2 (mm)	Dial 3 (mm)	Dial 4 (mm)	Dial 5 (mm)
C0A-B	0.0	0.00	0.00	0.00	0.00	0.00
C1	33.4	-0.10	0.20	0.43	0.25	0.13
C2	66.7	-0.10	0.41	1.04	0.58	0.23
C3	100.1	-0.13	0.66	1.80	0.94	0.28
C4	133.5	-0.08	0.91	2.74	1.37	0.30
C5	166.8	0.05	1.22	3.99	2.34	0.36
C6	200.2	0.13	1.70	5.31	2.90	0.46
C7	233.5	0.20	2.03	6.68	3.76	0.53
C8	266.9	0.30	2.74	8.20	4.67	0.61
C9	300.3	0.41	3.30	10.19	6.45	0.71
C10	322.5	0.84	3.76	13.31	10.54	0.94
Max	333.6	1 47	4.14	17.27	16.92	1.27
End	0.0	1.30	1.37	8.31	12.07	1.32

* Does not include self-weight shears of 6.6 kN for specimen D-3 and 6.3 kN for specimen D-4

Table A.8 Dapped End Specimens D-3 and D-4 – Strain Measurements – Loading 1.

Load Stage	1 D3 H0A-A	DEMEC Gauge Readings - Strain (mm/m) 2 D3 H1A	3 D3 H1B	4 D3 H1C	5 D3 H1D	6 D3 H2A	7 D3 H2B	8 D3 H2C
C0A	0.000	0.100	0.100	0.000	0.000	0.050	0.050	0.050
C0B	0.000	-0.100	-0.100	0.000	0.000	-0.050	-0.050	-0 050
C1	0.000	0.000	-0.100	0.000	-0.100	-0.050	-0.050	-0.050
C2	0.000	0 000	0.000	-0.100	0.000	-0.050	-0.050	-0.050
C3	-0.100	-0.100	0 000	-0.100	-0.100	-0.150	-0.050	-0.050
C4	-0.100	-0.100	0.400	0 000	0.000	-0.150	-0.050	0 050
C5	0 000	-0.100	0 800	0 200	-0.100	-0.050	-0.050	0.050
C6	0.000	0.100	1.400	0.500	-0.100	-0.150	-0.050	-0.050
C7	0.000	0.100	1.400	0.900	-0.100	-0.150	0.050	-0.150
C8	-0.100	0 200	1.400	0.900	-0.100	-0.150	0.150	-0.150
C9	0.000	0.400	1.500	0.900	-0.100	-0.150	0.350	-0.150
C10	0.300	0.400	1.600	0 900	0.000	-0.150	0.450	-0.050

Table A.8 *(Cont'd)* Dapped End Specimens D-3 and D-4 – Strain Measurements – Loading 1.

	DEMEC Gauge Readings - Strain (mm/m)							
Load	9	10	11	12	13	14	15	16
Stage	D3 H2D	D3 H3A	D3 H3B	D3 H3C	D3 H3D	D3 H4A	D3 H4D	D3 H5A
C0A	0.000	0.000	0.000	-0.050	0.000	0.050	0.000	0.050
C0B	0.000	0.000	0.000	0 050	0.000	-0 050	0.000	-0.050
C1	0.000	-0 100	0.000	0 050	0.100	-0.050	0.000	-0.150
C2	0.000	-0.100	-0.100	0.050	0 100	-0.150	0.000	-0 150
C3	0.100	-0.200	-0.100	0.050	0.100	-0.150	0.300	-0.250
C4	0.100	-0.200	-0.100	0.050	0 100	-0.150	0.300	-0.250
C5	0.100	-0.100	-0.100	0.050	0.300	-0.250	0.700	-0.350
C6	1.700	-0 200	-0.100	2.350	1 000	-0.150	0.800	-0.350
C7	2.800	-0.200	-0.200	3 250	1.000	-0 150	0 900	-0.350
C8	2.700	-0.200	-0 100	4.050	0.900	-0 150	0 600	-0 450
C9	2.700	-0 200	-0.100	4.950	0.800	-0 150	0 500	-0 350
C10	2.800	-0.200	-0.100	5.750	0.800	-0 150	0.500	-0 450

Table A.8 *(Cont'd)* Dapped End Specimens D-3 and D-4 – Strain Measurements – Loading 1.

	DEMEC Gauge Readings - Strain (mm/m)							
Load	17	18	19	20	21	22	23	24
Stage	D3 H5D	D3 V0A-A	D3 V1A	D3 V1B	D3 V1C	D3 V1D	D3 V2A	D3 V2B
C0A	0.100	0.000	0.050	0 050	0.050	0 050	-0 050	0 100
C0B	-0.100	0.000	-0.050	-0.050	-0 050	-0.050	0.050	-0 100
C1	0.000	-0 100	-0.050	0.050	0 050	0.050	0.050	-0.100
C2	0.000	-0.200	0.050	0.050	0 050	-0 050	0 050	0 000
C3	0 500	-0.200	0 150	0 050	-0 050	-0 050	0.050	-0 100
C4	0.900	-0.300	0.550	0.350	0 150	-0 050	0.150	-0.100
C5	1.300	-0.200	0.350	0 450	0.250	-0.050	0 150	0.000
C6	1.800	-0.100	0.550	0.650	0.550	0 150	0 050	0 000
C7	2.200	-0.200	0.750	0 850	0 850	0 450	0 150	0 100
C8	2.400	-0.100	0.950	1.050	1 150	0 650	0.250	0.200
C9	2.800	0.100	1.050	1.150	1.250	0 950	0 350	0 300
C10	3.000	0.300	1.150	1.250	1 450	1.150	0 450	0 300

Table A.8 *(Cont'd)* Dapped End Specimens D-3 and D-4 – Strain Measurements – Loading 1

	DEMEC Gauge Readings - Strain (mm/m)							
Load	25	26	27	28	29	30	31	32
Stage	D3 V2C	D3 V2D	D3 V3A	D3 V3B	D3 V3C	D3 V3D	D3 V4A	D3 V4D
C0A	0.000	0.000	0.050	0.050	0.050	-0.050	0.050	0.000
C0B	0.000	0.000	-0 050	-0.050	-0.050	0 050	-0.050	0.000
C1	0.100	0.300	-0.050	-0.050	-0.050	0.050	-0 050	-0.200
C2	0.100	0.100	0.050	0.050	-0.050	-0.150	-0.050	0.000
C3	0.000	0.200	-0.050	0.050	-0.050	-0.050	0.050	0.100
C4	0.100	0.100	-0.050	-0.050	-0.150	-0.050	-0.050	-0.200
C5	0.100	0.000	-0.050	0.050	-0.050	0.050	-0.050	0.300
C6	0.200	0.400	0.050	0.450	1 250	0.750	0.550	0.200
C7	0.400	0.800	0.250	0.750	1.750	1.050	0.850	0.200
C8	0.600	1.700	0.250	0.950	2.350	1.350	1.050	0.500
C9	0.600	2.000	0.250	1.050	3.850	1.350	1.250	0.600
C10	0.600	2.400	0.150	0.950	5.350	1 450	1.550	0.600

Table A.8 *(Cont'd)* Dapped End Specimens D-3 and D-4 – Strain Measurements – Loading 1.

Load Stage	DEMEC Gauge Readings - Strain (mm/m) 33 D3 V5A	34 D3 V5D	35 D3 D0A-A	36 D3 D1A	37 D3 D1B	38 D3 D1C	39 D3 D1D	40 D3 D2A
C0A	0.000	0.000	0.035	0.035	0 000	0.000	-0.035	0.000
C0B	0.000	0.000	-0.035	-0.035	0.000	0.000	0.035	0.000
C1	-0.100	0.000	0.035	0 035	-0 071	0.071	-0.106	-0.071
C2	0.000	0.000	-0.035	0.106	-0.071	0.071	-0.035	-0.071
C3	0.100	0.100	-0.035	0.035	-0.071	0.142	-0.248	-0.142
C4	0.000	0.100	0.035	0.035	0.071	0.213	-0.106	-0.142
C5	0.000	0.100	-0.106	0.035	0.284	0.213	-0.106	-0.213
C6	0.100	0.300	-0.106	-0 106	0.496	0.426	-0.248	-0.071
C7	0.200	0.500	-0.177	-0.106	0.496	0.638	-0.248	-0.142
C8	0.600	0.600	-0.177	0.035	0.709	0.709	-0.177	-0.142
C9	0.700	0.700	-0.106	0 035	0.780	0.638	-0.106	0.000
C10	0.900	0.800	-0.035	0.035	0.780	0.851	-0.106	0.071

Table A.8 *(Cont'd)* Dapped End Specimens D-3 and D-4 – Strain Measurements – Loading 1

Load Stage	DEMEC Gauge Readings - Strain (mm/m) 41 D3 D2B	42 D3 D2C	43 D3 D2D	44 D3 D3A	45 D3 D3B	46 D3 D3C	47 D3 D3D	48 D3 D4A
C0A	0.035	0.000	0.000	0.000	-0.035	-0.035	-0.035	-0.035
C0B	-0.035	0.000	0 000	0.000	0.035	0.035	0.035	0.035
C1	-0.035	0.000	0.071	0.000	0.035	0.035	0.035	0.035
C2	-0.035	0.000	0 071	0.071	0.177	0.035	0.035	0.035
C3	-0.106	-0.071	0.000	0.000	-0 035	-0.035	-0.035	-0.035
C4	-0.177	-0.142	-0.071	0.000	-0.035	-0.035	-0.035	-0.035
C5	-0.177	-0.142	-0.071	-0.071	-0.106	-0.035	-0.035	-0.177
C6	-0.106	-0.142	-0.213	-0.142	-0.106	-0.106	-0.106	-0.106
C7	-0.248	-0.213	-0.355	-0.142	-0.248	0.035	-0.106	-0.177
C8	-0.177	-0.142	-0.426	-0.142	-0.177	0.248	-0.248	-0.106
C9	-0.106	-0.213	-0.496	-0.213	-0.248	0.390	-0.319	-0.177
C10	-0.106	-0.213	-0.426	-0.142	-0.177	0.674	-0.177	-0.035

Table A.8 *(Cont'd)* Dapped End Specimens D-3 and D-4 – Strain Measurements – Loading 1.

Load Stage	DEMEC Gauge Readings - Strain (mm/m) 49 D3 D4D	50 D3 D5A	51 D3 D5D	52 D3BK H0A	53 D3BK V0A	54 D3BK D0D	55 D3 I0A-A	56 D3 I0A1B
C0A	-0.035	0.000	0.000	0.050	0.050	-0.035	0.035	0.035
C0B	0.035	0.000	0.000	-0.050	-0.050	0.035	-0.035	-0.035
C1	0.035	0.000	0.142	-0.050	-0.050	0.177	0.035	0.035
C2	0.106	0.000	0.142	-0.050	-0.150	0.035	0.248	0.177
C3	0.106	-0.071	0.284	-0.050	-0.050	0.106	0.390	0.319
C4	0.177	-0.142	0.355	-0.050	-0.050	0.035	0.532	0.603
C5	0.177	-0.142	0.284	0.050	-0.150	0.035	0.745	0.957
C6	0.248	-0.142	0.355	0.050	-0.150	-0.035	0.957	1.170
C7	0.177	-0.213	0.284	0.050	-0.150	-0.035	1.170	1.170
C8	0.035	0.071	0.284	-0.050	-0.150	-0.106	1.454	1.454
C9	0.035	0.213	0.284	-0.050	-0.250	-0.106	1.738	1.454
C10	0.106	0.355	0.355	-0.150	-0.250	-0.035	1.950	1.738

Table A.8 *(Cont'd)* Dapped End Specimens D-3 and D-4 – Strain Measurements – Loading 1.

	DEMEC Gauge Readings - Strain (mm/m)							
Load	57	58	59	60	61	62	63	64
Stage	D3 I1C	D3 H12B	D3 H0A1B	CL H56D	CL H56E	D4 H0A-A	D4 H0B-A	D4 H1A
C0A	0.035	0.035	0.000	0.000	0.000	-0.050	-0.050	-0.050
C0B	-0.035	-0.035	0.000	0.000	0.000	0.050	0.050	0.050
C1	-0.035	0.106	0.000	0.071	0.071	-0.050	0.050	-0.050
C2	0.035	0.106	0.000	0.142	0.213	-0.050	0.050	-0.050
C3	0.035	0.035	-0.071	0.213	0.284	-0.050	0.050	-0.050
C4	0.106	-0.035	-0.355	0.496	0.496	-0.050	0.050	0.150
C5	0.248	0.035	0.922	0.567	0.709	-0.050	0.150	0.150
C6	0.603	-0.035	1.277	0.780	0.851	-0.050	0.150	0.150
C7	0.957	0.035	1.348	0.922	0.993	0.050	0.250	0 150
C8	1.241	0.177	1.489	1.064	1.206	0.050	0.350	0.050
C9	1.454	0.177	1.702	1.206	1.348	0.050	0.350	0 050
C10	1.667	0 390	1.844	1.348	1.560	0.050	0.350	0 050

Table A.8 *(Cont'd)* Dapped End Specimens D-3 and D-4 – Strain Measurements – Loading 1.

	DEMEC Gauge Readings - Strain (mm/m)							
Load	65	66	67	68	69	70	71	72
Stage	D4 H1B	D4 H1C	D4 H1D	D4 H2A	D4 H2B	D4 H2C	D4 H2D	D4 H3A
C0A	0.000	-0.050	-0.050	-0 050	-0.050	-0.050	0 000	0.050
C0B	0.000	0.050	0.050	0.050	0.050	0.050	0.000	-0.050
C1	0.100	0.050	0.050	-0.050	0.050	0.050	0.100	0.050
C2	0.000	0 050	0.050	-0 050	0.050	-0 050	0.000	-0 050
C3	0.100	0 050	0.050	-0.150	0 050	0.050	0.100	-0.050
C4	0.000	0.050	0 050	-0.050	0.050	0.050	0.100	-0 050
C5	0.000	0.050	0.050	-0.050	0.450	-0.150	0 800	-0 050
C6	0.000	-0.050	0 050	-0.050	0.550	-0.150	1.000	-0 050
C7	-0.100	-0 050	-0 050	-0.150	0.450	-0 250	2.300	-0.050
C8	0.000	-0.050	-0.050	-0 050	0.550	-0.250	3.300	-0.050
C9	0.000	-0.050	0.250	-0.050	0.550	-0.250	6.700	0.050
C10	0.000	0.150	0.950	-0.050	0.550	-0.250	13 400	0.550

Table A.8 *(Cont'd)* Dapped End Specimens D-3 and D-4 – Strain Measurements – Loading 1.

	DEMEC Gauge Readings - Strain (mm/m)							
Load	73	74	75	76	77	78	79	80
Stage	D4 H3D	D4 H4A	D4 H4D	D4 V0A-A	D4 V0B-A	D4 V1A	D4 V1B	D4 V1C
C0A	-0.050	0.000	0.050	0.050	0.050	0 100	0 050	0.050
C0B	0.050	0.000	-0.050	-0.050	-0.050	-0.100	-0.050	-0.050
C1	0.050	0.000	0.050	0.050	0.050	0.100	-0.050	-0.050
C2	0.050	0.000	0.150	-0.050	-0.050	-0.200	-0.050	-0.050
C3	0.250	-0.100	0.150	0.050	0.050	0.100	-0.050	-0 150
C4	0.350	-0.100	0.150	0.150	-0.050	0.000	0.050	-0.150
C5	0.350	-0.200	0 250	0.050	0.050	0.000	0.050	0.050
C6	0.250	-0.200	0.250	0.050	0.250	0.100	0.150	0.050
C7	0.150	-0.500	0.350	0.150	0.750	0.300	0.050	0.050
C8	0.150	-0.300	0.350	0.250	1.250	0.200	0.150	0.250
C9	0.150	-0.300	0.450	0.350	1.650	0.300	0.250	0.350
C10	0.050	-0.300	0.550	0.450	1.850	0.500	0.450	0.050

Table A.8 *(Cont'd)* Dapped End Specimens D-3 and D-4 – Strain Measurements – Loading 1.

	DEMEC Gauge Readings - Strain (mm/m)							
Load Stage	81 D4 V1D	82 D4 V2A	83 D4 V2B	84 D4 V2C	85 D4 V2D	86 D4 V3A	87 D4 V3D	88 D4 V4A
C0A	0.050	0.050	0.100	0.000	-0.050	-0.050	0.000	0.050
C0B	-0.050	-0.050	-0.100	0.000	0.050	0.050	0.000	-0.050
C1	0.050	0.150	-0.200	0.000	-0.050	0.150	0.000	0.150
C2	0.050	0.050	0.000	0.000	-0.050	0.150	0.000	0.150
C3	0.050	0.050	0.000	0.000	-0.050	0.250	0.000	0.150
C4	-0.050	0.050	0.100	0.000	-0.150	0.350	0.100	0.150
C5	0.450	0.250	0.500	0.500	0.450	0.450	0.200	0.250
C6	0.550	0.250	0.700	0 800	0.650	0.650	0.200	0.250
C7	0.750	0.350	1.000	1.400	1.650	1.050	0.200	0.250
C8	1.050	0.450	1.300	1.900	2.450	1.550	0.300	0.250
C9	1.850	0.450	1.700	2.100	8.850	2.650	0.600	0.350
C10	5.750	0.650	7.400	7.000	15.750	8.250	1.100	0.650

Table A.8 *(Cont'd)* Dapped End Specimens D-3 and D-4 – Strain Measurements – Loading 1.

	DEMEC Gauge Readings - Strain (mm/m)							
Load Stage	89 D4 V4D	90 D4 D0A-A	91 D4 D0B-A	92 D4 D1A	93 D4 D1B	94 D4 D1C	95 D4 D1D	96 D4 D2A
C0A	0.000	0,000	0.000	0.000	0.000	-0.071	-0.071	-0.035
C0B	0.000	0.000	0.000	0.000	0.000	0.071	0.071	0.035
C1	-0.100	0 000	0.071	0.000	0.000	0.071	0.071	-0.035
C2	-0.100	-0.142	0.000	0.071	0.071	0.071	0.071	-0.035
C3	-0.100	-0.071	0.142	0.071	0.071	0.071	0.142	-0.106
C4	0.000	-0.071	0.000	-0.142	0.000	0.071	0.071	-0.035
C5	0.000	-0.142	0.213	0.000	0.000	-0.071	-0.142	-0.177
C6	0.000	-0.213	0.142	0.000	-0.071	-0.071	-0.142	-0.248
C7	0.100	-0.213	0.142	0.071	0.000	-0.071	-0.213	-0.248
C8	0.100	-0.071	0.355	0.213	0.071	-0.071	-0.142	-0.177
C9	0.000	0.000	0.709	0.213	0.142	-0.071	-0.071	-0.248
C10	0.300	0.071	0.851	0.284	0.142	-0.142	0.496	-0.248

Table A.8 *(Cont'd)* Dapped End Specimens D-3 and D-4 – Strain Measurements – Loading 1.

	DEMEC Gauge Readings - Strain (mm/m)							
Load Stage	97 D4 D2B	98 D4 D2C	99 D4 D2D	100 D4 D3A	101 D4 D3D	102 D4 D4A	103 D4 D4D	104 D4BK H0A
C0A	-0.035	-0.035	-0.071	0.000	-0.035	-0.071	-0.035	-0.100
C0B	0.035	0.035	0.071	0.000	0.035	0.071	0.035	0.100
C1	0.177	0.106	0.071	0.071	0.035	0.000	0.106	0.100
C2	0.177	0.177	0.142	0.071	0.177	0.071	0.177	0.000
C3	0.106	0.106	0 142	0.071	0.177	0.000	0.106	0.000
C4	0.106	0.106	0.142	0.071	0.177	0.000	0.106	0.000
C5	0.035	0.106	0.071	-0.071	0.177	-0.071	0.106	0.000
C6	-0.035	-0.106	0.000	-0.071	0.106	-0.142	0.035	0.000
C7	-0.035	-0.106	-0.142	-0.142	0.035	-0.213	0.106	-0.100
C8	-0.106	-0.106	0.000	-0.071	0.106	-0.213	0.177	0.000
C9	-0.106	-0.106	-0.071	-0.071	0.106	-0.071	0.177	0.000
C10	-0.390	-0.106	-0.071	-0.071	-0.106	-0.213	0.177	0.000

Table A.8 *(Cont'd)* Dapped End Specimens D-3 and D-4 – Strain Measurements – Loading 1.

	DEMEC Gauge Readings - Strain (mm/m)						
Load Stage	105 D4BK V0A	106 D4BK D0D	107 D4 I0A-A	108 D4 I0A1B	109 D4 I1C	110 D4 H12B	111 D4 H0A1B
C0A	-0.050	0.035	-0.035	-0.071	0.000	0.000	0.035
C0B	0.050	-0.035	0.035	0.071	0.000	0.000	-0.035
C1	0.050	-0.035	0.106	0.071	0.071	0.000	0.035
C2	0.050	0.035	0.106	0.213	0.071	0.000	0.248
C3	0.050	0.035	0.177	0.355	0.213	0.000	0.532
C4	-0.050	-0.106	0.248	0.496	0.496	0.142	0.674
C5	-0.050	0.035	0.319	0.709	0.780	0.284	0.887
C6	-0.050	-0.035	0.461	0.851	0.993	0.355	1.028
C7	-0.050	-0.035	0.603	0.993	1.135	0.355	1.170
C8	-0.050	-0.106	0.887	1.135	1.206	0.426	1.383
C9	-0.050	-0.177	1.099	1.348	1.348	0.426	1.525
C10	0.050	-0.177	1.241	1.631	1.206	0.284	1.525

Table A.9 Dapped End Specimen D-3 – Measured Loads – Loading 2.

	Measured Loads and Deflections			
Load Stage	Shear* (kN)	Dial 1 (mm)	Dial 2 (mm)	Dial 3 (mm)
E0	0.0	0.00	0.00	0.00
E1	200.2	-0.36	2.03	4.14
E2	289.1	-0.56	2.84	5.99
E3	333.6	-0.58	3.30	6.98
E4	367.0	1.80	6.25	9.09
End	0.0	0.69	6.32	6.45

* Does not include self-weight shear of 5.4 kN

Table A.10 Dapped End Specimens D-3 and D-4 – Strain Measurements – Loading 2.

	DEMEC Gauge Readings - Strain (mm/m)							
Load Stage	1 D3 H0A-A	2 D3 H1A	3 D3 H1B	4 D3 H1C	5 D3 H1D	6 D3 H2A	7 D3 H2B	8 D3 H2C
E0	0.000	0.000	0.300	0.200	-0.100	-0.150	-0.050	-0.150
E1	0.200	0.200	1.000	0.400	-0.100	-0.150	0.250	-0.250
E2	0.300	0.300	1.400	0.500	-0.100	-0.250	0.450	-0.250
E3	0.500	0.300	1.500	0.600	-0.100	-0.250	0.550	-0.250
E4	0.400	0.300	1.200	0.500	-0.300	-0.250	0.650	-2.650

Table A.10 *(Cont'd)* Dapped End Specimens D-3 and D-4 – Strain Measurements – Loading 2.

	DEMEC Gauge Readings - Strain (mm/m)							
Load Stage	9 D3 H2D	10 D3 H3A	11 D3 H3B	12 D3 H3C	13 D3 H3D	14 D3 H4A	15 D3 H4D	16 D3 H5A
E0	1.200	-0.300	-0.100	1.750	0.500	-0.150	0.100	-0.150
E1	1.500	-0.300	-0.100	4.250	0.600	-0.250	0.200	-0.250
E2	1.600	-0.400	-0.200	5.450	0.600	-0.250	0.200	-0.250
E3	1.700	-0.400	-0.200	6.250	0.600	-0.350	0.200	-0.250
E4	6.700	-0.100	0.000	20.850	0.400	0.350	0.100	-0.350

Table A.10 *(Cont'd)* Dapped End Specimens D-3 and D-4 – Strain Measurements – Loading 2.

	DEMEC Gauge Readings - Strain (mm/m)							
Load Stage	17 D3 H5D	18 D3 V0A-A	19 D3 V1A	20 D3 V1B	21 D3 V1C	22 D3 V1D	23 D3 V2A	24 D3 V2B
E0	0.600	-0.100	0.050	0.150	0.250	0.150	0.150	0.300
E1	1.600	0.200	0.650	0.750	0.950	0.850	0.350	0.500
E2	2.100	0.300	0.850	1.050	1.250	1.150	0.350	0.500
E3	2.300	0.400	1.050	1 350	1.350	1.250	0.450	0.600
E4	2.100	0.400	0.950	1.050	1.050	1.550	0.650	1.300

Table A.10 *(Cont'd)* Dapped End Specimens D-3 and D-4 – Strain Measurements – Loading 2.

	DEMEC Gauge Readings - Strain (mm/m)							
Load Stage	25 D3 V2C	26 D3 V2D	27 D3 V3A	28 D3 V3B	29 D3 V3C	30 D3 V3D	31 D3 V4A	32 D3 V4D
E0	0.100	1.600	0.050	0.050	3.850	-0.250	0.650	0.200
E1	0.300	2.800	0.250	0 750	5.050	0.650	1.150	0.500
E2	0.400	3.200	0.250	1.050	5.950	1.050	1.550	0.600
E3	0.400	3.500	0.250	1.150	6.650	1.250	1.750	0.800
E4	0.600	18.000	0.450	1.450	19.550	6.750	5.950	0.800

Table A.10 *(Cont'd)* Dapped End Specimens D-3 and D-4 – Strain Measurements – Loading 2.

	DEMEC Gauge Readings - Strain (mm/m)							
Load Stage	33 D3 V5A	34 D3 V5D	35 D3 D0A-A	36 D3 D1A	37 D3 D1B	38 D3 D1C	39 D3 D1D	40 D3 D2A
E0	0.100	0.200	0.177	0.248	0.213	0.426	-0.106	0.071
E1	0.200	0.200	0.177	0.177	0.426	0.567	-0.177	0.071
E2	0.100	0.300	0.106	0.248	0.709	0.709	-0.177	0.071
E3	0.000	0.300	0.106	0.177	0.780	0.780	-0.177	0.071
E4	0.000	0.300	0.177	0.248	0.638	0.496	-0.106	0.000

Table A.10 *(Cont'd)* Dapped End Specimens D-3 and D-4 – Strain Measurements – Loading 2.

	DEMEC Gauge Readings - Strain (mm/m)							
Load Stage	41 D3 D2B	42 D3 D2C	43 D3 D2D	44 D3 D3A	45 D3 D3B	46 D3 D3C	47 D3 D3D	48 D3 D4A
E0	-0.035	-0.071	-0.071	0.142	0.106	0.887	0.035	0.177
E1	-0.035	-0.071	-0.213	0.000	-0.035	0.674	-0.106	-0.035
E2	-0.106	-0.142	-0.355	-0.071	-0.106	0.745	-0.106	0.035
E3	-0.106	-0.213	-0.426	-0.142	-0.248	0.674	-0.248	-0.035
E4	-0.106	0.213	2.270	-0.071	-0.248	2.092	0.035	0.319

Table A.10 *(Cont'd)* Dapped End Specimens D-3 and D-4 – Strain Measurements – Loading 2.

	DEMEC Gauge Readings - Strain (mm/m)							
Load	49	50	51	52	53	54	55	56
Stage	D3 D4D	D3 D5A	D3 D5D	D3BK H0A	D3BK V0A	D3BK D0D	D3 I0A-A	D3 I0A1B
E0	0.177	0.284	0.071	-0.050	-0.150	0.106	0.461	0.248
E1	0.177	-0.071	0.567	-0.050	-0 250	-0.035	1.241	1.099
E2	0.106	-0.142	0.709	-0.150	-0.350	-0.035	1.738	1.809
E3	0.177	-0.213	0.709	-0.150	-0.350	-0.106	1.879	1.950
E4	0.035	-0.284	0.709	-0.150	-0.350	-0.106	1.667	1.950

Table A.10 *(Cont'd)* Dapped End Specimens D-3 and D-4 – Strain Measurements – Loading 2

	DEMEC Gauge Readings - Strain (mm/m)				
Load	57	58	59	60	61
Stage	D3 I1C	D3 H12B	D3 H0A1B	CL H56D	CL H56E
E0	0.106	0.106	0.426	0.142	0.213
E1	0.957	0.319	1.277	0.638	0.851
E2	1.383	0.461	1.915	1.135	1.206
E3	1.667	0.603	2.199	1.206	1.418
E4	0.887	0.674	1.986	1.064	1.277

A.5 Web Hole Specimens H-1 and H-2

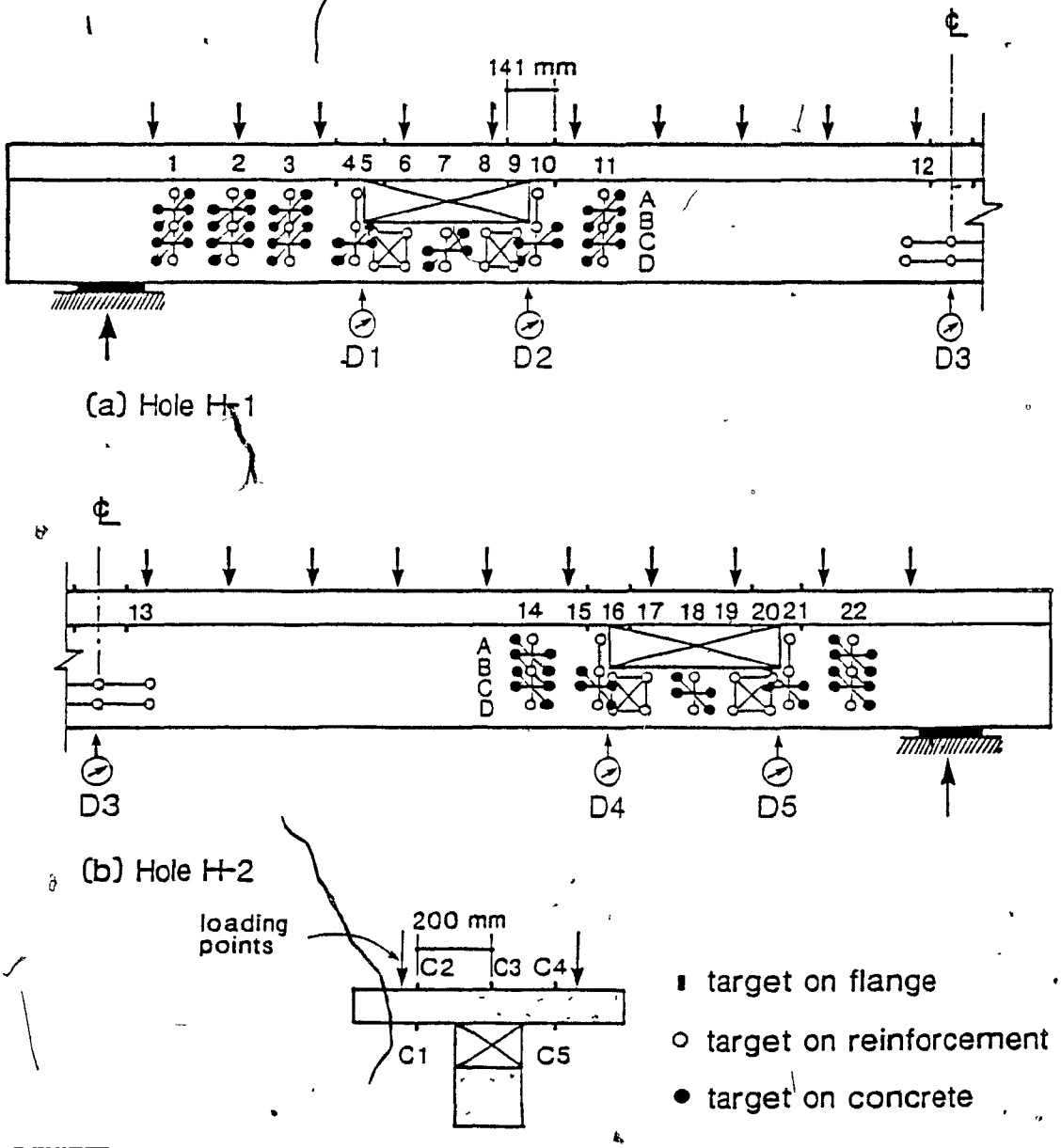

Figure A.4 Initial Test Set-Up and Instrumentation for Web Hole Specimens H-1 and H-2.

Table A.11 Web Hole Specimens H-1 and H-2 - Measured Loads - Loading 1.

Load Stage	Loading* (kN/m)	Measured Loads and Deflections Dial 1 (mm)	Dial 2 (mm)	Dial 3 (mm)	Dial 4 (mm)	Dial 5 (mm)
1A-D	0.0	0.00	0.00	0.00	0.00	0.00
3	11.1	0.46	1.57	1.96	1.37	0.61
4	18.0	0.89	3.07	3.96	2.67	1.12
5	28.4	2.34	5.11	6.65	4.42	1.78
6	39.3	3.23	8.00	10 26	6.93	2.79
7	48.4	6.35	11.30	14.48	9.86	3.84
8	64.2	6.73	15.49	19.89	13.59	5.21
9	75.0	9.83	19.61	24.99	17.30	6.48
10	83.8	12.65	24.49	31.22	22.20	10.69
11	93.0	15 44	29.74	37.80	28.07	13.49
12	95.4	18 75	33.83	43.00	33.73	17.15
13	43.6	12.85	25.37	32.16	26 72	14.53
13-1	30.4	13.49	23.98	30.23	25.58	14.15
13-2	0.0	8 00	15.32	18.92	17.48	10.49
14A-B	0.0	8.00	15.32	18.92	17.48	10.49
15	42.6	15.85	25.78	32.69	27.18	17.25
16	82.1	20.73	35.56	45.56	36.20	21.31
17	90.8	22 53	39.45	50.80	40.75	23.60
18	94.9	24.69	44.20	57.10	47.17	27.36
19	92.4	26.72	48.19	64 31	53.85	30.68
20	72.5	27.58	49.25	68.91	63.99	36.96
20-1	61.0	26.44	47.30	66.42	62.46	36.22
20-2	45.3	24.51	43.64	61.41	58.93	34.52
20-3	30.2	22.43	39.65	55 95	54 87	32.46
20-4	14.4	19.81	34 67	49.10	49.48	29.72
20-5	0.0	16.61	28.60	40.46	41.94	26.06

* Does not include uniform self-weight loading of 4.3 kN/m.

Table A.12 Web Hole Specimens H-1 and H-2 – Strain Measurements – Loading 1.

Load Stage	DEMEC Gauge Readings - Strain (mm/m) 1 H1 C1 4	2 H1 C2 4	3 H1 C3 4	4 H1 C4 4	5 H1 C5 4	6 H1 C1 10	7 H1 C2 10	8 H1 C3 10
1A	—	—	—	—	0.000	-0.230	-0.024	—
1B	0.024	-0.035	-0.035	-0.035	0.000	0.195	-0.024	0.000
1C	-0.047	0.035	0.035	0.035	0.000	-0.089	0.047	0.000
1D	0.024	—	—	—	—	0.124	—	—
3	-0.047	0.106	0.177	0.035	0.213	0.053	-0.024	-0.142
4	-0.189	0.106	0.177	0.106	-0.426	0.124	-0.165	-0.355
5	-0.402	0.177	0.390	0.177	-0.567	0.124	-0.307	-0.496
6	-0.402	0.319	0.461	0.106	-0.638	0.904	-0.591	-0.851
7	-0.544	0.319	0.674	0.248	-0.851	0.975	-0.875	-1.064
8	-0.898	0.319	1.170	0 390	-0.780	1.046	-1.229	-1.277
9	-0.969	0.390	1.667	0.603	-0.993	1.684	-1.442	-1.560
10	-1.395	0.319	2.234	0.603	-1.348	2.323	-1.655	-1.915
11	-1.324	0.319	2.376	0.674	-1.418	3.174	-2.009	-2.199
12	-1.466	0.319	2.518	0.674	-1.631	3.245	-2.222	-2.340
13	-1.466	0.177	2.092	0.532	-1.418	2.394	-1.655	-1.773
14A	-1.040	-0.035	1.454	0.248	-1.064	1.543	-1.087	-1.277
14B	-0.969	-0.177	1.383	0.177	-1 064	1.543	-1.158	-1.418
15	-1.395	-0.106	1.879	0.319	-1.489	2.394	-2.009	-2.057
16	-1.749	0.106	2.518	0.461	-1.915	3.103	-2.364	-2.624
17	-1.820	0.177	2.801	0.603	-1.986	3.316	-2.648	-2.766
18	-2.600	0.106	3.085	0.603	-2.766	2.819	-2.790	-2.979
19	-2.104	-0.035	3.227	0.674	-2.199	2.961	-3.712	-3.050
20	-1.749	0.106	3.085	0.674	-1.986	3.528	-2.648	-2.837

Table A.12 *(Cont'd)* Web Hole Specimens H-1 and H-2 – Strain Measurements – Loading 1.

Load Stage	DEMEC Gauge Readings - Strain (mm/m) 9 H1 C4 10	10 H1 C5 10	11 CL C1 12	12 CL C2 12	13 CL C3 12	14 CL C4 12	15 CL C5 12	16 H2 C1 15
1A	—	—	—	—	—	-0.071	-0.047	—
1B	-0.035	0.000	—	0 000	0.000	0.000	0.024	-0.071
1C	0.035	0.000	-0.071	0.000	0.000	0.071	0.024	-0.071
1D	—	—	0.071	—	—	—	—	0.142
3	-0.106	0.284	0.000	0.000	0.071	-0.071	-0.047	0.142
4	-0.319	0.071	-0.355	-0.142	-0.071	-0.142	-0.331	0.284
5	-0.390	-0.142	-0.567	-0.284	-0.213	-0.284	-0.189	0.355
6	-0.674	0.213	0.142	-0.426	-0.567	-0.496	0.024	1.277
7	-0.887	0.780	-0.284	-0.496	-0.567	-0.496	0.165	1.773
8	-1.241	1.206	0.355	-0.851	-0.851	-0.780	-0.615	2.411
9	-1.454	1.489	0.426	-0 851	-0.922	-0.851	0.307	3.191
10	-1.667	1.915	-0.284	-0.993	-0.993	-0.993	-0.047	3.830
11	-1.950	3.191	0.284	-1.206	-1.277	-1.206	0.165	5.816
12	-2.092	3.191	-0.142	-1.206	-1.277	-1.206	0.024	8.794
13	-1.596	2.482	-0.496	-0.851	-0.851	-0.780	-0.118	7.660
14A	-1.099	1.348	-0.638	-0.496	-0.496	-0.567	-0.260	5.177
14B	-1.170	1.418	-0.426	-0.496	-0.567	-0.496	-0.189	5.390
15	-1.879	2.411	-0.213	-0.922	-1.064	-0.993	-0.118	7.447
16	-2.305	3.262	-0.142	-1.348	-1.489	-1.489	0.024	9.645
17	-2.589	4.255	-0.284	-1.631	-1.631	-1.702	0.024	11.277
18	-2.730	2.270	0.142	-1.631	-1.844	-1.631	-0.118	14.326
19	-2.801	3.830	0.426	-1.844	-2.057	-1.915	-0.189	15.957
20	-2.447	4.184	-0.071	-1.631	-1.844	-1.702	0.095	21.844

Table A.12 *(Cont'd)* Web Hole Specimens H-1 and H-2 – Strain Measurements – Loading 1.

	DEMEC Gauge Readings - Strain (mm/m)							
Load	17	18	19	20	21	22	23	24
Stage	H2 C2 15	H2 C3 15	H2 C4 15	H2 C5 15	H2 C1 21	H2 C2 21	H2 C3 21	H2 C4 21
1A	-0.071	-0.095	-0.047	0.071	—	-0.024	-0 024	-0 047
1B	0.000	0.047	0.024	0 000	-0.095	-0.024	-0 024	0.024
1C	0.071	0.047	0.024	-0 071	0.047	0 047	0.047	0.024
1D	—	—	—	—	0 047	—	—	—
3	0.142	0.189	0.095	0.000	0.189	0.189	0.118	0 236
4	-0.355	-0.095	-0.260	0 000	-0.236	0.118	0.189	0 095
5	-0.426	-0.591	-0.331	0 213	-0.307	0 402	0.544	0.307
6	-0.567	-0.591	-0.615	0.284	-0.662	0.898	0.969	0 449
7	-0.851	-0.733	-0.757	0.567	-0.520	1.608	1.608	0.946
8	-1.135	-1.300	-1.111	0.851	-0 946	2.388	2 459	1.655
9	-1.348	-1.300	-1.395	1 702	-1 087	3.310	3.452	2 222
10	-1.773	-1.868	-1.678	1.702	-1.229	4 586	4.799	3 215
11	-1.986	-1.939	-2.104	3.475	-1.939	7.069	7.423	5 272
12	-2.128	-2.009	-2.175	3.404	-2.364	9 976	10 189	7 896
13	-1.631	-1.513	-1.678	2 695	-2 364	8 983	9 125	6.974
14A	-1.064	-1 229	-1.111	1.844	-1.939	6.572	6.785	5 201
14B	-1.135	-1.300	-1 324	1.773	-1.726	6 572	6 714	5 130
15	-1.773	-1.797	-1 962	2 553	-2 648	8 629	8.771	6 690
16	-2.340	-2.364	-2.530	3.262	-3 002	10.756	10.969	8 818
17	-2.553	-2 506	-2 600	3.475	-3 499	12.459	12.600	9 669
18	-2.624	-2.648	-2.742	3.262	-4.279	15 579	15.437	12.151
19	-2.482	-2.648	-2.813	2.908	-4.563	20.827	20.331	16.336
20	-1.773	-1.797	-1.891	2.908	-5.626	27.494	26.714	22.719

Table A.12 *(Cont'd)* Web Hole Specimens H-1 and H-2 – Strain Measurements – Loading 1.

	DEMEC Gauge Readings - Strain (mm/m)							
Load	25	26	27	28	29	30	31	32
Stage	H2 C5 21	H1 H1A	H1 H1C	H1 V1A	H1 V1C	H1 D1A	H1 D1B	H1 D1C
1A	0.000	-0.067	-0.067	-0.067	-0 067	0 035	—	—
1B	0.000	0.033	0.033	0 033	0.033	—	-0 035	-0 071
1C	0.000	0.033	0.033	0.033	0 033	-0 035	0.035	0 071
1D	—	—	—	—	—	—	—	—
3	-0.142	0.133	0 133	-0 067	-0.067	-0 035	0.177	-0 071
4	-0.355	0 033	0.133	-0.067	-0.067	-0.035	0.248	0.000
5	-0.567	-0.067	0.033	0.033	-0.067	0.177	0.106	0.071
6	-0.567	0.033	0.033	0.033	-0.067	-0.248	0 106	-0 709
7	-0.567	0.033	0.033	0.033	0.033	-0 248	-0 035	-0 284
8	-0.851	0.033	0.033	0 033	0.033	-0 674	-0.248	-0.709
9	-1.277	0.033	0 433	0.133	0.333	-0.603	-0 319	-0 426
10	-1.702	-0.167	0 833	0.233	0.533	-0.461	-0.461	-0.496
11	-2.057	-0.167	1.233	0.433	0.633	-0.603	-0 390	-0.355
12	-2.624	-0.267	1.333	0.333	0.833	-0.603	-0.603	-0 567
13	-2.411	-0.267	0.933	0.433	0 633	-0.532	-0.532	-0.426
14A	-1.915	-0.067	0.933	0.333	0.633	-0.674	-0 603	-0.496
14B	-1.915	-0.267	0.833	0.333	0.533	-0.603	-0.390	-0.496
15	-2.482	-0.267	1.233	0 233	0.633	-0.745	-0.674	-0.567
16	-2.979	-0.467	1.533	0.333	0.833	-0.816	-0.674	-0.709
17	-3.333	-0.467	1.633	0 433	1.033	-0.816	-0.816	-0.780
18	-4.610	-0.467	1.833	0.433	0.933	-0.887	-0.887	-0.709
19	-4.752	-0.567	1.933	0.433	1.033	-0.887	-0.816	-0.709
20	-4.752	-0.367	1.733	0.333	0.833	-0.957	-0.887	-0.780

Table A.12 *(Cont'd)* Web Hole Specimens H-1 and H-2 – Strain Measurements – Loading 1.

	DEMEC Gauge Readings - Strain (mm/m)							
Load Stage	33 H1 H2A	34 H1 H2C	35 H1 V2A	36 H1 V2C	37 H1 D2A	38 H1 D2B	39 H1 D2C	40 H1 H3A
1A	-0.100	-0.175	-0.100	—	0.047	0.118	-0.142	0.000
1B	0.000	0.025	0.000	-0.100	-0.165	-0 095	0.071	0.000
1C	0.100	0.025	0.000	0 000	0.118	-0.024	0.071	0.000
1D	—	0.125	0.100	0.100	—	—	—	0.000
3	0.100	0.125	0.000	-0.100	-0.095	-0.165	-0.142	0.000
4	0.100	0 025	0 000	-0.100	-0.236	-0.307	-0.071	-0.100
5	0.100	0.025	0.000	-0.100	-0.307	-0.165	-0.071	0.000
6	0.100	0.125	0.000	0.000	-0.024	-0.520	-0 213	-0 300
7	0.000	0.525	0.100	0.200	-0.378	-0.449	-0.142	-0.400
8	0.000	1.425	0.500	0.800	-0.520	-0.733	0 213	0.200
9	-0.100	1.725	0.900	1.200	-0.449	-0.591	0.426	1.000
10	-0.200	2.025	1.200	1.400	-0.378	-0.520	0.426	2.500
11	-0.300	2.325	1.300	1 700	-0.307	-0.520	0.496	4.300
12	-0.400	2.425	1.500	1.800	-0.520	-0.875	0.567	5.500
13	-0.400	2.025	1.000	1.200	-0.307	-0.733	0.284	5.000
14A	-0.100	1.425	0.400	0.700	-0.378	-0.591	0.213	3.600
14B	-0.100	1.225	0 400	0.600	-0.307	-0.591	0.284	3.600
15	-0.400	2.025	0.900	1.100	-0.733	-1.229	0.213	5.100
16	-0.400	2.125	1.400	1.700	-0.662	-1.017	0.355	6.100
17	-0.500	2.825	1.600	2.000	-0.733	-0.946	0.426	6.900
18	-0.600	3.125	1.700	2.100	-0.591	-0.875	0.496	7.700
19	-0.700	3.125	1.900	2.000	-0.662	-1.017	0.496	8.200
20	-0.600	2.925	1.800	1.800	-0.662	-0.875	0.496	8.000

Table A.12 *(Cont'd)* Web Hole Specimens H-1 and H-2 – Strain Measurements – Loading 1.

	DEMEC Gauge Readings - Strain (mm/m)							
Load Stage	41 H1 H3C	42 H1 V3A	43 H1 V3C	44 H1 D3A	45 H1 D3B	46 H1 D3C	47 H1 H4C	48 H1 V4A
1A	-0.325	-0.225	-0.275	—	—	0 095	0.075	-0.200
1B	0.075	-0.025	-0.075	0 071	-0.035	-0.118	-0.125	0.000
1C	0.075	0.175	0.225	-0.071	0.035	0.024	-0.025	0.100
1D	0.175	0.075	0.125	—	—	—	0.075	0.100
3	0.175	-0.225	-0.075	0.000	-0.106	-0.118	0.075	0.000
4	0.175	-0.225	-0.075	0.142	-0.106	-0.047	0.375	0.000
5	0.175	-0.125	-0.075	-0.142	-0.248	-0.189	0.975	0.200
6	0.975	0.275	0.225	-0.426	-0.390	-0.473	1.275	0.600
7	1.475	0.575	0.525	-0.142	-0.674	-0.118	1.575	0.800
8	1.675	1.175	0.825	-0.284	-0.674	-0.047	2.075	1.200
9	1.775	1.575	1.125	-0.213	-0.745	-0.331	3.075	1.500
10	2.175	2.075	1.325	-0.426	-0.887	0.024	3.575	1.600
11	2.675	3.375	1.525	-0.709	-1.028	0.378	4.375	1.600
12	2.875	4.275	1.525	-0.993	-1.099	0.307	4.875	1.700
13	1.975	3.475	10.925	-0.993	-0.816	0.378	3.275	1.000
14A	1.475	2.575	10.325	-0.851	-0.887	0.024	2.275	0.400
14B	1.475	2.475	10.325	-0.709	-0.745	-0.047	2.375	0.300
15	2.275	3.275	10.825	-1.418	-1.028	0.165	3.575	1.000
16	3.075	4.275	11.425	-1.348	-1.170	0.378	5.175	1.600
17	3.275	5.175	11.725	-1.418	-1.312	0.449	5.875	2.100
18	3.575	6.075	11.725	-1.418	-1.383	0.520	7.075	2.300
19	3.475	6.475	11.725	-1.631	-1.241	0.591	7.075	2.300
20	3.275	6.175	11.425	-1.560	-1.312	0.591	6.975	1.900

Table A.12 *(Cont'd)* Web Hole Specimens H-1 and H-2 – Strain Measurements – Loading 1.

Load Stage	DEMEC Gauge Readings - Strain (mm/m) 49 H1 V4C	50 H1 D4C	51 H1 H56B	52 H1 H56D	53 H1 V5C	54 H1 V6C	55 H1 D56DB	56 H1 D56BD
1A	-0.150	-0.024	-0.025	-0.025	—	—	-0.118	-0.071
1B	-0.050	-0 095	-0.025	-0 025	-0.067	0.000	0.024	0.071
1C	0.150	0.118	-0 025	-0 025	0.033	0.000	0 095	—
1D	0.050	—	0.075	0.075	0.033	0 000	—	—
3	0.050	0.047	0 075	-0.025	-0.067	0.000	-0 047	0 071
4	0.050	0.118	0.075	-0.025	-0.067	0 000	0.095	0.142
5	0.250	0.331	0.375	-0.025	-0.167	-0.100	0.095	0 213
6	0.450	0 473	0 175	0 075	-0.167	0 000	-0.331	0.213
7	0.650	0.615	0 275	0.175	-0.067	0 300	-0 260	0 638
8	0.950	0 898	0.575	0.375	0.033	0 800	-0.047	1 135
9	1.350	1.253	0.375	0.575	0.233	1 400	0.165	1.560
10	1.450	1 820	0 475	0.775	0.933	2 300	-0 331	2 695
11	1.550	2.600	0 375	0.875	1.933	2 700	-0 473	3.546
12	1.650	3 026	0 475	0.975	2.533	3 000	-0.473	3.972
13	0.950	2.104	0.175	0 575	2 433	3 000	-0.473	3.546
14A	0.450	1.111	0 075	0 575	1.833	2.500	-0 686	2 624
14B	0.450	1 111	-0.125	0 475	1 833	2.500	-0 686	2 766
15	1.050	1.962	0 475	0.775	2 233	3 000	-0 686	3.546
16	1.750	2.884	0 575	1.175	2.833	3.600	-0.757	4.752
17	1.950	3.310	0.575	1 275	3 433	3 900	-0 757	5 106
18	1.950	4.303	0.675	1 275	3.833	3.900	-0.757	5.461
19	1.850	4.657	0 375	1 075	4 033	4 000	-0.898	5 248
20	1.550	4.303	0 175	0 975	3 933	4 000	-0.827	5 035

Table A.12 *(Cont'd)* Web Hole Specimens H-1 and H-2 – Strain Measurements – Loading 1.

Load Stage	DEMEC Gauge Readings - Strain (mm/m) 57 H1 H7C	58 H1 V7C	59 H1 D7C	60 H1 H89B	61 H1 H89D	62 H1 V8C	63 H1 V9C	64 H1 D89DB
1A	-0.025	-0.175	0 000	0 050	0.025	-0 325	-0.325	—
1B	-0.025	0.025	0.000	-0 050	0.025	-0 125	0 075	0 000
1C	-0.025	0.025	0.000	-0.050	-0.075	0 275	0.075	0 000
1D	0.075	0.125	—	0 050	0.025	0.175	0.175	—
3	-0.025	-0.075	0 071	-0 150	-0 075	-0.025	-0 125	0.000
4	0.275	-0 075	0.142	-0 050	-0.075	-0.025	-0 125	0.071
5	0.175	0.125	0.000	-0.150	0.225	0.075	-0.125	0 071
6	0.375	0 125	-0 071	-0 350	0 625	0.175	-0.225	0 000
7	0.675	0.325	-0 071	-0 350	1.225	0 275	-0 225	0 000
8	0.975	0.925	-0 213	-0.550	1.725	0 575	-0.325	-0 213
9	0.975	1.625	-0.284	-0 850	2.225	1.175	-0.025	-0 496
10	0.475	2.325	-0 355	-0 850	2.725	2.675	0.175	-0.709
11	0.275	2.925	-0.355	-1 050	3.525	3.975	0 375	-1.064
12	0.175	3.525	-0 355	-1 050	3.825	4.675	0.775	-1.206
13	0.075	3.125	-0.355	-1.250	2.725	4.375	1 075	-0 922
14A	0.175	2 925	-0.496	-0 750	1.625	3.575	1.475	-0 709
14B	0.175	2.925	-0.496	-0 850	1.625	3.675	1,375	-0.922
15	0.075	3 425	-0 567	-1 050	3.025	4.475	1.375	-1.064
16	-0.025	4.225	-0.567	-0.950	4.225	5.375	1.075	-1.560
17	-0.025	4 425	-0 567	-0 950	4.825	5 875	0.975	-1.418
18	-0.125	4.625	-0.567	-0 950	5.325	6.175	1.075	-1.489
19	-0.125	4 725	-0.638	-1.050	5.325	6.375	1.075	-1.702
20	-0.225	4.425	-0 638	-1 150	5.025	6.175	1.075	-1.773

Table A.12 *(Cont'd)* Web Hole Specimens H-1 and H-2 – Strain Measurements – Loading 1.

Load Stage	DEMEC Gauge Readings - Strain (mm/m) 65 H1 D89DB	66 H1 H10C	67 H1 V10A	68 H1 V10C	69 H1 D10C	70 H1 H11A	71 H1 H11C	72 H1 V11A
1A	0.000	0.000	-0.125	-0.200	—	-0.150	-0.075	-0.150
1B	0.000	0.000	0.075	-0.100	-0.035	0.050	0.025	0.050
1C	0.000	0 000	-0.025	0.200	0.035	0.050	0.025	0.050
1D	—	0.000	0.075	0.100	—	0.050	0.025	0.050
3	0.071	0.200	0.075	0.000	0.106	0.150	0.225	0.050
4	0.000	0.100	0.075	-0.100	-0.035	0.150	0.325	0.050
5	0.071	0.300	0.075	-0.100	-0.177	0.350	0.725	0.050
6	0.213	0.400	0.175	-0.100	0.035	0.450	0.825	0.050
7	0.426	0.600	0.375	0.000	0.248	0.750	1.025	0.250
8	1.064	0.600	0.675	0.300	0.248	1.250	1.125	0.750
9	1.773	0.700	0.875	0.200	0.390	1.950	1.325	1.150
10	3.191	0.600	0 975	0.500	0.461	2.250	1.425	1.450
11	4.752	0.500	0.875	0.400	0.674	2 550	1.525	1.750
12	5.532	0.600	0.975	0.400	1.099	2.650	1.525	1.950
13	4.539	0.100	0.675	0.900	0.745	1.850	1.025	1.150
14A	3.475	-0.400	0.375	0 100	0 177	1.150	0.425	0 550
14B	3.546	-0.300	0.575	0.300	0 248	1.150	0.525	0.450
15	4.681	0.100	0.775	0.500	0.461	2.050	1.125	1.250
16	6.028	0 500	1.075	0.700	0.887	2.750	1.725	1.950
17	6.809	0.700	1 075	0 500	1.241	2.950	1.825	2.150
18	7.234	1.500	1.075	0 500	1.879	3 050	1.925	2.450
19	7.589	1.500	1.175	0 700	2.163	2.950	1.725	2.450
20	7.234	1.300	0.975	0.100	1.879	2.550	1.425	2.050

Table A.12 *(Cont'd)* Web Hole Specimens H-1 and H-2 – Strain Measurements – Loading 1.

Load Stage	DEMEC Gauge Readings - Strain (mm/m) 73 H1 V11C	74 H1 D11A	75 H1 D11B	76 H1 D11C	77 CL H12C	78 CL H12D	79 CL H13C	80 CL H13D
1A	-0.100	—	—	-0.095	-0.095	-0.118	-0.118	-0.095
1B	0.000	-0.035	-0 035	0.047	-0 095	-0.047	-0.047	0.047
1C	0.000	0.035	0.035	0 047	0.189	0.165	0.165	0.047
1D	0.100	—	—	—	—	—	—	—
3	0.100	0.177	0 035	0.189	0.118	0.095	-0.118	-0.024
4	0.100	0.035	0.106	0.189	0.331	0.236	-0.047	0.118
5	0.100	0.035	0.106	0.260	0.473	0.449	0.165	0.331
6	0.200	-0.035	0.177	0.331	0 615	0.591	0.307	0.615
7	0.200	-0.106	0.319	0.473	0.827	0.875	0.804	1.040
8	0.500	-0.106	0.248	0.757	1.111	1.087	1.017	1.466
9	0.700	0.106	0.248	0.827	1.253	1.300	1.371	1.820
10	0.900	0.177	0.177	0.827	1.608	1.371	1.371	2.175
11	1.000	0.319	0.177	0.969	1.749	1.442	1.584	2.600
12	1.200	0.603	0.106	0.969	2.033	1.584	1.797	2.671
13	0.700	0.390	0.035	0.615	2.388	0.875	0.946	1.608
14A	0.500	0.248	-0.106	0.118	0.331	0.236	0.024	0.544
14B	0.500	0.177	-0.106	0 118	0.331	0.095	0.024	0.473
15	0.900	0.319	-0.106	0.473	1.040	0.875	0.875	1.466
16	1.200	0.603	0.035	0.827	1.678	1.442	1.726	2.530
17	1.400	0.745	-0.035	0.827	1.749	1.513	1.868	2.742
18	1.400	0.887	-0.106	0.827	1.962	1.868	2.222	3.097
19	1.200	1.028	0.106	0.969	5.012	5.414	2.080	2.530
20	1.200	0.957	-0.106	-0.024	4.728	9.173	1.726	2.600

Table A.12 *(Cont'd)* Web Hole Specimens H-1 and H-2 – Strain Measurements – Loading 1.

	DEMEC Gauge Readings - Strain (mm/m)							
Load Stage	81 H2 H14A	82 H2 H14C	83 H2 V14A	84 H2 V14C	85 H2 D14A	86 H2 D14B	87 H2 D14C	88 H2 H15C
1A	0.000	0.025	-0.075	-0.100	0.024	—	—	-0 025
1B	-0.100	-0.075	0.025	0.000	-0.118	-0 035	-0.035	-0.125
1C	0.000	0.025	0.025	0.100	0.095	0.035	0.035	0.075
1D	0.100	0.025	0.025	0.000	—	—	—	0.075
3	0.000	0.125	0.025	0.000	-0.189	-0.177	0.035	-0.025
4	0.000	0.325	-0 075	-0 100	-0.260	-0.106	-0.035	-0 025
5	0.000	0.325	0.025	-0.100	-0.260	-0 106	0.035	0 175
6	0.200	0.725	0.025	0.000	-0.260	-0.035	0.177	0.175
7	0.100	0.925	0.325	0 300	-0.189	0.177	0 532	0 275
8	0.000	1.225	0.425	0 300	-0.260	0 319	0.816	0 375
9	0.000	1.425	0.625	0.400	-0 331	0 461	1 099	0 375
10	-0.300	1.625	0.825	0 500	-0.402	0.745	1.525	0 375
11	-0.600	1.525	0.925	0 600	-0 544	0.674	1 596	0 575
12	-0 800	1.325	1.425	0 800	-0 473	0 532	1.454	0 975
13	-0.400	1.025	1.025	0 500	-0.189	0 319	1.099	0 675
14A	-0.400	0.425	0.425	0 400	-0 473	0.035	0 390	0 175
14B	-0.500	0.525	0.525	0 400	-0 402	0 177	0 532	0 075
15	-0 600	0.825	0 925	0.500	-0 402	0.106	0.957	0 575
16	-0.600	1 325	1.425	0 900	-0 331	0 390	1.454	0.975
17	-0.700	1.425	1.825	0 900	-0 189	0.532	1 525	1 575
18	-0.600	1.025	2.325	1 100	0 165	0 248	1.383	2 575
19	3 800	0.925	2.825	1 100	-0.402	-0.532	1.312	3.075
20	10.400	2.525	2.225	0 600	-3 381	-0.957	2.234	9 075

Table A.12 *(Cont'd)* Web Hole Specimens H-1 and H-2 – Strain Measurements – Loading 1

	DEMEC Gauge Readings - Strain (mm/m)							
Load Stage	89 H2 V15A	90 H2 V15C	91 H2 D15C	92 H2 H167B	93 H2 H167D	94 H2 V16C	95 H2 V17C	96 H2 D16BD
1A	-0.050	—	—	0 050	-0.125	-0.100	-0.150	0 071
1B	-0.050	0 033	-0.106	-0.150	-0.025	0.000	-0.050	-0.071
1C	0.050	0.033	0.106	0.050	-0 025	0 100	0.150	0 000
1D	0.050	-0.067	—	0 050	0.175	0 000	0.050	—
3	-0.050	0.033	-0 035	-0 150	0.175	0.000	-0.050	-0 071
4	-0.050	-0 067	-0.035	-0 250	0.075	0.000	-0.250	0.000
5	-0.050	0.033	0 177	-0.450	0.275	0.000	0 150	0.071
6	0.250	0.033	0.319	-0.550	0 675	-0.100	0 050	0 000
7	0.850	0.333	0.319	-0.750	0.875	-0.100	0.450	-0 071
8	1.050	0.433	0.248	-0.850	1.275	-0 200	0.750	-0.142
9	1.350	0.633	0 300	-1.150	1.875	-0 100	1.550	-0 213
10	2.250	0.833	0 106	-1.450	2.675	0.100	2 350	-0 496
11	3.250	0.833	—	-2.150	3.875	0.400	3 050	-0 780
12	3.350	0.833	—	-2.750	3.475	0.100	5.450	-1 206
13	2.750	0.733	—	-2.550	3.075	0.200	6.250	-0 993
14A	2.250	0.233	—	-2.550	2.375	0.400	5.150	-0 851
14B	2.350	0.333	—	-2 350	2.275	0.500	5.350	-0 922
15	2.650	0.733	—	-2.750	2.775	0.300	5.950	-1.277
16	3.250	-0.667	—	-2.650	3.275	0.300	7.150	-1.489
17	3.450	0.833	—	-2.950	3.575	-0.100	9.050	-1.489
18	3.350	1.533	—	-4.850	2.275	0.100	15.050	-1.702
19	0.950	4.033	—	-6.850	7.075	9.500	34.050	5.603
20	14.850	—	—	—	21.075	—	52.250	5.887

Table A.12 *(Cont'd)* Web Hole Specimens H-1 and H-2 – Strain Measurements – Loading 1.

Load Stage	DEMEC Gauge Readings - Strain (mm/m) 97 H2 D16DB	98 H2 H18C	99 H2 V18C	100 H2 D18C	101 H2 H192B	102 H2 H192D	103 H2 V19C	104 H2 V20C
1A	-0.142	0.100	-0.075	-0.024	-0.033	0.000	0.025	—
1B	0.142	-0.100	0.025	-0 024	-0.033	-0.200	0.025	-0.100
1C	—	0 000	0.025	0.047	0.067	0.100	0.025	0.100
1D	—	0.000	0.025	—	—	0.100	-0.075	—
3	0.000	0 000	0.125	-0 095	0.267	0.000	-0.075	-0.300
4	0.071	0.100	0.025	-0 024	0.367	0.000	-0.075	-0.200
5	0.213	0.300	0.025	-0 095	0.667	0.000	-0.075	-0.300
6	0.284	0.300	0.225	-0.165	0.867	-0.100	-0.075	0.000
7	0.567	0.400	0 425	-0.165	1.067	-0.100	0.225	0.400
8	1.064	0.400	0 825	-0.165	1.367	0.300	0.925	0.900
9	1.631	0 400	1.325	-0.236	1.567	0.600	1.725	1.600
10	2.553	-0.100	2.425	-0.095	1.667	1.000	3.625	2.600
11	3.404	0.900	6.825	4.941	1.867	-0.900	5.125	6.500
12	4.681	0.200	16.425	13.735	1.767	-1.300	6.625	7.100
13	3.333	0.300	16.325	13.806	1.867	-0.800	6.325	6.700
14A	3.333	0.100	12.825	11 537	1.167	-0.700	5.525	5.200
14B	3.262	0.100	12.825	11 537	1.267	-0 600	5.525	5.300
15	4.184	0.100	15.325	13.097	1.567	-0.700	6.325	6.100
16	5.390	0.200	19.525	16.288	1.867	-0.900	7.625	7.000
17	6.170	0 100	22.625	19.480	1.867	-0.400	8.325	7.600
18	7.943	-0.400	27.625	26.785	1.967	0.100	9.325	8.000
19	16.454	-0.300	—	31.537	2.167	0.200	9 525	8.300
20	36.383	-0.600	26 525	—	2.367	1.100	9.625	8.700

Table A.12 *(Cont'd)* Web Hole Specimens H-1 and H-2 – Strain Measurements – Loading 1.

Load Stage	DEMEC Gauge Readings - Strain (mm/m) 105 H2 D19BD	106 H2 D19DB	107 H2 H21C	108 H2 V21A	109 H2 V21C	110 H2 D21C	111 H2 H22A	112 H2 H22C
1A	—	0.118	-0.033	-0.100	0.000	-0.165	0.025	0.050
1B	-0.106	-0.095	-0.033	0.000	0.000	0.118	0.025	-0.050
1C	0.106	-0.024	0.067	0.100	0.000	0.047	-0.075	-0.050
1D	—	—	—	—	—	—	0.025	0.050
3	-0.177	-0.165	0.267	0.000	0.100	-0.095	-0.075	-0.150
4	-0.035	-0.095	0.367	0.000	0.300	-0.024	-0.175	-0.150
5	-0.035	0.047	0.767	0.100	0.400	0.118	-0.175	-0.050
6	-0.035	0.260	1.167	0.500	0.600	0.260	0.925	0.550
7	0.035	0 686	1.767	0.700	0.900	0.473	1.725	0.550
8	-0.177	1.678	2.167	0.900	1.200	0.757	2.825	0.550
9	-0.248	2.813	2.667	1.200	1.500	1.040	4.025	0.550
10	-0.745	4.870	3.467	1.100	1.500	1.466	7.125	0.750
11	-1.312	6.927	4.767	1.700	1.400	2.459	10.025	0.850
12	-2.447	8.487	6.267	2.500	2.100	2.813	12.425	1.050
13	-1.809	7.920	4.967	1.700	1.700	2.459	11.225	1.250
14A	-1.525	6.501	3.167	1.400	1.100	1.820	7.325	0.650
14B	-1.667	6.430	3.167	1.400	1.100	1.820	7.525	0.750
15	-1.950	7.707	4.567	2.100	2.100	2.175	10.725	1.150
16	-2.163	9.054	6.267	3.100	3.100	2.671	13.425	1.450
17	-2.234	10.118	7.867	3.600	3.600	3.239	15.225	1.850
18	-2.163	11.111	10.967	4.400	4.400	4.161	18.025	3.150
19	-2.163	11.678	14.167	5.300	3.900	5.934	22.025	3.950
20	-2.021	11.962	17.567	6.500	3.800	7.494	26.125	5.550

Table A.12 *(Cont'd)* Web Hole Specimens H-1 and H-2 – Strain Measurements – Loading 1.

Load Stage	DEMEC Gauge Readings - Strain (mm/m) 113 H2 V22A	114 H2 V22C	115 H2 D22A	116 H2 D22B	117 H2 D22C
1A	—	-0.075	-0.047	-0.035	-0.213
1B	-0.133	-0.075	-0.047	0.035	0.071
1C	0.167	0.125	0.095	—	0.142
1D	-0.033	0.025	—	—	—
3	-0.133	0.025	-0.118	-0.035	0.000
4	-0.133	0.025	-0.189	-0.106	0.000
5	-0.133	0.025	-0.189	-0.106	-0.071
6	0.167	0.325	-0.331	-0.177	-0.213
7	0.367	0.525	-0.402	-0.248	-0.213
8	0.867	0.925	-0.615	-0.461	-0.213
9	1.667	1 225	-0.757	-0.461	-0.284
10	2.267	1.625	-1.182	-0.319	-0.355
11	2.767	1.925	-1.537	-0.177	-0.213
12	2.767	2.225	-1.891	-0 461	-0.709
13	2.267	1.625	-1.537	-0.106	-0.426
14A	1.767	1.125	-1.182	-0 177	-0.567
14B	1.767	1.225	-1.111	-0.177	-0.638
15	2.367	1.625	-1.608	-0.106	-0.567
16	2.867	2.225	-2.175	-0.390	-0.780
17	2.967	2.225	-2.317	-0.248	-0.780
18	0.267	2.325	-2.530	-0.106	-0.709
19	18.967	2.225	-2.530	0.035	-0.567
20	3.367	1.025	-2.600	0 390	-0.567

Table A.13 Web Hole Specimen H-1 – Measured Loads – Loading 2.

Load Stage	Measured Loads and Deflections Loading* (kN/m)	Dial 1 (mm)	Dial 2 (mm)	Dial 3 (mm)
B1A-B	0.0	0.00	0.00	0.00
B2	43.0	2.59	5.03	4.47
B3	82.3	4.90	9.50	8.51
B4	93.1	5.56	10.80	9.65
B5	108.8	6.48	12.55	11.28
B6	124.4	7.47	14.50	13.18
B7	0.0	0.53	1.37	0.89
B7-1	29.8	2.39	4.47	4.04
B7-2	58.0	4 01	7.72	6.93
B7-3	85.6	5.51	10.64	9.47
B7-4	111.4	6.88	13.31	12.01
B7-5	133.8	8.10	15.70	14.27
B8	143.1	8.71	16.87	15.27
B9	0.0	0.69	1.45	0.97
B9-1	29.2	2.62	4.95	4.24
B9-2	57.0	4.27	8.23	6.05
B9-3	85.7	5.82	11.28	9.96
B9-4	114.1	7.29	14.20	12.60
B9-5	141.1	8.66	16.92	15.06
B10	157.4	9.80	19.46	17.15
B11	170.4	11.76	24.99	20.57
B12	173.1	17.22	38.40	26.57
B12-1	118.7	16.18	36.60	24.79
B12-2	89.2	14.63	33.40	22.00
B12-3	59.3	12.83	29.62	18.82
B12-4	30.0	10.62	24.89	15.16
B12-5	0.0	7.32	17.45	9.75

* Does not include uniform self-weight loading of 4.3 kN/m.

Table A.14 Web Hole Specimen H-1 – Strain Measurements – Loading 2.

Load Stage	DEMEC Gauge Readings - Strain (mm/m) 1 H1 C1 4	2 H1 C2 4	3 H1 C3 4	4 H1 C4 4	5 H1 C5 4	6 H1 C1 10	7 H1 C2 10	8 H1 C3 10
B1A	-1.182	-0.177	1.950	0.106	-1.418	1.968	-1.726	-1.844
B1B	-1.395	-0.248	1.879	0.035	-1.418	1.897	-1.655	-1.915
B2	-1.608	-0.248	2.234	0.177	-1.702	2.394	-2.080	-2.340
B3	-1.820	-0.177	2.518	0.248	-1.986	2.890	-2.506	-2.695
B4	-1.962	-0.177	2.660	0.248	-2.340	2.961	-2.648	-2.908
B5	-2.033	-0.319	2.730	0.319	-2.411	2.961	-2.790	-3.050
B6	-2.104	-0.106	2.943	0.390	-2.199	3.387	-2.931	-3.262
B8	-2.175	-0.106	2.943	0.319	-2.411	3.670	-3.144	-3.475
B10	-2.317	-0.035	3.014	0.390	-2.624	4.167	-3.357	-3.759
B11	-2.600	-0.177	3.440	0.390	-2.766	5.160	-3.924	-4.397
B12	-2.884	-0.177	3.085	0.603	-3.333	9.060	-7.896	-4.113

Table A.14 *(Cont'd)* Web Hole Specimen H-1 – Strain Measurements – Loading 2.

	DEMEC Gauge Readings - Strain (mm/m)							
Load Stage	9 H1 C4 10	10 H1 C5 10	11 CL C1 12	12 CL C2 12	13 CL C3 12	14 CL C4 12	15 CL C5 12	26 H1 H1A
B1A	-1.596	2.128	-0.496	-0.993	-1.206	-1.064	-0.118	-0.467
B1B	-1.596	2.270	-0.426	-1.064	-1.206	-1.135	0.024	-0.467
B2	-2.021	2.766	-0.426	-1.277	-1.277	-1.277	-0.047	-0.567
B3	-2.376	3.333	-0.355	-1.489	-1.489	-1.489	-0.047	-0.767
B4	-2.518	3.617	-0.355	-1.489	-1.560	-1.631	-0.189	-0.667
B5	-2.730	3.688	-0.213	-1.631	-1.631	-1.702	0 095	-0.767
B6	-2.801	3.830	-0.284	-1.702	-1.773	-1.702	0.095	-0.667
B8	-3.014	4.113	-0.213	-1.844	-1.844	-1.844	0.165	-0.767
B10	-3.298	4.752	-0.284	-1 844	-1.915	-1.915	0.165	-0.667
B11	-3.865	5.887	-0.142	-2.057	-2 057	-2.057	0.165	-0 967
B12	-4.504	7.376	-0 213	-1.915	-1.986	-1.986	0 165	-0.867

Table A.14 *(Cont'd)* Web Hole Specimen H-1 – Strain Measurements – Loading 2.

	DEMEC Gauge Readings - Strain (mm/m)							
Load Stage	27 H1 H1C	28 H1 V1A	29 H1 V1C	30 H1 D1A	31 H1 D1B	32 H1 D1C	33 H1 H2A	34 H1 H2C
B1A	1.033	0.133	0 233	-0.745	-0.532	-0.426	-0.300	1.725
B1B	1.133	0.133	0.333	-0.745	-0.603	-0.426	-0.400	1.725
B2	1.233	0.333	0.633	-0.887	-0.816	-0 567	-0.600	2.225
B3	1.433	0.233	0.833	-0.957	-0.816	-0 638	-0.700	2.725
B4	1.633	0.233	0.833	-1.099	-1.099	-0.780	-0.700	2.825
B5	1.733	0.233	0.933	-1 099	-1.454	-0.780	-0.800	2.925
B6	1.933	0.433	1.133	-1.241	-1.099	-0.780	-0.800	3.125
B8	2.233	0.333	1.233	-1.312	-1.383	-0.922	-0.800	3.525
B10	2.433	0.333	1.333	-1.454	-1.738	-0.993	-0.900	3 925
B11	2.733	0.533	1 533	-1.454	-1.454	-1.064	-1.000	4.325
B12	3.133	0.433	1.633	-1.596	-1.596	-1.064	-1.200	5.025

Table A.14 *(Cont'd)* Web Hole Specimen H-1 – Strain Measurements – Loading 2.

	DEMEC Gauge Readings - Strain (mm/m)							
Load Stage	35 H1 V2A	36 H1 V2C	37 H1 D2A	38 H1 D2B	39 H1 D2C	40 H1 H3A	41 H1 H3C	42 H1 V3A
B1A	0.700	0.600	-0.591	-0.733	0.284	4.800	1.575	4.475
B1B	0.700	0.700	-0 520	-0 662	0.355	4.700	1.575	4.575
B2	1.200	1.000	-0.662	-0 733	0.284	6.400	2.175	5.075
B3	1.500	1.500	-0.662	-0.875	0.355	7.300	2.775	5.475
B4	1.600	1.500	-0.804	-0.946	0.355	7.500	2.975	5.575
B5	1.600	1.500	-0.804	-1.087	0.426	7.800	3.175	5.775
B6	1.900	2.000	-0 804	-1.087	0.496	8.100	3.475	6.175
B8	2.400	2.100	-0.946	-1.158	0.496	9.100	3.775	6.675
B10	2.500	2.400	-1 087	-1.229	0.426	10.300	3.975	7.275
B11	3.300	2.800	-1.087	-1.229	0.355	12.500	4.275	9.475
B12	4.200	3.700	-1.300	-1.158	0.213	14.200	6.775	14.975

Table A.14 *(Cont'd)* Web Hole Specimen H-1 – Strain Measurements – Loading 2.

	DEMEC Gauge Readings - Strain (mm/m)							
Load Stage	43 H1 V3C	44 H1 D3A	45 H1 D3B	46 H1 D3C	47 H1 H4C	48 H1 V4A	49 H1 V4C	50 H1 D4C
B1A	10.225	-0.638	-0.887	0.024	4.475	0.500	0.450	2.388
B1B	10.325	-0.496	-0.816	0.024	4.475	0.600	0.550	2.388
B2	10.525	-1 277	-0 957	0.236	5.375	0.900	0.650	2.884
B3	10.825	-1.560	-1.170	0.378	6.275	1.300	0.950	3.452
B4	10.925	-1.631	-1.241	0.378	6.575	1.600	1.050	3 664
B5	11.125	-1 560	-1.241	0.520	6.975	1.600	1.250	3.948
B6	11.425	-1.773	-1.383	0.520	7.375	1.800	1.550	4.161
B8	11.525	-2.128	-1.525	0.378	7.875	2.000	1.750	4.303
B10	11.625	-2.553	-1.525	0.520	8.175	2.000	1.750	4.657
B11	11.825	-2.766	-1.525	0.662	11.875	2.300	1.850	7.210
B12	12.425	4.468	-9.184	1.584	17.475	3.900	2.750	8.771

Table A.14 *(Cont'd)* Web Hole Specimen H-1 – Strain Measurements – Loading 2.

	DEMEC Gauge Readings - Strain (mm/m)							
Load Stage	51 H1 H56B	52 H1 H56D	53 H1 V5C	54 H1 V6C	55 H1 D56DB	56 H1 D56BD	57 H1 H7C	58 H1 V7C
B1A	0.075	0.575	1.933	2.200	-1.040	3.191	0.075	3.025
B1B	0.075	0.575	2.033	2.300	-0.969	3.191	0.075	3.125
B2	0.275	0.775	2.433	2.900	-1.040	3.972	-0.025	3.625
B3	0.175	0.975	2.933	3.300	-1.111	4.681	-0.125	4.325
B4	0.275	1.075	3.133	3.500	-1.111	4.823	-0.125	4.425
B5	0.275	1.175	3.233	3.600	-1.040	5.177	-0.125	4.625
B6	0.375	1 275	3.533	3 900	-1.111	5.532	-0.125	5.025
B8	0.575	1.575	3.833	4.200	-1.182	5.957	-0.225	5.425
B10	0.675	1.575	4.033	4.300	-1.111	6.170	-0.225	5.625
B11	0.575	1.675	4.633	4.500	-1.040	6.525	-0.325	5.625
B12	0.475	2.875	5.033	5.800	-1.537	8.440	-0.025	8.325

Table A.14 *(Cont'd)* Web Hole Specimen H-1 – Strain Measurements – Loading 2.

	DEMEC Gauge Readings - Strain (mm/m)							
Load Stage	59 H1 D7C	60 H1 H89B	61 H1 H89D	62 H1 V8C	63 H1 V9C	64 H1 D89DB	65 H1 D89DB	66 H1 H10C
B1A	-0.709	-0.850	2.725	3.775	1.275	-1.064	4.326	0.600
B1B	-0.709	-0.850	2.625	3.675	1.275	-1.135	4.326	0.700
B2	-0.780	-0.950	3 625	4.575	1.175	-1.206	5.319	0.900
B3	-0.780	-0.950	4.425	5.275	1.075	-1.348	6.383	1.200
B4	-0.709	-0.950	4.625	5.475	0.875	-1.560	6.596	1.300
B5	-0.709	-0.950	4.925	5.575	0.775	-1.631	6.809	1.400
B6	-0.638	-0.950	5.225	5.975	0.875	-1.631	7.305	1.600
B8	-0.709	-0.750	5.725	6.375	0.775	-1.844	7.801	1.700
B10	-0.709	-0.650	6.625	6.675	0.675	-2.057	8.652	2.300
B11	-0.709	-0.950	9.325	7.475	-0.025	-2.553	10.355	3.900
B12	-0.426	-6.050	15.125	10.075	-0.725	-4.184	13.262	5.600

Table A.14 *(Cont'd)* Web Hole Specimen H-1 – Strain Measurements – Loading 2.

	DEMEC Gauge Readings - Strain (mm/m)							
Load	67	68	69	70	71	72	73	74
Stage	H1 V10A	H1 V10C	H1 D10C	H1 H11A	H1 H11C	H1 V11A	H1 V11C	H1 D11A
B1A	0.375	0.100	1.170	1.250	0.525	0.550	0.300	0.461
B1B	0.275	0.100	1.170	1.350	0.525	0.550	0.300	0.532
B2	0.475	0.100	1.241	1.750	0.825	0.950	0.500	0.461
B3	0.575	0.000	1.454	2.050	1.225	1.250	0.700	0.603
B4	0.475	-0.100	1.454	2.250	1.425	1.350	0.800	0.532
B5	0.575	-0.200	1.596	2.450	1.525	1.550	0.800	0.674
B6	0.775	0.100	1.738	2.650	1.825	1.650	1.000	0.674
B8	0.775	0.100	1.738	2.850	1.825	1.850	1.000	0.745
B10	0.875	0.000	2 163	3.050	2.025	1.950	1.100	0.816
B11	0.975	0.300	3.936	3.350	2.125	2.050	1.200	0.816
B12	0.775	0.100	5.993	2.650	2.025	1.150	0.900	0.390

Table A.14 *(Cont'd)* Web Hole Specimen H-1 – Strain Measurements – Loading 2.

	DEMEC Gauge Readings - Strain (mm/m)					
Load	75	76	77	78	79	80
Stage	H1 D11B	H1 D11C	CL H12C	CL H12D	CL H13C	CL H13D
B1A	-0.035	0.260	3.381	3.712	0.307	0.898
B1B	0.035	0.189	3.381	3.712	0.236	0.898
B2	-0.106	0.402	3.806	4.279	0.591	1.324
B3	-0.035	0.615	4.090	4.563	1.087	1.749
B4	-0.035	0.615	4.161	4.704	1.158	1.891
B5	0.035	0.827	4.303	4.846	1.371	2.033
B6	-0.035	0.827	4.444	5.059	1.584	2.317
B8	-0.035	0.898	4.586	5.201	1.655	2.530
B10	0.106	0.969	4.728	5.485	1.868	2.813
B11	-0.035	0.969	4.799	5.556	1.868	2.884
B12	0.248	1.111	4.657	5.414	1.726	2.671